Laboratorio de Neurobiología del Sueño

Departamento de Fisiología

Facultad de Medicina

Universidad de la República

Estudio de las oscilaciones gamma del EEG durante la vigilia, el sueño y en un modelo farmacológico de psicosis

Tesis de Doctorado en Ciencias Biológicas

PEDECIBA

Santiago Castro Zaballa

Orientador:

Prof. Dr. Pablo Torterolo

Montevideo, 2018

AGRADECIMIENTOS

A mi tutor Pablo Torterolo por respaldarme en la puesta en práctica de esta idea que llevó al desarrollo de este nuevo trabajo, y por su constante impulso a la superación.

A Atilio Falconi por sus aportes y buenos consejos.

A Matías Cavelli, por su contribución.

A Noelia Velázquez y Joaquín Gonzalez por su apoyo técnico.

Al amor de mi vida, mi esposa Andrea Murieda, por su gran soporte, sin el cual todo esto no hubiera sido posible.

RESUMEN

Para generar los procesos cognitivos, distintas áreas corticales interactúan intensamente entre sí y con regiones subcorticales como el tálamo. Se ha postulado que las oscilaciones en la banda gamma de frecuencia (30 a 45 Hz) del electroencefalograma (EEG), son producto de estas interacciones y por lo tanto están involucradas en las funciones cognitivas.

En el presente trabajo, utilizando el gato como modelo animal, nos propusimos estudiar las oscilaciones gamma del EEG de distintas regiones corticales. Para ello utilizamos distintas funciones matemáticas, pero principalmente la "coherencia cruzada cuadrada". La actividad gamma fue estudiada durante la vigilia y el sueño, así como en un modelo farmacológico de psicosis (dosis subanestésica de ketamina). También, utilizando antagonistas de receptores muscarínicos (atropina y escopolamina), estudiamos el rol del sistema colinérgico (componente de los sistemas activadores) en la modulación de la actividad gamma.

Demostramos que durante la vigilia alerta (AW) hay un gran aumento de la coherencia en la banda gamma entre áreas corticales intrahemisféricas con respecto a los demás estados. A medida que el animal pasa a vigilia tranquila y luego al sueño NREM, la coherencia disminuye hasta valores moderados. La coherencia alcanza valores mínimos durante el sueño REM. Esta disminución de coherencia gamma durante el sueño REM se extiende hasta la banda gamma alta de frecuencias (60-100 Hz). La coherencia gamma entre áreas corticales interhemisféricas fue similar a la de las áreas intrahemisféricas excepto entre áreas interhemisféricas homólogas, donde la coherencia gamma durante el sueño REM fue similar a la encontrada durante el sueño NREM

También estudiamos la actividad gamma durante el sueño REM (REMc) y cataplejía (vigilia con atonía muscular, CA) producidos por microinyecciones de carbacol (agonista colinérgico) en el nucleus pontis

oralis. Estos experimentos permitieron contrastar dos estados que difieren en su aspecto cognitivo (vigilia alerta durante la CA y probable actividad onírica durante el sueño REMc), pero mantienen el mismo comportamiento (parálisis con atonía muscular característica del sueño REM). La coherencia gamma fue máxima durante la CA con valores similares a los de la AW. En contraste, la coherencia gamma fue mínima durante REMc (valores similares al sueño REM natural).

En el modelo de psicosis inducido por ketamina comprobamos la presencia de una disminución de la coherencia gamma entre todas las regiones corticales, efecto similar a lo que se observamos durante el sueño REM.

Por último, la administración de atropina o escopolamina provoca un enlentecimiento del EEG, con aumento de las ondas delta y los husos del sueño (como en el sueño NREM); sin embargo, los animales permanecen activos. Este estado disociado fue acompañado por valores de potencia y coherencia gamma, similares a la QW y la AW, respectivamente. Esta gran conectividad funcional en la banda gamma de frecuencias podría explicar por qué los animales permanecen despiertos a pesar de la presencia de ondas lentas y husos en el EEG.

Concluimos que las interacciones funcionales entre áreas corticales son radicalmente diferentes en dos estados comportamentales con activación cortical: vigilia y sueño REM. La virtual ausencia de coherencia en la banda gamma de frecuencia durante el sueño REM podría sustentar en parte el procesamiento cognitivo único que ocurre durante la actividad onírica, que es un fenómeno asociado principalmente con este estado. A su vez, demostramos que esta conectividad gamma durante el sueño REM se asemeja a lo que ocurre en un modelo farmacológico de psicosis. Por último, nuestros datos sugieren que la acetilcolina, actuando sobre receptores muscarínicos, no sería crítica en la generación de la actividad gamma, ya que esta se mantiene a pesar del bloqueo de sus receptores.

ABREVIATURAS

A1: corteza auditiva primaria

AW: vigilia alerta

AWm: alerta generada por la colocación de un espejo en frente del animal

AWml: alerta generada por una luz en movimiento

AWs: alerta generada con un estímulo sonoro

CA: cataplejía

ECG: electrocardiograma

EEG: electroencefalograma

EOG: electrooculograma

HIP: electrograma hipocámpico

QW: vigilia tranquila

M1: corteza motora primaria

NPO: núcleo pontis oralis

NREM: sueño no REM

Pf: corteza prefrontal

Pfdl: corteza prefrontal dorsolateral

Pfr: corteza prefrontal rostral

PGO: ondas ponto-geniculo-occipitales

Pp: corteza parietal posterior

REM: sueño REM

REMc: sueño REM inducido por carbacol

S1: corteza somestésica primaria

SRAA: sistema reticular activador ascendente

V1: corteza visual primaria

ÍNDICE

ESTRATEGIA DE INVESTIGACION Y ORGANIZACIÓN DE LA TESIS

En el presente trabajo estudiamos las oscilaciones gamma de distintas regiones corticales utilizando varios algoritmos matemáticos, tales como el análisis del espectro de potencias, la "coherencia cruzada cuadrada" y correlaciones. Éstas fueron estudiadas durante la vigilia y el sueño fisiológico o inducido farmacológicamente, así como en un modelo farmacológico de psicosis (dosis subanestésica de ketamina). También estudiamos el efecto de fármacos que bloquean neurotransmisores que forman parte de los sistemas activadores y que afectan la actividad cognitiva.

La Tesis está dividida en 5 capítulos:

Capítulo I: Fundamentos.

Capítulo II: Oscilaciones gamma del EEG durante la vigilia y el sueño.

Capítulo III: Oscilaciones gamma del EEG en un modelo farmacológico de psicosis.

Capítulo IV: Rol del sistema colinérgico en la modulación de las oscilaciones gamma del EEG.

Perspectivas.

En el Capítulo II; en una primera etapa comparamos el acoplamiento de las oscilaciones gamma de diferentes regiones corticales durante la vigilia alerta, la vigilia tranquila, el sueño no REM (NREM) y el sueño REM (del inglés: "*rapid eye movements*"). Esto lo hicimos tanto entre regiones corticales que se encuentran en el mismo hemisferio cerebral (conexiones intrahemisféricas), como para regiones corticales que se encuentran en diferentes hemisferios cerebrales (conexiones interhemisféricas).

En una segunda etapa realizamos microinyecciones de agonistas colinérgicos en el nucleus pontis oralis (NPO), lo que genera un estado con características fisiológicas indistinguibles de las del sueño REM (REMc), o un estado disociado de vigilia con atonía muscular conocido como cataplejía (CA). Comparamos el acoplamiento de las oscilaciones gamma entre diferentes regiones corticales durante estos 2 estados.

En la sección Resultados se expondrán tres trabajos publicados, precedidos por un breve comentario previo a cada uno de ellos. En la Discusión, se complementará la discusión presente en cada uno de los artículos con los avances en la temática desde que estos trabajos fueron publicados.

En el Capítulo III estudiamos como las oscilaciones gamma y su nivel de acoplamiento entre áreas corticales es afectado en un modelo farmacológico de psicosis. En este trabajo comparamos el acoplamiento de las oscilaciones gamma de diferentes regiones corticales durante vigilia, sueño NREM, sueño REM (modelo natural de psicosis) y bajo el efecto de la ketamina. Este trabajo aun no fue publicado, por lo que es descripto y discutido en su totalidad.

En el Capítulo IV estudiamos el efecto de la atropina y la escopolamina, ambos antagonistas de los receptores muscarínicos de acetilcolina, sobre la actividad gamma del EEG. La administración de atropina o escopolamina en animales de experimentación provoca un enlentecimiento del EEG, con aumento de las ondas delta y los husos (como en el sueño NREM); sin embargo, los animales permanecen activos y con una gran actividad gamma. Este trabajo tampoco fue publicado por lo que lo que es descrito y discutido en su totalidad.

Posteriormente presento perspectivas de trabajos futuros que continuarán el trabajo de esta Tesis.

En el Anexo 1 se presenta el trabajo titulado: "Las oscilaciones gamma neocorticales coherentes disminuyen durante el sueño REM en la rata".

En el Anexo 2 se introduce el trabajo titulado: "Ausencia de coherencia gamma de EEG en un estado cortical activado localmente: un rasgo conservado de sueño REM".

En el Anexo 3 se expone el trabajo titulado: "Potencia y coherencia de las oscilaciones corticales de alta frecuencia durante la vigilia y el sueño".

CAPITULO I

FUNDAMENTOS

1.1. Ciclo sueño-vigilia

El ciclo sueño-vigilia es el ritmo biológico más evidente en aves y mamíferos. Dicho ciclo está compuesto por dos estados comportamentales: la vigilia (W, del inglés *wakefulness*) y el sueño, que poseen diferencias tanto fisiológicas como comportamentales (Carskadon, 2005).

El sueño se puede definir como un estado comportamental reversible donde la respuesta y la interacción con el medio se encuentran disminuidas. En este se distinguen dos grandes estados: sueño NREM o sueño lento, y sueño REM (Carskadon, 2005).

Cada estado se caracteriza por un conjunto de correlatos fisiológicos tales como la actividad eléctrica de diversas áreas del encéfalo, el movimiento de los ojos y el tono muscular que pueden ser registrados mediante el electroencefalograma (EEG), electrooculograma (EOG) y electromiograma (EMG). El registro de las 3 variables en forma simultánea se denomina Polisomnografía.

Durante la vigilia existe una interacción óptima con el ambiente que nos permite desarrollar diversos comportamientos necesarios para la supervivencia. En el ser humano, la vigilia se acompaña de consciencia del medio que nos rodea y de ciertos estímulos generados internamente.

Desde el punto de vista electroencefalográfico la vigilia se caracteriza por la activación del neocortex, evidenciado por un aumento de la frecuencia y una disminución de la amplitud del trazado. La presencia de tono muscular es reflejada en la alta amplitud en el EMG. El electrograma del hipocampo (HIP) presenta un ritmo theta durante la vigilia activa. El EOG no presenta particularidades durante este estado (Torterolo & Vanini,

2010). En la Figura 1 se puede observar un registro polisomnográfico típico de vigilia en el gato.

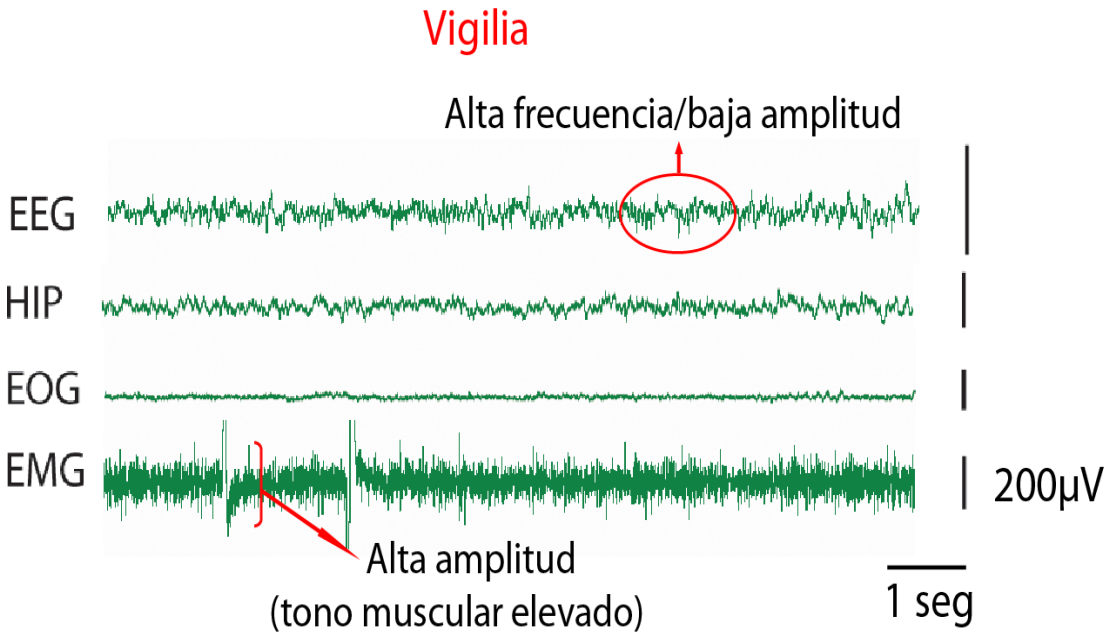

Figura 1. Registro polisomnográfico durante la vigilia. Se observan 4 registros bioeléctricos: el electroencefalograma de la corteza fronto-parietal (EEG), el registro eléctrico del hipocampo (HIP), el electrooculograma (EOG) y el electromiograma (EMG), obtenidos de un gato crónicamente implantado con electrodos para polisomnografía. En el EEG cortical se observa actividad oscilatoria con una frecuencia entre 15 y 50 Hz, y con una amplitud de 20 a 50 µV.

En el sueño existe una marcada disminución de la interacción con el ambiente, un aumento del umbral de reacción a estímulos externos, una disminución de la actividad y tono muscular, así como la adopción de una postura adecuada para conservar el calor. En humanos adultos, de la vigilia se ingresa al sueño NREM, en el cual se reconocen 3 fases relacionadas con la profundidad del estado. El sueño NREM presenta en forma característica un EEG con ondas de baja frecuencia (0.5 a 4 Hz, banda delta de frecuencias) y alta amplitud, así como por la presencia de husos de sueño (11 a 16 Hz, banda sigma de frecuencias), ambos generados por

la actividad sincronizada de neuronas talámicas y corticales (Torterolo & Vanini, 2010).

El sueño NREM se acompaña además de un aumento tónico de la actividad parasimpática que determina cambios característicos de la actividad visceral (Torterolo & Vanini, 2010). En el HIP se observan ondas lentas de alta amplitud. El EOG no presenta particularidades (Figura 2). En las etapas más profundas del NREM no existe o es mínima la actividad cognitiva (actividad onírica) (Dement et al., 1957; Pace-Schott et al., 2005).

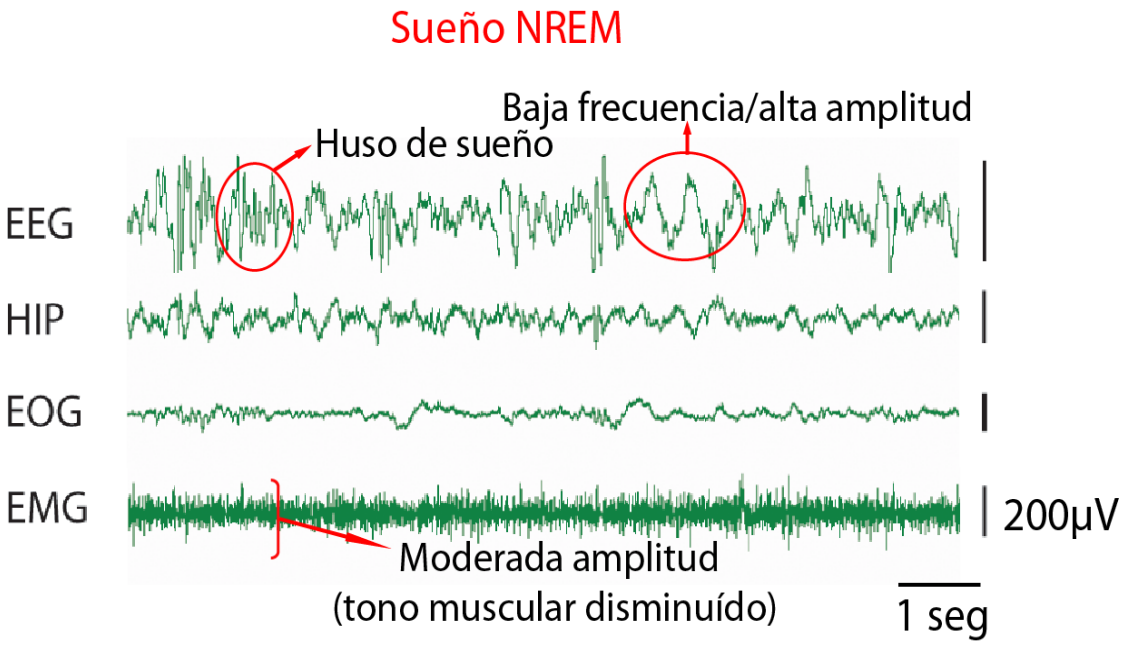

Figura 2. Registro polisomnográfico durante el sueño NREM. Se observan 4 registros eléctricos, el electroencefalograma de la corteza fronto-parietal (EEG), el registro eléctrico del hipocampo, el electrooculograma (EOG) y el electromiograma (EMG). En el EEG cortical es posible observar los husos de sueño y las ondas lentas. Asimismo, se puede observar el EMG con una amplitud disminuida correspondiente a un menor tono muscular que en vigilia.

En forma periódica y siempre precedida de NREM (con excepción de los neonatos), se ingresa al estado de sueño REM. A pesar de que el sueño es profundo, el EEG es similar al de vigilia. Esta asociación inusual

de parámetros había sido identificada y descripta en humanos por Aserinsky y Kleitman como sueño REM (Aserinsky & Kleitman, 1953), mientras que fue denominado sueño paradójico por Jouvet et al. (1959). El sueño REM también ha sido denominado sueño desincronizado, sueño activo y sueño con actividad onírica ("dream sleep"), ya que es en este estado donde principalmente ocurren los sueños.

El sueño REM se distingue por el EEG activado, movimientos oculares rápidos registrados en el EOG y una baja amplitud en el EMG que refleja atonía muscular (Figura 3) (Ursin & Sterman, 1981).

Como se observa en la Figura 3, durante el sueño REM el electrograma del hipocampo expresa una actividad rítmica en la banda theta de frecuencias (4-8 Hz), similar a la encontrada durante la vigilia con actividad motora. Por otro lado, el electrograma del núcleo geniculado lateral del gato presenta en forma distintiva ondas de gran amplitud que aparecen típicamente aisladas o en trenes (Ursin & Sterman, 1981). Estas ondas también pueden ser registradas en el tegmento pontino y en la corteza occipital, por lo que son llamadas ondas ponto-geniculo-occipitales (PGO).

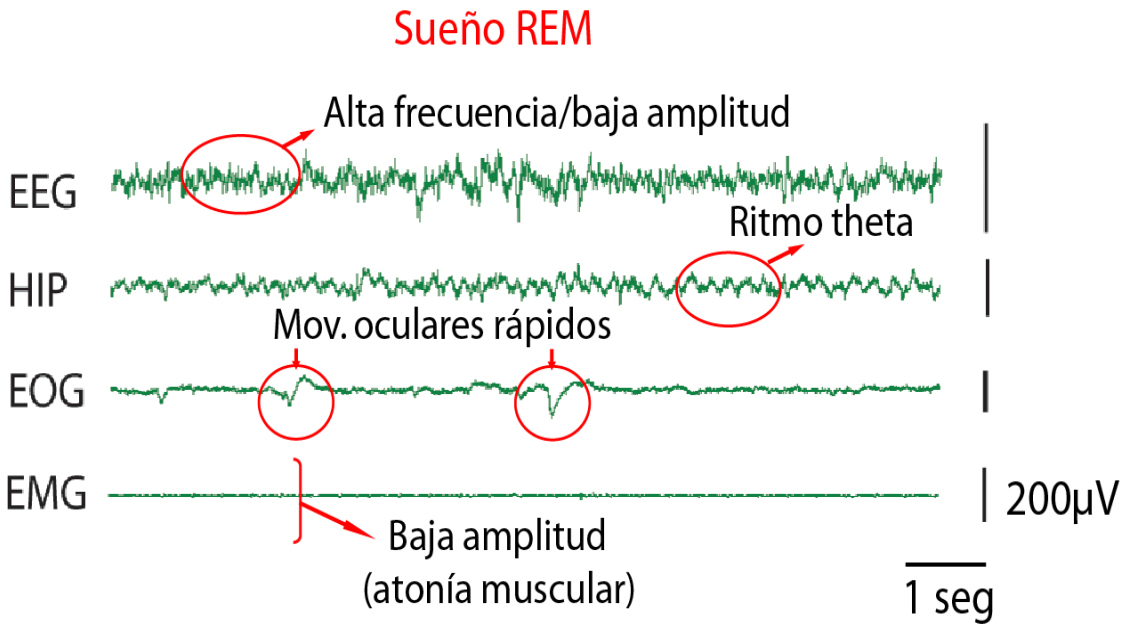

Figura 3. Registro polisomnográfico durante el sueño REM. Se observan 4 registros bioeléctricos, el electroencefalograma de la corteza fronto-parietal (EEG), el registro eléctrico del hipocampo (HIP), el electrooculograma (EOG) y el electromiograma (EMG). El EMG presenta baja amplitud producida por la atonía muscular; en el hipocampo se observa ritmo theta característico del sueño REM. En el EEG se observa la activación cortical y en el EOG los movimientos oculares rápidos.

1.2. Banda gamma y la integración en el procesamiento de la información

El problema de la integración ("*the binding problem*") es uno de los interrogantes más importantes que la neurociencia cognitiva tiene para resolver. A modo de ejemplo, distintas áreas corticales visuales procesan distintos aspectos de una imagen (color, forma, tamaño, movimiento por el campo visual, etc.). Sin embargo, estos aspectos se perciben en forma integrada.

Singer et al. (1995) propusieron que si las descargas de neuronas se sincronizan entre sí, participan en la codificación de información relacionada. Se cree que esta sincronización se basa en un proceso de auto-organización que está mediado por una red selectiva de conexiones cortico-corticales y cortico-talámicas. Por lo tanto, los grupos distribuidos de neuronas que codifican una característica particular, serían identificables como miembros de un conjunto, porque sus respuestas contendrían episodios durante los cuales sus descargas son sincrónicas.

A su vez, Siegel et al. (2012) propusieron que las oscilaciones a frecuencias específicas correlacionadas entre circuitos corticales distribuidos pueden funcionar como índices o huellas digitales de las interacciones que sostienen los procesos cognitivos.

Se ha visto que la banda gamma de frecuencias del EEG, es crítica para la integración en el procesamiento de la información y actividades cognitivas. Se considera que esta está compuesta por oscilaciones que van

de 30 a 100 Hz, siendo común que se la divida en gamma baja (30-50 Hz) y gamma alta (50-100 Hz); se considera también que la frecuencia más importante para la fenomenología cognitiva estaría alrededor de los 40 Hz (Llinas & Ribary, 1993; Bressler et al., 1993). Se ha propuesto que en la percepción sensorial, la resolución de problemas, la memoria, la vigilia y el sueño REM, estarían involucrados oscilaciones de frecuencia gamma (Eckhorn et al., 1988; Garcia-Rill 2015; Gray & Singer 1989, Phillips & Takeda 2009; Palva et al., 2009; Voss et al., 2009).

Sobre los mecanismos de generación de las oscilaciones gamma registradas en la corteza cerebral, Buzsaki y Wang (2012) proponen lo siguiente: 1. La ritmogénesis de banda gamma está ligada a la inhibición perisomática. 2. Las oscilaciones gamma son de corta duración y normalmente surgen de la interacción coordinada de excitación e inhibición, que puede ser detectada como potenciales de campo locales. 3. el ritmo gamma generalmente está asociado con disparos irregulares de neuronas individuales, y la frecuencia de las oscilaciones gamma de la red varía ampliamente dependiendo del mecanismo subyacente. 4. la magnitud de la oscilación gamma está modulada por ritmos más lentos. Tal acoplamiento entre frecuencias puede servir para sincronizar partes activas de circuitos corticales (Buzsaki & Wang, 2012).

Varias observaciones han llevado a la hipótesis de que las interneuronas GABAérgicas parvalbúmina positivas juegan un papel crítico en las oscilaciones gamma. 1. Aunque las neuronas piramidales y muchos tipos de interneuronas disparan durante las oscilaciones gamma, solo interneuronas GABAérgicas parvalbúmina positivas disparan rítmicamente en casi todos los ciclos (Ylinen et al., 1995). 2. Las redes aisladas de interneuronas GABAérgicas parvalbúmina positivas pueden generar oscilaciones gamma, mientras que el bloqueo de las sinapsis inhibidoras altera estas oscilaciones (Whittington et al., 1995). 3. Las interneuronas parvalbúmina positivas están interconectadas a través de sinapsis químicas y eléctricas (Galarreta et al., 1999), de modo que el aumento de la

frecuencia gamma en una interneurona GABAérgicas parvalbúmina positiva inducirá el disparo rítmico en una segunda interneurona conectada (Tamas et al., 2000). 4. Las interneuronas GABAérgicas parvalbúmina positivas proyectan a la región perisomática de las neuronas piramidales, y los registros de potencial de campo e imágenes de colorante sensibles al voltaje sugieren que esta región es el origen de las fluctuaciones de voltaje de frecuencia gamma (Mann et al., 2005).

Cardin et al.(2009) expresaron selectivamente "*channelrhodopsin-2*" (ChR2) en interneuronas de parvalbúmina o neuronas piramidales en la corteza somatosensorial y luego activaron ChR2 con trenes rítmicos de destellos de luz (8-200 Hz) mientras registraban potenciales de campo. Los autores observaron que la estimulación rítmica de las interneuronas de parvalbúmina puede generar oscilaciones de potenciales de campo *in vivo* en frecuencias gamma (30–60 Hz), pero no en otras frecuencias. En otro trabajo con optogenética, Sohal et al. (2009) demostraron que la inhibición de las interneuronas GABAérgicas parvalbúmina positivas, suprimió las oscilaciones gamma mientras que otras frecuencias no se vieron afectadas.

Evidencias recientes sugieren que las interneuronas somatostatinérgicas peri-dendríticas también tendrían un rol en la generación de actividad en la banda gamma inducida por estímulos visuales (Veit et al., 2017).

Los mecanismos neuronales detrás de la actividad gamma también incluyen neuronas piramidales de descarga rítmica rápida (Cunningham et al., 2004), y neuronas piramidales de la capa V que suman potenciales de acción dendríticos en la frecuencia gamma (Larkum et al., 2001). Además, las neuronas excitadoras talamo-corticales tienen propiedades intrínsecas necesarias para generar oscilaciones gamma subumbrales (Pedroarena et al., 1997). Sin embargo, se sabe que otras regiones manifiestan actividad gamma además de la corteza y el tálamo, incluidos el hipocampo, los ganglios basales, el cerebelo y diversas áreas de la formación reticulada

mesopontina (Garcia-Rill 2017). Estas regiones modularían la actividad gamma cortical.

La actividad gamma del EEG aumenta con la activación cortical. Por ejemplo, los estímulos táctiles la aumentan en las áreas sensitivas somáticas y área asociativa parietal posterior (Bauer et al., 2006). La potencia de la banda gamma aumenta durante la actividad cognitiva, ya sea procesando información sensorial, o simplemente pensando o procesando imágenes internas (Bouyer et al., 1981; Desmedt et al., 1994; Steriade et al., 1996). Además de aumentar la "potencia" de la actividad gamma durante las funciones cognitivas, también aumenta la coherencia gamma entre diferentes áreas corticales (Cantero et al., 2004)(ver Recuadro 1).

La función de las oscilaciones gamma sigue siendo incierta. Sin embargo, se ha propuesto la sincronización gamma local como base de la integración sensorial (Singer, 2002), y el acoplamiento de las oscilaciones gamma de áreas corticales alejadas como base de la integración de procesos cognitivos (Miltner et al., 1999; Rodríguez et al., 1999; Varela et al., 2001; Cantero et al., 2004).

Recuadro 1. Potencia y coherencia

Potencia

La potencia o densidad espectral de potencia, que se calcula por medio de la transformación rápida de Fourier, es una representación de la distribución de la energía o la amplitud de una señal, en las distintas frecuencias de las que está formada. El aumento de la potencia del EEG en una frecuencia determinada refleja el grado de sincronización local del potencial extracelular a esa frecuencia (Buzsáki et al., 2012).

Coherencia espectral

La coherencia electroencefalográfica proporciona un índice objetivo de las interacciones funcionales entre diferentes regiones de la corteza cerebral. Para ser completamente coherentes dos ondas deben tener un desfasaje constante a una frecuencia determinada y la relación entre las amplitudes a esa frecuencia debe mantenerse constante. Esto implica que dos áreas corticales que coordinan su actividad eléctrica, van a presentar un aumento de la coherencia entre sus actividades eléctricas aunque la latencia debida a la distancia y/o a múltiples sinapsis determine un desfasaje temporal entre sus actividades eléctricas (Schoffelen et al., 2005). Se ha propuesto entonces, que el grado de coherencia entre el EEG de distintas cortezas registrados simultáneamente reflejaría la fuerza de las interconexiones funcionales (reentradas) que ocurren entre ellas (Edelman & Tononi, 2000; Bullock et al., 2003). La coherencia matemáticamente se obtiene de la densidad espectral cruzada, *cross spectral density* (csd) entre las dos ondas, normalizada por la potencia de la densidad espectral o *power spectral density* (psd) de cada onda. Por lo tanto, la coherencia entre dos ondas a y b, a una frecuencia determinada *f, se* obtiene de la siguiente manera:

$$\mathrm{coh}(f) = \frac{\left|\sum \mathrm{csd}_{ab}(f)\right|^2}{\sum \mathrm{psd}_a(f) \sum \mathrm{psd}_b(f)}$$

La sumatoria se aplica sobre bloques de información. Con un solo bloque, el resultado será siempre la unidad. Se necesitan al menos 10 bloques para obtener un resultado confiable (nosotros utilizamos 100).

1.3. Modelo animal

En la presente Tesis utilizamos el gato (Felis catus) como modelo animal. Este tiene ventajas experimentales comparativas tanto con estudios en seres humanos, como con otro tipo de animales de experimentación. Además de las dificultades éticas que implica el trabajo experimental en seres humanos, los registros de superficie en humanos (EEG o MEG) no permiten una clara localización espacial de la señal y el acceso a áreas corticales y subcorticales profundas. En cambio, en el gato, el EEG se puede registrar mediante electrodos superficiales de corteza (electrocorticograma) así como con electrodos profundos.

Comparado con roedores, los gatos tienen más desarrolladas las áreas de asociación, facilitando el estudio de las funciones cognitivas (Figura 4). Además, la corteza cerebral de gato ha sido ampliamente mapeada (Figura 5).

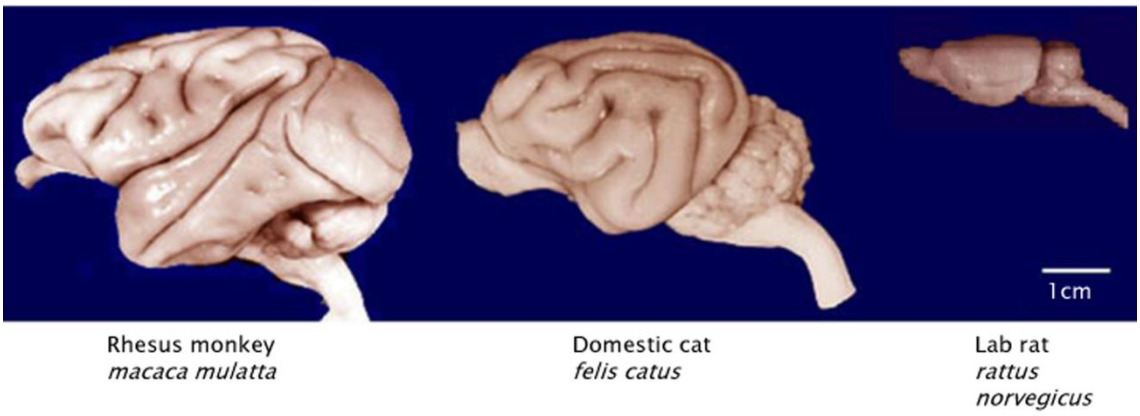

Figura 4. Cerebros de mono Rhesus, gato y rata. Se puede observar que el encéfalo del gato presenta más similitudes al del mono Rhesus, ya sea por su tamaño como por su complejidad (número de cisuras y circunvoluciones en la corteza cerebral). Tomado de la Universidad de Wisconsin (www.brainmuseum.org).

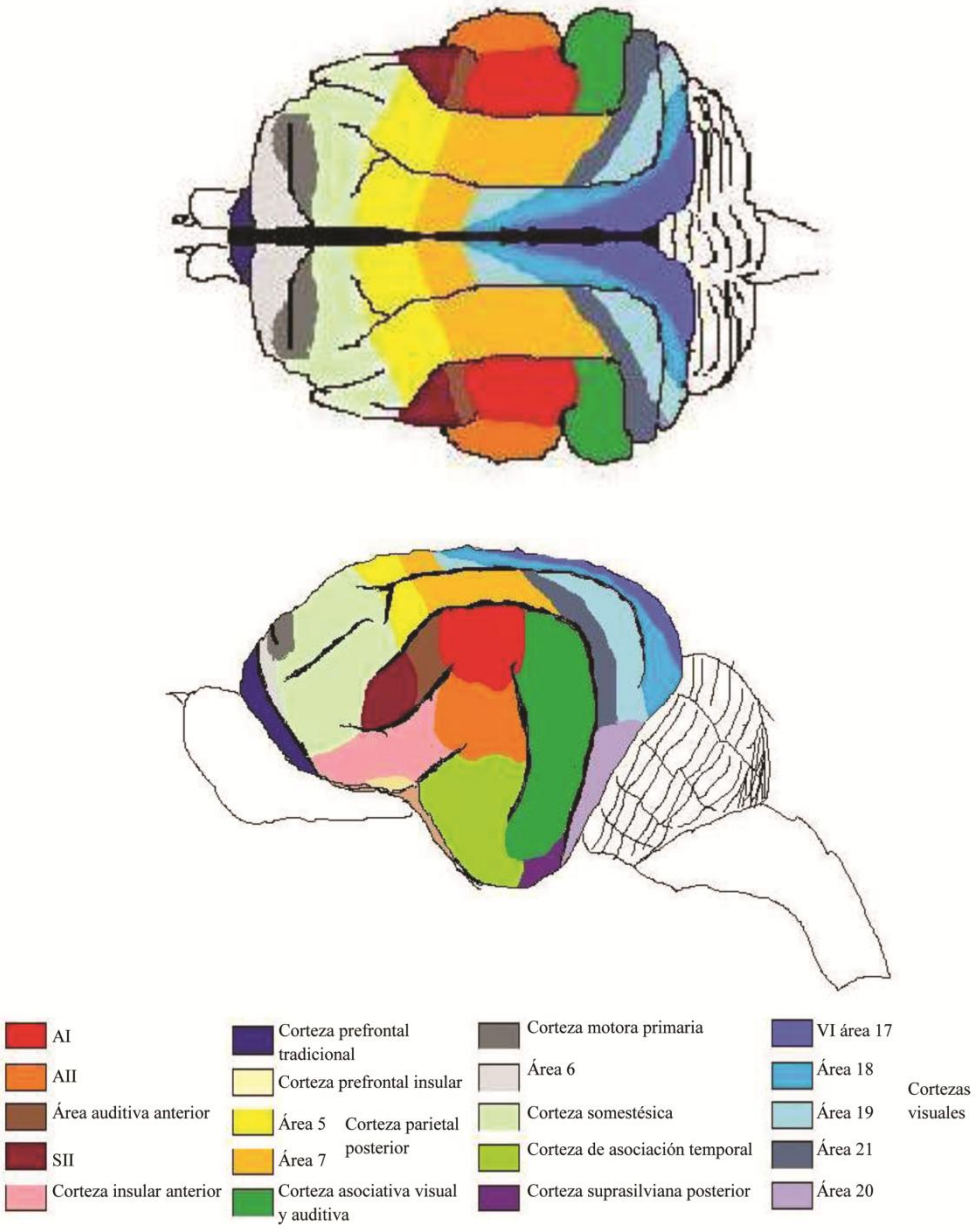

Figura 5. Mapa anátomo-funcional de la corteza cerebral del gato. Se muestra una vista superior y lateral del cerebro con las diferentes áreas corticales marcadas según el código de colores que se encuentra debajo. Este mapa fue confeccionado de acuerdo a los trabajos de Thompson et al(1963), Markowitsch & Pritzel(1977), Berman & Jones(1982) y Scannell et al(1995).

Otra ventaja de este modelo animal es que es posible observar directamente las oscilaciones en la banda gamma de frecuencias en

registros crudos de EEG sin la necesidad de realizar ningún procesamiento de los mismos (Figura 6). Los registros de EEG en humanos no permiten la observación directa de estas oscilaciones debido a que son filtradas por el cráneo y el cuero cabelludo, y porque son enmascaradas por artefactos generados por la actividad muscular (Hipp & Siegel, 2013). Los registros en roedores tampoco permiten la observación directa de las oscilaciones gamma con la misma claridad (Maloney et al., 1997).

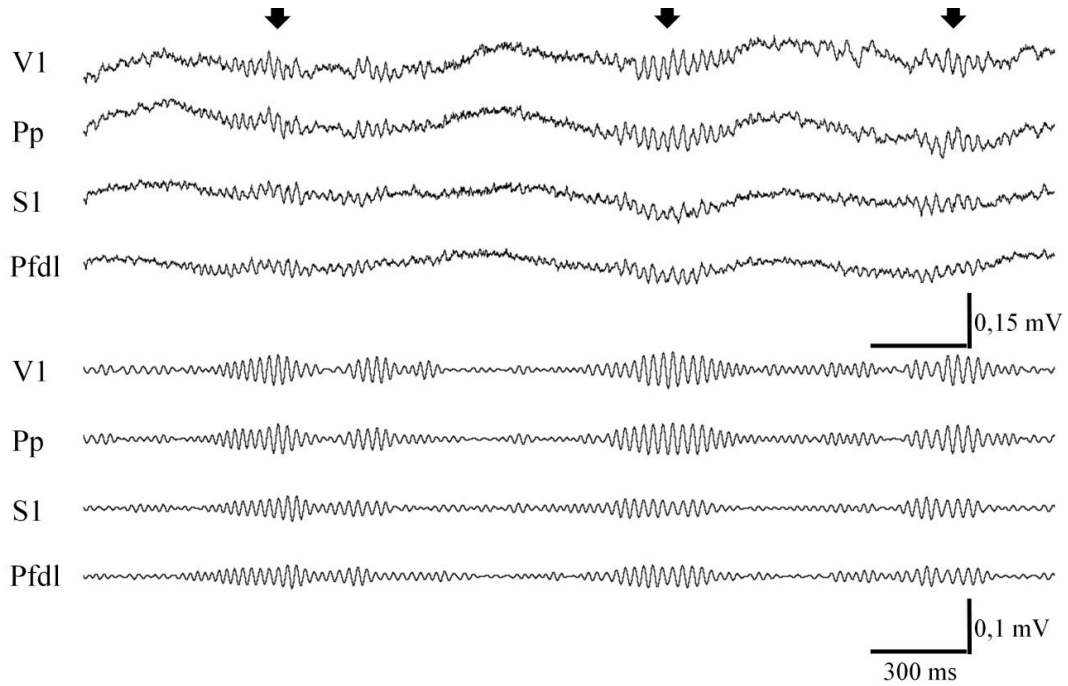

Figura 6. Oscilaciones gamma en el EEG del gato. Registros corticales simultáneos, crudos y filtrados (30-45 Hz), de las cortezas prefrontal dorsolateral (Pfdl), somatosensorial primaria (S1) parietal posterior (Pp) y visual primaria (V1) durante la vigilia alerta. Las oscilaciones gamma, que se pueden observar claramente en el registro crudo (flechas), están acopladas en las cuatro áreas corticales.

Por otra parte, el gato es un animal empleado habitualmente para el estudio del sueño, ya que posee etapas bien definidas de sueño y de duración suficiente como para realizar análisis prolongados de las distintas etapas. Es interesante destacar que lesiones en el tegmento pontino

dorsal en gatos genera sueño REM sin atonía, y libera comportamientos elaborados durante el mismo. Estos son comportamientos de alerta, saltos, predación, caza, sugiriendo que los gatos tienen experiencias oníricas similares a las humanas durante el sueño REM (Sastre & Jouvet, 1979; Morrison, 1983).

Por último, nuestro equipo de investigación tiene amplia experiencia en el uso de este animal de experimentación (Torterolo et al., 2002, 2003, 2009, 2011a, 2011b, 2015, 2016).

CAPITULO II

OSCILACIONES GAMMA DEL EEG DURANTE LA VIGILIA Y EL SUEÑO

1. Introducción

1.1. Actividad gamma durante el sueño

Las experiencias oníricas son un fenómeno asociado al sueño REM. La mayoría de individuos al ser despertados durante este estado sostienen haber estado soñando (Dement et al., 1957; Pace-Schott et al., 2005). La probabilidad de obtener reportes de experiencias oníricas despertando a individuos durante el sueño NREM es marcadamente menor. A su vez, la escasa actividad onírica que ocurre durante el sueño NREM presenta características diferentes, ya que es breve y con poca riqueza sensorial y emocional. Además, está más relacionada con la vida real y es congruente en el tiempo, espacio y personajes.

La actividad onírica durante el sueño REM se caracteriza por su riqueza y claridad sensorial, discontinuidades e incongruencias en el tiempo, espacio y personajes (distorsión de la realidad), así como falta de consciencia de estar soñando. Algunas de las características de las experiencias oníricas del sueño REM como la pérdida del control voluntario (el individuo no sabe lo que va a pasar a continuación, la atención es inestable y está dirigida en forma rígida), la violación de leyes físicas, incongruencias en el tiempo, espacio y personajes, recuerdan la disfunción de la corteza prefrontal dorsolateral (Corsi-Cabrera et al., 2003). Esto se relaciona con la evidencia de que la actividad de la corteza prefrontal medida por tomografía de emisión de positrones disminuye durante el sueño REM (Braun et al., 1997). A su vez, la actividad de las áreas

asociativas multimodales (tanto frontales como parietales) disminuye, mientras que aumenta la actividad de las áreas límbicas relacionadas con el control emocional (Braun et al., 1997).

¿Qué pasa con la coherencia de la banda de gamma de frecuencias durante el sueño? En la presente Tesis, presento evidencias que responden este interrogante estudiando la coherencia entre diferentes áreas corticales para la banda gamma de frecuencias del EEG durante la vigilia y el sueño.

La entrada colinérgica del núcleo tegmental laterodorsal y pedunculopontina al NPO es crítica para la generación del sueño REM. Se considera que la NPO ejerce un control ejecutivo sobre la iniciación y el mantenimiento del sueño REM. Las microinyecciones de carbacol, un agonista colinérgico mixto, en el núcleo pontis oralis (NPO) del gato, induce la generación de sueño REM (REM inducido por carbacol o REMc), con una latencia muy corta (hasta 30 s) con duraciones que pueden superar las 2 h. Las microinyecciones de carbacol dentro de la NPO también pueden inducir atonía muscular durante W (López-Rodríguez et al., 1994) o cataplejía, un signo patológico de narcolepsia (Guilleminault & Fromherz., 2011, Mignot., 2011, Chase., 2013, Dauvilliers et al., 2014). La cataplejía inducida por el carbacol (CA) ocurre cuando el carbacol es microinyectado durante AW (López-Rodriguez et al., 1994). Además, las alternancias entre REMc a CA son comunes, y CA puede ser inducida desde REMc por la estimulación sensorial (Torterolo et al., 2015). Por lo tanto, en este estudio también comparamos la coherencia gamma EEG durante REMc y CA, dos estados diferentes que presentan la misma actividad somato-motora (atonía muscular).

2. Hipótesis de trabajo

Dado que existen diferencias importantes en las funciones cognitivas entre la vigilia y el sueño, esperamos encontrar diferencias significativas entre la coherencia en la banda gamma de frecuencias del EEG entre

distintas áreas corticales al comparar la vigilia con las diferentes etapas de sueño.

3. Objetivos

3.1. Objetivo general

Estudiar las interacciones funcionales entre diferentes áreas corticales en la banda gamma del EEG durante la vigilia y el sueño

3.2. Objetivos específicos

Analizar el acoplamiento de las oscilaciones en la banda gamma entre distintas áreas corticales intrahemisféricas durante la vigilia y el sueño (Trabajo 1).

Estudiar el acoplamiento de las oscilaciones en la banda gamma entre distintas áreas corticales interhemisféricas durante la vigilia y el sueño (Trabajo 2).

Evaluar el acoplamiento de las oscilaciones en la banda gamma entre distintas áreas corticales durante el sueño REM y cataplejía inducidos farmacológicamente (Trabajo 3).

4. Material y métodos.

En esta sección se hará una breve reseña general de la metodología. Los detalles se expondrán en los trabajos adjuntos.

4.1. Animales de experimentación

Se utilizaron gatos adultos obtenidos de la Unidad de Reactivos y Biomodelos de Experimentación (URBE). Los animales permanecieron en jaulas individuales, con un ciclo luz-oscuridad (12-12 Hs) y temperatura controladas. Los procedimientos se llevaron a cabo de acuerdo con la Guía para el uso y cuidado de animales de laboratorio (8va edición, National Academy Press, Washington. DC 2010). A su vez, los estudios se realizaron de acuerdo a la Ley Nacional de Experimentación Animal (Nº

18.611). Los protocolos experimentales fueron aprobados por la Comisión Honoraria de Experimentación Animal (CHEA). Se realizó el mayor esfuerzo para minimizar el número de animales empleados, y se tomaron medidas para evitarles dolor, incomodidad o estrés.

4.2. Procedimientos quirúrgicos

Los procedimientos fueron similares a los utilizados previamente por nuestro grupo (Torterolo et al., 2002, 2003, 2009, 2011a, 2011b, 2015).

Los animales previamente a la anestesia, fueron tratados con xilazina (2.2 mg/Kg, i/m.), atropina (0.05 mg/Kg, i/m), antibióticos (ceftriaxona 50 mg/Kg, i/m) y analgésicos (ketoprofeno, 2 mg/Kg, s/c). La anestesia fue inducida con ketamina 15 (mg/Kg, i.m.) y mantenida con una mezcla gaseosa de isoflourano (1-3%) en oxígeno.

La cabeza del animal fue posicionada en un aparato estereotáctico y la calota fue expuesta. Se colocaron electrodos en la porción orbital del hueso frontal para el registro del EOG. Se realizaron perforaciones en el cráneo donde se colocaron macroelectrodos de acero inoxidable (1.4 mm de diámetro) en diferentes áreas corticales y subcorticales, siguiendo las coordenadas estereotácticas del atlas de Berman y Jones (1982).

A su vez, se colocó un electrodo indiferente sobre el seno frontal. Utilizando cemento acrílico se fijó en la calota un conector en el que se soldaron los electrodos implantados.

Para el Objetivo 3, realizamos una perforación en el cráneo guiados por la posición estereotáctica del NPO (Torterolo et al., 2012).

Finalizada la cirugía, se administró un analgésico c/24 hs por 48 hs (Ketoprofeno, 1mg/Kg, s.c.). Los márgenes de incisión fueron mantenidos limpios y se aplicó antibiótico tópico diariamente.

Una vez recuperados de la cirugía, los animales fueron adaptados a las condiciones experimentales, por un período de no menos de dos semanas.

4.3. Sesiones experimentales

Se realizaron registros polisomnográficos en los que se registraron simultáneamente la actividad múltiples áreas corticales con electrodos monopolares. Se utilizo un electrodo indiferente común para las estructuras registradas. Éste se ubicó en el seno frontal izquierdo. Esta ubicación es adecuada debido a que la actividad registrada es escasa; un electrodo indiferente inactivo es crítico para el análisis de coherencia (Bullock et al., 1995a; Bullock., 1997; Nunez et al., 1997; Cantero et al., 2000). También se monitorizó el EMG de los músculos de la nuca (registrado con electrodos bipolares colocados en forma aguda sobre la piel que cubre los músculos). Para obtener una serie de datos completa, cada animal fue registrado diariamente durante aproximadamente 30 días.

Los registros fueron realizados en condiciones semirestringidas. La ventaja de esta condición es que las diferencias observadas en el EEG entre los estados comportamentales se deben a diferencias genuinas, no influenciadas por posturas o movimientos, reduciendo también la posibilidad de artefactos.

Las señales bioeléctricas fueron amplificadas (1000x), filtradas (0.1-500 Hz), digitalizadas (1024 Hz, 2^{16} bits) y almacenadas en una PC utilizando el software Spike 2 (Cambridge Electronic Design).

Los datos fueron obtenidos en QW, sueño NREM y REM espontáneos. La QW fue identificada por la presencia de EEG desincronizado, con actividad en el EMG y escasa actividad en el EOG. El sueño NREM fue identificado por la presencia de ondas lentas de alta amplitud y la presencia de husos de sueño en el EEG. El sueño REM fue identificado por un EEG desincronizado con ondas PGO y atonía en el EMG.

La AW fue inducida por estímulos sonoros de 300 segundos de duración, aproximadamente 30 minutos después del inicio del registro. El estímulo sonoro consistió en clics (0.1 ms de duración) de 60 a 100 dB SPL en intensidad con una frecuencia de presentación variable (1 a 500 Hz,

modificada de una forma al azar por el operador) para así evitar la habituación.

En experimentos seleccionados, la AW fue también inducida por la presentación de una luz en movimiento o colocando un espejo en frente del animal.

Para el Objetivo 3, se realizaron microinyecciones de carbacol (0,8 µg en 0,2 µl de solución salina) unilateralmente durante un período de 1 minuto en el NPO, con una jeringa Hamilton (Torterolo et al., 2000; Torterolo et al., 2009; Torterolo et al., 2011). Las microinyecciones de carbachol se realizaron durante el sueño NREM o durante W (López-Rodriguez et al., 1994). Ocasionalmente se aplicó estimulación auditiva o somatosensorial leve a los animales para inducir CA desde un estado de REMc (ver sección de Resultados, Trabajo 3).

4.4. Análisis de datos

Los estados de sueño y vigilia fueron determinados en épocas de 10 segundos de duración.

Para analizar coherencia entre pares de canales de EEG se examinaron 12 periodos de 100 segundos libres de artefactos para cada estado comportamental (1200 segundos por estado comportamental). Los datos fueron obtenidos en 4 sesiones de registro; de cada sesión de registro se obtuvieron 3 ventanas de análisis para cada estado comportamental.

En cada periodo de 100 segundos fue analizada la coherencia (Magnitude Squared Coherence) utilizando el algoritmo matemático descripto en el recuadro 1. Este algoritmo matemático fue descripto por Bullock & McClune (1989) y validado por varios autores (Bouyer et al., 1981; Bullock & McClune, 1989; Bullock et al., 1995b; Achermann & Borbely, 1998a, b; Cantero et al., 2004).

Para obtener los valores de coherencia se utilizó el *script* de Spike 2 COHER 1S (Cambridge Electronic Design). Este algoritmo divide el

periodo de tiempo (ventana de 100 segundos analizado en 100 bloques para una frecuencia de muestreo de 1024 Hz), con un tamaño de bin de 2048 muestras y una resolución de frecuencias de 0.5 Hz.

En experimentos preliminares, establecimos que el valor de coherencia entre un registro cortical y el EMG (del músculo de la nuca, masetero o temporal), EOG o ECG fue de 0.1 o menor. Por lo tanto, valores menores o iguales a 0.1 indican ausencia de coherencia entre las cortezas analizadas.

Aplicamos la transformación z´ de Fisher a los valores de coherencia para normalizar nuestros datos y analizarlos por medio de test estadísticos paramétricos.

Se analizaron los perfiles de coherencia z´ para épocas de 100 segundos para cada par de registros corticales, así como el promedio de las 12 épocas. Los valores de coherencia z´ fueron promediados para cada estado, para cada gato independientemente, y fue expresado como media ± error estándar. La significancia de las diferencias entre los diferentes estados comportamentales se evaluó por medio del test ANOVA y el *post hoc* de Tamhane. El criterio utilizado para descartar la hipótesis nula fue $p < 0.05$.

Registros seleccionados fueron filtrados (pasa banda 30 - 45 Hz) utilizando filtros digitales de tipo (“*finite impulse response*") del Spike 2.

La amplitud de los pares de registros simultáneos filtrados fue analizada por medio de la correlación de Pearson. Por último, la estructura de las ondas y la correlación entre ellas fueron analizadas mediante las funciones de autocorrelación y correlación cruzada, respectivamente.

5. Resultados

5.1. Trabajo 1. Las oscilaciones neocorticales coherentes de 40 Hz no están presentes durante el sueño REM.

Durante los procesos cognitivos hay una gran interacción entre varias regiones de la corteza cerebral. Se ha postulado que las oscilaciones en la banda gamma de frecuencias (≈ 40 Hz) del EEG, son producto de esta interacción. Estas están involucradas en la integración de eventos neuronales espacialmente separados, pero temporalmente correlacionados, lo que da como resultado una experiencia perceptual unificada. El alcance de estas interacciones puede examinarse mediante un algoritmo matemático llamado "coherencia", que refleja la "fuerza" de las interacciones funcionales entre áreas corticales. El presente estudio se realizó para analizar la coherencia del EEG en la banda gamma de frecuencias del gato durante la AW, QW, NREM y el sueño REM.

Los gatos fueron implantados con electrodos en las cortezas frontal, parietal y occipital para controlar la actividad de EEG. Se analizaron los valores de coherencia dentro de la frecuencia gamma (30-45 Hz y 60-100 Hz) de los pares de registros de EEG.

Se observó un gran aumento en la coherencia entre todas las regiones corticales en la frecuencia gamma durante AW en comparación con los otros estados conductuales. A medida que el animal pasó de AW a QW, y de QW a NREM, la coherencia disminuyó a un nivel moderado. Sorprendentemente, prácticamente no hubo coherencia en la banda gamma del EEG durante el sueño REM.

Llegamos a la conclusión de que las interacciones funcionales entre las áreas corticales son radicalmente diferentes durante el sueño y la vigilia. La virtual ausencia de coherencia gamma durante el sueño REM puede ser la base del procesamiento cognitivo único que ocurre durante las experiencias oníricas, que son principalmente un fenómeno relacionado al sueño REM.

EJN fens EUROPEAN JOURNAL OF NEUROSCIENCE

European Journal of Neuroscience, pp. 1–10, 2013 doi:10.1111/ejn.12143

Coherent neocortical 40-Hz oscillations are not present during REM sleep

Santiago Castro,[1] Atilio Falconi,[1] Michael H. Chase[2,3] and Pablo Torterolo[1]
[1]Department of Physiology, School of Medicine, Universidad de la República, General Flores 2125, 11800, Montevideo, Uruguay
[2]WebSciences International, Los Angeles, CA, USA
[3]UCLA School of Medicine, Los Angeles, CA, USA

Keywords: cat, consciousness, cortex, EEG, synchronisation

Abstract

During cognitive processes there are extensive interactions between various regions of the cerebral cortex. Oscillations in the gamma frequency band (≈40 Hz) of the electroencephalogram (EEG) are involved in the binding of spatially separated but temporally correlated neural events, which results in a unified perceptual experience. The extent of these interactions can be examined by means of a mathematical algorithm called 'coherence', which reflects the 'strength' of functional interactions between cortical areas. The present study was conducted to analyse EEG coherence in the gamma frequency band of the cat during alert wakefulness (AW), quiet wakefulness (QW), non-rapid eye movement (NREM) sleep and rapid eye movement (REM) sleep. Cats were implanted with electrodes in the frontal, parietal and occipital cortices to monitor EEG activity. Coherence values within the gamma frequency (30–100 Hz) from pairs of EEG recordings were analysed. A large increase in coherence occurred between all cortical regions in the 30–45 Hz frequency band during AW compared with the other behavioral states. As the animal transitioned from AW to QW and from QW to NREM sleep, coherence decreased to a moderate level. Remarkably, there was practically no EEG coherence in the entire gamma band spectrum (30–100 Hz) during REM sleep. We conclude that functional interactions between cortical areas are radically different during sleep compared with wakefulness. The virtual absence of gamma frequency coherence during REM sleep may underlie the unique cognitive processing that occurs during dreams, which is principally a REM sleep-related phenomenon.

Introduction

The brain integrates fragmentary neural events that occur at different times and locations into a unified perceptual experience. Understanding the mechanisms that are responsible for this integration, 'the binding problem', is one of the most important challenges that cognitive neuroscience has to solve (von der Malsburg, 1995; Velik, 2009).

Electroencephalographic oscillations in the gamma frequency band (≈ 40 Hz) are involved in the integration or binding of spatially separated, but temporally correlated, neural events; recent studies based on magnetoencephalography and electrocorticography have also reported that gamma band oscillations between 60 and 200 Hz may also play a role in this process (Uhlhaas *et al.*, 2011).

An increase in gamma power typically appears during states/behaviors that are characterised by the active cognitive processing of external percepts or internally generated thoughts and images (Uhlhaas *et al.*, 2009, 2011; Rieder *et al.*, 2010). Gamma activity has been observed during attentive wakefulness not only in humans, but also in animals (Bouyer *et al.*, 1981; Llinas & Ribary, 1993; Tiitinen *et al.*, 1993; Steriade *et al.*, 1996; Maloney *et al.*, 1997). Gamma-band rhythmogenesis is inextricably tied to perisomatic inhibition wherein the key ingredient is $GABA_A$-receptor-mediated inhibition (Buzsaki & Wang, 2012).

The degree of EEG coherence between two cortical regions is believed to reflect the strength of the functional interconnections (re-entries) that occur between them (Edelman & Tononi, 2000; Bullock *et al.*, 2003). Recently, Siegel *et al.* (2012) have proposed that frequency-specific correlated oscillations in distributed cortical networks provide indices, or 'fingerprints', of the network interactions that underlie cognitive processes; measures of the association between brain areas based on such frequency-specific signals are likely to provide more detailed information than corresponding measures based on broadband electrophysiological signals or blood oxygen level-dependent functional magnetic resonance imaging (BOLD-fMRI) signals (Siegel *et al.*, 2012).

Coherent EEG activity in the gamma frequency band increases during different behaviors and cognitive functions in both animals and humans (Bouyer *et al.*, 1981; Bressler *et al.*, 1993; Harle *et al.*, 2004). In addition, gamma activity and gamma coherence between different brain areas have been viewed as a possible neural correlate of consciousness (Llinas *et al.*, 1998). In this regard, coherence in

Correspondence: Dr P. Torterolo, as above.
E-mail: ptortero@fmed.edu.uy

Received 12 March 2012, revised 19 December 2012, accepted 29 December 2012

the gamma frequency band is lost during narcosis (unconsciousness) induced by anesthesia (John, 2002; Mashour, 2006).

Cognitive activities not only occur during wakefulness. Dreams, which occur more prominently during REM sleep, are considered a special kind of cognitive activity or proto-consciousness (Hobson, 2009). REM sleep dreams are characterised by their vividness, single-mindedness, bizarreness and loss of voluntary control over the plot. Attention is unstable and rigidly focused, facts and reality are not checked, violation of physical laws and bizarreness are passively accepted, contextual congruence is distorted and time is altered (Rechtschaffen, 1978; Hobson, 2009; Nir & Tononi, 2010). Interestingly, some authors have suggested that cognition during REM sleep mimics frontal lobe dysfunction (Corsi-Cabrera *et al.*, 2003). In contrast, during deep non-REM (NREM) sleep there is an absence of, or at least a strong reduction in, cognitive functions (Hobson, 2009).

What occurs with respect to coherence in the gamma frequency band during sleep? In a pioneering study utilising magnetoencephalographic recordings, Llinas & Ribary (1993) found that during REM sleep in humans, as in wakefulness, there is large widespread 40-Hz coherent activity that is characterised by a fronto-occipital phase shift over the brain (Llinas & Ribary, 1993); however, recent studies have challenged these results (see Discussion). In the present report, we answered the preceding question by studing gamma band coherence among different cortical areas during natural sleep and wakefulness in the cat. Preliminary data have been presented in abstract form (Castro *et al.*, 2010, 2011).

Material and methods

Experimental animals

Four adult cats were used in this study. The animals were obtained from, and determined to be in good health by, the Institutional Animal Care Facility. All of the experimental procedures were conducted in accord with the *Guide for the Care and Use of Laboratory Animals* (8th edition, National Academy Press, Washington DC, 2010) and approved by the Institutional Animal Care Commission (protocol no. 71140-1235-09, School of Medicine, Universidad de la República). All efforts were made to use the minimal number of animals necessary to produce reliable scientific data.

Surgical procedures

Surgical procedures that were employed were similar to those used in previous studies (Torterolo *et al.*, 2002, 2009, 2011b). Accordingly, the animals were chronically implanted with electrodes to monitor the states of sleep and wakefulness. Prior to being anesthetised, each cat was premedicated with xylazine (2.2 mg/kg, i.m.), atropine (0.04 mg/kg, i.m.) and antibiotics (Tribrissen®, 30 mg/kg, i.m.). Anesthesia, which was initially induced with ketamine (15 mg/kg, i.m.), was maintained with a gas mixture of isoflourane in oxygen (1–3%). The head was positioned in a stereotaxic frame and the skull was exposed. In order to record the EEG, stainless steel screw electrodes (1.4 mm diameter) were placed on the surface (above the dura matter) of prefrontal and sensory cortical regions (Fig. 1). To reduce volume conduction, the inter-electrode distance was at least 6 mm (between posterior-parietal and auditory primary cortices); the greatest was 22 mm (between prefrontal and visual primary cortices).

The electrodes were connected to a Winchester plug, which together with two plastic tubes (which were used to maintain the animal's head fixed without pain or pressure) were bonded to the skull with acrylic cement.

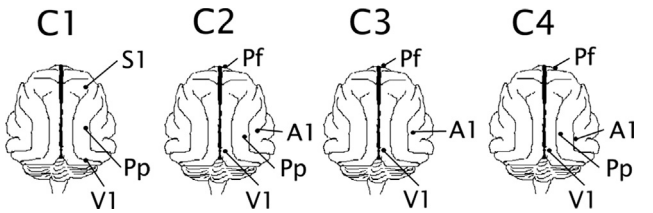

FIG. 1. Position of recording electrodes. The figure depicts the position of the recording electrodes on the surface of the primary sensory, association sensory and prefrontal cerebral cortices. Recordings from these electrodes were referred to a common inactive electrode, which was located over the frontal sinus. The electrodes were located in accordance with previous reports (Thompson *et al.*, 1963; Markowitsch & Pritzel, 1977; Berman & Jones, 1982; Scannell *et al.*, 1995). C1–C4, individual animals. A1, auditory primary cortex; Pf, prefrontal cortex; Pp, posterior-parietal cortex; S1, somato-sensory primary cortex; V1, visual primary cortex.

At the end of these surgical procedures an analgesic (Buprenex®, 0.01 mg/kg, i.m.) was administered. Incision margins were kept clean and a topical antibiotic was administered on a daily basis. After the animals had recovered from the preceding surgical procedures, they were adapted to the recording environment for a period of at least 2 weeks.

Experimental sessions

Experimental sessions of 4 h in duration were conducted between 11:00 and 15:00 in a temperature-controlled environment (21–23 °C). All animals had free access to water and food until 1 h prior to the beginning of each recording session. During these sessions (as well as during adaptation sessions), the animal's head was held in a stereotaxic position by four steel bars that were placed into the plastic tubes while the body rested in a sleeping bag (semirestricted condition).

The activity of three cortical areas, from the same cerebral hemisphere, was recorded simultaneously with monopolar electrodes. A common electrode reference montage was employed. The reference electrode was placed in the left frontal sinus; this location is excellent for a common inactive reference electrode, which is critical for the analysis of coherence (Bullock *et al.*, 1995a; Bullock, 1997; Nunez *et al.*, 1997; Cantero *et al.*, 2000). The electromyogram (EMG, of the nuchal muscle which was recorded by means of acutely placed bipolar electrodes) was also monitored. The EMG of the gastrocnemious and temporal muscles, as well as electrocardiogram and electrooculogram (EOG), (via acutely placed electrodes on the sides of the eyes' orbits) were also recorded in control experiments. Each cat was recorded daily for a period of approximately 30 days in order to obtain complete data sets.

Bioelectric signals were amplified (× 1000), filtered (0.1–100 Hz), sampled (512 Hz, 2^{16} bits) and stored in a PC using Spike 2 software (Cambridge Electronic Design, Cambridge, UK). To discard artifacts in coherence analysis due to digitisation of the raw recordings, control experiments were also performed with different combinations of filters (500 Hz highpass filters, with and without a 50-Hz notch filter) as well as with sampling rates of 1024 Hz. No differences were observed in the data obtained in these experiments compared with the data presented in the Results.

Data were obtained during spontaneously occurring QW, REM sleep and NREM sleep. The presence of a desynchronised EEG and a high level of EMG activity were used to identify wakefulness. NREM sleep was determined by the occurrence of high-amplitude

slow waves (0.5–4 Hz) and sleep 'spindles' (9–14 Hz) in the EEG, while REM sleep was identified by a desynchronised EEG with ponto-geniculo-occipital waves and atonia (Ursin & Sterman, 1981).

AW was induced for a period of 300 s by a sound stimulus, which was introduced approximately 30 min after the beginning of the recording. The sound stimulus consisted of clicks (0.1 ms in duration) of 60–100 dB SPL in intensity with a variable frequency of presentation (1–500 Hz, modified at random by the operator) in order to avoid habituation (Torterolo *et al.*, 2003, 2011a). In selected experiments, AW was also induced either by the presentation of a moving light or by placing a mirror in front of the cat. Because the state of alertness always outlasted the duration of the stimulus, a waking state was considered as QW when there was a relatively low EMG and EOG activity several minutes after stimulation.

Data analysis

Sleep and waking states were determined for 10-s epochs. To analyse coherence between pairs of EEG channels, 12 artifact-free periods of 100 s were examined during each behavioral state (1200 s for each behavioral state). For each pair of recordings, data were obtained during four recording sessions.

For each 100-s period, the magnitude squared coherence was analysed as follows – $coh_{ab}(f) = [\sum csd_{ab}(f)]^2/[\sum psd_a(f) \sum psd_b(f)]$, where psd is the power spectral density, and a and b are the waves that were analysed. csd, which is the cross spectra density or the Fourier analysis of the cross covariance function, provides a reflection of how common activity between two processes is distributed across frequencies. Coherence between two waveforms is a function of frequency and ranges from 0 for totally incoherent waveforms to 1 for maximal coherence. In order for two waveforms to be completely coherent at a particular frequency over a given time range, the phase shift between the waveforms must be constant and the amplitudes of the waves must have a constant ratio. This mathematical approach was described in detail by Bullock & McClune (1989) and has been validated by several investigators (Bouyer *et al.*, 1981; Bullock & McClune, 1989; Bullock *et al.*, 1995b; Achermann & Borbely, 1998a,b; Cantero *et al.*, 2004).

Magnitude squared coherence was measured using the Spike 2 script COHER 1S (Cambridge Electronic Design). With this algorithm we analysed the coherence between two EEG channels that were recorded simultaneously during 100-s periods. This period of analysis was divided into 100 time-blocks for a sample rate of 512 Hz, with a bin size of 1024 samples and a resolution of 0.5 Hz.

In pilot recordings and analyses, we determined that the level of coherence between cortical leads and EMG recordings (neck, gastrocnemious or temporal), the electrocardiogram or the EOG, was approximately 0.1 (Fig. S1).

In this report, we concentrated on examining the coherence of the EEG in the gamma frequency band (30–45 Hz), as originally described by Jasper & Andrews (1938); this narrow band corresponds to the 40-Hz cognitive rhythm introduced by Das & Gastaut (1955). We chose this narrow band of the gamma spectrum for analysis because in preliminary studies we observed that when an animal is alerted by different means, there is a noticeable peak in coherence in this frequency (see Fig. 6). Although some data suggest a role in cognitive functions of higher gamma (60–100 Hz) oscillations, the mechanisms and functions are not clear (Uhlhaas *et al.*, 2011). Nevertheless, we also examined 60–100 Hz oscillations with the aim of determining if some of the observed phenomena extend to higher frequencies.

To normalise the data and evaluate them by means of parametric statistical tests, we applied the Fisher z′ transform to the gamma coherence values. Thereafter, the profile of the z′-coherence of the gamma band in 100-s epochs for each pair of EEG recordings, as well as the average of 12 epochs, was analysed; the results were presented in graphic form (see Figs 6–8). The z′-coherence of the gamma band for each pair of EEG channels, which was also averaged across behavioral states independently for each cat, was expressed as the mean ± standard error. The significance of the differences among behavioral states was evaluated with ANOVA and Tamhane *post-hoc* tests. The criterion used to reject the null hypotheses was $P < 0.05$.

Selected recordings were filtered (band pass 35–45 Hz) using Spike 2 digital finite impulse response filters. The amplitude of simultaneously recorded pairs of filtered EEG signals was also analysed by means of the Pearson correlation. Autocorrelations and cross-correlation functions were also performed.

Results

Raw and filtered (30–45 Hz) EEG recordings during AW and REM sleep

The EEG fluctuates from a desynchronised pattern of activity during wakefulness and REM sleep to synchronised activity during NREM sleep. Although EEG activity during wakefulness and REM sleep is similar, there are subtle but striking differences. Representative EEG recordings (prefrontal and posterior parietal leads) are shown in Figs 2 and 3. 'Bursts' of 35–40 Hz oscillations can be readily observed in raw recordings during AW (Fig. 2); in contrast, these electrographic events are difficult to find during REM sleep (Fig. 3). These oscillations were unmasked after digital filtering of the recordings to include only 30–45 Hz activity (Figs 2 and 3). During AW, the 'bursts' of gamma oscillations exhibited spindle morphology with an amplitude and duration of approximately 25 μV and 200–500 ms, respectively. These gamma oscillations during AW, which are clearly observed in the autocorrelation histogram, are accompanied by high values of gamma band power (Fig. 4). In contrast, during REM sleep the amplitude and duration of these events are drastically reduced (Figs 3 and 4).

A strong coupling of EEG signals recorded in different cortical sites was present during AW, but not during REM sleep (Figs 2–4). This high level of coupling between EEG oscillations can be observed in filtered recordings. Coupling is highlighted when the amplitudes of the signals between pairs of simultaneous EEG recordings are correlated. During AW, there was a high correlation between both EEG signals, which was absent during REM sleep (Figs 2–4).

A visual form to represent the increase in gamma power as well as the coupling among different cortices during AW is shown in Fig. 5. Compared with AW, during REM sleep, gamma power was reduced and coupling was not present. However, note that gamma band power during REM sleep is similar to QW and larger than NREM sleep.

Coherent 30–45 Hz activity is present during wakefulness but not during REM sleep

In spite of the fact that EEG coupling was not present during REM sleep when analysed by filtered recordings and correlation methods, we applied the 'coherence' algorithm for an in-depth analysis of different pairs of EEG signals that were simultaneously recorded during wakefulness and sleep.

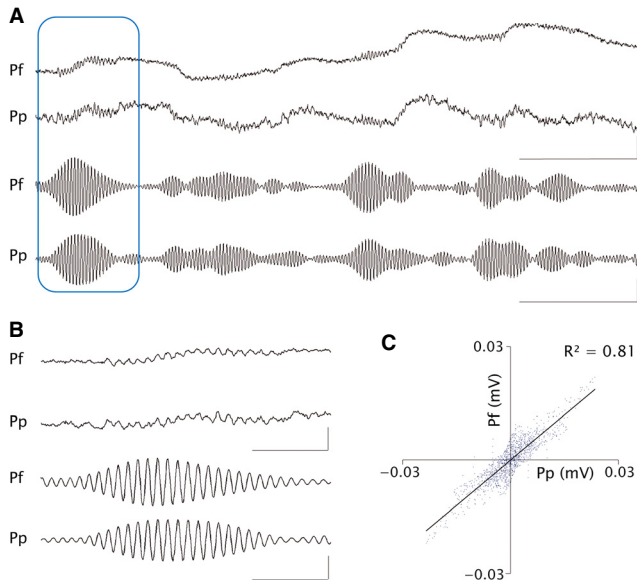

FIG. 2. Gamma oscillations during alert wakefulness. (A) Simultaneous raw and filtered (35–40 Hz) cortical recordings from the prefrontal (Pf) and posterior-parietal cortices (Pp) during alert wakefulness. Gamma oscillations, which are readily observed in the raw recordings, are highlighted after filtering. Scale bars – 1 s and 200 μV for raw recordings and 20 μV for filtered recordings. (B) Gamma oscillations enclosed in A are presented with a longer calibration time. Scale bars – 0.2 s, voltage calibration as in A. (C) Regression and correlation coefficient between the amplitudes of Pf and Pp were analysed from representative filtered recordings during 6 s of alert wakefulness. Regression line equation – $y = 0.8x + 2^{-5}$.

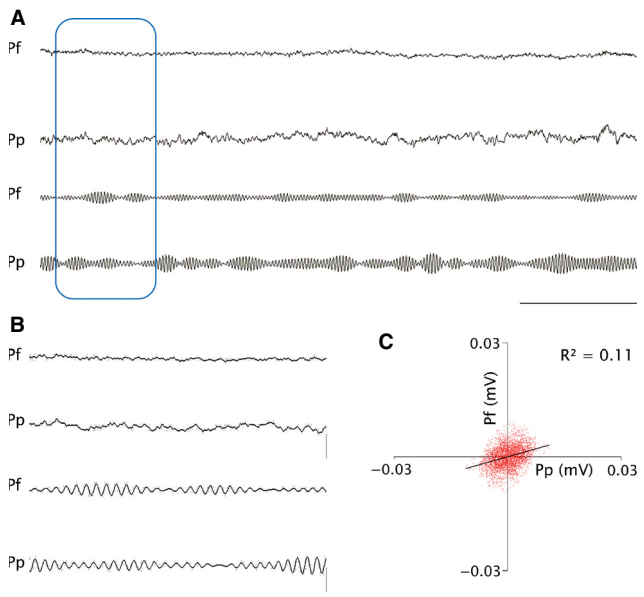

FIG. 3. Gamma oscillations during REM sleep. (A) Simultaneous raw and filtered (35–40 Hz) cortical recordings from the prefrontal (Pf) and posterior-parietal cortices (Pp) during REM sleep. The amplitude and duration of gamma oscillations decreased compared with alert wakefulness (see Fig. 2). Scale bars – 1 s and 200 μV for raw recordings and 20 μV for filtered recordings. (B) Gamma oscillations enclosed in A are shown with a longer calibration time. Scale bars – 0.2 s, voltage calibration as in A. (C) Regression and correlation coefficient between the amplitudes of Pf and Pp were analysed from representative filtered recordings during 6 s of REM sleep. Regression line equation – $y = 0.28x + 2^{-6}$.

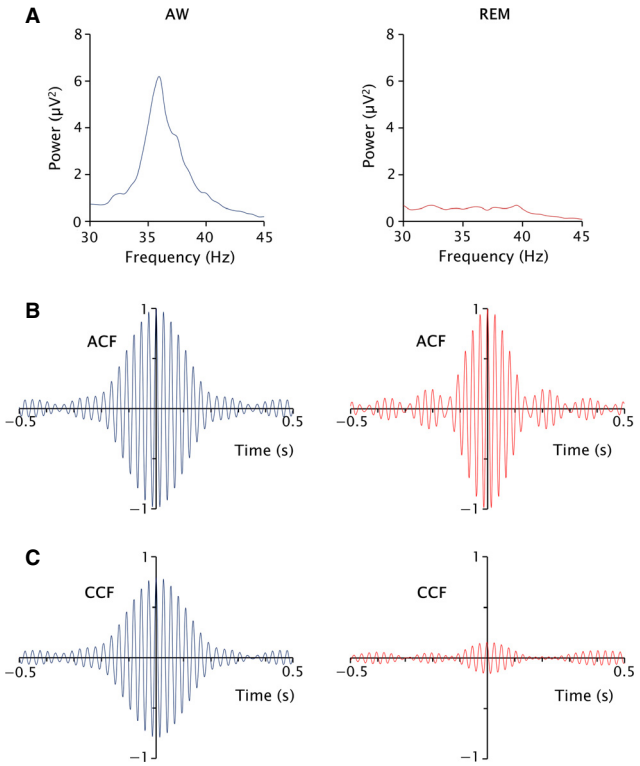

FIG. 4. Gamma oscillations during alert wakefulness (AW) and REM sleep. (A) Gamma band power during AW (left) and REM sleep (right), of the EEG recorded from the prefrontal cortex (100-s window). (B) Autocorrelation function (ACF) from filtered (35–40 Hz) 300-s EEG recordings from the prefrontal cortex during AW (left) and REM sleep (right). (C) Cross-correlation function (CCF) from filtered (35–40 Hz) 300 s of simultaneous EEG recordings from the prefrontal cortex and posterior parietal cortex during AW (left) and REM sleep (right).

In pilot studies we analysed the EEG coherence from 0.5 up to 100 Hz (Fig. 6). It is readily observed that when an animal is alerted by different means, there is a clear increase in coherence between 30 and 45 Hz, with a narrow peak between 35 and 40 Hz; hence, this band was selected for further analysis.

z′-Coherence profiles for representative pairs of EEG leads are shown in Fig. 7; the profile of 12 100-s periods and their average for each behavioral state are shown. It is readily observed that z′-coherence profiles for all of the 100-s periods, as well as the average, were larger during AW, with a restricted peak at 35–40 Hz. The z′-coherence decreased during QW and NREM sleep, and was virtually absent during REM sleep.

Examples of the averaged gamma (30–45 Hz) band z′-coherence profiles for different combination of EEG recordings are shown in Fig. 8. For these cortical combinations, the z′-coherence was larger during AW and was drastically reduced during REM sleep. Note that in Fig. 8A, the results of three different procedures for the induction of AW (sound, moving light or exposure to a mirror) were included; the results of these procedures were similar. During AW, the z′-coherence peak reached values up to 2.1, which corresponds to a coherence of 0.97.

The averaged z′-coherence in the 35–40 Hz band across behavioral states for all combinations of cortical recordings is presented in Table 1. In these 15 independent analyses, the results were consistent. During AW, there was a significant increase in z′-coherence in most of the combinations, while during REM sleep there was a significant decrease in this parameter. During QW and NREM sleep,

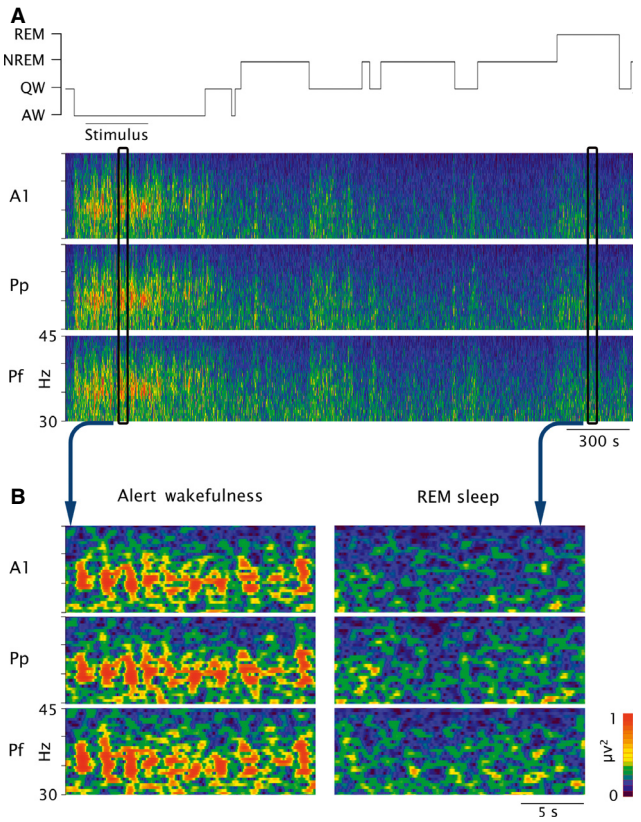

FIG. 5. Gamma band power during alert wakefulness and REM sleep. (A) Hypnogram and simultaneous gamma power spectrogram from EEG recordings of the primary auditory (A1), posterior parietal (Pp) and prefrontal cortices (Pf). During alert wakefulness, gamma power values are larger and more coupled between the recorded cortices than during other behavioral states. A bar under the hypnogram indicates the time of sound stimulation. (B) Twenty-second windows of alert wakefulness and REM sleep. The dynamic of gamma power during alert wakefulness was very similar in the cortices that were simultaneously recorded; this fact was not evident during REM sleep.

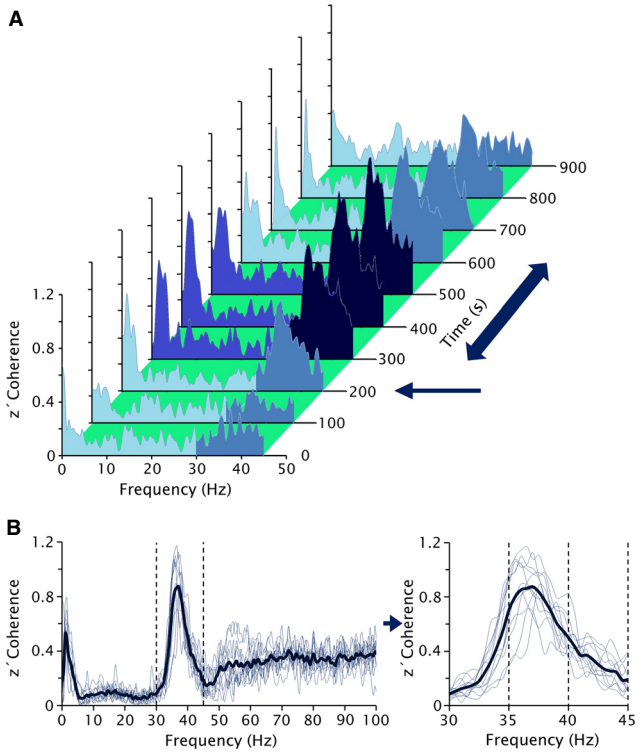

FIG. 6. Profile of EEG coherence during wakefulness. (A) z′-Coherence spectra (0–45 Hz) between the EEG recorded from prefrontal and posterior parietal cortices (1000 s in 100-s epochs). The thin arrow indicates the moment when the experimenter entered the recording room; the thick double-headed arrow indicates the time when sound stimulation was applied. When the animal was alerted by a novel stimulus, there was a clear peak in gamma (30–45 Hz) coherence. The increase in gamma coherence outlasted the sound stimulation. (B) Twelve z′-coherence profiles (thin lines), from a representative pair of recordings (prefrontal and posterior-parietal cortices) during alert wakefulness. The average of these profiles (thick line) is also shown. The profiles were constructed from periods of 100 s, during sound stimulation, with a resolution of 0.5 Hz. The coherence for the gamma band (30–45 Hz) is highlighted to the right.

z′-coherence values were intermediate, and in several combinations they were larger during QW than during NREM sleep. Differences in the extent of coherence between different recording pairs during the same behavioral state could be related to either the distance between the electrodes and/or the degree of reciprocal connections between them (Cantero *et al.*, 2000).

The z′-coherence, normalised to AW values, highlights the differences between wakefulness and REM sleep (Fig. 9). Depending on the pair of cortical areas analysed, z′-coherence during REM sleep ranged from 60 to 2.6% of the AW values.

Coherence in high (60–100 Hz) gamma band during sleep and wakefulness

Figure 6B shows EEG coherence from 0.5 to 100 Hz during AW. A coherence peak in the 30–45 Hz band occurs during AW; this phenomenon is not observed at higher frequencies.

The dynamic evolution of EEG coherence in high gamma during wakefulness and sleep is shown in Fig. 10. While changes in z′-coherence during AW, QW and NREM sleep were subtle, z′-coherence was drastically reduced during REM sleep (Fig. 10). As shown in Table 2, a significant decrease in z′-coherence during REM sleep occurred in all cortical combinations that were analysed.

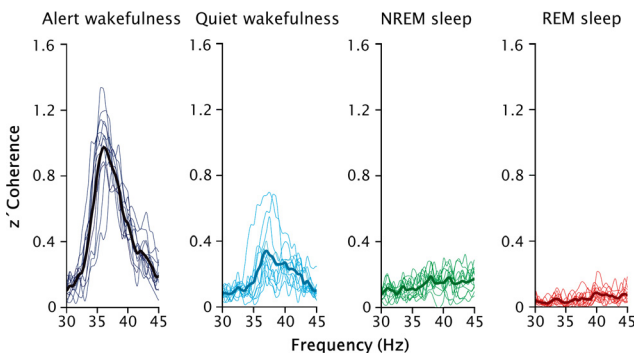

FIG. 7. Profile of EEG gamma (30–45 Hz) coherence during wakefulness and sleep. Twelve profiles of z′-coherences (thin lines) of a representative pair of recordings (prefrontal and posterior-parietal cortices) as well as the averages of these 12 profiles (thick lines) are shown for alert and quiet wakefulness, NREM and REM sleep. The profiles were constructed from periods of 100 s with a resolution of 0.5 Hz. Gamma coherence was maximal during alert wakefulness and practically absent during REM sleep.

Figure 10C presents 60–100 Hz power spectrum profiles from representative 100-s time epochs. In comparison to AW or QW, high gamma power is reduced during NREM sleep. Note that even

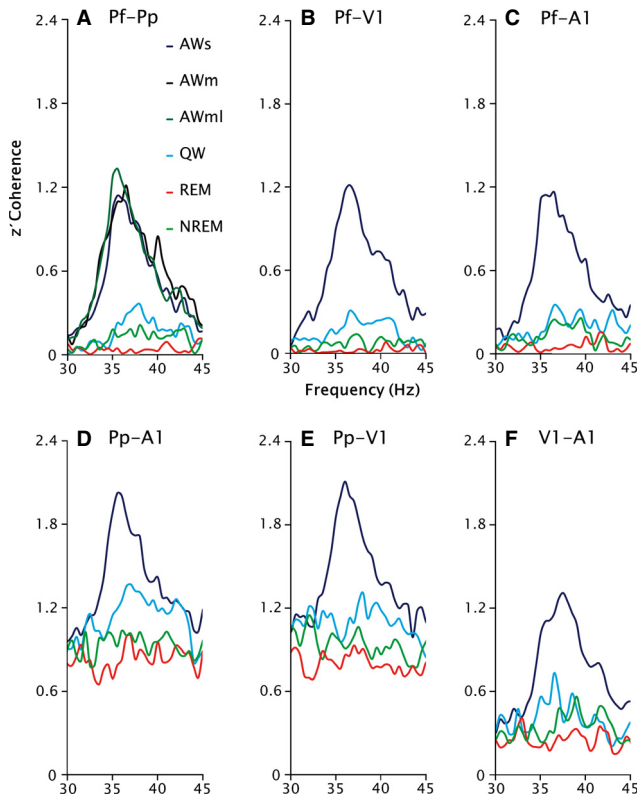

FIG. 8. Gamma band z′-coherence profiles from representative prefrontal-perceptual and perceptual regions during sleep and wakefulness. Graphics at the top (A–C) show z′-coherence between prefrontal and perceptual cortices. At the bottom (D–F), z′-coherences profiles between perceptual cortices are shown. In A, three types of stimuli produced alert wakefulness – sound (AWs), mirror (AWm) and moving light (AWml). In B–F, alertness was produced only by sound stimulation. For all combinations of recordings, z′-coherence in the gamma band was larger during AW than during REM sleep. QW, quiet wakefulness; NREM, non-REM sleep; REM, REM sleep; A1, auditory cortex; Pf, prefrontal cortex; Pp, posterior-parietal cortex; V1, visual primary cortex.

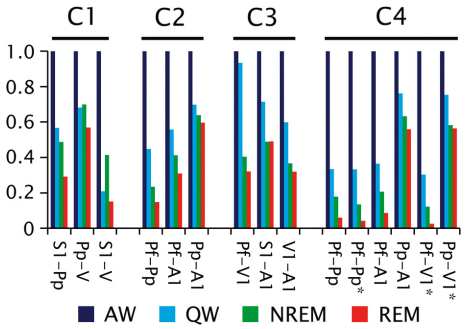

FIG. 9. Gamma band (35–40 Hz) z′-coherence for all analysed cortical combinations. The data from Table 1 were normalised to the values obtained during alert wakefulness. C1–C4, individual animals. A1, auditory cortex; Pf, prefrontal cortex; Pp, posterior-parietal cortex; S1, somato-sensory primary cortex; V1, visual primary cortex. In the derivatives indicated by an asterisk, AW was produced by light stimulation. AW, alert wakefulness; QW, quiet wakefulness; NREM, non-REM sleep; REM, REM sleep.

though high gamma coherence is reduced during REM sleep (Fig. 10A), high gamma power is similar than waking levels.

Discussion

In the present study, we demonstrated that the EEG intra-hemispheric coherence in the gamma (30–45 Hz) frequency band is larger during AW than during QW. In addition, gamma coherence decreased to a lower level during NREM sleep, and was absent during REM sleep; the lack of coherence during REM sleep also extended to high gamma (60–100 Hz) band frequencies. Therefore, during REM sleep, the coupling of high-frequency neuronal activity among different cortical regions is practically non-existent.

Animal model

We used the cat as an animal model because it has well-defined, consolidated sleep and waking states. In addition, there are data

TABLE 1. Gamma (35–40 Hz) z'-coherence values during sleep and wakefulness

Animal	Derivates	AW	QW	NREM	REM	Statistical significance	*F*
C1	S1-Pp	1.09 ± 0.05	0.62 ± 0.06	0.53 ± 0.04	0.32 ± 0.01	AW vs. all‡; REM vs. QW and NREM†	54
	Pp-V1	1.31 ± 0.06	0.89 ± 0.06	0.92 ± 0.06	0.75 ± 0.06	AW vs. all‡; REM vs. QW and NREM†	46
	S1-V1	0.70 ± 0.05	0.15 ± 0.01	0.29 ± 0.04	0.11 ± 0.01	AW vs. all‡; REM vs. NREM†; NREM vs. QW†	54
C2	Pf-Pp	0.67 ± 0.02	0.30 ± 0.04	0.16 ± 0.01	0.10 ± 0.01	AW vs. all‡; REM vs. QW and NREM†; NREM vs. QW†	114
	Pf-A1	0.87 ± 0.05	0.49 ± 0.03	0.36 ± 0.01	0.27 ± 0.01	AW vs. all‡; REM vs. QW and NREM†	86
	Pp-A1	1.27 ± 0.04	0.89 ± 0.05	0.81 ± 0.01	0.76 ± 0.01	AW vs. all‡; REM vs. QW and NREM†	29
C3	Pf-V1	0.14 ± 0.01	0.13 ± 0.02	0.06 ± 0.01	0.05 ± 0.01	AW vs. REM and NREM†; REM vs. QW†; NREM vs. QW†	18
	S1-A1	0.99 ± 0.02	0.70 ± 0.03	0.48 ± 0.01	0.48 ± 0.01	AW vs. all‡; REM vs. QW†; NREM vs. QW†	137
	V1-A1	0.76 ± 0.02	0.46 ± 0.03	0.28 ± 0.01	0.24 ± 0.03	AW vs. all‡; REM vs. QW†; NREM vs. QW‡	102
C4	Pf-Pp	0.80 ± 0.05	0.27 ± 0.04	0.14 ± 0.01	0.05 ± 0.01	AW vs. all‡; REM vs. QW and NREM‡	118
	Pf-Pp*	0.94 ± 0.03	0.31 ± 0.02	0.13 ± 0.01	0.04 ± 0.00	AW vs. all‡; REM vs. all‡; NREM vs. AW and REM‡	121
	Pf-A1	0.79 ± 0.04	0.29 ± 0.04	0.16 ± 0.01	0.07 ± 0.01	AW vs. all‡; REM vs. QW and NREM‡; NREM vs. QW†	173
	Pp-A1	1.57 ± 0.03	1.20 ± 0.03	0.99 ± 0.02	0.88 ± 0.01	AW vs. all‡; REM vs. QW and NREM‡; NREM vs. QW‡	515
	Pf-V1*	0.86 ± 0.02	0.26 ± 0.02	0.10 ± 0.00	0.02 ± 0.00	AW vs. all‡; REM vs. QW‡; NREM vs. QW‡	616
	Pp-V1*	1.70 ± 0.02	1.28 ± 0.03	0.99 ± 0.02	0.96 ± 0.02	AW vs. all‡; REM vs. QW and NREM‡; NREM vs. QW‡	235

ANOVA with Tamhane tests. The degrees of freedom were 3 (between groups) and 44 (within groups) for all the derivates that were analysed. A1, auditory cortex; Pf, prefrontal cortex; Pp, posterior-parietal cortex; S1, somato-sensory primary cortex; V1, visual primary cortex. AW, alert wakefulness; QW, quiet wakefulness; NREM, non-REM sleep; REM, REM sleep. *In these cortical pairs AW was induced by light stimulation. The values represent mean ± standard error. $^{†}P < 0.05$ and $^{‡}P < 0.0001$.

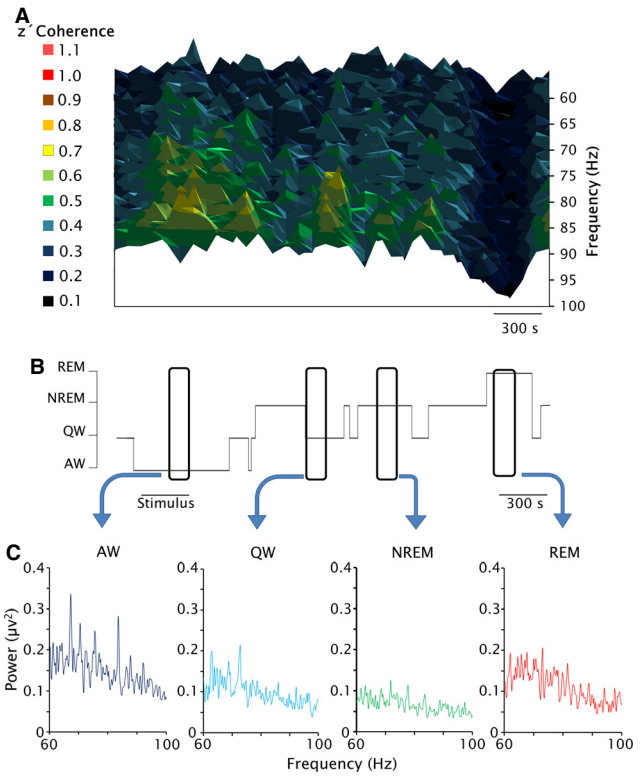

FIG. 10. Dynamic evolution of EEG coherence during sleep and wakefulness. (A) Three-dimensional spectrogram of z′-coherence of the EEG (60–100 Hz) from simultaneous recordings from prefrontal and posterior parietal cortices (3300 s). Time and frequency are shown on the horizontal and vertical (depth) axes, respectively, while z′-coherence is represented in a color code. z′-Coherence is drastically reduced during REM sleep. (B) Hypnogram of recordings analysed in A. The bar under the hypnogram indicates the time of sound stimulation. (C) Gamma band power spectrum profiles from representative 100-s time epochs enclosed in B during AW, QW, NREM sleep and REM sleep.

that suggest that complex, dream-like, cognitive processes are present during REM sleep in this species (Sastre & Jouvet, 1979; Morrison, 1983). Experimental lesions targeted to the dorsal pontine reticular formation elicit REM sleep without atonia; in this condition, dream-like behaviors with complex motor activities, such as jumps and predation-like movements, are released (Sastre & Jouvet, 1979; Morrison, 1983). Furthermore, cortical development is greater in the cat than in rodents, especially in associative cortices; consequently, the cat is an special attractive species in which to study cognitive processes (Thompson *et al.*, 1963; Markowitsch & Pritzel, 1977; Fuster, 1989; Scannell *et al.*, 1995).

Recordings were carried out in semirestricted condition. The advantage is that the differences among states are the states *per se*; changes in postures or movements did not influence the recordings, reducing the possibility of artifacts.

Extra-cerebral potentials did not explain gamma band coherence

There are two main arguments against the possibility that extra-cerebral potentials generated by muscles, heart or eye movements could produce the large 'coherence' observed during AW. First, gamma coherence between the EEG and the activity of different muscles EMGs, electrocardiogram or EOG recorded by means of either bipolar or monopolar electrodes was negligible (a portion of these results are shown in Fig. S1). Second, there was a variable latency between most of the peaks of the gamma waves between the different cortices that were recorded simultaneously. This latency was proportional to the distance between the recorded cortices (not shown); it would not be present if the potentials were produced from an extra-cerebral source. This fact also allows one to reject the volume conduction as an important component of gamma band coherence in the present study.

Data in humans indicate that saccadic eye movements can be a source of gamma wave oscillations in frontal derivations (Yuval-Greenberg *et al.*, 2008). In addition to the lack of coherence between the EEG and the EOG, the absence of gamma coherence during REM sleep, when saccadic eye movements predominate, indicates that these movements did not play a role in the generation of gamma coherence in the cat.

TABLE 2. Gamma (60–100 Hz) z'-coherence values during sleep and wakefulness

Animal	Derivates	AW	QW	NREM	REM	Statistical significance	*F*
C1	S1-Pp	0.63 ± 0.02	0.53 ± 0.01	0.40 ± 0.02	0.19 ± 0.01	REM vs. all‡; AW vs. QW and NREM†	149
	Pp-V1	0.83 ± 0.01	0.76 ± 0.01	0.61 ± 0.02	0.48 ± 0.01	REM vs. all‡; AW vs. NREM‡	122
	S1-V1	0.40 ± 0.01	0.35 ± 0.01	0.21 ± 0.01	0.04 ± 0.01	REM vs. all†; AW vs. QW and NREM†	175
C2	Pf-Pp	0.43 ± 0.01	0.34 ± 0.03	0.31 ± 0.01	0.12 ± 0.01	REM vs. all‡; AW vs. QW and NREM†	58
	Pf-A1	0.51 ± 0.01	0.45 ± 0.02	0.45 ± 0.01	0.25 ± 0.01	REM vs. all‡; AW vs. NREM†	70
	Pp-A1	0.98 ± 0.04	0.86 ± 0.05	0.88 ± 0.02	0.71 ± 0.01	REM vs. all†	10
C3	Pf-V1	0.08 ± 0.00	0.08 ± 0.00	0.05 ± 0.01	0.02 ± 0.00	REM vs. all†; NREM vs. AW and QW†	48
	S1-A1	0.61 ± 0.01	0.43 ± 0.01	0.36 ± 0.02	0.30 ± 0.01	REM vs. all‡; AW vs. QW and NREM†; QW vs. NREM†	46
	V1-A1	0.39 ± 0.02	0.36 ± 0.01	0.18 ± 0.02	0.12 ± 0.02	REM vs. AW and QW‡; NREM vs. AW and QW†	93
C4	Pf-Pp	0.35 ± 0.02	0.31 ± 0.01	0.31 ± 0.03	0.07 ± 0.01	REM vs. all‡	53
	Pf-Pp*	0.37 ± 0.02	0.30 ± 0.02	0.26 ± 0.02	0.03 ± 0.00	REM vs. all‡	110
	Pf-A1	0.31 ± 0.01	0.27 ± 0.01	0.28 ± 0.03	0.07 ± 0.01	REM vs. all†	49
	Pp-A1	0.92 ± 0.02	0.89 ± 0.01	0.85 ± 0.04	0.64 ± 0.05	REM vs. all‡; AW vs. QW and NREM†	16
	Pf-V1*	1.07 ± 0.02	1.11 ± 0.02	0.93 ± 0.02	0.70 ± 0.01	REM vs. all‡; QW vs. NREM†	100
	Pp-V1*	0.45 ± 0.02	0.37 ± 0.02	0.31 ± 0.00	0.06 ± 0.02	REM vs. all‡; AW vs. NREM†	113

ANOVA with Tamhane tests. The degrees of freedom were 3 (between groups) and 44 (within groups) for all the derivates that were analysed. A1, auditory cortex; Pf, prefrontal cortex; Pp, posterior-parietal cortex; S1, somato-sensory primary cortex; V1, visual primary cortex. AW, alert wakefulness; QW, quiet wakefulness; NREM, non-REM sleep; REM, REM sleep. *In these cortical pairs AW was induced by light stimulation. The values represent mean ± standard error. †$P < 0.05$ and ‡$P < 0.0001$.

Coherence analysis in a 100-s window

To determine general trends in coherence analyses, we employed time windows of 100 s, although the timescale for functionally significant events and fluctuations in the brain is much shorter. In relation to cognitive functions, Libet *et al.* (1991) demonstrated that appropriate neuronal activation of approximately 500 ms in duration is required to elicit a conscious sensory experience (Libet *et al.*, 1991). Therefore, from an electrophysiological point of view, in 100-s time-windows one can average the results of different EEG events that occur during wakefulness (i.e. sensory or motor-evoked events), during NREM sleep (i.e. spindles and slow waves) or REM sleep (i.e. ponto-geniculo-occipital waves and tonic EEG desynchronisation). Nevertheless, an increase in gamma coupling was also evident during shorter periods of analysis. Good correlation ($R^2 = 0.81$) was evident in filtered recordings during 6-s epochs of AW. Furthermore, coupling was readily observed in the 200–500 ms gamma 'bursts' that were present in the raw and filtered recordings during AW; these synchronised gamma 'bursts' are also identified by their power in Fig. 5 (see also the cross correlation function in Fig. 4). In contrast, gamma band coupling disappeared during REM sleep (Figs 3–5).

Gamma coherence during wakefulness

It is well known that gamma power and gamma coherence increase during wakefulness in animals and humans (Llinas & Ribary, 1993; Maloney *et al.*, 1997; Rieder *et al.*, 2010). In the cat, gamma band coherence increases during AW between electrodes located in cortical and thalamic sites (Bouyer *et al.*, 1981). In accordance with these results, we demonstrated that during AW, coherence increases between different cortical areas; this fact was clearly observed at frequencies of $\approx$ 40 Hz, but not at higher gamma bands. This increase in coherence occurs during alert behaviors that were induced either by sound, moving light stimulation or when a mirror was located in front of the animal (or immediately after these procedures, as shown in Fig. 6). Coherence also increased when the level of alertness was high at the beginning of the recording or when an individual entered into the recording room (Fig. 6). Therefore, it is the state of alertness, *per se*, and not the stimuli that increase gamma band coherence.

Gamma coherence during sleep

The intercortical dialogue during wakefulness and sleep has been analysed with standard EEG recordings in humans (Achermann & Borbely, 1998a,b), and an increase in gamma band (up to 50 Hz) coherence during REM sleep in comparison with NREM sleep was observed (Achermann & Borbely, 1998a,b). This effect was subtle and mainly present between anterior inter-hemispheric homologous leads. However, the preceding authors were cautious in interpreting their findings because of the low amplitude of high-frequency signals of the standard EEG recordings.

Nir *et al.* (2008) studied inter-hemispheric correlations of envelopes (0.1 Hz) of gamma oscillations during REM sleep and Stage 2 NREM sleep in comparison with wakefulness (Nir *et al.*, 2008). However, the coupling of gamma waves, *per se*, was not the focus of this study. In rats, Gervasoni *et al.* (2004) analysed pooled gamma (30–55 Hz) coherence between neocortical, hippocampal as well as subcortical loci (caudate-putamen and thalamus). They found that REM sleep was the state of maximum pooled coherence in the gamma range; however, gamma coherence among different neocortical sites was not analysed.

The results of the present study led to a different conclusion compared with the study of Llinas & Ribary (1993), who reported that during REM sleep magneto-EEG 40-Hz oscillations were similar in distribution, phase and amplitude to those observed during wakefulness; in contrast, gamma coherent activity was reduced during NREM sleep. They also found that gamma oscillations become robustly coherent in short time windows after sensory stimulation during waking; in other words, sensory stimuli 'reset' gamma oscillations. This effect was not observed during REM sleep. The preceding authors considered that dreams during REM sleep represent a state of hyper-attentiveness in which sensory inputs cannot address the processes that generate conscious experience (Llinas & Ribary, 1993). The discrepancies with our data may arise from the different analytical approaches; Llinas & Ribary (1993) analysed coherence by superimposing 37 traces (filtered at 35–45 Hz) recorded during 0.6–3-s epochs. It is likely that small time periods of high gamma coherence may appear in humans during phasic periods of REM sleep; in fact an increase in gamma activity was found during these periods (Gross & Gotman, 1999). However, we hypothesise that this increase in gamma coherence would not be maintained if larger periods of REM sleep (that include tonic REM sleep) were analysed.

In contrast to the references cited in the preceding paragraphs, several reports are in agreement with our results. Perez-Garci *et al.* (2001) reported that there is a decrease in correlation spectra in 2-s epochs of fast (27–48 Hz) frequencies restricted to intra-hemispheric frontal-perceptual cortical regions during REM sleep in humans (Perez-Garci *et al.*, 2001). However, among perceptual regions, correlation values for REM sleep and wakefulness were similar. Cantero *et al.* (2004) employed human intracranial EEG recordings for coherence analyses during sleep, which allow a much finer spatial scale than do scalp-recorded signals. They found that local (within neocortical regions) and long-range (between intra-hemispheric neocortical regions) gamma coherence was significantly greater during wakefulness than during sleep (Cantero *et al.*, 2004). However, no differences in coherence in the 35–58 Hz frequency band were found between NREM and REM sleep. Furthermore, functional gamma-range coupling between the neocortex and hippocampus was observed during wakefulness, but not during REM sleep. A recent study by Voss *et al.* (2009) demonstrated that coherence for all EEG spectra decreases during REM sleep compared with wakefulness (Voss *et al.*, 2009); interestingly, during lucid dreaming, coherence values are intermediate between wakefulness and REM sleep.

In the present paper, we have demonstrated in the cat that gamma intra-hemispheric coherence is practically absent during REM sleep. This was true for coherence measured between prefrontal and perceptual regions of the cortex, and among perceptual cortices, including primary as well as associative sensory areas. Interestingly, gamma band uncoupling during REM sleep was readily observed by simple inspection of filtered recordings. Future studies are needed to analyse the degree of gamma band coupling of cortical and subcortical areas that increase their activity during REM sleep, such as the limbic cortices and amygdala (Schwartz & Maquet, 2002).

Our demonstration that there is a radical reduction in gamma coherence during REM sleep between different and distant cortical regions does not contradict findings from Steriade's group, which show an increase in local coupling (within a column or among closely cortical sites) during activated states (Steriade *et al.*, 1996; Destexhe *et al.*, 1999). In fact, as suggested in Figs 5 and 10, gamma power values (as a reflection of local gamma synchronisation) during REM sleep were similar to QW and greater than during NREM sleep.

Absence of gamma coherence during REM sleep – impact on cognitive functions

A proper understanding of cognitive functions cannot be achieved without an understanding of consciousness, which involves a system's capacity to integrate information (Tononi, 2010). Recently, utilising transcranial magnetic stimulation and high-density EEG recordings in humans, Massimini *et al.* (2010) demonstrated that although during NREM sleep transcranial magnetic stimulation elicited local and stereotypical cortical activations, during REM sleep transcranial magnetic stimulation triggered a widespread and differentiated patterns of cortical activation that were similar to those observed during wakefulness. These data indicate that there is a significant impairment in intracortical dialogue during NREM sleep, although during REM sleep interactions among cortical sites are operative (Massimini *et al.*, 2010). However, in this study the frequency bands of the cortical interactions were not analysed. Our results in the cat and previous results from humans clearly show that, compared with wakefulness, during REM sleep there is a failure in the capacity of integration among different cortices, at least in high frequency ranges (Perez-Garci *et al.*, 2001; Cantero *et al.*, 2004; Voss *et al.*, 2009). This phenomenon may underlie some of the unique patterns of REM sleep mentation (Hobson, 2009; Nir & Tononi, 2010); in fact, the prevalence of thoughts decreases from wakefulness to NREM sleep and reach a nadir during REM sleep (the same as gamma coherence), while hallucinations and emotions follow an inverse pattern (Fosse *et al.*, 2001).

Bullock *et al.* (2003) considered that the following processes result in an increase in coherence between two structures: (1) both structures are driven by the same generator, (2) both structures can mutually drive each other and (3) one of the structures drives the other one. It is likely that differential activation of regulatory (cholinergic, monoaminergic and peptidergic) systems during REM sleep may be the foundation for cortical uncoupling (Watson *et al.*, 2010). Although it is not clear what role is played by these neuromodulatory systems with respect to large-scale cortical interactions, it is accepted that at least some of these systems alter the frequency range and the strength of local cortical oscillations (Munk *et al.*, 1996; Rodriguez *et al.*, 2004; Roopun *et al.*, 2010). Recent studies have demonstrated the presence of gamma activity in the reticular activating system, and have suggested that this activity helps to stabilise coherence related to arousal (reviewed by Urbano *et al.*, 2012); however, the role of gamma activity in the reticular activating system during REM sleep is unknown. Nevertheless, the study of mechanisms that support the modification of gamma coherence during sleep and wakefulness was beyond the scope of the present report.

Conclusions

During REM sleep in the cat, despite an activated (desynchronised) EEG, there is an absence of cross-talk between different cortical regions in the gamma frequency band. Therefore, functional interactions among different cortical areas (re-entries), which are critical for cognitive functions, are different during wakefulness and REM sleep. This uncoupling of gamma frequency activity during REM sleep may be involved in the distinctiveness of the cognitive operations that take place during mentation that occur during wakefulness and REM sleep (dreams).

Supporting Information

Additional supporting information can be found in the online version of this article:
Fig. S1. Gamma (30–45 Hz) coherence was not produced by extracerebral signals.

Acknowledgements

We thank Luciana Benedetto and Matias Cavelli for their technical assistance. We are also grateful to Dr Giancarlo Vanini for critical comments regarding the manuscript. We are indebted to several anonymous reviewers for comments on the manuscript. The 'Programa de Desarrollo de Ciencias Básicas' (PEDECIBA), Uruguay, partially supported this work.

Conflict of interest

None.

Abbreviations

AW, alert wakefulness; EEG, electroencephalogram; EMG, electromyogram; EOG, electrooculogram; NREM, non-rapid eye movement; QW, quiet wakefulness; REM, rapid eye movement.

References

Achermann, P. & Borbely, A.A. (1998a) Coherence analysis of the human sleep electroencephalogram. *Neuroscience*, **85**, 1195–1208.

Achermann, P. & Borbely, A.A. (1998b) Temporal evolution of coherence and power in the human sleep electroencephalogram. *J. Sleep Res.*, **7**(Suppl. 1), 36–41.

Berman, A.L. & Jones, E.G. (1982) *The Thalamus and Basal Telencephalum of the Cat. A Citoarchitectonic Atlas with Stereotaxic Coordinates*. University of Wisconsin, Madison.

Bouyer, J.J., Montaron, M.F. & Rougeul, A. (1981) Fast fronto-parietal rhythms during combined focused attentive behaviour and immobility in cat: cortical and thalamic localizations. *Electroen. Clin. Neuro.*, **51**, 244–252.

Bressler, S.L., Coppola, R. & Nakamura, R. (1993) Episodic multiregional cortical coherence at multiple frequencies during visual task performance. *Nature*, **366**, 153–156.

Bullock, T.H. (1997) Signals and signs in the nervous system: the dynamic anatomy of electrical activity is probably information-rich. *Proc. Natl. Acad. Sci. USA*, **94**, 1–6.

Bullock, T.H. & McClune, M.C. (1989) Lateral coherence of the electrocorticogram: a new measure of brain synchrony. *Electroen. Clin. Neuro.*, **73**, 479–498.

Bullock, T.H., McClune, M.C., Achimowicz, J.Z., Iragui-Madoz, V.J., Duckrow, R.B. & Spencer, S.S. (1995a) EEG coherence has structure in the millimeter domain: subdural and hippocampal recordings from epileptic patients. *Electroen. Clin. Neuro.*, **95**, 161–177.

Bullock, T.H., McClune, M.C., Achimowicz, J.Z., Iragui-Madoz, V.J., Duckrow, R.B. & Spencer, S.S. (1995b) Temporal fluctuations in coherence of brain waves. *Proc. Natl. Acad. Sci. USA*, **92**, 11568–11572.

Bullock, T.H., McClune, M.C. & Enright, J.T. (2003) Are the electroencephalograms mainly rhythmic? Assessment of periodicity in wide-band time series. *Neuroscience*, **121**, 233–252.

Buzsaki, G. & Wang, X.J. (2012) Mechanisms of gamma oscillations. *Annu. Rev. Neurosci.*, **35**, 203–225.

Cantero, J.L., Atienza, M. & Salas, R.M. (2000) Clinical value of EEG coherence as electrophysiological index of cortico-cortical connections during sleep. *Rev. Neurol.*, **31**, 442–454.

Cantero, J.L., Atienza, M., Madsen, J.R. & Stickgold, R. (2004) Gamma EEG dynamics in neocortex and hippocampus during human wakefulness and sleep. *Neuroimage*, **22**, 1271–1280.

Castro, S., Benedetto, L., Gutierrez, M., Falconi, A. & Torterolo, P. (2010) 'Coherence' in the cortical electrical activity during sleep and wakefulness. In *3rd International Congress on Sleep Medicine and 12th Brazilian Congress on Sleep Medicine*. San Pablo.

Castro, S., Gutierrez, M., Falconi, A., Chase, M. & Torterolo, P. (2011) Absence of EEG gamma (35-40 Hz) coherence characterizes REM sleep and differentiates it from wakefulness. In *41st Annual Meeting of the Society for Neuroscience*. Washington.

Corsi-Cabrera, M., Miro, E., del-Rio-Portilla, Y., Perez-Garci, E., Villanueva, Y. & Guevara, M.A. (2003) Rapid eye movement sleep dreaming is characterized by uncoupled EEG activity between frontal and perceptual cortical regions. *Brain Cogn.*, **51**, 337–345.

Das, N.N. & Gastaut, H. (1955) Variations de l'activite electrique du cerveau, du coeur et des muscles squellettiques au cours de la meditation et de l'extase yoguique. *Electroen. Clin. Neuro.*, **6**, 211.

Destexhe, A., Contreras, D. & Steriade, M. (1999) Spatiotemporal analysis of local field potentials and unit discharges in cat cerebral cortex during natural wake and sleep states. *J. Neurosci.*, **19**, 4595–4608.

Edelman, G.M. & Tononi, G. (2000) *A Universe of Consciousness*. Basic Books, New York.

Fosse, R., Stickgold, R. & Hobson, J.A. (2001) Brain-mind states: reciprocal variation in thoughts and hallucinations. *Psychol. Sci.*, **12**, 30–36.

Fuster, J.M. (1989) *The Prefrontal Cortex*. Raven Press, New York.

Gervasoni, D., Lin, S.C., Ribeiro, S., Soares, E.S., Pantoja, J. & Nicolelis, M.A. (2004) Global forebrain dynamics predict rat behavioral states and their transitions. *J. Neurosci.*, **24**, 11137–11147.

Gross, D.W. & Gotman, J. (1999) Correlation of high-frequency oscillations with the sleep–wake cycle and cognitive activity in humans. *Neuroscience*, **94**, 1005–1018.

Harle, M., Rockstroh, B.S., Keil, A., Wienbruch, C. & Elbert, T.R. (2004) Mapping the brain's orchestration during speech comprehension: task-specific facilitation of regional synchrony in neural networks. *BMC Neurosci.*, **5**, 40.

Hobson, J.A. (2009) REM sleep and dreaming: towards a theory of protoconsciousness. *Nat. Rev. Neurosci.*, **10**, 803–813.

Jasper, H.H. & Andrews, H.L. (1938) Brain potentials and voluntary muscle activity in man. *J. Neurophysiol.*, **1**, 87–100.

John, E.R. (2002) The neurophysics of consciousness. *Brain Res. Brain Res. Rev.*, **39**, 1–28.

Libet, B., Pearl, D.K., Morledge, D.E., Gleason, C.A., Hosobuchi, Y. & Barbaro, N.M. (1991) Control of the transition from sensory detection to sensory awareness in man by the duration of a thalamic stimulus. The cerebral 'time-on' factor. *Brain*, **114**, 1731–1757.

Llinas, R. & Ribary, U. (1993) Coherent 40-Hz oscillation characterizes dream state in humans. *Proc. Natl. Acad. Sci. USA*, **90**, 2078–2081.

Llinas, R., Ribary, U., Contreras, D. & Pedroarena, C. (1998) The neuronal basis for consciousness. *Philos. Trans. R. Soc. Lond. B Biol. Sci.*, **353**, 1841–1849.

Maloney, K.J., Cape, E.G., Gotman, J. & Jones, B.E. (1997) High-frequency gamma electroencephalogram activity in association with sleep-wake states and spontaneous behaviors in the rat. *Neuroscience*, **76**, 541–555.

von der Malsburg, C. (1995) Binding in models of perception and brain function. *Curr. Opin. Neurobiol.*, **5**, 520–526.

Markowitsch, H.J. & Pritzel, M. (1977) A stereotaxic atlas of the prefrontal cortex of the cat. *Acta Neurobiol. Exp. (Wars)*, **37**, 63–81.

Mashour, G.A. (2006) Integrating the science of consciousness and anesthesia. *Anesth. Analg.*, **103**, 975–982.

Massimini, M., Ferrarelli, F., Murphy, M., Huber, R., Riedner, B., Casarotto, S. & Tononi, G. (2010) Cortical reactivity and effective connectivity during REM sleep in humans. *Cogn. Neurosci.*, **1**, 176–183.

Morrison, A.R. (1983) A window on the sleeping brain. *Sci. Am.*, **248**, 94–102.

Munk, M.H., Roelfsema, P.R., Konig, P., Engel, A.K. & Singer, W. (1996) Role of reticular activation in the modulation of intracortical synchronization. *Science*, **272**, 271–274.

Nir, Y. & Tononi, G. (2010) Dreaming and the brain: from phenomenology to neurophysiology. *Trends Cogn. Sci.*, **14**, 88–100.

Nir, Y., Mukamel, R., Dinstein, I., Privman, E., Harel, M., Fisch, L., Gelbard-Sagiv, H., Kipervasser, S., Andelman, F., Neufeld, M.Y., Kramer, U., Arieli, A., Fried, I. & Malach, R. (2008) Interhemispheric correlations of slow spontaneous neuronal fluctuations revealed in human sensory cortex. *Nat. Neurosci.*, **11**, 1100–1108.

Nunez, P.L., Srinivasan, R., Westdorp, A.F., Wijesinghe, R.S., Tucker, D.M., Silberstein, R.B. & Cadusch, P.J. (1997) EEG coherency. I: statistics, reference electrode, volume conduction, Laplacians, cortical imaging, and interpretation at multiple scales. *Electroen. Clin. Neuro.*, **103**, 499–515.

Perez-Garci, E., del-Rio-Portilla, Y., Guevara, M.A., Arce, C. & Corsi-Cabrera, M. (2001) Paradoxical sleep is characterized by uncoupled gamma activity between frontal and perceptual cortical regions. *Sleep*, **24**, 118–126.

Rechtschaffen, A. (1978) The single-mindedness and isolation of dreams. *Sleep*, **1**, 97–109.

Rieder, M.K., Rahm, B., Williams, J.D. & Kaiser, J. (2010) Human gamma-band activity and behavior. *Int. J. Psychophysiol.*, **79**, 39–48.

Rodriguez, R., Kallenbach, U., Singer, W. & Munk, M.H. (2004) Short- and long-term effects of cholinergic modulation on gamma oscillations and response synchronization in the visual cortex. *J. Neurosci.*, **24**, 10369–10378.

Roopun, A.K., Lebeau, F.E., Ramell, J., Cunningham, M.O., Traub, R.D. & Whittington, M.A. (2010) Cholinergic neuromodulation controls directed temporal communication in neocortex in vitro. *Front. Neural Circuits*, **4**, 8.

Sastre, J.P. & Jouvet, M. (1979) Oneiric behavior in cats. *Physiol. Behav.*, **22**, 979–989.

Scannell, J.W., Blakemore, C. & Young, M.P. (1995) Analysis of connectivity in the cat cerebral cortex. *J. Neurosci.*, **15**, 1463–1483.

Schwartz, S. & Maquet, P. (2002) Sleep imaging and the neuro-psychological assessment of dreams. *Trends Cogn. Sci.*, **6**, 23–30.

Siegel, M., Donner, T.H. & Engel, A.K. (2012) Spectral fingerprints of large-scale neuronal interactions. *Nat. Rev. Neurosci.*, **13**, 121–134.

Steriade, M., Amzica, F. & Contreras, D. (1996) Synchronization of fast (30–40 Hz) spontaneous cortical rhythms during brain activation. *J. Neurosci.*, **16**, 392–417.

Thompson, R.F., Johnson, R.H. & Hoopes, J.J. (1963) Organization of auditory, somatic sensory, and visual projection to association fields of cerebral cortex in the cat. *J. Neurophysiol.*, **26**, 343–364.

Tiitinen, H., Sinkkonen, J., Reinikainen, K., Alho, K., Lavikainen, J. & Naatanen, R. (1993) Selective attention enhances the auditory 40-Hz transient response in humans. *Nature*, **364**, 59–60.

Tononi, G. (2010) Information integration: its relevance to brain function and consciousness. *Arch. Ital. Biol.*, **148**, 299–322.

Torterolo, P., Morales, F.R. & Chase, M.H. (2002) GABAergic mechanisms in the pedunculopontine tegmental nucleus of the cat promote active (REM) sleep. *Brain Res.*, **944**, 1–9.

Torterolo, P., Yamuy, J., Sampogna, S., Morales, F.R. & Chase, M.H. (2003) Hypocretinergic neurons are primarily involved in activation of the somatomotor system. *Sleep*, **1**, 25–28.

Torterolo, P., Benedetto, L., Lagos, P., Sampogna, S. & Chase, M.H. (2009) State-dependent pattern of Fos protein expression in regionally-specific sites within the preoptic area of the cat. *Brain Res.*, **1267**, 44–56.

Torterolo, P., Ramos, O.V., Sampogna, S. & Chase, M.H. (2011a) Hypocretinergic neurons are activated in conjunction with goal-oriented survival-related motor behaviors. *Physiol. Behav.*, **104**, 823–830.

Torterolo, P., Sampogna, S. & Chase, M.H. (2011b) A restricted parabrachial pontine region is active during non-rapid eye movement sleep. *Neuroscience*, **190**, 184–193.

Uhlhaas, P.J., Pipa, G., Lima, B., Melloni, L., Neuenschwander, S., Nikolic, D. & Singer, W. (2009) Neural synchrony in cortical networks: history, concept and current status. *Front. Integr. Neurosci.*, **3**, 17.

Uhlhaas, P.J., Pipa, G., Neuenschwander, S., Wibral, M. & Singer, W. (2011) A new look at gamma? High- (>60 Hz) gamma-band activity in cortical networks: function, mechanisms and impairment. *Prog. Biophys. Mol. Biol.*, **105**, 14–28.

Urbano, F.J., Kezunovic, N., Hyde, J., Simon, C., Beck, P. & Garcia-Rill, E. (2012) Gamma band activity in the reticular activating system. *Front. Neurol.*, **3**, 6.

Ursin, R. & Sterman, M. (1981). *Manual for Standardized Scoring of Sleep and Waking States in Adult Cats*. BIS/BRI, University of California, Los Angeles.

Velik, R. (2009) From single neuron-firing to consciousness – towards the true solution of the binding problem. *Neurosci. Biobehav. Rev.*, **34**, 993–1001.

Voss, U., Holzmann, R., Tuin, I. & Hobson, J.A. (2009) Lucid dreaming: a state of consciousness with features of both waking and non-lucid dreaming. *Sleep*, **32**, 1191–1200.

Watson, C., Baghdoyan, H. & Lydic, R. (2010). A neurochemical perspective on states of consciousness. In Hudetz, A.G. & Pearce, R. (Eds), *Supressing the Mind, Contemporary Clinical Neuroscience*. Humana Press, New York, pp. 33–79.

Yuval-Greenberg, S., Tomer, O., Keren, A.S., Nelken, I. & Deouell, L.Y. (2008) Transient induced gamma-band response in EEG as a manifestation of miniature saccades. *Neuron*, **58**, 429–441.

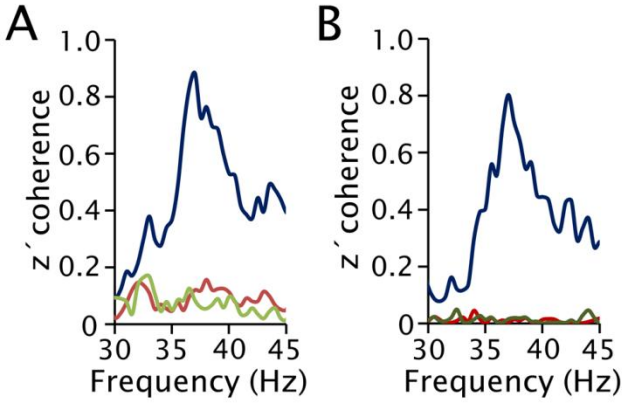

Supplementary Figure 1.Gamma (30-45Hz) coherence was not produced by extra-cerebral signals. A. Gamma coherence between the simultaneous recordings of the EEG from prefrontal (Pf) and posterior parietal (Pp) cortices (blue); Pf and temporal electromiogram (EMG, red) and Pp and temporal EMG (green). B. Gamma coherence between the simultaneous recordings of the EEG from prefrontal (Pf) posterior parietal (Pp) cortices (blue); Pf and ipsilateral electro-oculogram (EOG, green) and Pp and ipsilateral EOG (red). All the recordings were monopolar; the indifferent electrode was located in the frontal sinus.

5.2. Trabajo 2. Coherencia interhemisférica de oscilaciones gamma neocorticales durante el sueño y la vigilia

Como continuación del Trabajo 1, el presente estudio se realizó para analizar la coherencia interhemisférica de la banda gamma de frecuencias del EEG en el gato durante la AW, QW, NREM y sueño REM.

Los gatos fueron implantados con electrodos en las cortezas frontal, parietal y occipital para controlar la actividad de EEG. Se analizó el grado de coherencia en las bandas de frecuencia gamma baja (30-45 Hz) y alta (60-100 Hz) de los pares de registros de EEG.

Hubo un gran aumento en la coherencia entre todas las regiones corticales interhemisféricas en las bandas gamma bajas durante AW en comparación con los otros estados conductuales. Además, la coherencia gamma baja y alta, entre las cortezas heterotópicas interhemisféricas (diferentes áreas corticales de ambos hemisferios) disminuyeron durante el sueño REM; este es un patrón que informamos previamente entre las áreas corticales del mismo hemisferio (coherencia intrahemisférica) en el Trabajo 1. En contraste, entre la mayoría de las áreas corticales homotópicas interhemisféricas (áreas equivalentes o especulares de ambos hemisferios), la coherencia gamma baja fue similar durante el NREM en comparación con el sueño REM.

Concluimos que a pesar de las diferencias sutiles entre las cortezas interhemisféricas homotópicas y heterotópicas, las interacciones funcionales a alta frecuencia disminuyen durante el sueño REM.

Neuroscience Letters 578 (2014) 197–202

Contents lists available at ScienceDirect

Neuroscience Letters

journal homepage: www.elsevier.com/locate/neulet

Inter-hemispheric coherence of neocortical gamma oscillations during sleep and wakefulness

Santiago Castro[a], Matias Cavelli[a], Patricia Vollono[a], Michael H. Chase[b,c], Atilio Falconi[a], Pablo Torterolo[a,*]

[a] Laboratorio de Neurobiología del Sueño, Departamento de Fisiología, Facultad de Medicina, Universidad de la República, Montevideo, Uruguay
[b] WebSciences International, Los Angeles, CA, USA
[c] UCLA School of Medicine, Los Angeles, CA, USA

HIGHLIGHTS

- The electroencephalogram of adult cats was recorded during sleep and wakefulness.
- The inter-hemispheric coherence of the EEG gamma frequency band was analyzed.
- The coherence was larger in alert wakefulness and almost absent during REM sleep.

ARTICLE INFO

Article history:
Received 17 March 2014
Received in revised form 18 May 2014
Accepted 20 June 2014
Available online 30 June 2014

Keywords:
Cortex
Consciousness
EEG
Synchronization
REM

ABSTRACT

Oscillations in the gamma frequency band (mainly ≈40 Hz) of the electroencephalogram (EEG) have been involved in the binding of spatially separated but temporally correlated neural events that result in a unified perceptual experience. The extent of these interactions can be examined by means of a mathematical algorithm called "coherence", which reflects the "strength" of functional interactions between cortical areas. As a continuation of a previous study of our group, the present study was conducted to analyze the inter-hemispheric coherence of the EEG gamma frequency band in the cat during alert wakefulness (AW), quiet wakefulness (QW), non-REM (NREM) sleep and REM sleep. Cats were implanted with electrodes in the frontal, parietal and occipital cortices to monitor EEG activity. The degree of coherence in the low (30–45 Hz) and high (60–100 Hz) gamma frequency bands from pairs of EEG recordings was analyzed. A large increase in coherence between all inter-hemispheric cortical regions in the low gamma bands during AW was present compared to the other behavioral states. Furthermore, both low and high gamma coherence between inter-hemispheric heterotopic cortices (different cortical areas of both hemispheres) decreased during REM sleep; this is a pattern that we previously reported between the cortical areas of the same hemisphere (intrahemispheric coherence). In the high gamma band, coherence during REM sleep also decreased compared to the other behavioral states. In contrast, between most of the inter-hemispheric homotopic cortical areas (equivalent or mirror areas of both hemispheres), low gamma coherence was similar during NREM compared to REM sleep. We conclude that in spite of subtle differences between homotopic and heterotopic inter-hemispheric cortices, functional interactions at high frequency decrease during REM sleep.

1. Introduction

Inter-hemispheric communication is achieved by information that is carried by the corpus callosum, anterior commisure and subcortical pathways [1]. Classical split-brain research wherein the corpus callosum is severed has demonstrated that inter-hemispheric communication subserves a large range of behaviors and cognitive functions [16]. For example, recent experiments have pointed out that transient coherent inter-hemispheric coordination underlies functions such as lexical processing [13].

Electroencephalographic (EEG) oscillations in the gamma frequency band (mainly ≈40 Hz) are involved in the integration or binding of spatially separated but temporally correlated neural events. An increase in gamma power typically appears during states/behaviors that are characterized by active cognitive

* Corresponding author at: Facultad de Medicina, Universidad de la República, General Flores 2125, 11800 Montevideo, Uruguay. Tel.: +598 2924 34 14x3234.
E-mail address: ptortero@fmed.edu.uy (P. Torterolo).

http://dx.doi.org/10.1016/j.neulet.2014.06.044
0304-3940/

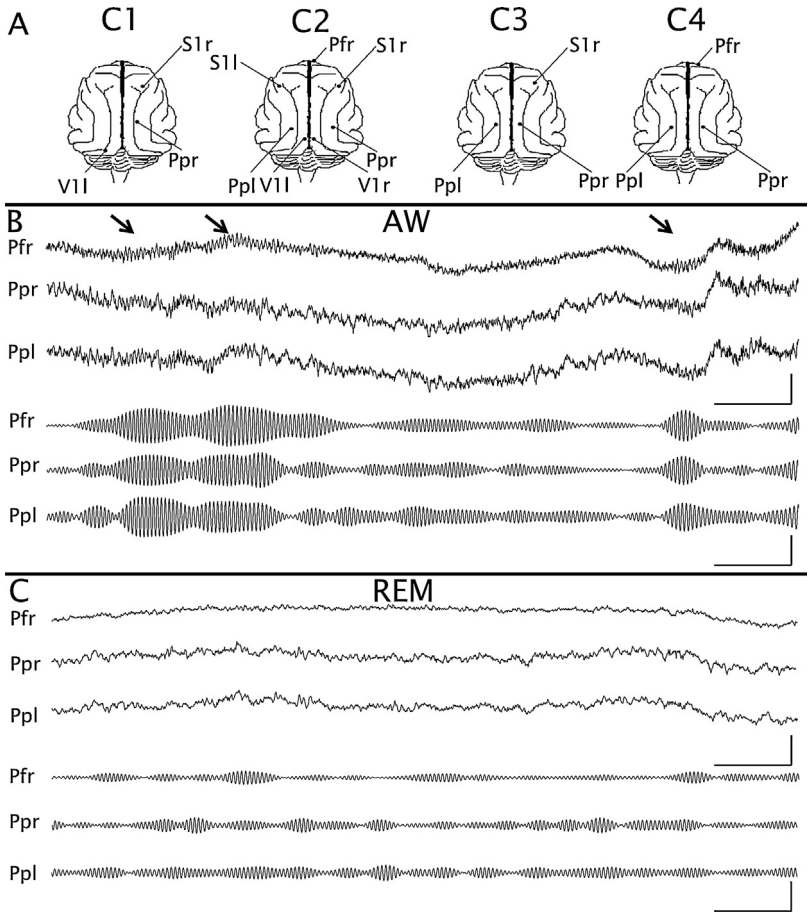

Fig. 1. Gamma oscillations during alert wakefulness and REM sleep. (A) Summary of the position of electrodes on the surface of the primary sensory, association sensory and prefrontal cerebral cortices. These electrodes were referred to a common indifferent electrode, which was located over the frontal sinus. C1–C4, are the animals' names. Pf, prefrontal cortex; Pp, posterior-parietal cortex; S1, somatosensory cortex; V1, visual primary cortex; r, right; l, left. (B) Simultaneous raw and filtered (35–40 Hz) cortical recordings from the right prefrontal (rPf), right posterior-parietal cortex (rPp) and left posterior-parietal cortex (lPp) during alert wakefulness. Gamma oscillations, which are readily observed in the raw recordings (arrows), are highlighted after filtering. Calibration bars: 1 s and 200 μV for raw recordings and 20 μV for filtered recordings. (C) Simultaneous raw and filtered (35–40 Hz) cortical recordings during REM sleep. The amplitude and duration of gamma oscillations decreased compared to alert wakefulness. Calibration bars, as in B.

processing of external percepts or internally generated thoughts and images in humans, and during attentive wakefulness in animals [8,28,29].

The degree of EEG coherence between two cortical regions is believed to reflect the strength of the functional interconnections that occur between them [7]. Coherent EEG activity in the gamma frequency band increases during different behaviors and cognitive functions in both animals and humans [5,6]. In this regard, both gamma activity and gamma coherence between different brain areas has been viewed as a possible neural correlate of consciousness [22].

In the cat, EEG "bursts" of 35–40 Hz oscillations of 200–500 ms and approximately 25 μV can be easily observed in raw EEG recordings ([10] and Fig. 1). Furthermore, EEG intra-hemispheric coherence at 35–40 Hz is greater during alert (AW) than quiet (QW) wakefulness [10]. In addition, intra-hemispheric coherence in the low (35–40 Hz) and high (60–100 Hz) gamma bands decrease to a lower level during non-REM (NREM) sleep, but reaches its nadir during REM sleep. Therefore, during REM sleep, the coupling of high frequency neuronal activity among different cortical areas of the same hemisphere is practically eliminated [10]; comparable results were obtained by other authors utilizing different experimental approaches [9,25,31]. Note that cognitive activities not only occur during wakefulness; dreams, that occur more prominently during rapid eye movement (REM) sleep, are considered a special kind of cognitive activity or proto-consciousness [19].

How is the functional interaction in the gamma frequency band between both hemispheres? Interestingly, a recent study showed that in the condition of corpus callosum agenesia, the gamma coherence (30–55 Hz) did not change during the resting state [18]. However, a subtle increase in gamma band (up to 50 Hz) coherence during REM sleep has been observed in EEG recordings in humans between anterior inter-hemispheric homotopic (equivalent areas of both cerebral hemispheres) leads [2,3]. Consequently, the present study was conducted to determine the interhemispheric coherence in the low (30–45 Hz) and high (60–100 Hz) gamma band between homotopic and heterotopic (different areas of both cerebral hemispheres) cortical areas, during sleep and wakefulness, utilizing the cat as the animal model.

2. Materials and methods

2.1. Experimental animals

Four adult cats (the same as in [10]) were used in this study. The animals were obtained from, and determined to be in good health, by the Institutional Animal Care Facility. All experimental procedures were conducted in accord with the *Guide for the Care and Use of Laboratory Animals* (8th edition, National Academy Press, Washington, DC, 2011) and approved by the Institutional Animal Care Commission. Adequate measures were taken to minimize pain, discomfort or stress of the animals. In addition, all efforts were made in

order to use the minimum number of animals necessary to produce reliable scientific data.

For details regarding the surgical and experimental procedures see [10]. Briefly, the animals were implanted with electrodes to monitor the states of sleep and wakefulness. Stainless steel screw electrodes (1.4 mm diameter) were placed on the surface (above the dura matter) of different cortical areas. Fig. 1A shows the place of the recording electrodes used in this study. The electrodes were connected to a Winchester plug that together with two plastic tubes, were bonded to the skull with acrylic cement in order to maintain the animal's head fixed in stereotaxic position without pain or pressure [10]. After the animals had recovered from the preceding surgical procedures, they were adapted to the recording environment for a period of at least two weeks.

Experimental sessions of 4 h in duration were conducted between 11 A.M. and 3 P.M. in a temperature-controlled environment (21–23 °C). During these sessions (as well as during the adaptation sessions), the animal's head was held in a stereotaxic position by four steel bars that were placed into the chronically implanted plastic tubes, while the body rested in a sleeping bag.

The simultaneous activity of three cortical areas from the same cerebral hemisphere was recorded with monopolar electrodes, utilizing a common reference electrode located in the left frontal sinus. The electromyogram (EMG) of the nuchal muscle, which was recorded by means of acutely placed bipolar electrode, was also monitored. Each cat was recorded daily for a period of approximately 30 days in order to obtain complete data sets.

Bioelectric signals were amplified (×1000), filtered (0.1–100 Hz), sampled (512 Hz, 2^{16} bits) and stored in a PC using the Spike 2 software (Cambridge Electronic Design). Data were obtained during spontaneously occurring quiet wakefulness (QW), REM sleep and non-REM sleep (NREM). Alert wakefulness (AW) was induced for a period of 300 s by a sound stimulus, which was introduced approximately 30 min after the beginning of the recording [10]. The sound stimulus consisted of clicks (0.1 ms in duration) of 60–100 dB SPL in intensity with a variable frequency of presentation (1–500 Hz, modified at random by the operator) in order to avoid habituation [10].

Sleep and waking states were quantified in epochs of 10 s. Selected recordings were filtered (band pass 30–45 Hz) and were processed by means of spectrograms (Fig. 2).

In order to analyze coherence between pairs of EEG channels, 12 manually selected artifact-free periods of 100 s were examined during each behavioral state (1200 s for each behavioral state). For each pair of recordings, data were obtained during four recording sessions.

For each 100 s period, the Magnitude Squared Coherence was analyzed by means of Spike 2 script COHER 1S (Cambridge Electronic Design) (see [10] for details in coherence definition).

The coherence between two EEG channels that were recorded simultaneously during 100 s periods was analyzed. This period of analysis was divided into 100 time-blocks with a sample rate of 512 Hz, a bin size of 1024 samples and a resolution of 0.5 Hz. Coherence between two waveforms is a function of frequency and ranges

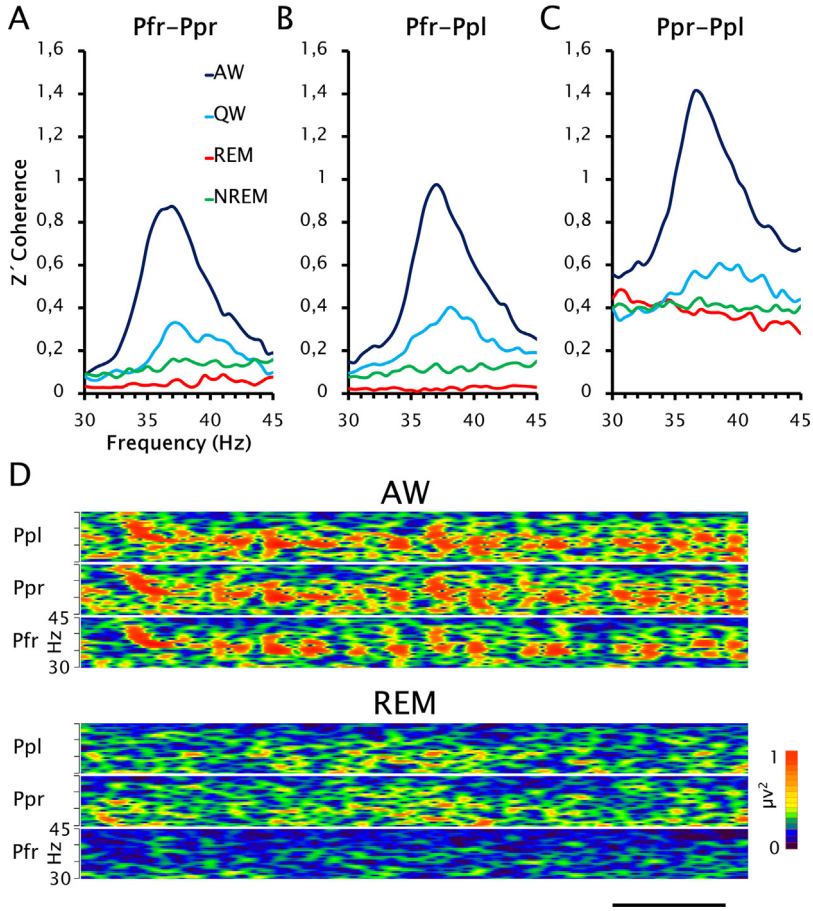

Fig. 2. Graphics that show the averaged z′-coherences profiles between representative intra-hemispheric (A), inter-hemispheric heterotopic (B) and inter-hemispheric homotopic (C) cortical areas during alert wakefulness (AW), quiet wakefulness (QW), non-REM sleep (NREM) and REM sleep in cat 4. (D) Spectrogram of the EEG gamma band of left posterior parietal (Ppl), right posterior parietal (Ppr) and right prefrontal cortex (Pfr). The dynamic of the gamma power during alert wakefulness is very similar in the recorded cortices. On the contrary, during REM sleep the gamma power coupling was reduced. However, the dynamic of the gamma power have some similarities between left and right parietal posterior cortices, but is very different between any of them and the prefrontal cortex. Calibration bar: 5 s.

Table 1
Gamma (35–40 Hz) z′-coherence values during sleep and wakefulness.

Animal	Derivates	AW	QW	NREM	REM	Statistical significance	*F*
C1	S1r-V1l	0.76 ± 0.03	0.35 ± 0.01	0.22 ± 0.02	0.18 ± 0.01	+AW vs. all; +QW vs. REM and NREM; +NREM vs. REM	202
	Ppr-V1l	1.31 ± 0.06	0.89 ± 0.06	0.92 ± 0.06	0.75 ± 0.06	+AW vs. all; +QW vs. REM; +NREM vs. REM	46
C2	Pfr-Ppl	0.49 ± 0.01	0.26 ± 0.02	0.16 ± 0.01	0.09 ± 0.01	++AW vs. all; +QW vs. NREM and REM; +NREM vs. REM	55
	Ppr-Ppl	0.95 ± 0.04	0.46 ± 0.05	0.27 ± 0.04	0.20 ± 0.03	++AW vs. all; +QW vs. NREM and REM	73
	V1r-V1l	1.70 ± 0.02	1.48 ± 0.01	1.42 ± 0.01	1.35 ± 0.01	+AW vs. all; +QW vs. REM; +NREM vs. REM	40
	S1r-S1l	0.64 ± 0.02	0.46 ± 0.01	0.45 ± 0.02	0.38 ± 0.01	++AW vs. all; +QW vs. REM	107
C3	S1r-Ppl	0.23 ± 0.01	0.08 ± 0.01	0.04 ± 0.01	0.02 ± 0.01	++AW vs. all; +QW vs. NREM and REM; +NREM vs. REM	111
	Ppr-Ppl	0.43 ± 0.01	0.34 ± 0.04	0.05 ± 0.01	0.05 ± 0.01	+AW vs. all; +QW vs. NREM and REM	31
C4	Pfr-Ppl	0.78 ± 0.02	0.33 ± 0.02	0.12 ± 0.01	0.02 ± 0.01	++AW vs. all; +QW vs. NREM and REM; +NREM vs. REM	120
	Ppr-Ppl	1.20 ± 0.03	0.55 ± 0.07	0.41 ± 0.02	0.37 ± 0.01	++AW vs. all; +QW vs. NREM and REM	90

The values represent mean ± standard error. +$P < 0.05$. ++$P < 0.0001$, ANOVA with Tamhane tests. The degrees of freedom were 3 (between groups) and 44 (within groups) for all the derivates that were analyzed. A1, auditory primary cortex; Pf, prefrontal cortex; Pp, posterior-parietal cortex; S1, somatosensory cortex; V1, visual primary cortex; r, right; l, left. The underlined derivates correspond to homotopic cortices.

from 0 for totally incoherent waveforms to 1 for maximal coherence; in order for two waveforms to be completely coherent at a particular frequency over a given time range, the phase shift between the waveforms must be constant and the amplitudes of the waves must have a constant ratio. We established that the random level of coherence was approximately 0.1 [10].

In order to normalize the data and conduct parametric statistical tests, we applied the Fisher z′ transform to the gamma coherence values. Thereafter, the profile of the z′-coherence of the gamma band in 100 s epochs for each pair of EEG recordings as well as the average of twelve epochs was analyzed, and the results were presented in a graphic form (Fig. 2). The z′-coherence of the gamma band for each pair of EEG channels was also averaged across behavioral states independently for each cat, and was expressed as the mean ± standard error. The significance of the differences among behavioral states was evaluated with the ANOVA and Tamhane post hoc tests. The criterion used to reject the null hypotheses was $P < 0.05$.

3. Results

Examples of representative EEG recordings from cortical areas of the same and different hemispheres (right prefrontal, right posterior parietal and left posterior parietal) are shown in Fig. 1B and C. "Bursts" of 35–40 Hz oscillations can be readily observed in raw recordings during AW (Fig. 1B, arrows). On the contrary, they are difficult to perceive during REM sleep (Fig. 1C). After digital filtering of the recordings to include only the low gamma band, these oscillations were unmasked.

A strong coupling of EEG gamma oscillations recorded in different cortical sites, was present during AW (even between channels within different brain hemispheres), but not during REM sleep (Fig. 1B and C). However, during REM sleep filtered records of the right and left posterior parietal cortices (Ppr and Ppl, homotopic cortices) appeared to be more coupled than were recordings between them and the right prefrontal cortex (Pfr) (Fig. 1C).

The "coherence" algorithm was applied in order to conduct an in-depth analysis of different pairs of EEG signals that were simultaneously recorded during sleep and wakefulness. Examples of representative averaged low (30–45 Hz) gamma band z′-coherence profiles for intra-hemispheric, homotopic inter-hemispheric and heterotopic inter-hemispheric combinations of EEG recordings are shown in Fig. 2A–C. A narrow peak of coherence at 35–40 Hz is readily observed in all derivations during AW. Both for intra-hemispheric and heterotopic inter-hemispheric combinations, the z′-coherence was drastically reduced during REM sleep. For homotopic inter-hemispheric combinations, the z′-coherence was similar between NREM and REM sleep.

A visual form to represent the gamma power as well as the coupling among different cortices during AW is shown in Fig. 2D; note the presence of "gamma bursts" in the form of red "clouds" that were correlated in all the recordings. Compared to AW, during REM sleep, gamma power was reduced and the correlation of the "bursts" was almost absent. However, note that during REM sleep the dynamic of the gamma power have some similarities between left and right posterior parietal cortex but is very different between any of them and the prefrontal cortex. Similar pattern can be observed in the filtered recordings of Fig. 1C.

The averaged inter-hemispheric z′-coherence in the 35–40 Hz band across behavioral states for all combinations of cortical recordings is presented in Table 1. As it is shown in the representative examples of Figs. 1 and 2, during AW z′-coherence was significantly larger in both inter-hemispheric combinations (homotopic and heterotopic). During QW and NREM sleep, z′-coherence values were intermediate, and in some combinations they were larger during QW than during NREM sleep. z′-coherence decreased during REM sleep between pairs of non-correspondent (heterotopic) cortices of both hemispheres. In contrast, in most of the derivations

Table 2
Gamma (60–100 Hz) z′-coherence values during sleep and wakefulness.

Animal	Derivates	AW	QW	NREM	REM	Statistical significance	*F*
C1	S1r-V1l	0.35 ± 0.02	0.31 ± 0.02	0.17 ± 0.02	0.04 ± 0.01	+All vs. all	81
	Ppr-V1l	0.46 ± 0.02	0.41 ± 0.01	0.28 ± 0.01	0.13 ± 0.01	+All vs. all	144
C2	Pfr-Ppl	0.39 ± 0.05	0.24 ± 0.04	0.15 ± 0.01	0.08 ± 0.01	+AW vs. NREM and REM; +QW vs. REM; +NREM vs. REM	18
	Ppr-Ppl	0.75 ± 0.05	0.39 ± 0.06	0.24 ± 0.03	0.14 ± 0.02	+AW vs. all; +QW vs. NREM and REM	36
	V1r-V1l	1.69 ± 0.02	1.59 ± 0.01	1.51 ± 0.01	1.32 ± 0.03	+All vs. all	20
	S1r-S1l	0.80 ± 0.02	0.72 ± 0.01	0.73 ± 0.02	0.65 ± 0.03	+AW vs. NREM and REM; +QW vs. REM; +NREM vs. REM.	59
C3	S1r-Ppl	0.21 ± 0.01	0.17 ± 0.02	0.09 ± 0.01	0.02 ± 0.01	+AW vs. all; +QW vs. NREM and REM; +NREM vs. REM.	38
	Ppr-Ppl	0.21 ± 0.04	0.34 ± 0.01	0.05 ± 0.01	0.03 ± 0.01	+AW vs. NREM and REM; +QW vs. REM	13
C4	Pfr-Ppl	0.49 ± 0.03	0.43 ± 0.03	0.37 ± 0.02	0.04 ± 0.01	+All vs. all	81
	Ppr-Ppl	0.82 ± 0.01	0.56 ± 0.07	0.52 ± 0.03	0.18 ± 0.01	+AW vs. all; +QW vs. REM; +NREM vs. REM	45

The values represent mean ± standard error. +$P < 0.05$, ANOVA with Tamhane tests. The degrees of freedom were 3 (between groups) and 44 (within groups) for all the derivates that were analyzed. A1, auditory primary cortex; Pf, prefrontal cortex; Pp, posterior-parietal cortex; S1, somatosensory cortex; V1, visual primary cortex; r, right; l, left. The underlined derivates correspond to homotopic cortices.

(4 out of 5), the z′-coherence between inter-hemispheric homotopic regions was similar during NREM and REM sleep.

Table 2 presents an analysis of the inter-hemispheric z′-coherence for the 60–100 Hz frequency band. The z′-coherence during AW was larger than QW in most but not all derivations. During REM sleep, there was a significant decrease in z′-coherence for both inter-hemispheric and intra-hemispheric (homotopic and heterotopic) combinations.

4. Discussion

A gamma frequency band (30–45 Hz) in the EEG was originally described by Jasper and Andrews [20], and corresponds to the 40 Hz cognitive rhythm introduced by Das and Gastaut [11]. Several seminal studies then confirmed that this frequency band plays a critically important role in cognitive functions [22].

From a methodological point of view, our animal model have the advantage that by utilizing cortical surface electrodes, ≈40 Hz oscillations can be clearly observed directly in the raw EEG recordings. Therefore, the result of the coherence analysis can also be confirmed by direct observation of the recordings; e.g., the tracing of Fig. 1 corresponds to the analysis, which is presented in Fig. 2.

In the present study, we demonstrated that the EEG inter-hemispheric coherence in the low gamma (30–45 Hz) frequency band is greater during AW than QW. In this regard, callosal-dependent inter-hemispheric synchrony has been observed during visual stimulation in the cat [15]; and in humans, synchronized activity in ≈40 Hz has been found to spread across the hemispheres during a visual recognition task [26]. Gamma-band rhythmogenesis has been systematically studied and is considered to be inextricably tied to the presence of perisomatic inhibition of cortical neurons that occurs due to $GABA_A$-receptor mediated inhibition [8]. However, the locally generated gamma rhythms can become coupled over surprisingly long distances, i.e. between hemispheres or remote regions of the cerebral cortex [8,17,23]. Interestingly, recent studies suggest that coherent gamma activity that is present in several subregions of the ascending reticular activating system may function to stabilize EEG gamma coherence during arousal [30].

Gamma coherence decreased to a lower level during NREM and REM sleep compared to QW. Although between homotopic inter-hemispheric areas z′-coherence was similar during NREM and REM sleep, between non-symmetrical inter-hemispheric areas, gamma coherence reached its nadir during REM sleep, as we found for low gamma coherence concerning intra-hemispheric regions [10].

Interestingly, low gamma coupling during REM sleep between homotopic cortices of both hemispheres is of intermediate strength compared with the lack of coupling for intra-hemispheric remote cortical areas and the high degree of local coupling (within a column or among closely cortical sites) that produce high values of gamma power [10,27]. In the cat, as in other mammals, there is a great number of callosal fibers that connect between homotopic inter-hemispheric cortical areas [24]; these connections may facilitate functional coupling between these cortical sites.

Research in oscillations of higher frequencies than 40 Hz (up to 600 Hz) has been undertaken recently [29], and the role of these higher frequency bands in cognitive function is still unknown. Nevertheless, we included an investigation of frequencies from 60 up to 100 Hz in the present study and in our previous paper [10]. We found that inter-hemispheric and intra-hemispheric high gamma coherence shares the same characteristics. Alert wakefulness produced only a small increase in coherence in some derivations compared to QW, and there was significant reduction of coherence during REM sleep for both inter-hemispheric combinations (homotopic and heterotopic cortices). It is interesting to note that even though high gamma coherence is reduced during REM sleep, the power or potency (and sign of local synchronization) in this frequency band is similar than waking levels [10]. Unfortunately, the mechanisms that are responsible for these high frequency oscillations are still unclear [29]. However, it is important to note that the possibility that artifacts induced either by muscle or saccadic activity affected the data has been previously discussed and discarded [10].

In addition to the results of EEG coherence during REM sleep of Achermann and Borbely [2,3] (see Section 1), Leveille et al. demonstrated that although intra-hemispheric EEG coherence (up to beta band) during REM sleep is altered in autism, inter-hemispheric coherence did not change [21]. Inter-hemispheric communication during REM sleep was also assessed by means of paired-pulse transcranial magnetic stimulation [4,12]. The authors demonstrated a drastic decrease in callosal inhibition, and a significant increase in intra-cortical facilitation 10 and 15 ms after awakenings that followed REM sleep, suggesting that inter-hemispheric connectivity is modified during REM sleep. However, more studies are needed to understand the functional role of inter-hemispheric interaction during REM sleep.

5. Conclusions

Functional interactions among different cortical areas, including inter-hemispheric communication, are critical for cognitive functions [14]. In the present and a previous paper we demonstrated an uncoupling of gamma frequency activity during REM sleep between intra and inter-hemispheric cortices. This fact may contribute to the uniqueness of cognitive functions that take place during REM sleep, where most dreams occur [19].

Acknowledgments

The “Programa de Desarrollo de Ciencias Básicas” (PEDECIBA), and the “Agencia Nacional de Investigacion e Innovación” (ANII), Uruguay, partially supported this work.

References

[1] F. Aboitiz, J. Montiel, One hundred million years of interhemispheric communication: the history of the corpus callosum, Braz. J. Med. Biol. Res. 36 (2003) 409–420.
[2] P. Achermann, A.A. Borbely, Coherence analysis of the human sleep electroencephalogram, Neuroscience 85 (1998) 1195–1208.
[3] P. Achermann, A.A. Borbely, Temporal evolution of coherence and power in the human sleep electroencephalogram, J. Sleep Res. 7 (Suppl. 1) (1998) 36–41.
[4] M. Bertini, L. De Gennaro, M. Ferrara, G. Curcio, V. Romei, F. Fratello, R. Cristiani, F. Pauri, P.M. Rossini, Reduction of transcallosal inhibition upon awakening from REM sleep in humans as assessed by transcranial magnetic stimulation, Sleep 27 (2004) 875–882.
[5] J.J. Bouyer, M.F. Montaron, A. Rougeul, Fast fronto-parietal rhythms during combined focused attentive behaviour and immobility in cat: cortical and thalamic localizations, Electroencephalogr. Clin. Neurophysiol. 51 (1981) 244–252.
[6] S.L. Bressler, R. Coppola, R. Nakamura, Episodic multiregional cortical coherence at multiple frequencies during visual task performance, Nature 366 (1993) 153–156.
[7] T.H. Bullock, M.C. McClune, J.T. Enright, Are the electroencephalograms mainly rhythmic? Assessment of periodicity in wide-band time series, Neuroscience 121 (2003) 233–252.
[8] G. Buzsaki, X.J. Wang, Mechanisms of gamma oscillations, Annu. Rev. Neurosci. 35 (2012) 203–225.
[9] J.L. Cantero, M. Atienza, J.R. Madsen, R. Stickgold, Gamma EEG dynamics in neocortex and hippocampus during human wakefulness and sleep, Neuroimage 22 (2004) 1271–1280.
[10] S. Castro, A. Falconi, M.H. Chase, P. Torterolo, Coherent neocortical 40-Hz oscillations are not present during REM sleep, Eur. J. Neurosci. 37 (2013) 1330–1339.
[11] N.N. Das, H. Gastaut, Variations de l'activite electrique du cerveau, du coeur et des muscles squellettiques au cours de la meditation et de l'extase yoguique, Electroencephalogr. Clin. Neurophysiol. 6 (1955) 211.
[12] L. De Gennaro, M. Bertini, M. Ferrara, G. Curcio, R. Cristiani, V. Romei, F. Fratello, F. Pauri, P.M. Rossini, Intracortical inhibition and facilitation upon awakening from different sleep stages: a transcranial magnetic stimulation study, Eur. J. Neurosci. 19 (2004) 3099–3104.

[13] K.W. Doron, D.S. Bassett, M.S. Gazzaniga, Dynamic network structure of interhemispheric coordination, Proc. Natl. Acad. Sci. U.S.A. 109 (2012) 18661–18668.
[14] G.M. Edelman, G. Tononi, A Universe of Consciousness, Basic Books, New York, 2000.
[15] A.K. Engel, P. Konig, A.K. Kreiter, W. Singer, Interhemispheric synchronization of oscillatory neuronal responses in cat visual cortex, Science 252 (1991) 1177–1179.
[16] M.S. Gazzaniga, Shifting gears: seeking new approaches for mind/brain mechanisms, Annu. Rev. Psychol. 64 (2012) 1–20.
[17] G.G. Gregoriou, S.J. Gotts, H. Zhou, R. Desimone, High-frequency, long-range coupling between prefrontal and visual cortex during attention, Science 324 (2009) 1207–1210.
[18] L.B. Hinkley, E.J. Marco, A.M. Findlay, S. Honma, R.J. Jeremy, Z. Strominger, P. Bukshpun, M. Wakahiro, W.S. Brown, L.K. Paul, A.J. Barkovich, P. Mukherjee, S.S. Nagarajan, E.H. Sherr, The role of corpus callosum development in functional connectivity and cognitive processing, PLOS ONE 7 (2012) e39804.
[19] J.A. Hobson, REM sleep and dreaming: towards a theory of protoconsciousness, Nat. Rev. Neurosci. 10 (2009) 803–813.
[20] H.H. Jasper, H.L. Andrews, Brain potentials and voluntary muscle activity in man, J. Neurophysiol. 1 (1938) 87–100.
[21] C. Leveille, E.B. Barbeau, C. Bolduc, E. Limoges, C. Berthiaume, E. Chevrier, L. Mottron, R. Godbout, Enhanced connectivity between visual cortex and other regions of the brain in autism: a REM sleep EEG coherence study, Autism Res. 3 (2010) 280–285.
[22] R. Llinas, U. Ribary, D. Contreras, C. Pedroarena, The neuronal basis for consciousness, Philos. Trans. R. Soc. Lond. B: Biol. Sci. 353 (1998) 1841–1849.
[23] L. Melloni, C. Molina, M. Pena, D. Torres, W. Singer, E. Rodriguez, Synchronization of neural activity across cortical areas correlates with conscious perception, J. Neurosci. 27 (2007) 2858–2865.
[24] H. Nakamura, T. Kanaseki, Topography of the corpus callosum in the cat, Brain Res. 485 (1989) 171–175.
[25] E. Perez-Garci, Y. del-Rio-Portilla, M.A. Guevara, C. Arce, M. Corsi-Cabrera, Paradoxical sleep is characterized by uncoupled gamma activity between frontal and perceptual cortical regions, Sleep 24 (2001) 118–126.
[26] E. Rodriguez, N. George, J.P. Lachaux, J. Martinerie, B. Renault, F.J. Varela, Perception's shadow: long-distance synchronization of human brain activity, Nature 397 (1999) 430–433.
[27] M. Steriade, F. Amzica, D. Contreras, Synchronization of fast (30–40 Hz) spontaneous cortical rhythms during brain activation, J. Neurosci. 16 (1996) 392–417.
[28] P.J. Uhlhaas, G. Pipa, B. Lima, L. Melloni, S. Neuenschwander, D. Nikolic, W. Singer, Neural synchrony in cortical networks: history, concept and current status, Front. Integr. Neurosci. 3 (2009) 17.
[29] P.J. Uhlhaas, G. Pipa, S. Neuenschwander, M. Wibral, W. Singer, A new look at gamma? High- (>60 Hz) gamma-band activity in cortical networks: function, mechanisms and impairment, Prog. Biophys. Mol. Biol. 105 (2011) 14–28.
[30] F.J. Urbano, N. Kezunovic, J. Hyde, C. Simon, P. Beck, E. Garcia-Rill, Gamma band activity in the reticular activating system, Front. Neurol. 3 (2012) 6.
[31] U. Voss, R. Holzmann, I. Tuin, J.A. Hobson, Lucid dreaming: a state of consciousness with features of both waking and non-lucid dreaming, Sleep 32 (2009) 1191–1200.

5.3. Trabajo 3. Oscilaciones neocorticales de 40 Hz durante el sueño REM y la cataplejía inducidos por carbacol

En los Trabajos 1 y 2, se analizó el grado de conectividad funcional entre áreas corticales empleando el análisis de "coherencia cruzada cuadrada" de la banda gamma EEG; demostramos que la coherencia gamma es máxima durante la vigilia de alerta y casi no existe durante el sueño REM.

La entrada colinérgica desde el núcleo tegmental laterodorsal y pedunculopontino al NPO es crítica para la generación de sueño REM. Se considera que el NPO ejerce control ejecutivo sobre la iniciación y el mantenimiento del sueño REM. En el gato, dependiendo del estado previo del animal, una sola microinyección de carbacol (un agonista colinérgico) en el NPO puede producir ya sea sueño REM (sueño REM inducido por carbacol, REMc), o un estado de vigilia con atonía muscular (cataplejía) inducido por carbachol, CA).

En el presente estudio, en gatos a los que se les implantaron electrodos en diferentes áreas corticales para registrar la actividad polisomnográfica, comparamos la coherencia gamma (30-45 Hz) durante REMc, CA y estados conductuales naturales.

La coherencia gamma fue máxima durante CA y AW. Por el contrario, en la mayoría de los animales, la coherencia gamma estuvo casi ausente durante REMc, como en el sueño REM natural.

Concluimos que, a pesar de la misma parálisis muscular somática, hay diferencias notables en la actividad cortical entre REMc y CA, lo que confirma que la coherencia gamma del EEG (≈ 40 Hz) es un rasgo que diferencia la vigilia del sueño REM. Finalmente, estos datos sugieren que la presencia de coherencia gamma podría ser útil para detectar la presencia de consciencia en pacientes paralizados (síndrome de encerramiento, consciencia intraoperatoria, etc.).

EJN European Journal of Neuroscience FENS Federation of European Neuroscience Societies

European Journal of Neuroscience, Vol. 43, pp. 580–589, 2016 doi:10.1111/ejn.13151

NEUROSYSTEMS

Neocortical 40 Hz oscillations during carbachol-induced rapid eye movement sleep and cataplexy

Pablo Torterolo,[1] Santiago Castro-Zaballa,[1] Matías Cavelli,[1] Michael H. Chase[2] and Atilio Falconi[1]
[1]Laboratorio de Neurobiología del Sueño, Facultad de Medicina, Departamento de Fisiología, Universidad de la República, General Flores 2125, 11800 Montevideo, Uruguay
[2]WebSciences International and UCLA School of Medicine, Los Angeles, CA, USA

Keywords: cat, electroencephalogram, gamma, narcolepsy, nucleus pontis oralis, reticular formation

Edited by Thomas Klausberger
Received 18 July 2015, revised 3 December 2015, accepted 4 December 2015

Abstract

Higher cognitive functions require the integration and coordination of large populations of neurons in cortical and subcortical regions. Oscillations in the gamma band (30–45 Hz) of the electroencephalogram (EEG) have been involved in these cognitive functions. In previous studies, we analysed the extent of functional connectivity between cortical areas employing the 'mean squared coherence' analysis of the EEG gamma band. We demonstrated that gamma coherence is maximal during alert wakefulness and is almost absent during rapid eye movement (REM) sleep. The nucleus pontis oralis (NPO) is critical for REM sleep generation. The NPO is considered to exert executive control over the initiation and maintenance of REM sleep. In the cat, depending on the previous state of the animal, a single microinjection of carbachol (a cholinergic agonist) into the NPO can produce either REM sleep [REM sleep induced by carbachol (REMc)] or a waking state with muscle atonia, i.e. cataplexy [cataplexy induced by carbachol (CA)]. In the present study, in cats that were implanted with electrodes in different cortical areas to record polysomnographic activity, we compared the degree of gamma (30–45 Hz) coherence during REMc, CA and naturally-occurring behavioural states. Gamma coherence was maximal during CA and alert wakefulness. In contrast, gamma coherence was almost absent during REMc as in naturally-occurring REM sleep. We conclude that, in spite of the presence of somatic muscle paralysis, there are remarkable differences in cortical activity between REMc and CA, which confirm that EEG gamma (≈40 Hz) coherence is a trait that differentiates wakefulness from REM sleep.

Introduction

During wakefulness (W) there is awareness (consciousness) of the environment and internal stimuli such as hunger, thirst, etc. In contrast, during quiet or non-rapid eye movement (NREM) sleep, especially during the deep phase (N3) that occurs during the first half of the night, cognition is almost absent (Tononi, 2009). During rapid eye movement (REM) sleep there is a different cognitive state, which is when most dreams occur (Hobson, 2009; Tononi, 2009). However, the electroencephalogram (EEG) activity appears similar to that which takes place during W. Because of this fact, Jouvet (1965) called this state the 'paradoxical phase' of sleep. However, a detailed analysis of the EEG in cats and rats revealed that there is a high level of neocortical gamma (30–100 Hz) band coherence during alert W (AW), which decreases during quiet W (QW) and NREM sleep, and is almost absent during REM sleep (Castro *et al.*, 2013, 2014; Cavelli *et al.*, 2015). As EEG coherence between two cortical regions reflects the strength of the functional interconnections that occur between them (Edelman & Tononi, 2000; Bullock *et al.*, 2003), the differences in gamma band coherence indicate that the functional integration among separate cortical areas is not the same during W and REM sleep.

In order to confirm and expand knowledge about the dynamics of gamma neocortical activity during the activated behavioural states (W and REM sleep), we took advantage of the fact that microinjections of carbachol, a mixed cholinergic (muscarinic and nicotinic) agonist, into the nucleus pontis oralis (NPO) of the cat switch the behavioural state from W or NREM to REM sleep. Thus, a single microinjection of carbachol during NREM sleep induces the generation of REM sleep [REM sleep induced by carbachol (REMc)] with short latency (approximately 30 s). Interestingly, depending on the previous behavioural state of the animal, microinjections of carbachol within the NPO may also induce muscle atonia during W or cataplexy, which is similar to atonia during naturally-occurring REM sleep and REMc (Lopez-Rodriguez *et al.*, 1994). Cataplexy, which is a cardinal sign of the sleep pathology narcolepsy, consists of a sudden loss in muscle tone during W, which is most commonly elicited by an emotional response (Guilleminault & Fromherz, 2011; Mignot, 2011; Chase, 2013; Dauvilliers *et al.*, 2014).

Cataplexy induced by carbachol (CA) occurs most readily when carbachol is microinjected during AW (Lopez-Rodriguez *et al.*,

Correspondence: Pablo Torterolo, as above.
E-mail: ptortero@fmed.edu.uy

1994). In addition, transitions from REMc to CA are common, and CA can be induced from REMc by sensory stimulation (Torterolo *et al.*, 2015). Hence, in the present study we compared EEG gamma coherence during REMc and CA, which are two different states that present essentially the same somato-motor atonia. The direct transition of these carbachol-induced states from one to another allows a direct observation of the differences of the gamma activity between the activated states; W to REM sleep transitions do not take place during the natural sleep–W cycle. Because 40 Hz activity is prominent and readily observable in raw EEG recordings and is highly reactive to the level of alertness [which is not the case for higher frequency gamma activity (Castro *et al.*, 2013)], in the present report we only examined the 30–45 Hz frequency band of the gamma spectrum.

Materials and methods

Four adult cats were used in this study; these animals were also employed in a previous report (Torterolo *et al.*, 2015). The animals were determined to be in good health by veterinarians of the Department of Laboratory Medicine (Facultad de Medicina, Universidad de la República, Montevideo, Uruguay). All experimental procedures were conducted in accordance with the National Animal Care Law (no. 18611) and the Guide to the Care and Use of Laboratory Animals (8th Edn, National Academy Press, Washington D.C., 2010), and were approved by the Institutional Animal Care Committee (Comisión de Experimentación Animal). Efforts were made to use the minimal number of animals necessary to produce reliable data.

Surgical procedures were the same as those previously employed (Castro *et al.*, 2013; Torterolo *et al.*, 2015). The animals were chronically implanted with electrodes to monitor the states of sleep and W. Prior to being anaesthetized, each cat was premedicated with xylazine (2.2 mg/kg, i.m.), atropine (0.04 mg/kg, i.m.) and antibiotics (Tribrissen®, 30 mg/kg, i.m.). Anaesthesia, which was initially induced with ketamine (15 mg/kg, i.m.), was maintained with a gas mixture of isoflourane in oxygen (1–3%). Following anaesthesia, the head was positioned in a stereotaxic frame and stainless steel screw electrodes were placed in the skull to record the EEG. The position of the recording electrodes is illustrated in Fig. 1A. In addition, bipolar electrodes were implanted in both lateral geniculate nuclei in order to monitor ponto-geniculo-occipital (PGO) waves, and in the orbital portion of the the electro-oculogram. A Winchester plug (connected to the electrodes) and a chronic head- restraining bone to record restraining device were bonded to the skull with acrylic cement. A hole (5 mm diameter), which was drilled in the skull overlying the cerebellar cortex, was filled with bone-wax, and this hole was subsequently used to provide access to the pons for drug administration.

Experimental sessions

After the animals recovered from surgery and were adapted to the recording environment, polysomnographic recordings were conducted from 11:00 to 15:00 h in a temperature-controlled environment (21–23 °C). During these sessions, the head of the cat was held in a stereotaxic position by a head-restraining device. The EEG activity of three cortical areas was recorded with monopolar electrodes, utilizing a common reference electrode located in the left frontal sinus. Electro-oculogram, lateral geniculate nuclei, neck electromyogram (electrodes were placed acutely on the skin over neck muscles), ECG (electrodes were placed acutely on the skin over the precordial region) and respiratory activity (by means of a microeffort piezo crystal infant sensor) were also recorded. Each cat was recorded daily for a period of approximately 30 days in order to obtain complete data sets.

Bioelectric signals were amplified (×1000), filtered (0.1–100 Hz), sampled (512 Hz, 2^{16} bits) and stored on a PC using SPIKE 2 software (Cambridge Electronic Design). Data were obtained during QW, REM sleep and NREM sleep. AW was induced for a period of 300 s by a sound stimulus, which was introduced at approximately 30 min after the beginning of the recording (Castro *et al.*, 2013). The sound stimulus consisted of clicks (0.1 ms in duration) of 60–100 dB sound pressure level in intensity with a variable frequency of presentation (1–500 Hz) in order to avoid habituation (Castro *et al.*, 2013).

The eyes of the animals were examined throughout the recording sessions in order to determine if they were closed or open, and if the pupils were mydriatic or miotic. We also monitored the degree of relaxation of the nictitating membrane and whether the animals were able to track visual or auditory stimuli.

In order to induce REMc or CA, carbachol (0.8 μg in 0.2 μL of saline) was microinjected unilaterally for a period of 1 min into the NPO with a Hamilton syringe (Torterolo *et al.*, 2013, 2015). The coordinates were: AP, −2 to −3; L, 1.5–2.5; and H, −3.5 to −5, according to Berman (1968). Carbachol microinjections were performed either during NREM sleep or W (Lopez-Rodriguez *et al.*, 1994). Two successful carbachol microinjections (i.e. in these experiments REMc and CA episodes were generated) were carried out for each cat on different days. Mild auditory or somato-sensory stimuli were occasionally applied to the animals in order to induce CA from an ongoing state of REMc (see Results).

Sleep and coherence analyses

The states of AW, QW, NREM sleep, REM sleep, REMc and CA were determined on the basis of polysomnographic records that were divided into 10 s epochs and analysed according to standard criteria (Ursin & Sterman, 1981). The identification of REMc and CA is explained in the Results. Only well-defined periods of REMc and CA were analysed, and transitions between states were excluded.

Selected recordings were filtered (band pass 30–45 Hz) and processed by means of spectrograms. In order to analyse coherence between pairs of EEG recordings, 12 artefact-free periods of 100 s were examined during each behavioural state (1200 s for each behavioural state). For each pair of recordings, data were obtained during four separate recording sessions.

For each 100 s period, the magnitude squared coherence was analysed by means of SPIKE 2 script COHER 1S (Cambridge Electronic Design) (for details, see Castro *et al.*, 2013). The coherence between two EEG channels that were recorded simultaneously during 100 s periods was analysed. This period of analysis was divided into 100 time blocks with a sample rate of 512 Hz, bin size of 1024 and resolution of 0.5 Hz. We previously established that the random level of coherence was approximately 0.1 (Castro *et al.*, 2013).

Statistical analysis

In order to normalize the data and conduct parametric statistical tests, the Fisher z′ transform to the gamma coherence values was applied. Thereafter, the profile of the z′-coherence of the gamma band in 100 s epochs for each pair of EEG recordings, as well as the average of 12 epochs, was analysed, and the results were presented in a graphic form. In addition, for each cat, the z′-coherence

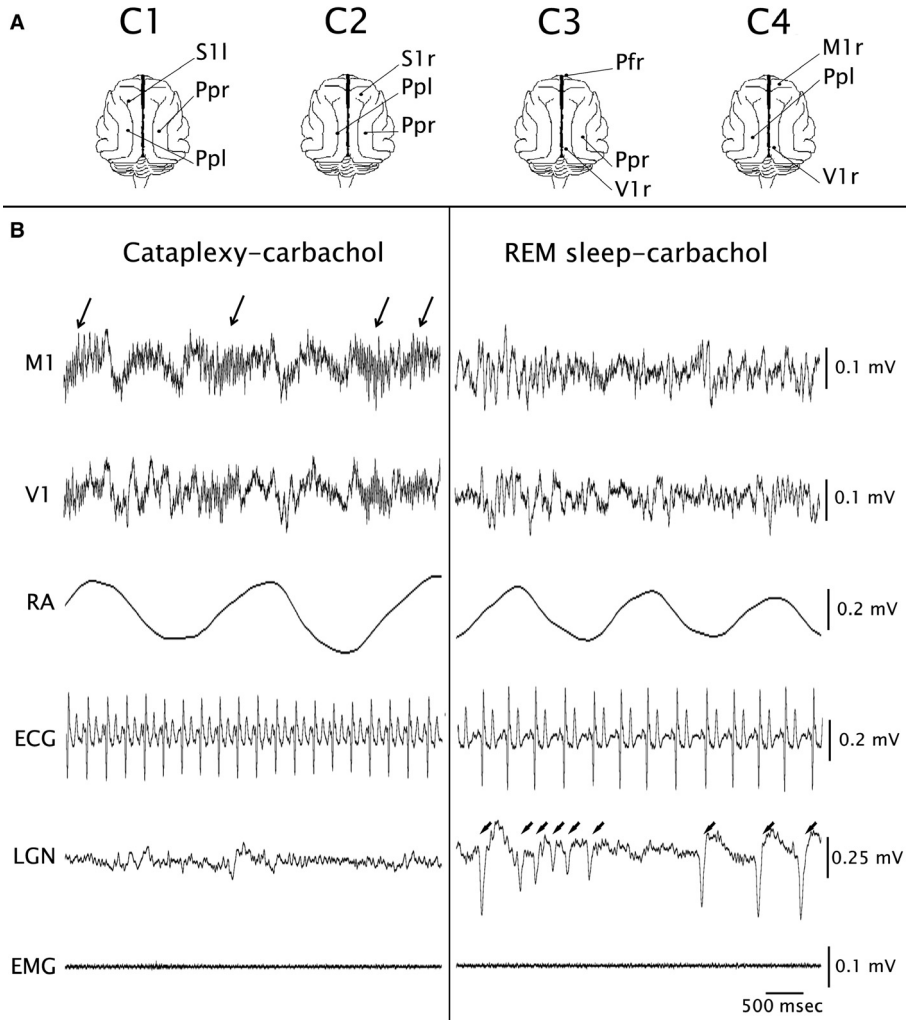

FIG. 1. (A) Location of recording electrodes. Recordings from these electrodes were referred to a common electrode, which was located over the frontal sinus. G1–G4, individual animals; M1, primary motor cortex; Pf, prefrontal cortex; Pp, posterior parietal cortex; S1, somato-sensory primary cortex; V1, visual primary cortex; r, right; l, left. (B) Polysomnographic recordings during Cataplexy induced by carbachol (CA). M1, V1 and lateral geniculate nuclei (LGN), electrogram, electromyogram (EMG), respiratory activity (RA) and electrocardiogram (ECG) during CA. Arrows indicate gamma oscillations. (C) Polysomnographic recordings during REMc. Arrowheads indicate PGO waves.

of the gamma band for all pairs of EEG channels was averaged across behavioural states and expressed as the mean ± SE. The significance of the differences between behavioural states was evaluated with the ANOVA and Tamhane *post hoc* tests. The criterion used to reject the null hypotheses was $P < 0.05$.

Results

Behavioural states induced by carbachol

As we have previously reported (Torterolo *et al.*, 2015), the microinjection of carbachol into the NPO induces either CA or REMc. The carbachol-induced states had a latency of 266 ± 29 s (mean ± SE). In addition, transitions from REMc to CA and vice versa were also observed spontaneously or provoked by sensory stimulation; the carbachol-induced states lasted 39–160 min. Figure 1B presents a representative recording during CA, and bursts of gamma oscillations are readily observed (at approximately 40 Hz, shown by arrows in Fig. 1B) in the primary motor cortex and primary visual cortex, as well as muscle atonia. In previous reports it has been established that this type of gamma activity is prominent during AW (Castro *et al.*, 2013, 2014). In addition, PGO waves were rarely observed during CA; the eyes were open with moderate pupillary dilatation and auditory and visual stimuli were tracked as during natural W (not shown). In contrast, as in naturally-occurring REM sleep, during REMc there were no clear gamma bursts in most of the animals (Fig. 1C) (Castro *et al.*, 2013, 2014). Furthermore, during REMc, PGO waves (shown by arrowheads in Fig. 1C) and muscle atonia were present. Additionally, the eyes were closed and the nictitating membrane was relaxed (not shown). Heart rate during REMc tended to be lower (Fig. 2A and B) (Torterolo *et al.*, 2015) and respiratory activity was more regular than during CA.

As previously reported (Torterolo *et al.*, 2015), mild auditory or somatic sensory stimulation during REMc aroused the animal even though atonia was maintained, i.e. CA was induced. There were also transitions from REMc to CA, which were triggered by spontaneous or uncontrolled environmental sounds. Spontaneous CA to REMc transitions were also observed. Interestingly, when the carbachol effect was diminishing and the animal aroused from REMc, it usually spent a few minutes in CA prior to entering into complete W.

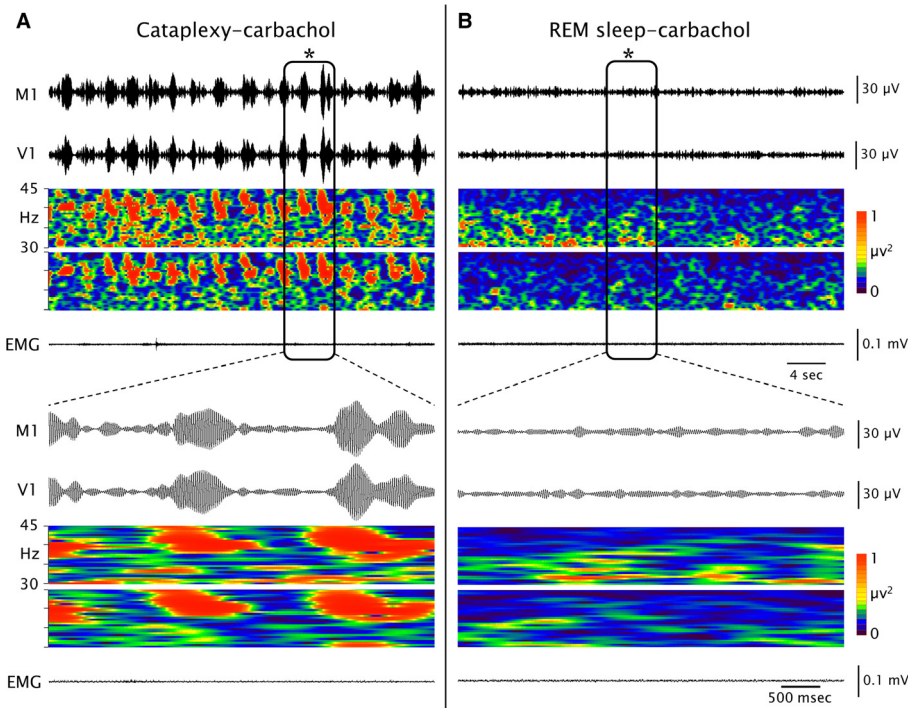

FIG. 2. Gamma band (30–45 Hz) oscillations and power during rapid eye movement (REM) sleep and Cataplexy induced by carbachol (CA). Simultaneous filtered (35–40 Hz) recordings and gamma power spectrograms from the primary motor cortex (M1) and primary visual cortex (V1) are shown together with electromyographic activity. Recordings are presented in a 40 s time window; below are shown recordings from the insets (*) with a 5 s time window. (A) CA. (B) REMc. Compared with REMc, gamma activity during cataplexy was larger and more strongly coupled between different areas.

This behaviour is similar to sleep paralysis, a clinical sign that often occurs in patients with narcolepsy (Guilleminault & Fromherz, 2011; Mignot, 2011).

Coherent gamma activity during cataplexy induced by carbachol and rapid eye movement sleep induced by carbachol

Gamma activity was unmasked after digital filtering, which included only 30–45 Hz oscillations. Filtered recordings and their spectrograms are shown during CA and REMc in Fig. 2. Note that, during CA, there was a strong coupling of EEG signals between the recorded cortices (Fig. 2A), as was demonstrated for AW (Castro *et al.*, 2013). This coherent gamma activity was present during CA in all of the animals studied. However, during REMc, gamma power was reduced and coupling was not present in three out of four animals (Fig. 2B). In one animal (labelled G1), coherent gamma activity was present during REMc; this special case will be analysed at the end of this section.

Coherence profiles for representative pairs of EEG leads are shown in Fig. 3A and B. The profile of twelve 100 s periods and their average during CA and REMc are shown in Fig. 3A. z′-coherence profiles for all 100 s periods as well as their average were larger during CA (with a restricted peak at 35–40 Hz), and were virtually absent during REMc. The average z′-coherence profile for a representative combination of cortices is shown for all naturally-occurring and carbachol-induced behavioural states in Fig. 3B. In spite of the presence of muscle atonia, the average gamma coherence profile during CA was similar to AW. However, gamma coherence during REMc was similar to naturally-occurring REM sleep. Intermediate values were present during QW and NREM sleep. The dynamic of gamma z′-coherence following carbachol microinjection into the NPO is shown in Fig. 3C and D; a high level of gamma coherence was present during CA but not during REMc.

The average z′-coherence in the 35–40 Hz band across behavioural states for all combinations of cortical recordings is presented in Table 1. In these independent analyses from different cortices from all cats, the results were consistent for CA, i.e. gamma z′-coherence was large and similar to AW. However, gamma coherence was minimal during REMc in most animals, and the values were similar to that present during naturally-occurring REM sleep.

Gamma power, which is shown in Fig. 4 and Table 2, was maximal during AW and CA. However, the gamma power during REMc was similar to that present during naturally-occurring REM sleep and QW. Gamma power values were minimal during NREM sleep.

In the animal G1, gamma power and coherence during naturally-occurring NREM and REM sleep, W and CA were similar to those present in the other animals (Tables 1 and 2). However, gamma activity during REMc was different. G1 showed long-duration bursts of high-amplitude coherent gamma oscillations during REMc, even though the classic features of REM sleep (atonia, PGO waves and relaxed nictitating membrane) were present. Values of gamma coherence and power were high in this animal (Tables 1 and 2).

Discussion

In the present report, we demonstrate that gamma coherence is significantly different during REMc and CA even though both states were induced by microinjections of carbachol into the NPO. The NPO of the cat (also called the medial pontine reticular formation or perilocus coeruleus α) and its corresponding nucleus in the rat, which is called the sublaterodorsal nucleus, is considered to exert

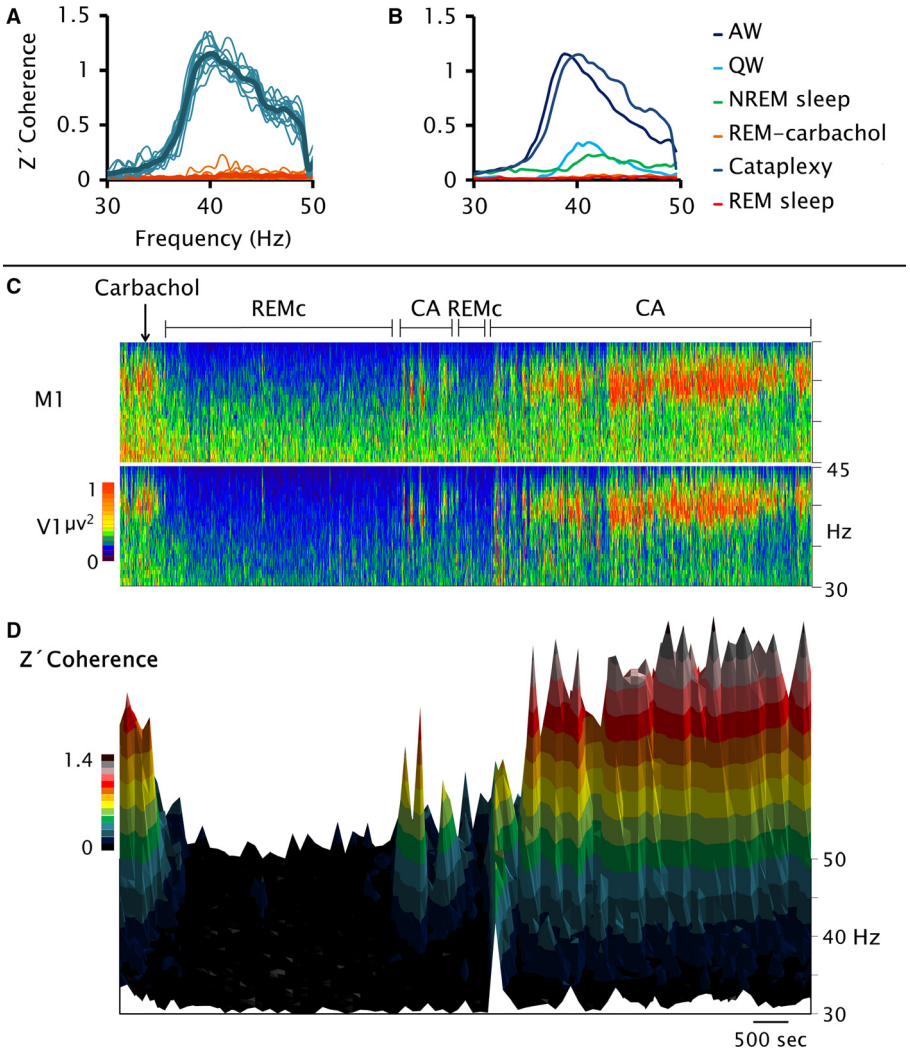

FIG. 3. Profile of electroencephalogram (EEG) gamma (30–45 Hz) coherence during rapid eye movement (REM) sleep and cataplexy induced by carbachol (CA). (A) Twelve profiles of z′-coherences (thin lines) of a representative pair of recordings (prefrontal and posterior parietal cortices of the same hemisphere) and averages of these 12 profiles (thick lines) are shown for REMc and CA. The profiles were constructed from periods of 100 s with a resolution of 0.5 Hz. Gamma coherence was maximal during CA and practically absent during REMc. (B) Averaged profiles during CA, REMc and naturally-occurring behavioural states. (C) Spectrograms of recordings from the primary motor cortex (M1) and primary visual cortex (V1) of the same hemisphere, following the microinjection of carbachol into the NPO. Episodes of REMc and CA are indicated. (D) Dynamic evolution of EEG coherence following the microinjection of carbachol into the NPO. Three-dimensional spectrogram of z′-coherence of the EEG (30–45 Hz) from simultaneous recordings from the M1 and V1. Time and frequency are shown on the horizontal and vertical (depth) axes, respectively; z′-coherence is represented by a colour code. z′-coherence was drastically reduced during REMc and was maximal during CA.

executive control over the initiation and maintenance of REM sleep (reviewed in Baghdoyan, 1997; Kubin, 2001; Reinoso-Suarez *et al.*, 2001; Luppi *et al.*, 2007; Siegel, 2011; Chase, 2013).

Gamma coherence

The EEG oscillations in the gamma frequency band (30–100 Hz) are involved in the integration or binding of spatially separated but temporally correlated neural events (Uhlhaas *et al.*, 2009, 2011; Rieder *et al.*, 2010). An increase in gamma power typically appears during states/behaviours that are characterized by active cognitive processing of external percepts or internally generated thoughts and images in humans, and during AW in animals (Llinas & Ribary, 1993; Tiitinen *et al.*, 1993; Castro *et al.*, 2013, 2014). Furthermore, gamma coherence between different brain areas, which is greatest during W, has been viewed as a neural correlate of consciousness (Llinas *et al.*, 1998); coherence in the gamma frequency band decreases during narcosis (unconsciousness) induced by anaesthesia (John, 2002; Mashour, 2006).

Gamma coherence during rapid eye movement sleep induced by carbachol

A single microinjection of carbachol into the NPO induces a state that is similar to naturally-occurring REM sleep, i.e. EEG desynchronization, PGO waves, rapid eye movements, muscle atonia, postsynaptic inhibition of motoneurons, hippocampal theta rhythm, respiratory depression and the absence of the 40 Hz rhythm of the olfactory bulb that occurs during W (Morales *et al.*, 1987; Lydic & Baghdoyan, 1989; Lopez-Rodriguez *et al.*, 1994; Garzon *et al.*, 1997).

In the present study, we demonstrated that, during REMc, coherent 40 Hz oscillations were practically absent in most animals, as in naturally-occurring REM sleep. However, although gamma coherence is strongly reduced during REMc and REM sleep, gamma

TABLE 1. Gamma (35–40 Hz) z′-coherence

	AW	QW	NREM	REM	REMc	CA	Statistical significances	F
G1								
Ppr-Ppl	1.13 ± 0.03	0.84 ± 0.07	0.77 ± 0.03	0.55 ± 0.03	1.50 ± 0.04	1.10 ± 0.04	REMc vs. ALL; CA vs. NREM, REM; AW vs. QW, NREM, REM; QW vs. REM; NREM vs. REM	61
S1 l-Ppl	0.98 ± 0.04	0.41 ± 0.03	0.53 ± 0.03	0.33 ± 0.01	1.36 ± 0.06	0.78 ± 0.02	REMc vs. ALL; CA vs. AW, QW, NREM, REM; AW vs. QW, NREM, REM; NREM vs. REM	114
G2								
Ppr-Ppl	0.43 ± 0.01	0.34 ± 0.04	0.05 ± 0.01	0.05 ± 0.01	0.03 ± 0.01	0.25 ± 0.02	REMc vs. CA, AW, QW, NREM; CA vs. AW, NREM, REM; AW vs. NREM, REM; QW vs. NREM, REM	101
S1r-Ppr	0.97 ± 0.02	0.60 ± 0.04	0.48 ± 0.01	0.48 ± 0.01	0.67 ± 0.01	0.82 ± 0.01	REMc vs. CA, AW, NREM, REM; CA vs. AW, QW, NREM, REM; AW vs. QW, NREM, REM	101
G3								
Pfr-Ppr	0.72 ± 0.05	0.27 ± 0.04	0.16 ± 0.01	0.10 ± 0.01	0.10 ± 0.01	0.84 ± 0.05	REMc vs. CA, AW, QW, NREM; CA vs. QW, NREM, REM; AW vs. QW, NREM, REM; QW vs. NREM, REM; NREM vs. REM	96
Pfr-V1r	0.88 ± 0.03	0.44 ± 0.01	0.37 ± 0.01	0.12 ± 0.01	0.19 ± 0.01	0.70 ± 0.03	REMc vs. CA, AW, QW, NREM; CA vs. QW, NREM, REM; AW vs. QW, NREM, REM; QW vs. NREM, REM; NREM vs. REM	210
Ppr-V1r	1.92 ± 0.03	1.47 ± 0.01	1.38 ± 0.01	1.05 ± 0.02	1.18 ± 0.01	1.92 ± 0.05	REMc vs. CA, AW, QW, NREM; CA vs. QW, NREM, REM; AW vs. QW, NREM REM; QW vs. NREM, REM; NREM vs. REM	208
G4								
M1r-V1r	0.91 ± 0.02	0.18 ± 0.01	0.15 ± 0.01	0.02 ± 0.01	0.02 ± 0.01	0.76 ± 0.05	REMc vs. CA, AW, QW, NREM; CA vs. QW, NREM, REM; AW vs. QW, NREM, REM; QW vs. NREM, REM; NREM vs. REM.	301
M1r-Ppl	0.77 ± 0.02	0.36 ± 0.04	0.18 ± 0.01	0.02 ± 0.01	0.01 ± 0.01	0.36 ± 0.04	REMc vs. CA, AW, QW, NREM; CA vs. AW, NREM, REM; AW vs. QW, NREM, REM; QW vs. NREM, REM; NREM vs. REM.	121

The values represent mean ± standard error. $P < 0.05$, ANOVA with Tamhane tests. All derivates have the same degrees of freedom (five between groups, 66 within groups). M1, primary motor cortex; Pf, prefrontal cortex; Pp, posterior-parietal cortex; S1, somato-sensory primary cortex; V1, visual primary cortex; r, right; l, left.
ALL, the rest of the behavioral states. AW, alert wakefulness; CA, cataplexy induced by carbachol; EEG, electroencephalogram; NPO, nucleus pontis oralis; NREM, non-rapid eye movement; PGO, ponto-geniculo-occipital; QW, quiet wakefulness; REM, rapid eye movement; REMc, rapid eye movement sleep induced by carbachol; W, wakefulness.

power during these states was similar to gamma power during QW and larger compared with NREM sleep.

A robust reduction of gamma coherence during naturally-occurring REM sleep has been previously demonstrated in the cat (Castro *et al.*, 2013, 2014), rat (Cavelli *et al.*, 2015) and humans (Perez-Garci *et al.*, 2001; Cantero *et al.*, 2004; Voss *et al.*, 2009). This significant diminution in gamma coherence strongly suggests that, during REM sleep, there is a decrease in the capacity for high-frequency integration among different neocortical areas. This phenomenon may underlie the distinctive pattern of REM sleep mentation, i.e. dreams (Hobson, 2009; Nir & Tononi, 2010).

In one animal there was coherent gamma activity during REMc. Interestingly, coherent gamma activity has been observed during REM sleep solely during lucid dreaming (Voss *et al.*, 2009). In fact, externally-imposed resonance at 40 Hz by means of electrical stimulation produces self-awareness (lucidity) during REM sleep (Voss *et al.*, 2014).

We do not have an explanation as to why gamma coherence during REMc in G1 differed from that in the other animals. However, it is possible that a small difference in the site of carbachol microinjection was responsible for the atypical electrocortical pattern of activity that was present during REMc in G1. As in our previous studies, the microinjection could spread into neighbouring areas, such as the locus coeruleus or the laterodorsal tegmental nucleus, that are critical in the promotion of W (Torterolo *et al.*, 2013). Recruiting mesopontine neurons with inherent gamma activity (Urbano *et al.*, 2012) could have induced a different pattern of gamma activity in the EEG.

Gamma coherence during cataplexy induced by carbachol

Emotionally-triggered cataplexy is observed in 60–70% of patients with narcolepsy; during cataplexy, REM sleep atonia emerges during W (Guilleminault & Fromherz, 2011; Mignot, 2011). Sleep

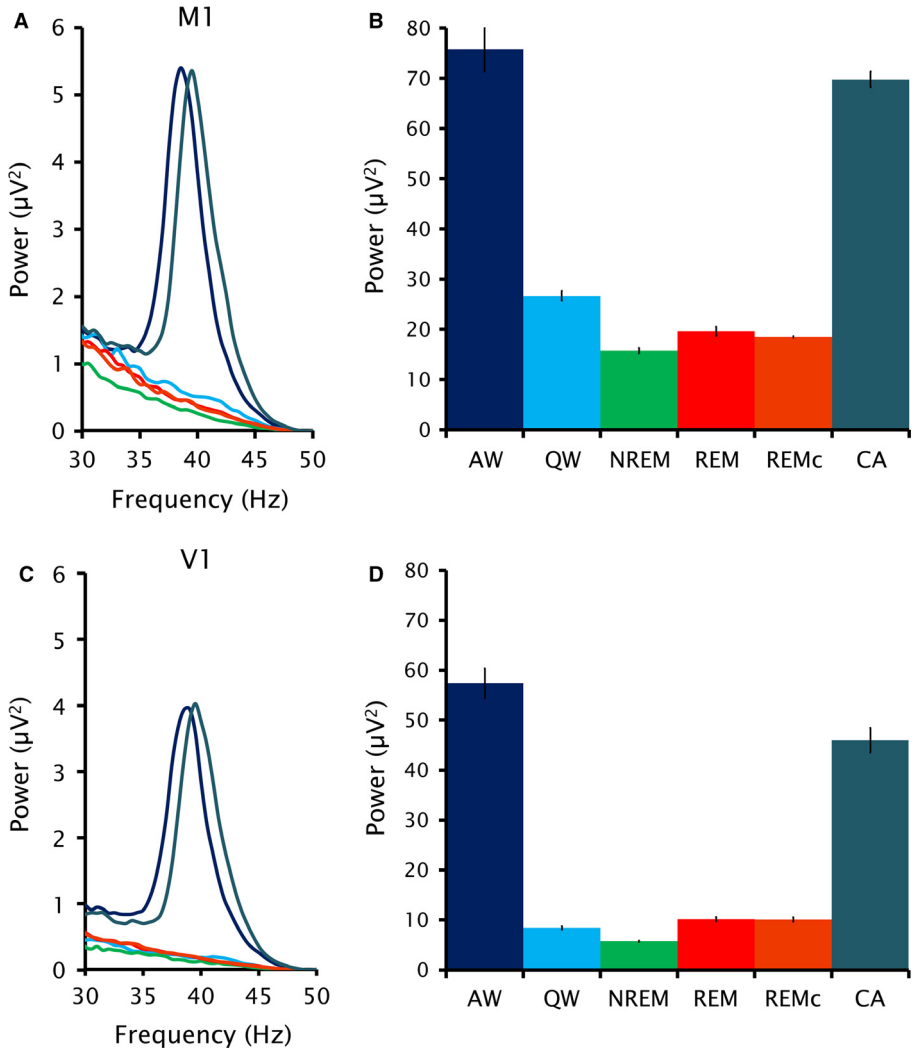

FIG. 4. Gamma band (30–45 Hz) power during naturally-occurring sleep, W and carbachol-induced states. (A) Averaged power profiles from primary motor cortex (M1) gamma activity (colours correspond to the colours of the bars in B). (B) Mean + SE of power values from the M1. (C) Averaged power profiles of gamma activity from the primary visual cortex (V1) (colours correspond to the colours of the bars in D). (D) Mean + SE of the power values from the V1. This example was obtained from animal G4 (see Table 2 for statistics).

paralysis is another condition in which REM sleep atonia takes place during W; this condition occurs in patients with narcolepsy but also as isolated periods of sleep paralysis in normal individuals (Sharpless & Grom, 2014). During sleep paralysis, the atonia is still maintained when individuals are aroused from REM sleep; fear is a common emotion during these periods (Sharpless & Grom, 2014). Interestingly, although we did not observe differences in somatomotor activity between CA and REMc, the gamma coherence during CA was high as in AW, suggesting that the animal was attentive and fully alert. However, as in naturally-occurring REM sleep, gamma coherence was absent during REMc.

Modulatory systems during rapid eye movement sleep and cataplexy

Cortical GABAergic neurons as well as glutamatergic thalamocortical neurons are critical for the generation of gamma band oscillations in the EEG (Llinas *et al.*, 1998; Buzsaki & Wang, 2012). Thalamocortical activity is modulated by regulatory systems that are comprised of small groups of neurons with a common neurotransmitter that project to various regions of the central nervous system (Jones, 2005). Cholinergic, monoaminergic and hypocretinergic neurons that integrate these systems play a critical role in the control of behavioural states (Torterolo & Vanini, 2010). By modulating the activity of the thalamocortical system, regulatory systems may control gamma oscillations and coherence.

The activity of regulatory neuronal systems has been studied during natural W and sleep states as well as during REMc by means of unit recordings or c-fos expression in different species (Yamuy *et al.*, 1995, 1998; Maloney *et al.*, 1999; Torterolo *et al.*, 2001, 2006; Lee *et al.*, 2005a,b; Lu *et al.*, 2006; Hassani *et al.*, 2009, 2010). In addition, the role of some of these systems has been assessed during cataplectic attacks in a canine model of narcolepsy (Wu *et al.*, 1999, 2004). Interestingly, as in naturally-occurring REM sleep, both serotonergic and noradrenergic neurons are inhibited during cataplectic attacks (Wu *et al.*, 1999, 2004). In contrast, although histaminergic neurons of the tuberomammillary nucleus of the hypothalamus are inhibited during naturally-occurring REM sleep, they are active during cataplexy (John *et al.*, 2004).

The activity of histaminergic neurons during cataplexy may also determine the presence and degree of gamma coherence during CA. However, as in naturally-occurring REM sleep, it is expected that,

TABLE 2. Gamma (35–40 Hz) power (μV^2)

	AW	QW	NREM	REM	REMc	CA	Statistical significance	F
G1								
Ppl	64.4 ± 2.4	18.3 ± 4.7	8.9 ± 0.3	15.1 ± 0.5	115.0 ± 12.6	32.3 ± 0.8	REMc vs. ALL; CA vs., NREM, REM; AW vs. QW, NREM, REM; NREM vs. REM	53
S1 l	15.3 ± 0.6	13.1 ± 0.9	7.6 ± 0.3	13.0 ± 0.6	28.5 ± 3.5	30.2 ± 0.7	REMc vs. ALL; CA vs. AW, QW, NREM, REM; AW vs. QW, NREM; QW vs. NREM; NREM vs. REM	27
G2								
Ppr	14.0 ± 0.8	10.8 ± 0.9	6.5 ± 0.6	9.7 ± 1.3	14.8 ± 0.6	25.3 ± 2.5	REMc vs. CA, QW, NREM, REM; CA vs. AW, QW, NREM, REM; AW vs. NREM; QW vs. NREM	26
S1r	26.2 ± 1.5	13.1 ± 0.9	6.1 ± 0.4	7.7 ± 0.5	10.2 ± 0.3	24.5 ± 2.5	REMc vs. CA, AW, NREM, REM; CA vs. QW, NREM, REM; AW vs. QW, NREM, REM; QW vs. NREM, REM	47
G3								
Pfr	60.9 ± 3.1	23.8 ± 3.6	12.5 ± 0.3	20.9 ± 0.4	20.3 ± 0.2	67.7 ± 4.7	REMc vs. CA, AW, NREM; CA vs. QW, NREM, REM; AW vs. QW, NREM, REM; NREM vs. REM	76
Ppr	57.6 ± 2.6	21.1 ± 3.9	10.3 ± 0.3	18.5 ± 0.5	12.0 ± 0.4	44.5 ± 3.8	REMc vs. CA, AW, NREM, REM; CA vs. QW, NREM, REM; AW vs. QW, NREM, REM; QW vs. NREM; NREM vs. REM	61
G4								
M1r	75.8 ± 4.3	26.7 ± 0.9	15.8 ± 0.5	19.6 ± 0.9	18.5 ± 0.2	69.8 ± 1.6	REMc vs. CA, AW, QW, NREM; CA vs. QW, NREM, REM; AW vs. QW, NREM, REM; QW vs. NREM, REM; NREM vs. REM.	195
V1r	57.4 ± 3.0	8.4 ± 0.3	5.8 ± 0.1	10.2 ± 0.5	10.1 ± 0.4	46.0 ± 2.6	REMc vs. CA, AW, NREM; CA vs. QW, NREM, REM; AW vs. QW, NREM, REM; QW vs. NREM; NREM vs. REM	195

The values represent mean ± standard error. $P < 0.05$. ANOVA with Tamhane tests. All derivates have the same degrees of freedom (five between groups, 66 within groups). The power unit is μV^2. M1, primary motor cortex; Pf, prefrontal cortex; Pp, posterior-parietal cortex; S1, somato-sensory primary cortex; V1, visual primary cortex; r, right; l, left.
ALL, the rest of the behavioral states. AW, alert wakefulness; CA, cataplexy induced by carbachol; EEG, electroencephalogram; NPO, nucleus pontis oralis; NREM, non-rapid eye movement; PGO, ponto-geniculo-occipital; QW, quiet wakefulness; REM, rapid eye movement; REMc, rapid eye movement sleep induced by carbachol; W, wakefulness.

during REMc, histaminergic neurons will drastically decrease their firing rate. Therefore, the activity of this neuronal group may be critically involved in promoting the alertness during cataplexy. Suppression of the activity of histaminergic neurons during REM sleep may be permissive for the induction of cognitive activities that are characteristic of this behavioural state, i.e. dreams.

A recent study highlighted the role of cortical-projecting GABAergic neurons of the basal forebrain in the generation of gamma oscillations in the EEG (Kim *et al.*, 2015). In addition, the authors suggested that cholinergic neurons within this area are not critical for the generation of these oscillations. The role of other wake-promoting neurons, such as dopaminergic and hypocretinergic neurons, in the generation of gamma power and coherence remains to be determined.

Gamma coherence in a paralysed body

During REM sleep, when dreams mainly occur, the networks that generate somato-motor atonia are activated. During pathological conditions such as cataplexy and sleep paralysis, REM sleep atonia is present in association with AW. Our data revealed that, when this type of paralysis is pharmacologically-induced, it is associated with a high degree of gamma power and coherence. In other words, high gamma coherence seems to be associated with alertness. Therefore, it is expected that in conditions such as the locked-in syndrome, which is mainly produced by lesions of descending motor pathways (Gosseries *et al.*, 2009) as well as during intraoperative awareness (Mashour & Avidan, 2015), gamma coherence would be high. Consequently, the present data suggest that measures of gamma power and coherence will be of assistance in diagnosing the presence of consciousness when communication with patients is not possible (Owens *et al.*, 2009).

Conclusions

In the present report, we conducted a comprehensive analysis of gamma coherence in cats during REMc, CA and naturally-occurring behavioural states. We determined that there are remarkable differences in cortical activity during REMc compared with CA, in spite of the presence of somatic muscle paralysis during both states. We conclude that EEG gamma (≈40 Hz) coherence is a trait that differentiates W from REM sleep.

Acknowledgements

This study was supported by the Programa de Desarrollo de Ciencias Básicas, PEDECIBA and by the Agencia Nacional de Investigación en Innovación (ANII) (FCE-2-2011-1-7030 grant) from Uruguay. S.C.-Z. and M.C.

currently have a postgraduate fellowship from the ANII. The authors are grateful to Giancarlo Vanini for his critical comments of the manuscript.

Abbreviations

AW, alert wakefulness; CA, cataplexy induced by carbachol; EEG, electroencephalogram; NPO, nucleus pontis oralis; NREM, non-rapid eye movement; PGO, ponto-geniculo-occipital; QW, quiet wakefulness; REM, rapid eye movement; REMc, rapid eye movement sleep induced by carbachol; W, wakefulness.

References

Baghdoyan, H.A. (1997) Cholinergic mechanism regulating REM sleep. In Schwartz, W.J. (Ed.), *Sleep Science: Integrating Basic Research and Clinical Practice. Monographs in clinical neuroscience*. Karger, Basel, pp. 88–116.

Berman, A.L. (1968) *The Brain Stem of the cat. A Cytoarchitectonic Atlas with Stereotaxic Coordinates*. University of Wisconsin, Madison.

Bullock, T.H., McClune, M.C. & Enright, J.T. (2003) Are the electroencephalograms mainly rhythmic? Assessment of periodicity in wide-band time series. *Neuroscience*, **121**, 233–252.

Buzsaki, G. & Wang, X.J. (2012) Mechanisms of gamma oscillations. *Annu. Rev. Neurosci.*, **35**, 203–225.

Cantero, J.L., Atienza, M., Madsen, J.R. & Stickgold, R. (2004) Gamma EEG dynamics in neocortex and hippocampus during human wakefulness and sleep. *NeuroImage*, **22**, 1271–1280.

Castro, S., Falconi, A., Chase, M.H. & Torterolo, P. (2013) Coherent neocortical 40-Hz oscillations are not present during REM sleep. *Eur. J. Neurosci.*, **37**, 1330–1339.

Castro, S., Cavelli, M., Vollono, P., Chase, M.H., Falconi, A. & Torterolo, P. (2014) Inter-hemispheric coherence of neocortical gamma oscillations during sleep and wakefulness. *Neurosci. Lett.*, **578**, 197–202.

Cavelli, M., Castro, S., Schwarzkopf, N., Chase, M.H., Falconi, A. & Torterolo, P. (2015) Coherent neocortical gamma oscillations decrease during REM sleep in the rat. *Behav. Brain Res.*, **281**, 318–325.

Chase, M.H. (2013) Motor control during sleep and wakefulness: clarifying controversies and resolving paradoxes. *Sleep Med. Rev.*, **17**, 299–312.

Dauvilliers, Y., Siegel, J.M., Lopez, R., Torontali, Z.A. & Peever, J.H. (2014) Cataplexy – clinical aspects, pathophysiology and management strategy. *Nat. Rev. Neurol.*, **10**, 386–395.

Edelman, G.M. & Tononi, G. (2000) *A Universe of Consciousness*. Basic Books, New York.

Garzon, M., de Andres, I. & Reinoso-Suarez, F. (1997) Neocortical and hippocampal electrical activities are similar in spontaneous and cholinergic-induced REM sleep. *Brain Res.*, **766**, 266–270.

Gosseries, O., Bruno, M., Vanhaudenhuyse, A., Laureys, S. & Schnakers, C. (2009) Consciousness in the locked-in syndrome. In Laureys, S. & Tononi, G. (Eds), *The Neurology of Consciousness: Cognitive Neuroscience and Neuropathology*. Elsevier, San Diego, pp. 191–203.

Guilleminault, C. & Fromherz, S. (2011) Narcolepsy: diagnosis and management. In Kryger, M.H., Roth, T. & Dement, W.C. (Eds), *Principles and Practices of Sleep Medicine*. Saunders, Philadelphia, pp. 957–968.

Hassani, O.K., Lee, M.G. & Jones, B.E. (2009) Melanin-concentrating hormone neurons discharge in a reciprocal manner to orexin neurons across the sleep-wake cycle. *Proc. Natl. Acad. Sci. USA.*, **106**, 2418–2422.

Hassani, O.K., Henny, P., Lee, M.G. & Jones, B.E. (2010) GABAergic neurons intermingled with orexin and MCH neurons in the lateral hypothalamus discharge maximally during sleep. *Eur. J. Neurosci.*, **32**, 448–457.

Hobson, J.A. (2009) REM sleep and dreaming: towards a theory of protoconsciousness. *Nat. Rev. Neurosci.*, **10**, 803–813.

John, E.R. (2002) The neurophysics of consciousness. *Brain Res. Brain Res. Rev.*, **39**, 1–28.

John, J., Wu, M.F., Boehmer, L.N. & Siegel, J.M. (2004) Cataplexy-active neurons in the hypothalamus: implications for the role of histamine in sleep and waking behavior. *Neuron*, **42**, 619–634.

Jones, B.E. (2005) From waking to sleeping: neuronal and chemical substrates. *Trends Pharmacol. Sci.*, **26**, 578–586.

Jouvet, M. (1965) The paradoxical phase of sleep. *Int. J. Neurol.*, **5**, 131–150.

Kim, T., Thankachan, S., McKenna, J.T., McNally, J.M., Yang, C., Choi, J.H., Chen, L., Kocsis, B., Deisseroth, K., Strecker, R.E., Basheer, R., Brown, R.E. & McCarley, R.W. (2015) Cortically projecting basal forebrain parvalbumin neurons regulate cortical gamma band oscillations. *Proc. Natl. Acad. Sci. USA.*, **112**, 3535–3540.

Kubin, L. (2001) Carbachol models of REM sleep: recent developments and new directions. *Arch. Ital. Biol.*, **139**, 147–168.

Lee, M.G., Hassani, O.K., Alonso, A. & Jones, B.E. (2005a) Cholinergic basal forebrain neurons burst with theta during waking and paradoxical sleep. *J. Neurosci.*, **25**, 4365–4369.

Lee, M.G., Hassani, O.K. & Jones, B.E. (2005b) Discharge of identified orexin/hypocretin neurons across the sleep-waking cycle. *J. Neurosci.*, **25**, 6716–6720.

Llinas, R. & Ribary, U. (1993) Coherent 40-Hz oscillation characterizes dream state in humans. *Proc. Natl. Acad. Sci. USA.*, **90**, 2078–2081.

Llinas, R., Ribary, U., Contreras, D. & Pedroarena, C. (1998) The neuronal basis for consciousness. *Philos. T. Roy. Soc. B.*, **353**, 1841–1849.

Lopez-Rodriguez, F., Kohlmeier, K., Morales, F.R. & Chase, M.H. (1994) State dependency of the effects of microinjection of cholinergic drugs into the nucleus pontis oralis. *Brain Res.*, **649**, 271–281.

Lu, J., Jhou, T.C. & Saper, C.B. (2006) Identification of wake-active dopaminergic neurons in the ventral periaqueductal gray matter. *J. Neurosci.*, **26**, 193–202.

Luppi, P.H., Gervasoni, D., Verret, L., Goutagny, R., Peyron, C., Salvert, D., Leger, L. & Fort, P. (2007) Paradoxical (REM) sleep genesis: The switch from an aminergic-cholinergic to a GABAergic-glutamatergic hypothesis. *J. Physiology-Paris*, **100**, 271–283.

Lydic, R. & Baghdoyan, H.A. (1989) Cholinoceptive pontine reticular mechanisms cause state-dependent respiratory changes in the cat. *Neurosci. Lett.*, **102**, 211–216.

Maloney, K.J., Mainville, L. & Jones, B.E. (1999) Differential c-Fos expression in cholinergic, monoaminergic, and GABAergic cell groups of the pontomesencephalic tegmentum after paradoxical sleep deprivation and recovery. *J. Neurosci.*, **19**, 3057–3072.

Mashour, G.A. (2006) Integrating the science of consciousness and anesthesia. *Anesth. Analg.*, **103**, 975–982.

Mashour, G.A. & Avidan, M.S. (2015) Intraoperative awareness: controversies and non-controversies. *Brit. J. Anaesth.*, **115**(Suppl 1), i20–i26.

Mignot, E. (2011) Narcolepsy: pathophysiology and genetic predisposition. In Krieger, M.H., Roth, T. & Dement, W. (Eds), *Principles and Practices of Sleep Medicine*. Saunders, Philadelphia, pp. 938–956.

Morales, F.R., Engelhardt, J.K., Soja, P.J., Pereda, A.E. & Chase, M.H. (1987) Motoneuron properties during motor inhibition produced by microinjection of carbachol into the pontine reticular formation of the decerebrate cat. *J. Neurophysiol.*, **57**, 1118–1129.

Nir, Y. & Tononi, G. (2010) Dreaming and the brain: from phenomenology to neurophysiology. *Trends Cogn. Sci.*, **14**, 88–100.

Owens, A., Schiff, N.D. & Laureys, S. (2009) The assessment of conscious awareness in the vegetative state. In Laureys, S. & Tononi, G. (Eds), *The Neurology of Consciousness: Cognitive Neuroscience and Neuropathology*. Elsevier, San Diego, pp. 163–172.

Perez-Garci, E., del-Rio-Portilla, Y., Guevara, M.A., Arce, C. & Corsi-Cabrera, M. (2001) Paradoxical sleep is characterized by uncoupled gamma activity between frontal and perceptual cortical regions. *Sleep*, **24**, 118–126.

Reinoso-Suarez, F., de Andres, I., Rodrigo-Angulo, M.L. & Garzon, M. (2001) Brain structures and mechanisms involved in the generation of REM sleep. *Sleep Med. Rev.*, **5**, 63–77.

Rieder, M.K., Rahm, B., Williams, J.D. & Kaiser, J. (2010) Human gamma-band activity and behavior. *Int. J. Psychophysiol.*, **79**, 39–48.

Sharpless, B.A. & Grom, J.L. (2014) Isolated sleep paralysis: fear, prevention, and disruption. *Behav. Sleep Med.*, 1–6.

Siegel, J.M. (2011) REM sleep. In Kryger, M.H., Roth, T. & Dement, W.C. (Eds), *Principles and Practices of Sleep Medicine*. Elsevier-Saunders, Philadelphia, pp. 92–111.

Tiitinen, H., Sinkkonen, J., Reinikainen, K., Alho, K., Lavikainen, J. & Naatanen, R. (1993) Selective attention enhances the auditory 40-Hz transient response in humans. *Nature*, **364**, 59–60.

Tononi, G. (2009) Sleep and dreaming. In Laureys, S. & Tononi, G. (Eds), *The Neurology of Consciousness: Cognitive Neuroscience and Neuropathology*. Elsevier, San Diego, pp. 89–107.

Torterolo, P. & Vanini, G. (2010) Nuevos conceptos sobre la generación y el mantenimiento de la vigilia. *Revista Neurología*, **50**, 747–758.

Torterolo, P., Yamuy, J., Sampogna, S., Morales, F.R. & Chase, M.H. (2001) Hypothalamic neurons that contain hypocretin (orexin) express c-fos during active wakefulness and carbachol-induced active sleep. *Sleep Res. Online*, **4**, 25–32.

Torterolo, P., Sampogna, S., Morales, F.R. & Chase, M.H. (2006) MCH-containing neurons in the hypothalamus of the cat: searching for a role in the control of sleep and wakefulness. *Brain Res.*, **1119**, 101–114.

Torterolo, P., Sampogna, S. & Chase, M.H. (2013) Hypocretinergic and non-hypocretinergic projections from the hypothalamus to the REM sleep executive area of the pons. *Brain Res.*, **1491**, 68–77.

Torterolo, P., Castro-Zaballa, S., Cavelli, M., Velasquez, N., Brando, V., Falconi, A., Chase, M.H. & Migliaro, E.R. (2015) Heart rate variability during carbachol-induced REM sleep and cataplexy. *Behav. Brain Res.*, **291**, 72–79.

Uhlhaas, P.J., Pipa, G., Lima, B., Melloni, L., Neuenschwander, S., Nikolic, D. & Singer, W. (2009) Neural synchrony in cortical networks: history, concept and current status. *Front. Integr. Neurosci.*, **3**, 17.

Uhlhaas, P.J., Pipa, G., Neuenschwander, S., Wibral, M. & Singer, W. (2011) A new look at gamma? High- (>60 Hz) gamma-band activity in cortical networks: function, mechanisms and impairment. *Prog. Biophys. Mol. Biol.*, **105**, 14–28.

Urbano, F.J., Kezunovic, N., Hyde, J., Simon, C., Beck, P. & Garcia-Rill, E. (2012) Gamma band activity in the reticular activating system. *Front. Neurol.*, **3**, 6.

Ursin, R. & Sterman, M. (1981) *Manual for Standardized Scoring of Sleep and Waking States in Adult Cats*. BIS/BRI, University of California, Los Angeles.

Voss, U., Holzmann, R., Tuin, I. & Hobson, J.A. (2009) Lucid dreaming: a state of consciousness with features of both waking and non-lucid dreaming. *Sleep*, **32**, 1191–1200.

Voss, U., Holzmann, R., Hobson, A., Paulus, W., Koppehele-Gossel, J., Klimke, A. & Nitsche, M.A. (2014) Induction of self awareness in dreams through frontal low current stimulation of gamma activity. *Nat. Neurosci.*, **17**, 810–812.

Wu, M.F., Gulyani, S.A., Yau, E., Mignot, E., Phan, B. & Siegel, J.M. (1999) Locus coeruleus neurons: cessation of activity during cataplexy. *Neuroscience*, **91**, 1389–1399.

Wu, M.F., John, J., Boehmer, L.N., Yau, D., Nguyen, G.B. & Siegel, J.M. (2004) Activity of dorsal raphe cells across the sleep-waking cycle and during cataplexy in narcoleptic dogs. *J. Physiol.*, **554**, 202–215.

Yamuy, J., Sampogna, S., Lopez-Rodriguez, F., Luppi, P.H., Morales, F.R. & Chase, M.H. (1995) Fos and serotonin immunoreactivity in the raphe nuclei of the cat during carbachol-induced active sleep: a double-labeling study. *Neuroscience*, **67**, 211–223.

Yamuy, J., Sampogna, S., Morales, F.R. & Chase, M.H. (1998) c-fos expression in mesopontine noradrenergic and cholinergic neurons of the cat during carbachol-induced active sleep: a double labeling study. *Sleep Res. Online*, **1**, 28–40.

6. Discusión

La banda gamma de frecuencias en el EEG fue descrita originalmente Jasper et al. (1938), y corresponde al ritmo cognitivo de 40 Hz introducido por Das et al. (1955). Varios estudios confirmaron que esta banda de frecuencia juega un papel importante en las funciones cognitivas (Llinas et al., 1998).

En el Trabajo 1, demostramos en el gato que la coherencia en la banda gamma de frecuencias entre EEG corticales intrahemisféricos es mayor durante la AW que durante la QW. Esta disminuyó a un valor menor durante el sueño NREM, y alcanzo su nadir durante el sueño REM. Por lo tanto, durante el sueño REM, el acoplamiento de la actividad neuronal entre diferentes áreas corticales a disminuye al mínimo.

En el Trabajo 2 demostramos que la coherencia inter-hemisférica EEG en la banda de frecuencias gamma baja (30-45 Hz) es mayor durante AW que QW. La coherencia gamma disminuyó a un nivel inferior durante el sueño NREM y REM en comparación con QW. Entre zonas homólogas interhemisféricas la coherencia z' fue similar durante el NREM y el sueño REM, mientras que entre las áreas interhemisféricas no simétricas (heterólogas), la coherencia gamma alcanzó su nadir durante el sueño REM, al igual que entre áreas intrahemisféricas.

En el Trabajo 3, demostramos que la coherencia gamma es significativamente diferente durante REMc y CA. Durante CA, la coherencia gamma fue similar a la de AW, a pesar de la atonía muscular generada por la inyección de carbacol en el NPO. Durante el REMc la coherencia gamma fue mínima, al igual que durante el sueño REM natural.

6.1. Consideraciones técnicas

6.1.1. La actividad gamma observada no es "artefacto"

Podemos descartar que los potenciales extracerebrales generados por músculos, corazón o movimientos oculares sean la causa de la gran coherencia observada durante AW basándonos en dos argumentos.

Primero, la coherencia gamma entre el EEG y la actividad de diferentes EMGs, ECG y EOG registrados ya sea por electrodos bipolares o monopolares, fue despreciable (parte de estos resultados se observan en la Figura suplementaria1 del Trabajo 1). Segundo, observamos que existe una latencia variable entre la gran mayoría de los picos de las ondas gamma entre los diferentes registros corticales registrados simultáneamente. Esta latencia es proporcional a la distancia entre los electrodos de registro corticales (datos no mostrados). Si estos potenciales fueran producidos por una fuente extracerebral, no se esperaría encontrar latencia entre los diferentes registros corticales. Este hecho también descarta la conducción de volumen como un componente importante de la coherencia en la banda gamma.

Otro aspecto importante es que durante la CA (donde es prácticamente nula la actividad muscular), la coherencia gamma fue alta como en AW. Esto contribuye a demostrar que el aumento del acoplamiento de las oscilaciones gamma se debe a el estado de alerta cognitivo del animal y no a su nivel de actividad muscular. Además, en un modelo farmacológico de psicosis (ketamina, ver Capítulo III) la coherencia gamma se reduce al nivel de sueño REM sin que se produzca la atonía muscular característica de este, y con una potencia gamma similar a la de la vigilia tranquila.

Datos obtenidos en EEG registrados en humanos indican que los movimientos sacádicos oculares son una fuente de oscilaciones gamma en derivaciones frontales (Yuval-Greenberg et al., 2008). Sin embargo, la ausencia de coherencia entre el EEG y el EOG, así como la ausencia de coherencia gamma durante el sueño REM, cuando movimientos sacádicos son intensos, indica que estos movimientos no tienen un impacto en la generación de la coherencia gamma en el gato.

Otra posibilidad es que la actividad gamma del bulbo olfatorio esté transmitiéndose a nuestros electrodos corticales (Libano et al., 2008), ya sea por conducción de volumen o porque sea registrado por nuestro

electrodo indiferente en el seno frontal. Para descartar estas opciones realizamos registros simultáneos del bulbo olfatorio y 7 áreas corticales. Si la actividad gamma del bulbo olfatorio estuviera transmitiéndose a nuestros electrodos corticales deberíamos observar una gran coherencia gamma entre el registro bulbar y los registros corticales. Sin embargo, eso no sucede. La coherencia gamma entre el registro bulbar y los registros corticales cercanos es mucho más baja que la coherencia entre las áreas corticales más alejadas (datos no mostrados). A su vez, existen desfasajes muy grandes entre las oscilaciones gamma del bulbo olfatorio y las corticales lo que descarta la conducción de volumen entre estos. Por último, la actividad gamma del bulbo olfatorio tiene un patrón diferente de frecuencias, es decir, un espectrograma diferente al de la actividad gamma de la corteza cerebral.

También hicimos experimentos en gato cambiando la posición del electrodo indiferente y obtuvimos los mismos resultados (datos no mostrados). Además realizamos registros bipolares corticales y talámicos en los que se observan las oscilaciones gamma lo que descarta que sean un artefacto introducido a través del electrodo indiferente.

Además, realizamos registros en rata y ratones con electrodos monopolares. Se colocó un electrodo de referencia común en el hueso por encima del cerebelo. En estos registros, al igual que en nuestro trabajo en gatos, también pudimos observar una disminución de la coherencia gamma durante el sueño REM a pesar de que la potencia gamma durante el mismo permaneció elevada (Anexo 1, 2, Cavelli et al., 2017).

6.1.2. Análisis de coherencia en ventanas de 100 segundos

Utilizamos ventanas de 100 segundos para discernir características generales del patrón de coherencias. Tambien utilizamos ventanas de 10 segundos para analizar la dinámica de la actividad gamma en la rata y gato (Anexo 3, Cavelli et al., 2017). Sin embargo, la escala temporal de los eventos funcionalmente significativos y fluctuaciones de la actividad

cerebral es mucho más corta. En relación a las funciones cognitivas, Libet et al. (1991) demostraron que para una experiencia sensorial consciente es necesaria una activación neuronal apropiada durante 500 ms. De modo que, desde un punto de vista electrofisiológico, en una ventana de 100 segundos estamos promediando los resultados de diferentes eventos ocurridos durante la vigilia (ej. potenciales evocados cognitivos, sensitivos o motores), durante el sueño NREM (ej. husos de sueño y ondas lentas) o el sueño REM (ej. ondas PGO y desincronización tónica del EEG). Sin embargo, también demostramos un incremento del acoplamiento gamma durante períodos cortos de análisis. Se evidenció una gran correlación (R^2 = 0.81) en registros filtrados durante 6 segundos de AW. Además, el acoplamiento fue observado en las “ráfagas” gamma de 200 a 500 ms de duración presentes en registros crudos y filtrados durante AW; estas “ráfagas” gamma acopladas también se identifican claramente por la función de correlación cruzada. En contraste, el acoplamiento de la banda gamma desapareció durante el sueño REM.

6.2. Coherencia gamma durante la vigilia

Es bien conocido que la potencia y la coherencia gamma aumentan durante la vigilia en animales y humanos (Llinas & Ribary, 1993; Maloney et al., 1997; Lieder et al., 2010). En el gato, la coherencia de la banda gamma se incrementa durante la AW entre electrodos localizados en sitios corticales y talámicos (Bouyer et al., 1981). En el presente trabajo demostramos que durante AW la coherencia gamma aumenta entre distintas áreas corticales. Este incremento de coherencia ocurre durante estados de alerta que son inducidos por estimulación con sonido, luz, o con la colocación de un espejo en frente del animal (o inmediatamente después de estos procedimientos). La coherencia gamma también aumenta cuando el nivel de alerta es alto al principio del registro o cuando un individuo entra en la sala de registros, especialmente si los individuos que entran son

desconocidos para el animal. Por lo tanto, es el estado de alerta *per se*, y no el estímulo lo que incrementa la coherencia en la banda gamma.

Es importante destacar que el incremento de coherencia gamma es muy marcado incluso si lo comparamos con la QW, y que se limita a una banda de frecuencias bastante estrecha entre 30 y 45 Hz con un máximo en aproximadamente 37 Hz.

Este aumento del acoplamiento de la actividad EEG en la banda gamma de frecuencias durante AW estuvo presente en todos los pares de áreas corticales analizadas. Eso fue así tanto para la coherencia medida entre cortezas prefrontal y perceptuales, así como entre las cortezas perceptuales. Áreas corticales tan alejadas como la corteza prefrontal y la corteza visual primaria también muestran un importante nivel de coherencia. Las diferencias entre los valores de coherencia entre diferentes pares de registros corticales durante AW pueden estar relacionadas con la distancia entre los electrodos y con el nivel de conexiones recíprocas entre ellos (Cantero et al., 2000).

Es importante destacar que al momento de realizar el estímulo sonoro fue necesario darle una gran variabilidad a la frecuencia de presentación, para que este aumento de la coherencia gamma se mantuviera por periodos de tiempo suficientemente largos para su análisis. Si el estimulo sonoro era repetitivo o muy homogéneo, la coherencia gamma se reducía rápidamente (a pocos segundos de haber iniciado el estímulo) a niveles de QW.

Durante las condiciones patológicas como la cataplejía y la parálisis del sueño (signos característicos de la narcolepsia), la atonía del sueño REM se asocia a la vigilia alerta. Nuestros datos revelaron que cuando este tipo de parálisis es farmacológicamente inducido, se asocia con un alto grado de potencia y coherencia gamma. Por lo tanto, es esperable que en las condiciones patológicas mencionadas, en el síndrome de encerramiento (producido principalmente por lesiones de las vías motoras descendentes, Gosseries et al., 2009), así como durante los raros casos de consciencia

durante la anestesia general quirúrgica (Mashour & Avidan, 2015), la coherencia gamma sea alta. Por lo tanto, la monitorización de la potencia gamma y la coherencia podría ser de ayuda en el diagnóstico de la presencia de consciencia cuando la comunicación con el paciente no es posible (Owens et al., 2009).

6.3. Aumento de la coherencia gamma durante AW: impacto en las funciones cognitivas

El cerebro es una red neuronal muy grande en la cual, si bien existen especializaciones funcionales marcadas, las neuronas tienen oportunidades de interactuar entre sí a través de pocas uniones sinápticas. Esta conectividad funcional y efectiva es necesaria para sustentar las funciones cognitivas, y permite la coexistencia en circuitos neuronales tálamocorticales, tanto la especialización funcional como la integración. Según Tononi (2010), estas características de la conectividad permiten a nuestras habilidades cognitivas ser dependientes del contexto y adaptarnos al mundo complejo que vivimos.

Nuestros datos muestran que el gran aumento del acoplamiento entre la actividad EEG en la banda gamma de frecuencias de distintas áreas corticales (incluso áreas corticales alejadas, ver Figura II.1), se asocia al estado de alerta provocado por la exposición a estímulos novedosos, más que al estado de vigilia propiamente dicho. Esto sugiere que dicho fenómeno podría estar en la base fisiológica de la integración del procesamiento de información sensorial permitiendo una percepción consciente unificada y selectiva de los estímulos ambientales que son importantes para el animal. En otras palabras, el acoplamiento de la actividad en la banda gamma de frecuencias podría ser la base de funciones cognitivas como la atención y la percepción.

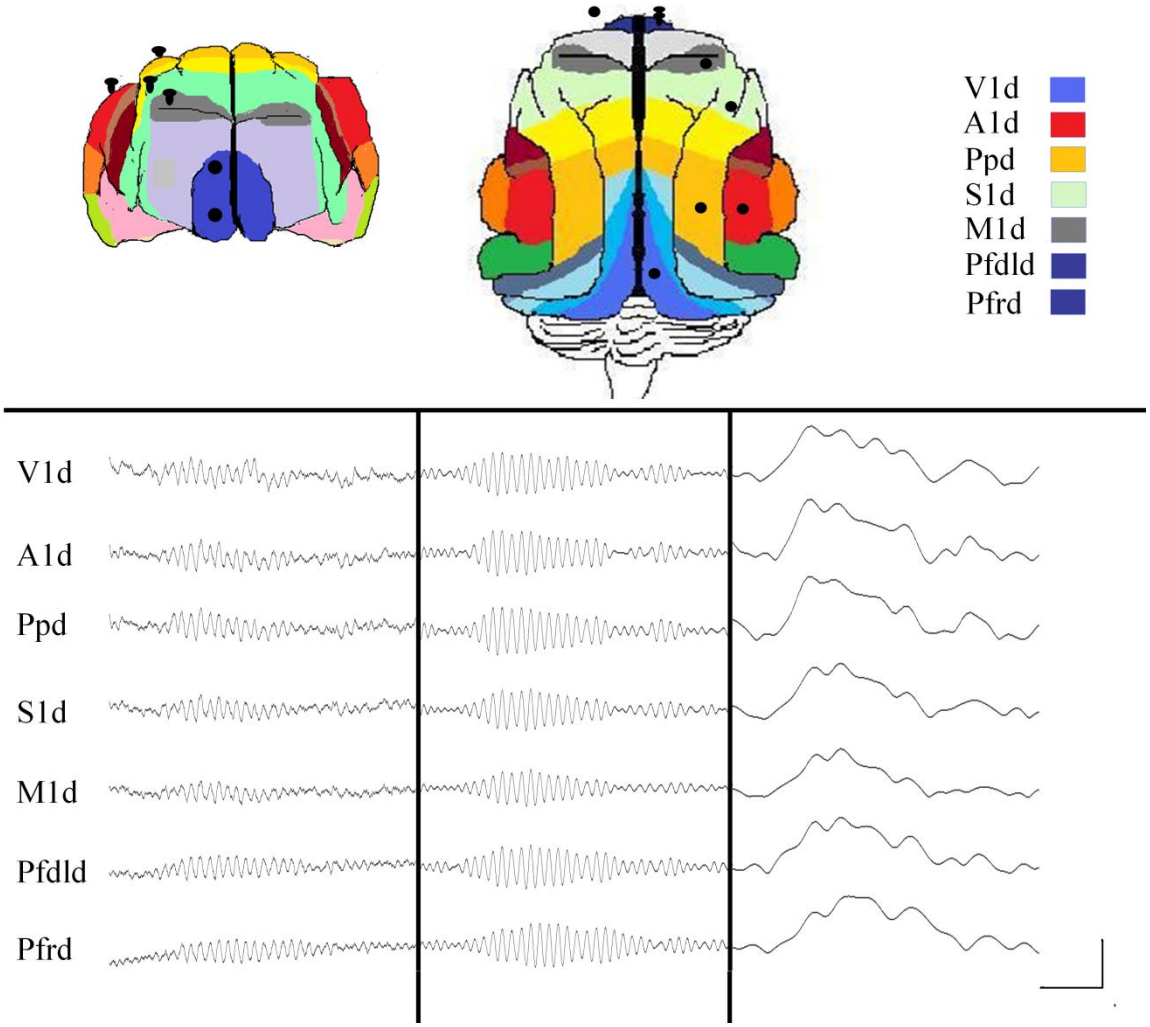

Figura II.1. **Oscilaciones gamma registradas simultáneamente en 7 áreas corticales.** En la parte superior de la imagen se puede observar una vista anterior y una vista superior del cerebro del gato donde se muestra la posición de 7 electrodos de registro corticales en el hemisferio cerebral derecho. En la parte inferior se puede observar el registro simultáneo de una oscilación gamma en 7 áreas corticales. A la izquierda se observa el registro crudo, en el medio el registro filtrado (pasa-banda 30-45 Hz) y a la derecha la envolvente de esa oscilación gamma. Se puede observar que existe un gran acoplamiento entre las diferentes áreas corticales. Barra de calibración horizontal: 200 ms, barra de calibración vertical: 200 µV en el registro crudo 100 µV en el registro filtrado y 50 µV en el registro de las envolventes. Pfrd: corteza prefrontal rostral derecha; Pfdld: corteza

prefrontal dorsolateral derecha; M1d: corteza motora primaria derecha; S1d: corteza somatosensorial primaria derecha; Ppd: corteza parietal posterior derecha; A1d: corteza auditiva derecha; V1d: corteza visual derecha.

6.4. Coherencia gamma durante el sueño

Varios estudios en seres humanos han evaluado el grado de acoplamiento en la banda gamma de frecuencias durante la vigilia y el sueño. Aunque los primeros trabajos sugieren ciertas diferencias con nuestros hallazgos, los trabajos más recientes (especialmente los trabajos de Ursula Voss, Allan Hobson y colaboradores) están de acuerdo con estos. A continuación, comentaremos los resultados de los principales estudios en seres humanos.

Llinas and Ribary (1993) describieron que durante el sueño REM las oscilaciones a 40 Hz en magneto-encefalograma (MEG) eran similares en distribución de fase y amplitud a aquellas observadas durante la vigilia; en contraste, la actividad gamma coherente estaba reducida durante el sueño NREM (Llinas & Ribary, 1993). Estos autores también mostraron que las oscilaciones gamma se hacían muy coherentes en ventanas temporales pequeñas (0.6 - 3 segundos) después de la estimulación sensorial durante la vigilia; en otras palabras, los estímulos sensoriales sincronizan (generan un "*reset*") las oscilaciones gamma. Este efecto no se observa durante el sueño REM. Estos autores hipotetizaron que la actividad onírica durante el sueño REM representan un estado de híper-alerta en el cual los estímulos sensoriales no pueden acceder al proceso que genera experiencias conscientes (Llinas & Ribary, 1993). También se observó un incremento de coherencia durante el sueño REM en comparación con el sueño NREM, en registros de EEG estándar en humanos (Achermann & Borbely, 1998a; b); este efecto fue más pronunciado entre áreas interhemisféricas anteriores homologas.

A diferencia de los estudios anteriores, Perez-Garci et al. (2001), describieron una disminución de la correlación espectral en épocas de 2 segundos en frecuencias rápidas (27-48 Hz) entre áreas corticales frontales

y perceptuales intrahemisféricas durante el sueño REM en humanos. (Perez-Garci et al., 2001). Sin embargo, los valores de correlación espectral entre regiones perceptuales fueron similares durante el sueño REM y durante la vigilia. Cantero et al. (2004) utilizaron registros EEG intracraneales en humanos para análisis de coherencia durante el sueño; estos registros tienen una resolución espacial mucho mayor que las señales registradas con electrodos sobre el cuero cabelludo. Ellos encontraron un aumento significativo de la coherencia gamma en la banda de 35-58 Hz durante la vigilia con respecto al sueño, tanto a nivel local como entre cortezas interhemisféricas distantes. Por el contrario, no encontraron diferencias entre el sueño NREM y el sueño REM. Además, encontraron acoplamiento funcional en la banda gamma entre la neocorteza y el hipocampo durante la vigilia, pero no durante el sueño REM. Mikulan et al. (2018) encontraron una disminución de la conectividad cortical durante el sueño NREM en comparación con la vigilia; el sueño REM no fue estudiado en este trabajo. Voss et al. (2009) demostraron que la coherencia para todo el espectro disminuye durante el sueño REM comparado con la vigilia; es interesante destacar que durante los sueños lúcidos (en el que el individuo es consciente de estar soñando), los valores de coherencia son intermedios entre los de vigilia y sueño REM. Voss et al. (2014) también demostraron que una resonancia a 40 Hz impuesta externamente mediante estimulación eléctrica, induce la autoconsciencia (lucidez) durante el sueño REM, mientras que si se estimula a otras frecuencias no obtienen el mismo efecto.

En el presente trabajo, demostramos en el gato que la coherencia gamma se reduce durante el sueño REM. Además, en el sueño REM inducido por una única microinyección de carbacol en el NPO, que es un estado comparable al sueño REM natural, el acoplamiento de las oscilaciones gamma a 40 Hz es prácticamente nulo, al igual que en el sueño REM natural. Eso fue así tanto para la coherencia medida entre cortezas prefrontal y perceptuales, así como entre cortezas perceptuales

incluyendo áreas sensoriales primarias y asociativas. Es interesante el hecho de que esta falta de acoplamiento durante el sueño REM se observa en la simple inspección de registros filtrados. Son necesarios más estudios para analizar el nivel de acoplamiento de la banda gamma entre áreas corticales y subcorticales que incrementan su actividad durante el sueño REM, como cortezas límbicas, amígdala, etc. (Schwartz & Maquet, 2002).

En rata encontramos resultados similares donde observamos una disminución de la coherencia gamma en el sueño REM en comparación con los demás estados mientras que la potencia gamma se mantuvo elevada (Anexos 1 y 2). El mismo perfil de coherencia espectral lo encontramos en estudios preliminares en ratones (Cavelli et al., 2017) y en neonatos humanos (Castro et al., 2014).

Nuestra demostración de que existe una reducción en la coherencia gamma durante el sueño REM entre distintas áreas corticales distantes no contradice los resultados de Steriade et al. (1996), que muestran un incremento del acoplamiento local (a lo largo de una columna cortical o entre sitios corticales cercanos) durante estados activados. De hecho, los valores de potencia gamma (una aproximación de la sincronización gamma local) durante el sueño REM fueron similares a los de la QW y mayores a los del sueño NREM.

6.5. Ausencia de coherencia gamma durante el sueño REM: relación con la actividad onírica

La ausencia de coherencia gamma durante el sueño REM en animales y humanos (ver arriba), sugiere que en este estado existe una disminución de la capacidad de integración entre diferentes cortezas, al menos para las altas frecuencias. Este fenómeno, podría estar relacionado con algunos de los patrones únicos de actividad mental del sueño REM. (Hobson, 2009; Nir & Tononi, 2010). Por ejemplo, la prevalencia de pensamientos decrece desde la vigilia al sueño NREM y alcanza un nadir durante el sueño REM (como la coherencia gamma), mientras que las

alucinaciones y las emociones siguen un patrón inverso (Fosse et al., 2001).

6.6. Coherencia gamma "alta" durante la vigilia y el sueño

Además de la actividad de la banda gamma 40 Hz, estudios recientes basados en MEG y electrocorticografía (ECog) también han reportado oscilaciones > 60 Hz que pueden alcanzar hasta 200 Hz (Crone et al., 2006; Jerbi et al., 2009). Estas denominadas "oscilaciones de banda gamma alta", se conocen también como oscilaciones U (Munk & Neuenschwander, 2000), “High gamma”, “Épsilon” o “High Frequency Oscillation" (Uhlhaas et al., 2011; Scheffzuk et al., 2011; Tort et al., 2013).

En nuestro trabajo encontramos en la banda de frecuencias 60-100 Hz una reducción de la coherencia durante el sueño REM. Esto lo confirmamos en un trabajo reciente que estudiamos en gato y rata, las relaciones dinámicas entre la sincronización local (potencia) y el acoplamiento entre áreas distantes (coherencia) en la banda gamma alta (52-98 Hz) durante la vigilia y el sueño. En ambas especies, durante el sueño REM, la potencia gamma aumentó, mientras que la coherencia gamma entre áreas neocorticales distantes disminuyó (Anexo 2). Estos resultados van en la misma línea que los de Pal et al. (2016). Estos autores encontraron, en comparación con la vigilia, una disminución de la coherencia gamma alta (85-155 Hz) en múltiples estados de inconsciencia tales como la anestesia con propofol, anestesia con sevoflurano, sueño NREM y REM.

A pesar de la caída de coherencia gamma alta durante el sueño REM, no se observaron mayores cambios entre AW, QW y sueño NREM. Esto sugiere que la banda de frecuencias 60-100 Hz representan un tipo diferente de oscilaciones neurales que la banda de frecuencias 30-45 Hz. Nuevos estudios son necesarios para aclarar este punto.

Muy pocos estudios han tratado las oscilaciones de EEG a frecuencias superiores a 100 Hz (Uhlhaas et al., 2011). Sin embargo, se ha

descrito un nuevo tipo de actividad oscilatoria cortical rápida que ocurre entre 110 y 160 Hz tanto en el hipocampo como en la neocorteza parietal (Sirota et al., 2008; Tort et al., 2008). Los autores denominaron oscilaciones de alta frecuencia (high-frequency oscillations HFO) a esta actividad (Tort et al., 2013). Al igual que con la actividad gamma, la actividad HFO también se ha relacionado con actividades cognitivas, como la toma de decisiones y los procesos de memoria (Tort et al., 2008). Recientemente estudiamos el espectro de potencia y coherencia de las HFO en la corteza frontal, parietal, occipital y bulbo olfatorio (OB) de la rata, durante la W y el sueño (Anexo 3). Demostramos que la potencia y coherencia HFO intra e inter-hemisférica, fue mayor durante W que durante el sueño a lo largo de la neocorteza y bulbo olfatorio. También encontramos un aumento moderado en la coherencia de HFO durante el sueño REM, aunque solo para la combinación intrahemisférica de electrodos localizados en las cortezas parietal y occipital.

6.7. Modulación de la actividad gamma

Las neuronas corticales GABAérgicas y las neuronas glutamatérgicas talamo-corticales son fundamentales para la generación de oscilaciones de la banda gamma en el EEG (ver Introducción). La actividad tálamo-cortical es modulada por los sistemas reguladores, que son pequeños grupos de neuronas con un neurotransmisor común que se proyectan a varias regiones del sistema nervioso central (SNC) (Jones, 2005). Las neuronas colinérgicas, monoaminérgicas y peptidérgicas que integran estos sistemas juegan un papel crítico en el control de estados conductuales. Mediante la modulación de la actividad del sistema tálamo-cortical, los sistemas reguladores pueden regular las oscilaciones gamma y su coherencia.

La actividad de los sistemas neuronales reguladores ha sido estudiada durante los estados naturales de W y de sueño, mediante registros unitarios o expresión de c-fos en diferentes animales (Yamuy et

al., 1995, Maloney et al. 1999, Torterolo et al., 2001, Lee et al., 2005a, Lee et al., 2005b, Lu et al., 2006, Torterolo et al., 2006, Hassani et al., 2009, Hassani et al., 2010). Además, el papel de algunos de estos sistemas se ha evaluado durante los ataques de cataplejía en modelos caninos de narcolepsia (Wu et al., 1999, Wu et al., 2004). Es interesante el hecho que al igual que en el sueño REM de origen natural, las neuronas serotoninérgicas y noradrenérgicas se inhiben durante la cataplejía (Wu et al., 1999; Wu et al., 2004). En contraste, aunque las neuronas histaminérgicas del núcleo tuberomammilar del hipotálamo se inhiben durante el sueño REM natural, se encuentran activas durante la cataplejía (John et al., 2004). Por lo tanto, este grupo neuronal puede estar implicado en la promoción de las diferencias cognitivas que existen durante el sueño REM y la cataplejía (sueños y estado de alerta, respectivamente). La actividad de las neuronas histaminérgicas durante la cataplejía también puede determinar la presencia y el grado de coherencia gamma durante CA. Por otro lado, como en el sueño REM natural, es esperable que durante REMc las neuronas histaminérgicas reduzcan drásticamente su frecuencia de disparo.

Un estudio reciente destacó el papel de las neuronas GABAérgicas de proyección cortical del prosencéfalo basal en la generación de oscilaciones gamma en el EEG (Kim et al., 2015). Además, los autores sugieren que las neuronas colinérgicas dentro de esta área no son críticas para la generación de estas oscilaciones (Capítulo IV). Queda por determinar el papel de otras neuronas activadoras, como las dopaminérgicas e hipocretinérgicas. A su vez, es importante conocer el rol en la generación de la actividad y coherencia gamma del EEG de las neuronas glutamatérgicas que forman parte del sistema reticular ascendente y que tienen importante actividad oscilatoria a esta frecuencia (García-Rill et al., 2017). Las neuronas MCHérgicas del hipotálamo, que aumentan su actividad durante el sueño REM (Torterolo et al., 2011; Monti

et al., 2013), también podrían estar relacionadas en la pérdida de la coherencia gamma que ocurre durante este estado.

7. CONCLUSIONES

Nuestros datos muestran una ausencia de interacciones funcionales entre diferentes áreas del neocortex en la banda gamma de frecuencias durante el sueño REM. Por otra parte, durante el estado de alerta provocado por la exposición a estímulos novedosos, estas interacciones aumentan en forma marcada con respecto a los demás estados. Por lo tanto, las interacciones funcionales entre diferentes áreas corticales (reentradas), que son críticas para las funciones cognitivas, son diferentes durante la vigilia y el sueño REM. Esta falta de acoplamiento de la actividad de frecuencia gamma durante el sueño REM podría estar involucrada en las peculiaridades de las operaciones cognitivas que ocurren durante las actividades mentales que ocurren durante las experiencias oníricas, que son un fenómeno característico del sueño REM.

REFERENCIAS

Achermann, P., & Borbely, A. A. (1998a) Coherence analysis of the human sleep electroencephalogram. *Neuroscience*. 85. 1195-1208.

Achermann, P., & Borbely, A. A. (1998b) Temporal evolution of coherence and power in the human sleep electroencephalogram. *Journal of Sleep Research*. 7 Suppl 1. 36-41.

Adams, B., & Moghaddam, B., (1998) Corticolimbic dopamine neurotransmission is temporally dissociated from the cognitive and locomotor effects of phencyclidine. *Journal of Neuroscience*. 18, 5545–5554.

Boucetta, S., Cisse, Y., Mainville, L., Morales, M. & Jones, B.E. (2014) Discharge Profiles across the Sleep-Waking Cycle of Identified Cholinergic, GABAergic, and Glutamatergic Neurons in the Pontomesencephalic Tegmentum of the Rat. *Journal of Neuroscience*. 34, 4708-4727.

Bauer, M., Oostenveld R., Peeters, M., Fries, P. (2006) Tactile Spatial Attention Enhances Gamma-Band Activity in Somatosensory Cortex and Reduces Low-Frequency Activity in Parieto-Occipital Areas. *Journal of Neuroscience*. 26(2):490-501.

Berman, A. L., & Jones, E. G. (1982) The thalamus and basal telencephalum of the cat. A citoarchitectonic atlas with stereotaxic coordinates. University of Wisconsin. Madison.

Bouyer, J.J., Montaron, M.F., & Rougeul, A., (1981) Fast fronto-parietal rhythms during combined focused attentive behavior and immobility in cat: cortical and thalamic localizations. *Electroencephalogram Clinical Neurophysiology*. 51. 244-252.

Bressler, S.L., Coppola, R., & Nakamura. R. (1993) Episodic multiregional cortical coherence at multiple frequencies during visual task performance. *Nature*. 366. 153-156.

Brunton, L. & Parker, K. (2008) Goodman and Gilman's Manual of Pharmacology and Therapeutics. McGraw Hill Medical, New York.

Bullock, T. H. (1997) Signals and signs in the nervous system: the dynamic anatomy of electrical activity is probably information-rich. *Proceedings of the National Academy of Science U S A*. 94. 1-6.

Bullock, T. H., & McClune., M. C. (1989) Lateral coherence of the electrocorticogram: a new measure of brain synchrony. *Electroencephalogram Clinical Neurophysiology*. 73. 479-498.

Bullock, T. H., McClune, M. C., Achimowicz, J. Z., Iragui-Madoz, V. J., Duckrow, R. B., & Spencer, S. S. (1995a) EEG coherence has structure in the millimeter domain: subdural and hippocampal recordings from epileptic patients. *Electroencephalogram Clinical Neurophysiology*. 95. 161-177.

Bullock, T. H., McClune, M. C., Achimowicz, J. Z., Iragui-Madoz, V. J., Duckrow, R. B., & Spencer. S. S. (1995b) Temporal fluctuations in coherence of brain waves. *Proceedings of the National Academy of Science U S A*.. 92. 11568-11572.

Bullock, T. H., McClune, M. C., & Enright. J.T. (2003) Are the electroencephalograms mainly rhythmic? Assessment of periodicity in wide-band time series. *Neuroscience*. 121. 233-252.

Buzsaki, G. & Wang, X. J. (2012) Mechanisms of gamma oscillations. *Annual Review Neuroscience.* 35. 203-225.

Buzsaki, G. (2006) Rhythms of the brain. Oxford university press.

Brando, V., Castro-Zaballa, S., Falconi, A., Torterolo, P., Migliaro, E. (2014) Statistical, spectral and non-linear analysis of the heart rate variability during sleep. *Archives italiennes de biologie.* 152(1):32-46.

Braun, A.R., Balkin, T.J., Wesenten, N.J., Carson, R.E., Varga, M., Baldwin, P., Selbie, S., Belenky, G. & Herscovitch, P. (1997) Regional cerebral blood

flow throughout the sleep-wake cycle. An H2 (15) O PET study. *Brain*. 120 1173-97

Cantero, J. L., Atienza, M., Madsen, J. R. & Stickgold, R. (2004) Gamma EEG dynamics in neocortex and hippocampus during human wakefulness and sleep. *Neuroimage*. 22. 1271-1280.

Cantero, J.L., Atienza, M. & Salas, R.M. (2000) [Clinical value of EEG coherence as electrophysiological index of cortico-cortical connections during sleep]. *Revista de Neurologia*. 31. 442-454.

Castro, S.,Cavelli, M., Torterolo, P., Falconi, A., Rava, M., Criado, A., Chiappella, L., Scavone, C., Ardanaz, J., Gonzalez, G. (2014) Análisis cuantitativo de la actividad eléctrica cortical en recién nacidos: estudio de la coherencia para la banda gamma de frecuencias. XXXIV Congreso Argentino de Neurología Infantil y II Congreso Uruguayo de Neuropediatría.

Cardin, J.A., Carlen, M., Meletis, K., Knoblich, U., Zhang, F., Deisseroth, K. (2009). Driving fast-spiking cells induces gamma rhythm and controls sensory responses *Nature*, 459 . 663-667

Carskadon, M. W. (2005). Normal Human Sleep: An Overview. In: Principles and practices of sleep medicine (Meir H. Kryger. T. R., William C. Dement. ed). 13-23 Philadelphia: Elsevier-Saunders.

Chow, K. L., Dement, W. C. & Mitchell, S. A. (1960) Self ratings. In: Drugs and Behavior, *Electroencephalogram dinamic Neurophysiology.* 11: 107, 1959.

Corsi-Cabrera, M., Miro, E., del-Rio-Portilla, Y., Perez-Garci, E., Villanueva, Y. & Guevara. M.A. (2003) Rapid eye movement sleep dreaming is characterized by uncoupled EEG activity between frontal and perceptual cortical regions. *Brain Cognition*. 51. 337-345.

Chase, M. H. (2013) Motor control during sleep and wakefulness: clarifying controversies and resolving paradoxes. *Sleep Medicine Review*. 17, 299-312.

Cunningham, M. O., Whittington, M. A., Bibbig, A., Roopun, A., LeBeau, F. E., et al. (2004). A role for fast rhythmic bursting neurons in cortial gamma oscillations in vitro. *Proceedings of the National Academy of Science U S A*.101:7152–7.

Dauvilliers, Y., Siegel, J.M., Lopez, R., Torontali, Z.A. & Peever, J.H. (2014) Cataplexy--clinical aspects, pathophysiology and management strategy. *Naional Review Neurol*ogy. 10, 386-395.

Das, N. N. & Gastaut, H. (1955) Variations de l'activite electrique du cerveau. du coeur et des muscles squellettiques au cours de la meditation et de l'extase yoguique. *Electroencephalogr Clin Neurophysiol*. 6:211.

Dement, W., & Kleitman, N., (1957) The relation of eye movements during sleep to dream activity: an objective method for the study of dreaming. *Journal of Experimental Psychology*. 53 339-46.

Eckhorn, R., Bauer, R., Jordan, W., Brosch, M., Kruse, W., Munk, M., & Reitboeck, H. J., (1988) Coherent oscillations: a mechanism of feature linking in the visual cortex? Multiple electrode and correlation analyses in the cat. *Biology Cybernetics*. 60 121-30.

Edelman, G.M. & Tononi. G. (2000) A universe of consciousness. Basic Books. New York.

Fuchs, E.C., Zivkovic, A.R., Cunningham. M.O., Middleton, S., Lebeau, F.E.,. Bannerman, D.M. (2007) Recruitment of parvalbumin-positive interneurons determines hippocampal function and associated behavior *Neuron*. 53 . 591-604

Fuster, J. M. (1989) The prefrontal cortex. Raven Press. New York.

Galarreta, M., Hestrin, S. (1999) A network of fast-spiking cells in the neocortex connected by electrical synapses *Nature*. 402 . 72-615

Garcia-Rill, E. (2015). Waking and the Reticular Activating System. New York. Academic Press. ISBN 9780128013854, 330. Doi: 10.1016/B978-0-12-801385- 4.00010-0

Garcia-Rill, E. (2017) Bottom-up gamma and stages of waking. *Medical Hypotheses.* 104 58–62

Gosseries, O., Bruno, M., Vanhaudenhuyse, A., Laureys, S. & Schnakers, C. (2009) Consciousness in the locked-in syndrome. In Laureys, S., Tononi, G. (eds.) The neurology of consciousness: cognitive neuroscience and neuropathology. Elsevier, San Diego. 191-203.

Gibson, J. R., Beierlein, M., Connors, B. W. (1999). Two networks of electrically coupled inhibitory neurons in neocortex. *Nature*. 402:75–9.

Guilleminault, C. & Fromherz, S. (2011) Narcolepsy: Diagnosis and Management. In Kryger, M.H., Roth, T., Dement, W.C. (eds.) Principles and practices of sleep medicine. Saunders, Philadelphia. 957-968.

Gray, C.M., Singer, W. (1989). Stimulus-specific neuronal oscillations in orientation columns of cat visual cortex. *Proceedings of the National Academy of Science U S A*. 86,1698-1702.

Hall, G.H. (1970) Effects of nicotine and tobacco smoke on the electrical activity of the cerebral cortex and olfactory bulb. *Journal of Pharmacology*. 38, 271-286.

Harle, M., Rockstroh, B. S., Keil, A., Wienbruch, C. & Elbert, T. R. (2004) Mapping the brain's orchestration during speech comprehension: task-specific facilitation of regional synchrony in neural networks. *BMC Neuroscience*. 5. 40.

Hipp, J. F., & Siegel, M. (2013) Dissociating neuronal gamma-band activity from cranial and ocular muscle activity in EEG. *Frontiers in human neuroscience*. doi:10.3389/fnhum.00338.

Hobson, J. A. (2009) REM sleep and dreaming: towards a theory of protoconsciousness. *Nature Review Neuroscience*. 10. 803-813.

Jasper, H. H. & Andrews, H. L. (1938) Brain potentials and voluntary muscle activity in man. *Journal of Neurophysiology*. 1. 87-100.

John, G., Proakis, D. G., Manolakis. (2013)Tratamiento digital de señales. Principios, algoritmos y aplicaciones. Prentice Hall, ISBN 0-13-373762-4

John, E.R. (2002) The neurophysics of consciousness. *Brain Research Review*. 39. 1-28.

John, J., Wu, M.F., Boehmer, L.N. & Siegel, J.M. (2004) Cataplexy-active neurons in the hypothalamus: implications for the role of histamine in sleep and waking behavior. *Neuron*. 42, 619-634.

Jouvet, M. (1965) [The paradoxical phase of sleep]. *International Journal of Neurology*. **5**, 131-150.

Kim, T., Thankachan, S., McKenna, J.T., McNally, J.M., Yang, C., Choi, J.H., Chen, L., Kocsis, B., Deisseroth, K., Strecker, R.E., Basheer, R., Brown, R.E. & McCarley, R.W. (2015) Cortically projecting basal forebrain parvalbumin neurons regulate cortical gamma band oscillations. *Proedures National Academy of Science U S A*. 112, 3535-3540.

Kubin, L. (2001) Carbachol models of REM sleep: recent developments and new directions. *Archives Italiennes de Biologie*. 139, 147-168.

Larkum, M. E., Zhu. J. J., Sakmann. B. (2001) Dendritic mechanisms underlying the coupling of the dendritic with the axonal action potential initiation zone of adult rat layer 5 pyramidal neurons. *Journal of Physiology*. 533:447–66.

Libano, R. D., Kay L. M. (2008) Olfactory system gamma oscillations: the physiological dissection of a cognitive neural system. *Cogn Neurodyn*. 2008 Sep; 2(3): 179–194. Published online 2008 Jun 19. doi: 10.1007/s11571-008-9053-1

Libet, B., Pearl, D. K., Morledge, D. E., Gleason, C. A., Hosobuchi, Y., & Barbaro, N. M. (1991) Control of the transition from sensory detection to sensory awareness in man by the duration of a thalamic stimulus. The cerebral 'time-on' factor. *Brain*. 114 . 1731-1757.

Lin, L., Faraco, J., Li, R., Kadotani, H., Rogers, W., Lin, X., (1999) The sleep disorder canine narcolepsy is caused by a mutation in the hypocretin (orexin) receptor 2 gene. *Cell*; 98: 365-76.

Llinas, R., & Ribary, U. (1993) Coherent 40-Hz oscillation characterizes dream state in humans. *Proceedings of the National Academy of Science U S A*. 90. 2078-2081.

Llinas, R., Ribary, U., Contreras, D., & Pedroarena, C. (1998) The neuronal basis for consciousness. *Philosoohical Transactions of the Royal Society of London B Biological Sciences*. 353. 1841-1849.

Llinas, R.R., Grace, A.A. &Yarom, Y. (1991) In vitro neurons in mammalian cortical layer 4 exhibit intrinsic oscillatory activity in the 10- to 50-Hz frequency range. *Proceedings of the National Academy of Science U S A*. 88, 897-901.

Lopez-Rodrguez, F., Kohlmeier, K., Morales, F. R., Chase, M. H. (1994) State dependency of the effects of microinjection of cholinergic drugs into the nucleus pontis oralis. *Brain Research.* 649 (1994) 271-281

Lu, J., Jhou, T.C. & Saper, C.B. (2006) Identification of wake-active dopaminergic neurons in the ventral periaqueductal gray matter. *Journal of Neuroscience*. 26, 193-202.

Luppi, P.H., Gervasoni, D., Verret, L., Goutagny, R., Peyron, C., Salvert, D., Leger, L. & Fort, P. (2007) Paradoxical (REM) sleep genesis: The switch from an aminergic-cholinergic to a GABAergic-glutamatergic hypothesis. *Journal of Physiology (Paris)*. 100, 271-283.

Mann, E. O., Suckling, J. M., Hajos, N., Greenfield, S.A., Paulsen, O. (2005) Perisomatic feedback inhibition underlies cholinergically induced fast network oscillations in the rat hippocampus in vitro *Neuron*. 45 . 105-117

Mota-Rolim, S. A., and Araujo, J. F. (2013). Neurobiology and clinical implications of lucid dreaming. *Medical Hypotheses*. 81, 751–756. doi: 10.1016/j.mehy.2013. 04.049

Maloney, K.J., Cape, E. G., Gotman, J. & Jones, B. E. (1997) High-frequency gamma electroencephalogram activity in association with sleep-wake states and spontaneous behaviors in the rat. *Neuroscience*. 76. 541-555.

Maquet, P., Franck, G., 1997. REM sleep and amygdala. *Molecular. Psychiatry*. 2, 195–196.

Maquet, P., Peters, J. M., Aerts, J., Delfiore, G., Degueldre, C., Luxen, A., Franck, G., 1996. Functional neuroanatomy of human rapid-eye-movement sleep and dreaming. *Nature.* 383, 163–166.

Markowitsch, H. J. & Pritzel. M. (1977) A stereotaxic atlas of the prefrontal cortex of the cat. *Acta Neurobiologiae Experimentalis (Wars)*. **37**. 63-81.

Martin, W.R. &Eades, C.G. (1960) A comparative study of the effect of drugs on activating and vasomotor responses evoked by midbrain stimulation: atropine, pentobarbital, chlorpromazine and chlorpromazine sulfoxide. *Psychopharmacologia*. 1, 303-335.

Mashour, G. A. (2006) Integrating the science of consciousness and anesthesia. *Anesthesia & Analgesia*. 103. 975-982.

Mashour, G. A., & Avidan, M.S. (2015) Intraoperative awareness: controversies and non controversies*. British Journal of Anaesthesia*. Nov;115(5):800-1.

Massimini, M., Ferrarelli, F., Huber, R., Esser, S. K., Singh, H. &Tononi, G. (2005) Breakdown of cortical effective connectivity during sleep. *Science*. 309, 2228-2232.

Miltner, W.H., Braun, C., Arnold, M., Witte, H., Taub, E., (1999). Coherence of gamma-band EEG activity as a basis for associative learning. *Nature.* 397, 434 – 436.

Mikulan, E., Hesse, E., Sedeño, L., Bekinschtein, T., Sigman, M., Garcia, M., Silva, W., Ciraolo, C., Garcia, A, Ibañez, A. (2018) Intracranial high-γ connectivity distinguishes wakefulness from sleep. *NeuroImage*. DOI: 10.1016/j.neuroimage.2017.12.015

Morrison, A. R. (1983) A window on the sleeping brain. *Scientific American*. 248. 94-102.

Monti, J. M. (2013) The neurotransmitters of sleep and wake, a physiological reviews series. *Sleep Medicine Review*. 17, 313-315.

Mota., N. B, Resende., A, Sérgio A. Mota-Rolim, Mauro Copelli and Ribeiro., S (2016). Psychosis and the Control of Lucid Dreaming *Frontiers in Psychology.* 7(185) · March DOI: 10.3389/fpsyg.2016.00294 · License: CC BY 4.0

Munk, M. H., Roelfsema, P. R., Konig, P., Engel, A. K., & Singer, W. (1996) Role of reticular activation in the modulation of intracortical synchronization. *Science*. 272.

Morales, F.R., Engelhardt, J.K., Soja, P.J., Pereda, A.E. & Chase, M.H. (1987) Motoneuron properties during motor inhibition produced by microinjection of carbachol into the pontine reticular formation of the decerebrate cat. *Journal of Neurophysiology*. 57, 1118-1129.271-274.

Nir, Y., Mukamel, R., Dinstein, I., Privman, E., Harel, M., Fisch, L., Gelbard-Sagiv, H., Kipervasser, S., Andelman, F., Neufeld, M.Y., Kramer, U., Arieli, A., Fried, I., & Malach, R. (2008) Interhemispheric correlations of slow

spontaneous neuronal fluctuations revealed in human sensory cortex. *Nature Neuroscience*. 11. 1100-1108.

Nir,, Y. & Tononi, G. (2010) Dreaming and the brain: from phenomenology to neurophysiology. *Trends in Cognitive Science*. 14. 88-100.

Nishino, S., Ripley, B., Overeem. S., Lammers, G. J., Mignot, E. (2000) Hypocretin (orexin) deficiency in human narcolepsy. *Lancet*; 355: 39-40.

Nunez, P. L., Srinivasan, R., Westdorp, A. F., Wijesinghe, R. S., Tucker, D. M., Silberstein, R. B. & Cadusch, P. J. (1997) EEG coherency. I: Statistics. reference electrode. volume conduction. Laplacians. cortical imaging. and interpretation at multiple scales. *Electroencephalogr Clinical Neurophysiology*. 103. 499-515.

Núñez, A., Rodrigo-Angulo, M. L., De Andrés, I., Garzón, M. (2009) Hypocretin/orexin neuropeptides: participation in the control of sleep-wakefulness cycle and energy homeostasis. *Current Neuropharmacology*. 7: 50-9

Owens, A., Schiff, N.D. & Laureys, S. (2009) The assesement of conscious awareness in the vegetative state. In Laureys, S., Tononi, G. (eds.) The neurology of Conciousness Elsevier.

Pal, D., Silverstein, B. H, Lee, H., Mashour, G. A (2016) Neural Correlates of Wakefulness, Sleep, and General Anesthesia: An Experimental Study in Rat. *Anesthesiology.* 125: 929-942.

Palva, S., Monto, S., Palva, J.M. (2009). Graph properties of synchronized corticalnetworks during visual working memory maintenance. *Neuroimage.* 49, 3257-3268. Doi: 10.1016/j. 11.031

Pace-Schott, E., The neurobiology of dreaming. In M.H. Kryger. T. Roth and W.C. Dement (Eds.). (2005). Principles and practices of sleep medicine. Elsevier-Saunders. Philadelphia.. 551-564.

Perez-Garci, E., del-Rio-Portilla, Y., Guevara, M.A., Arce, C., & Corsi-Cabrera, M. (2001) Paradoxical sleep is characterized by uncoupled gamma activity between frontal and perceptual cortical regions. *Sleep*. 24. 118-126.

Pedroarena, C., Llinás, R. R. Dendritic calcium conductances generate highfrequency oscillation in thalamocortical neurons. *Proceedings of the National Academy of Science U S A*. 1997;94:724–8.

Piper. D. C., Upton, N., Smith, M. I., Hunter, AJ. (2000) The novel brain neuropeptide, orexin-A modulates the sleep-wake cycle of rats. *European Journal of Neuroscience.* 12: 726-30

Philips, S., Takeda, Y. (2009). Greater frontal-parietal synchrony at low gamma-band frequencies for inefficient then efficient visual search in human EEG. *International Journal of Psychophysiology.* 73, 350-354. Doi: 10.1016/j.ij 05.011

Rechtschaffen, A. (1978) The single-mindedness and isolation of dreams. *Sleep*. 1. 97-109.

Rieder, M. K., Rahm, B., Williams, J. D., & Kaiser, J. (2010) Human gamma-band activity and behavior. *International Journal of Psychophysiol*. 79. 39-48.: 387.

Rodriguez, E., George, N., Lachaux, J.P., Martinerie, J., Renault, B., Varela, F.J., 1999. Perception's shadow: long-distance synchronization of human brain activity. *Nature.* 397, 430 – 433

Rajkowski, J., Kubiak, P., & Aston-Jones, G- (1994) Locus coeruleus activity in monkey: phasic and tonic changes are associated with altered vigilance. *Brain Research.* 35:607-616.

Reinoso-Suarez, F., de Andres, I., Rodrigo-Angulo, M. L. & Garzon, M. (2001) Brain structures and mechanisms involved in the generation of REM sleep. *Sleep Medicine Review*. 5, 63-77.

Sastre, J. P. & Jouvet. M. (1979). Oneiric behavior in cats. *Physiology Behaviour*. 22. 979-989.

Scannell, J. W., Blakemore, C. & Young, M .P. (1995) Analysis of connectivity in the cat cerebral cortex. *Journal of Neuroscience*. 15. 1463-1483.

Scheffzuk, C., Kukushka, V.I., Vyssotski, A.L., Draguhn, A., Tort, A.B.L., Brankak, J., (2011) Selective coupling between theta phase and neocortical fast gamma oscillations during REM-sleep in mice. *PLoS ONE. 6*, e28489.

Schwartz, S., & Maquet, P. (2002) Sleep imaging and the neuro-psychological assessment of dreams. *Trends in Cognitive Science*. 6. 23-30.

Schwartz, T. L., Sachdeva, S., & Stahl SM (2012) Genetic data supporting the NMDA glutamate receptor hypothesis for schizophrenia. *Current Pharmacology.* 18: 1580–1592.

Schoffelen, J. M., Oostenveld, R. & Fries, P., (2005) Neuronal coherence as a mechanism of effective corticospinal interaction. *Science.* 308 111-3.

Sharpless, B.A. & Grom, J.L. (2014) Isolated Sleep Paralysis: Fear, Prevention, and Disruption. *Behavioural Sleep Medicine*. 1-6.

Sohal, V. S., Zhang, F., Yizhar, O.(2009).Deisseroth Parvalbumin neurons and gamma rhythms enhance cortical circuit performance *Natur.,* 459 . 698-702

Siegel, M., Donner, T.H., & Engel, A.K. (2012) Spectral fingerprints of large-scale neuronal interactions. *National Review Neuroscience*. 13. 121-134.

Singer, W., Gray, C. (1995). Visual feature integration and the temporal correlation hypothesis. Annu. Rev. *Neuroscience*. 18:555-86

Singer, W., 2002. Gamma oscillations and cognition. In: Reisin, R.C., Nuwer, M., Hallet, M., Medina, C. (Eds.), *Advances in Clinical Neurophysiology*. Clinical. Neurophysiology. (Suppl.), vol. 54. Elsevier, The Netherlands, . 3 – 22.

Sirota, A., Montgomery, S., Fujisawa, S., Isomura, Y., Zugaro, M., & Buzsáki, G. (2008) Entrainment of Neocortical Neurons and Gamma Oscillations by the Hippocampal Theta Rhythm. *Neuron*. 60, 683–697.

Steriade, M., Amzica, F. & Contreras, D. (1996) Synchronization of fast (30-40 Hz) spontaneous cortical rhythms during brain activation. *Journal of Neuroscience*. 16. 392-417.

Steriade, M., (1997) Synchronized activities of coupled oscillators in the cerebral cortex and thalamus at different levels of vigilance. *Cerebral Cortex*. 7 583-604.

Steriade, M, Llinás, R. R. (1988). The functional states of the thalamus and the associatedneuronal interplay. *Physiology Review*. 68:649–742.

Steriade, M. (1999). Cellular substrates of oscillations in corticothalamic systems during states of vigilance. In: Baghdoyan HA, Lydic R, editors. Handbook of behavioral state control. *Cellular and molecular mechanisms*. New York: CRC Press. 327–47.

Tamas, G., Buhl, E.H., Lorincz. A, Somogyi, P. (2000) Proximally targeted GABAergic synapses and gap junctions synchronize cortical interneurons *Nature Neuroscience*. 3. 366-371

Thompson R. F., Johnson, R. H., & Hoopes, J. J. (1963) Organization of auditory somatic sensory and visual projection to association fields of cerebral cortex in the cat. *Journal of Neurophysiology*. 26. 343-364.

Tiitinen, H., Sinkkonen, J., Reinikainen, K., Alho, K., Lavikainen, J.. & Naatanen, R. (1993) Selective attention enhances the auditory 40-Hz transient response in humans. *Nature*. 364. 59-60.

Tononi, G. (2009) Sleep and dreaming. In Laureys, S., Tononi, G. (eds.) *The neurology of consciousness: cognitive neuroscience and neuropathology*. Elsevier, San Diego, 89-107.

Tononi, G. (2010) Information integration: its relevance to brain function and consciousness. *Archives Italiennes de Biologie*. 148. 299-322.

Tort, A. B. L., Komorowski, R., Eichenbaum, H., & Kopell, N. (2010) Measuring Phase- Amplitude Coupling Between Neuronal Oscillations of Different Frequencies. *Journal.of Neurophysioogyl*. 104, 1195–1210.

Tort, A. B. L., Kramer, M., Thorn, C., Gibson, D. J., Kubota, Y., Graybiel, A. M., & Kopell, N.J. (2008) Dynamic cross-frequency couplings of local field potential oscillations in rat striatum and hippocampus during performance of a T-maze task. *Proceedings of the National Academy of Science U S A*. 105, 20517–20522.

Tort, A. B. L., Scheffer-Teixeira, R., Souza, B.C., Draguhn, A., & Brankačk, J. (2013) Theta-associated high-frequency oscillations (110-160Hz) in the hippocampus and neocortex. *Progress in Neurobiology.* 100, 1–14.

Torterolo, P., Benedetto, L., Lagos, P., Sampogna, S. & Chase. M.H. (2009) State-dependent pattern of Fos protein expression in regionally-specific sites within the preoptic area of the cat. *Brain Research*. 1267. 44-56.

Torterolo, P., Castro, S., Cavelli, M., Velazques, N., Brando, V., Falconi, A., Chase, M. H., Migliaro, E. (2015) Heart rate variavility during carbachol-induced sleep and cataplexy. *Behavioural Brain Research*. 291. 72. 79

Torterolo, P., Castro, S., Cavelli, M., Chase, M. H., Falconi, A. (2016) Neocortical 40 Hz oscillations during carbachol-induced rapid eye movement sleep and cataplexy. *European Journal of Neuroscience*. 1–10, 2016. doi:10.1111/ejn.13151.

Torterolo, P., Morales, F. R. & Chase, M. H. (2002) GABAergic mechanisms in the pedunculopontine tegmental nucleus of the cat promote active (REM) sleep. *Brain Research*. 944. 1-9.

Torterolo, P., Sampogna, S., & Chase M.H. (2012) Hypocretinergic and non-hypocretinergic projections from the hypothalamus to the REM sleep executive area of the pons. *Brain Research.* http://dx.doi.org/10.1016/j.brainres.2012.10.050

Torterolo, P., Ramos, O. V., Sampogna, S. & Chase. M.H. (2011a) Hypocretinergic neurons are activated in conjunction with goal-oriented survival-related motor behaviors. *Physiology Behaviour*. 104. 823-830.

Torterolo, P., Sampogna, S., & Chase, M. H. (2011b) A restricted parabrachial pontine region is active during non-rapid eye movement sleep. *Neuroscience*. 190. 184-193.

Torterolo, P., & Vanini, G. (2010) Nuevos conceptos sobre la generación y el mantenimiento de la vigilia. *Review Neurology*. 50: 747-58.

Torterolo, P., Yamuy, J., Sampogna, S., Morales, F. R., & Chase, M. H. (2003) Hypocretinergic neurons are primarily involved in activation of the somatomotor system. *Sleep*. 1. 25-28.

Uhlhaas, P. J., Pipa, G., Lima, B., Melloni, L., Neuenschwander, S., Nikolic, D. & Singer, W. (2009) Neural synchrony in cortical networks: history. concept and current status. *Frontiers in Integrative Neuroscience*. **3**. 17.

Uhlhaas, P. J., Pipa G., Neuenschwander, S., Wibral. M. & Singer, W. (2011) A new look at gamma? High- (>60 Hz) gamma-band activity in cortical networks: function. mechanisms and impairment. *Progress in Biophysics & Molecular Biology*. 105. 14-28.

Uslaner, J. M., Tye, S. J., Eddins, D. M., Wang, X., Fox, S. V., Savitz. A. T., Binns. J., Cannon, C. E., Garson, S. L., Hodgson, R., et al., (2013) Orexin Receptor Antagonists Differ from Standard Sleep Drugs by Promoting Sleep at Doses That Do Not Disrupt Cognition. *Science Translational. Medicine*. 5, 179 44. DOI: 10.1126/scitranslmed.3005213

Urbano, F.J., Kezunovic, N., Hyde, J., Simon, C., Beck, P. & Garcia-Rill, E. (2012) Gamma band activity in the reticular activating system. *Frontiers in Neurology*. **3**. 6.

Ursin, R., & Sterman. M. (1981) Manual for standardized scoring of sleep and waking states in adult cats. BIS/BRI. University of California. Los Angeles.

Vanini, G., Torterolo, P., Baghdoyan, H. A., & Lydic R. (2011) The shared circuits of sleep and anesthesia. *Neuroscientific foundations of anesthesiology*. DOI10.1093/med/9780195398243.003.0024

Varela, F., Lachaux, J.P., Rodriguez, E., Martinerie, J., (2001). The brainweb: phase synchronization and large-scale integration. *National Review Neuroscencei*. 2, 229 – 239

Veit, J., Hakim, R., Jadi, M. P., & Sejnowski, T. J., (2017). Cortical gamma band synchronization through somatostatin interneurons *Nature Neuroscience.* 20, 951–959 doi:10.1038/nn.4562

Von der Malsburg, C. (1995) Binding in models of perception and brain function. *Current Opinion in Neurobiology*. 5. 520-526.

Voss, U., Holzmann, R., Hobson, A., Paulus, W., Koppehele-Gossel, J., Klimke, A. & Nitsche, M.A. (2014) Induction of self awareness in dreams through frontal low current stimulation of gamma activity. *Nature Neuroscience*. 17, 810-812.

Voss, U., Holzmann, R., Tuin, I. & Hobson. J.A. (2009) Lucid dreaming: a state of consciousness with features of both waking and non-lucid dreaming. *Sleep*. 32. 1191-1200.

Watson, C., Baghdoyan, H. & Lydic, R. (2010) A neurochemical perspective on states of consciousness. In Hudetz. A.G., Pearce. R. (eds.) *Supressing the Mind. Contemporary Clinical Neuroscience*. Humana Press. . 33-79.

Wikler, A. (1952) Pharmacologic dissociation of behavior and EEG «sleep patterns» in dogs: Morphine,N-allylnormorphine and atropine**.** *Proceedings of the society for experimental biology.* N. Y. 79: 261.

Wu, M.F., Gulyani, S.A., Yau, E., Mignot, E., Phan, B. & Siegel, J.M. (1999) Locus coeruleus neurons: cessation of activity during cataplexy. *Neuroscience*. 91, 1389-1399.

Wu, M.F., John, J., Boehmer, L.N., Yau, D., Nguyen, G.B. & Siegel, J.M. (2004) Activity of dorsal raphe cells across the sleep-waking cycle and during cataplexy in narcoleptic dogs. *Journal of Physiology*. 554, 202-215.

Yamuy, J., Sampogna, S., Morales, F.R. & Chase, M.H. (1998) c-fos expression in mesopontine noradrenergic and cholinergic neurons of the cat during carbachol-induced active sleep: A double labeling study. *Sleep Res Online*, **1**, 28-40, http://www.sro.org/1998/Yamuy/1928States in Rabbits. *Japan. Journal of. Pharmacology*. 47, 123-134

Ylinen, A., Soltesz, I., Bragin, A., Penttonen, M., Sik, A., Buzsaki, G. (1995) Intracellular correlates of hippocampal theta rhythm in identified pyramidal cells, granule cells, and basket cells *Hippocampus*. 5 . 78-90

Yuval-Greenberg, S., Tomer, O., Keren, A.S., Nelken, I. & Deouell, L.Y. (2008) Transient induced gamma-band response in EEG as a manifestation of miniature saccades. *Neuron*. 58. 429-441

CAPITULO III

OSCILACIONES GAMMA DEL EEG EN UN MODELO FARMACOLÓGICO DE PSICOSIS

1. Modelos de psicosis

La actividad onírica y la psicosis comparten características importantes. Una de ellas, es la presencia de percepciones sensoriales en ausencia de estímulos, acompañado de una falta de crítica por su presencia (Mota et al., 2016). El sueño REM (donde ocurre principalmente la actividad onírica) comparte características electrofisiológicas, farmacológicas y neuroquímicas con la psicosis; por lo tanto, se considera un modelo de ésta (Gottesmann & Gottesman, 2007).

Las oscilaciones gamma son alteradas en la psicosis (Lewis et al., 2005; Lisman et al., 2008; Skosnik et al., 2015; White & Siegel., 2016). Se ha propuesto que esto ocurre por la disfunción de una clase específica de interneuronas inhibidoras GABAérgicas que expresan la proteína de unión al calcio denominada parvalbúmina (Lewis et al., 2005). Las interneuronas GABAérgicas parvalbúmina positivas representan aproximadamente el 40% de las neuronas inhibitorias corticales. Se caracterizan por un fenotipo electrofisiológico único de "aceleración rápida", es decir, pueden disparar a frecuencias muy altas (> 200 Hz). Varios grupos han encontrado alteraciones en interneuronas GABAérgicas parvalbúmina positivas, particularmente en la corteza prefrontal de pacientes con psicosis (Lewis et al., 2005). Estas interneuronas expresan niveles virtualmente indetectables de GAD67, que sintetiza el neurotransmisor GABA, lo que sugiere que estas neuronas son hipofuncionales. Este tejido también exhibe aumentos

en los receptores postsinápticos de GABA y disminuciones en los transportadores de GABA, que pueden representar una compensación por la liberación deficiente de GABA (Lewis et al., 2005). La alteración de este mecanismo podría conducir a una superposición anormal y coactuación de conjuntos neurales que procesan diferentes fragmentos de información, causando así algunas de las anomalías cognitivas y síntomas observados en la psicosis (Lisman et al., 2008; Skosnik et al., 2015).

Otro de los factores implicados en la psicosis, es la hipofunción del receptor glutamatérgico de N-metil-D-aspartato (NMDA) (Lewis et al., 2006). La ketamina es un antagonista del receptor glutamatérgico NMDA, que en dosis subanestésicas ha sido utilizado como modelo de psicosis (Krystal et al., 2005). La administración aguda de ketamina en dosis subanestésicas genera síntomas de psicosis tanto en humanos (Adler et al., 1999), como en animales de experimentación (Adams & Moghaddam, 1998). Ésta produce alteraciones perceptuales, desorganización conceptual, manierismos (actividad motora organizada, repetitiva, estereotipada y sin propósito), recuerdos alterados y síntomas negativos (falta de interés o iniciativa, retraimiento social, apatía) (Krystal et al., 2005).

Como mencionamos en el Capítulo II, al igual que las funciones cognitivas, la potencia y la coherencia gamma se modifican al pasar de la vigilia al sueño. Las alteraciones de las funciones cognitivas y el estado de consciencia que provoca las dosis subanestésicas de ketamina, hacen que sea importante conocer como es afectado el acoplamiento de la actividad en la banda gamma entre diferentes áreas corticales.

En este trabajo vamos a centrarnos en las oscilaciones gamma bajas (30-45 Hz). Esta estrecha banda es altamente reactiva al nivel de alerta (Capítulo II).

1.2. Hipótesis de trabajo

Dado que existen similitudes importantes en las funciones cognitivas entre la psicosis y las experiencias oníricas, esperamos encontrar similitudes entre la coherencia en la banda gamma de frecuencias del EEG de distintas combinaciones de áreas corticales, entre el sueño REM (modelo natural de psicosis) y la ketamina a dosis subanestésicas (modelo farmacológico de psicosis).

2. Objetivos

2.1. Objetivo general

Analizar como las oscilaciones gamma y su nivel de acoplamiento entre áreas corticales es afectado en la psicosis.

2.2. Objetivos específicos

Analizar la actividad y el acoplamiento de las oscilaciones en la banda gamma entre distintas áreas corticales en un modelo farmacológico de psicosis, y compararlo con el sueño REM.

3. Material y métodos.

Gran parte de la metodología fue descrita previamente. Solo se comentarán los detalles diferenciales de esta serie experimental.

3.1. Sesiones experimentales

Se realizaron registros polisomnográficos en los que se registraron simultáneamente la actividad múltiples áreas corticales con electrodos monopolares (las áreas corticales en cada animal se muestran en la Figura III.1.A). Los datos que se utilizaron como control fueron obtenidos durante AW (mediante estímulos sonoros; ocasionalmente por medio de estímulo visuales, ver Figura III.3.), QW, sueño NREM y REM de la misma forma que en el Capítulo II. También se realizaron registros bajo el efecto de ketamina (Ketonal 50 de Richmond Veterinaria S.A) a dosis de 5, 10 y 15

mg/kg, i/m (50 mg/ml diluido en cloruro de bencetonio, ácido clorhídrico y agua; solución de uso veterinario). Las distintas dosis de la droga fueron administradas en días distintos, en forma randomizada, en 4 sesiones experimentales (por dosis) en 5 animales. Se dejó por lo menos dos días de descanso entre las administraciones de drogas. Es importante destacar que cuando se administra como agente único, la dosis anestésica de ketamina en gatos es mayor o igual a 25 mg/kg (Arnbjerg 1979; Hanna et al., 1988).

Bajo el efecto de ketamina también ser realizaron estímulos sonoros de 300 segundos de duración, 10 minutos después de la inyección de ketamina. Estos estímulos fueron iguales a los utilizados para inducir AW.

3.2. Análisis de los datos

Se compararon la potencia y la coherencia de la banda gamma baja (30-45 Hz) del EEG bajo el efecto de la ketamina con los estados de W y sueño. La potencia y coherencia gamma de la ketamina se evaluó tanto en ventanas tomadas tanto durante el estímulo, como alejadas temporalmente (300 segundos) de este. Las ventanas de análisis se eligieron durante el efecto máximo de la ketamina (entre 5 y 20 minutos luego de la inyección).

El análisis de potencia y coherencia se realizó de la misma forma que en el Capítulo II. En experimentos piloto se administró salina (para descartar que el efecto obtenido fuera por el dolor causado por la inyección) y el análisis del EEG mostró resultados similares a los observados en registros basales; por lo tanto, se utilizaron registros basales como registros control.

Para las Figuras III.2 y III.5 se usaron dos enfoques diferentes para estimar la potencia de EEG. En la Figura III.2, se utilizó un método multitaper como se describe en (Babadi & Brown, 2014). El método utiliza una serie de secuencias discretas de esferoide estirado hacia los polos (Slepian) para la Transformada Rápida de Fourier en ventanas. El procedimiento reduce la varianza, ofreciendo una mejor estimación de

potencia. En la Figura III.5, se aplicó una transformación wavelet para mejorar la localización de tiempo y frecuencia. La wavelet elegida fue Morlet, debido a su probada idoneidad para el análisis de EEG (Roach & Mathalon, 2008). Ambos análisis se realizaron empleando "Chronux Toolbox" y "ND Tools Toolbox", que se ejecutan en rutinas generadas en MATLAB.

Los datos se expresaron como media ± error estándar. Se evaluó la significancia de las diferencias entre estados conductuales para cada gato con ANOVA unidireccional y prueba de Tamhane. Para analizar el efecto de los fármacos en todo el grupo de animales (Figura III.6), se estudio la media de la coherencia z' intra-hemisférica de la banda gamma entre áreas corticales anteriores (S1 para C1 y C3, Pf para C2 y C5 y M1 para C4) y posteriores (V1 para C4, y Pp para el resto de los animales; Figura III.1A). Para este propósito, utilizamos ANOVA de medidas repetidas (rmANOVA) y la prueba *post hoc* de Bonferroni. El criterio utilizado para rechazar hipótesis nulas fue $p < 0.05$.

4. Resultados

Se expondrán los datos de la siguiente forma. Primero, se describirán los distintos efectos de la dosis más alta (15 mg/kg). Posteriormente, se comentarán los distintos efectos en función de la dosis.

4.1. Comportamiento

Durante el registro en condiciones semirestringidas, luego de la administración de ketamina (independiente de la dosis) los animales se mantuvieron despiertos con los ojos abiertos hasta el final del registro (3 a 4 horas después de la inyección del fármaco). Cuando los animales se volvieron a colocar en condición de libre movimiento, deambularon normalmente.

4.2. Registros crudos y filtrados

En la Figura III.1 B y C se muestran registros simultáneos crudos y filtrados (pasa-banda 30-45 Hz) de la corteza prefrontal y parietal posterior durante AW, sueño REM y bajo efecto de ketamina (15 mg/kg). Se puede observar que durante la AW existen oscilaciones gamma que aparecen simultáneamente en ambos canales (están acopladas), mientras que durante el sueño REM estas oscilaciones tienen menor amplitud y duración a su vez aparecen en ambos canales, en diferentes momentos (no están acoplados). Bajo el efecto de la ketamina las oscilaciones gamma tienen características similares a las que se observan durante el sueño REM.

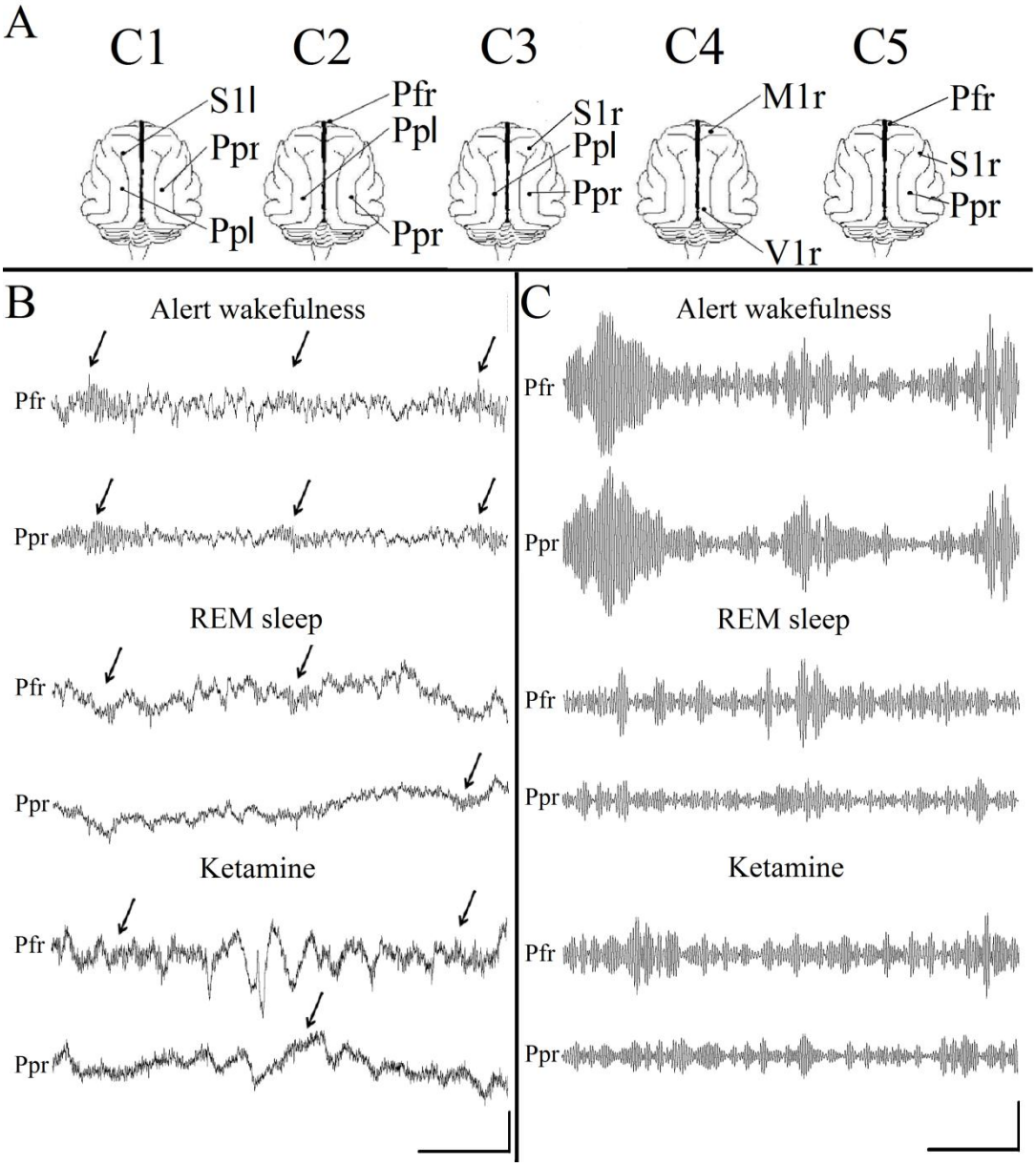

Figura III.1.**Las oscilaciones gamma bajo el efecto de la ketamina**. A. Posición de los electrodos de registro en la superficie de la corteza cerebral. Los registros de estos electrodos se derivaron a un electrodo indiferente inactivo común, que se ubicó sobre el seno frontal. C1-C5 nombre identificatorio de los animales. M1, corteza motora primaria; Pf, corteza prefrontal; Pp, corteza parietal posterior; S1, corteza somato-sensorial primaria; V1, corteza visual primaria; r, derecha; l, izquierda. B. Registros crudos simultáneos de la corteza prefrontal (Pf) y parietal posterior (Pp). B. Registros crudos durante la vigilia alerta, el sueño REM y bajo la administración de ketamina (15 mg/kg). Las flechas indican "ráfagas" gamma. C.

Registros filtrados (pasa-banda 30-45 Hz) de los mismos registros que en B. Barras de calibración, 1 segundo, 200 µV para B; 20 µV para C.

4.3. Evolución dinámica de la potencia y coherencia gamma

En Figura III.2. se muestra el análisis de potencia y coherencia de un registro representativo de C5, luego de la administración de ketamina (15 mg/kg). En la Figura III.2A se muestra la evolución dinámica de la potencia. Se puede observar que luego de un breve periodo de gran actividad gamma en la banda de 30-45 desencadenado por la inyección; la potencia gamma primero se reduce y luego aumenta abarcando un rango de frecuencias mucho más amplio (entre 30 y 60 Hz). Luego de 2 horas comienza a reaparecer el pico de potencia gamma entre 30 y 45 Hz. En la Figura III.2 B se muestra la evolución dinámica de la coherencia z´ entre las cortezas prefrontal y parietal-posterior. Se puede observar que luego de un breve aumento de la coherencia gamma (producido por la alerta post-inyección), ésta disminuyó a niveles muy bajos. El estímulo sonoro no tuvo ningún efecto sobre la potencia ni sobre la coherencia gamma. Luego de 1 hora de haber administrado el fármaco, la coherencia gamma comenzó a aumentar hasta alcanzar valores similares a los de AW aproximadamente 3 horas luego de la inyección.

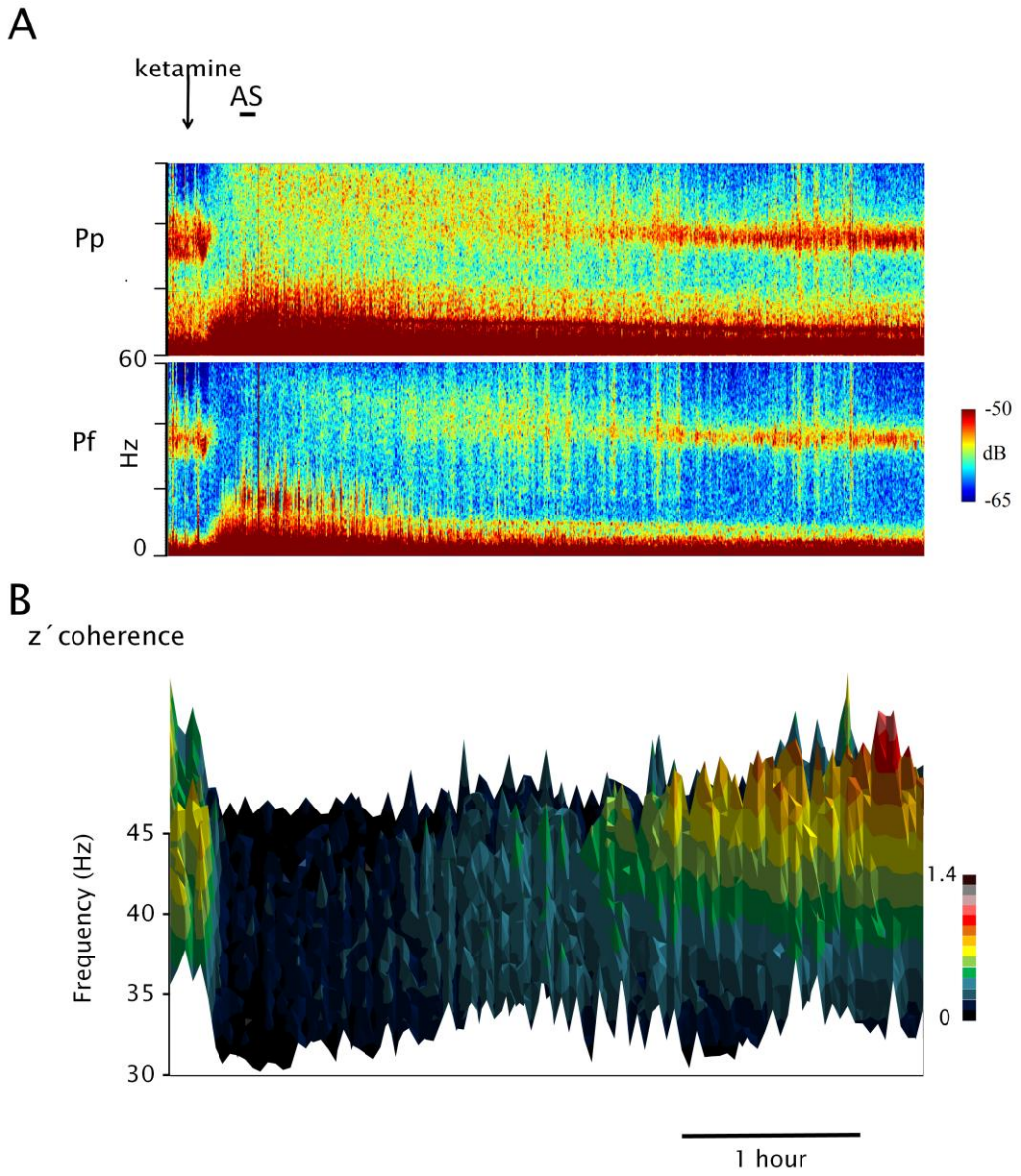

Figura III.2. **Evolución dinámica de la potencia y la coherencia z´ EEG durante la inyección de ketamina.** A. Espectrogramas de potencia gamma de corteza prefrontal (Pf) y Parietal posterior (Pp) luego de la inyección de ketamina (flecha). La barra horizontal representa la estimulación sonora (AS). B. Espectrograma tridimensional de la coherencia z 'del EEG (30-45 Hz) de los registros simultáneos de Pf y Pp (análisis del mismo registro que en A). El tiempo y la frecuencia se muestran en los ejes horizontal y vertical (profundidad), respectivamente; la coherencia-z' está representada en un código de colores.

La Figura III.3 muestra la evolución dinámica de la coherencia z´ entre las cortezas Pf y Pp en 2 registros representativos de C2. En el registro control mostrado en A, se realizó estimulación sonora durante 300 segundos y posteriormente un estimulo visual (colocando un espejo frente al animal durante 300 segundos). Luego de esto el animal presentó períodos de sueño (se indica un episodio de sueño REM). Tanto el estímulo sonoro como el visual provocaron un aumento de la coherencia gamma; durante el sueño REM la coherencia disminuye a un nivel mínimo. En B se muestra el efecto de la ketamina (15 mg/kg) en otro registro representativo. Luego de un breve aumento de la coherencia gamma debido al estímulo producido por la inyección, la coherencia gamma disminuyó al mismo nivel que durante el sueño REM. La estimulación sonora tampoco tuvo ningún efecto sobre la coherencia gamma. Estos cambios en la potencia y la coherencia gamma se observaron en los 5 animales con diferencias en la duración del efecto de la administración de ketamina, siendo C5 y C2 los que tuvieron la mayor y menor duración del efecto, respectivamente.

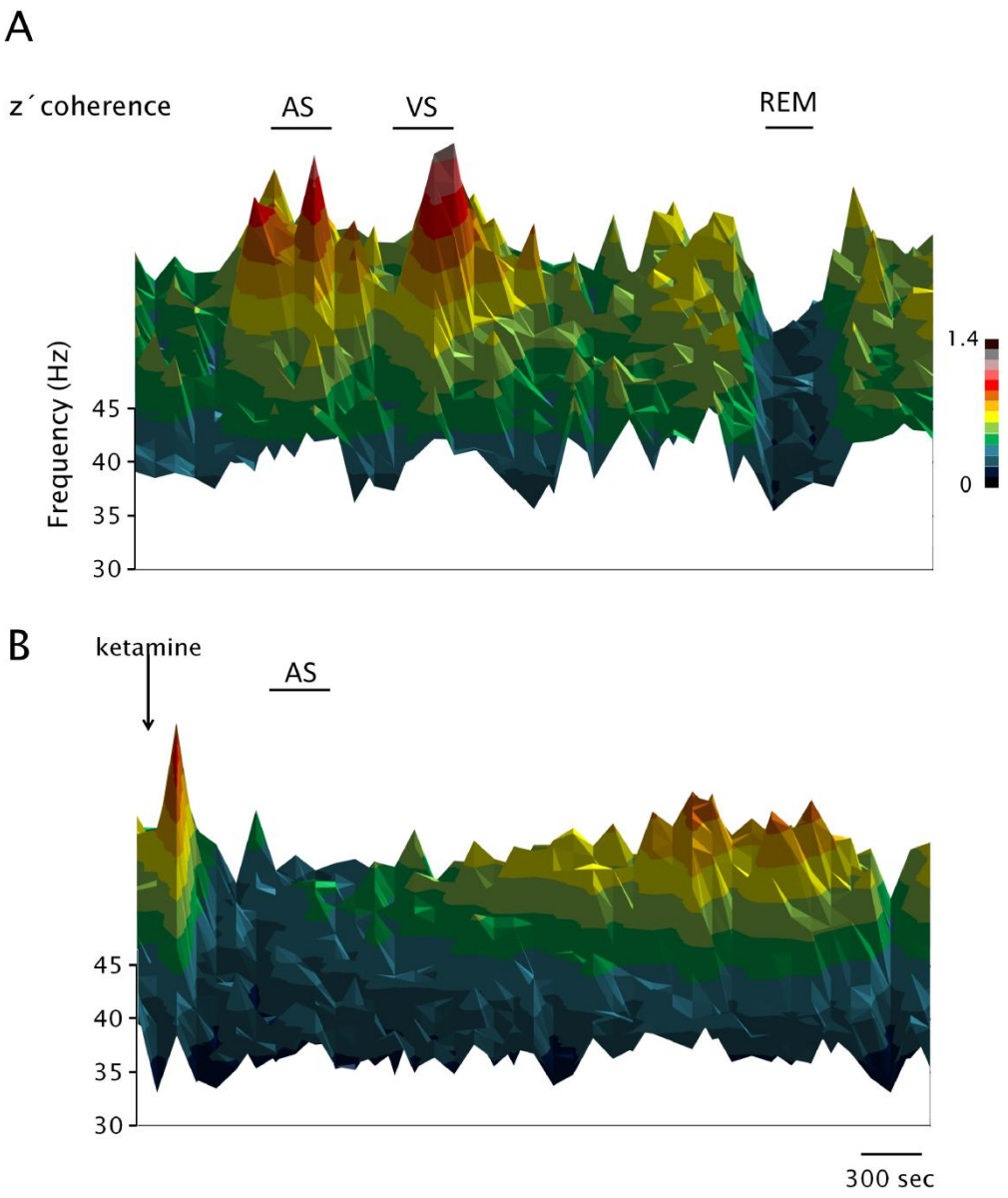

Figura III.3. **Evolución dinámica de la coherencia z´ del EEG (30–45 Hz) durante la vigilia y el sueño y bajo el efecto de la ketamina.** Espectrogramas 3D de coherencia z´ de registros simultáneos de las cortezas prefrontal y parietal posterior del C2. El eje horizontal indica el tiempo, el eje de profundidad indica frecuencia y el vertical indica coherencia z´ (representado por código de colores). En A se representa un registro basal, mientras que en B el efecto de la administración de ketamina (15 mg/kg). AS, estímulo sonoro; VS, estímulo visual.

4.4. Potencia y coherencia gamma

Bajo ketamina (independiente de la dosis), al contrastar los valores de potencia y coherencia gamma durante las ventanas afectadas por el estímulo sonoro y no afectadas por este (300 segundos antes o después), no hubo diferencias significativas (Figuras III.2 y III.3; datos cuantitativos no mostrados). Por lo tanto, para simplificar, solo se mostrará el análisis de las ventanas no afectadas por el estímulo sonoro.

La Figura III.4A muestra el análisis del espectro de potencia de la corteza prefrontal de C5 durante los distintos estados naturales y bajo ketamina. La ketamina genera alteraciones en las bandas de baja frecuencia y un pequeño pico en la banda beta (flechas). Si nos enfocamos en la banda gamma, la ketamina produce un nivel de potencia en la banda gamma baja menor a AW, pero comparable con QW o sueño REM. Sin embargo, el nivel de potencia en frecuencias por encima de 45 Hz (gamma alto, cabeza de flecha) es mayor que en los estados naturales.

Tabla III.1. Valores de potencia gamma (30-45 Hz) durante la W, sueño y luego de la administración de ketamina (15 mg/kg).

		AW	QW	NREM	REM	K	F
C1	Pp	64.4 ± 2.4 *	18.3 ± 4.7 *	8.9 ± 0.3 *	15.1 ± 0.5	28.0 ± 0.7	66
	S1	15.3 ± 0.6 *	13.1 ± 0.9 *	7.6 ± 0.3 *	13.0 ± 0.6	6.8 ± 0.1	7
C2	Pf	60.9 ± 3.1 *	23.8 ± 3.6 *	12.5 ± 0.3	20.9 ± 0.4 *	14.5 ± 2.6	50
	Pp	57.6 ± 2.6 *	21.1 ± 3.9	10.3 ± 0.3 *	18.5 ± 0.5	24.7 ± 1.4	37
C3	Pp	14.0 ± 0.8 *	10.8 ± 0.9 *	6.5 ± 0.6 *	9.7 ± 1.3	10.7 ± 0.3	26
	S1	26.2 ± 1.5 *	13.1 ± 0.9	6.1 ± 0.4 *	7.7 ± 0.5 *	15.4 ± 0.5	131
C4	M1	75.8 ± 4.3 *	26.7 ± 0.9	15.8 ± 0.5 *	19.6 ± 0.9	25.5 ± 0.9	73
	V1	57.4 ± 3.0 *	8.4 ± 0.6	5.8 ± 0.91 *	10.2 ± 0.5	9.8 ± 0.2	55
C5	Pf	132.0 ± 4.0 *	57.2 ± 5 *	20.5 ± 1.3 *	18.3 ± 1.1 *	33.4 ± 1.8	113
	S1	121.2 ± 4.9 *	69.8 ± 4.4 *	18.6 ± 1.8 *	37.0 ± 2.4 *	45.6 ± 2.8	121
	Pp	174.0 ± 11.2 *	79.8 ± 4.4 *	35.3 ± 3.2 *	39.9 ± 2.5	64.8 ± 3.4	85

Los valores representan la media ± error estándar. Los asteriscos muestran la significancia con respecto a ketamina (K). $p < 0.05$. ANOVA con pruebas *post hoc* de Tamhane. Todas las áreas corticales tienen los mismos grados de libertad (4 entre grupos, 55 dentro de grupos). M1, corteza motora primaria; Pf, corteza prefrontal; Pp, corteza parietal posterior; S1, corteza primaria somato-sensorial; V1, corteza visual primaria; r, derecha; l, izquierda.

En la Tabla III.1. se muestran los valores para cada gato y cortezas analizadas. La potencia bajo ketamina (15 mg/kg) se encuentra en valores comparables a QW y sueño REM; en la mayoría de los casos, son menores a AW y mayores a sueño NREM.

La Figura III.4B muestra perfiles de coherencia z' para un gato y par de cortezas representativas durante AW, sueño REM y bajo el efecto de ketamina (15 mg/kg). Los perfiles de coherencia z' con ketamina fueron similares a los de sueño REM. En la Figura III.4C se muestran los perfiles de coherencia promedio de la banda gamma para todos los estados conductuales. Se puede observar que la coherencia gamma bajo el efecto de la ketamina es tan baja como durante el sueño REM.

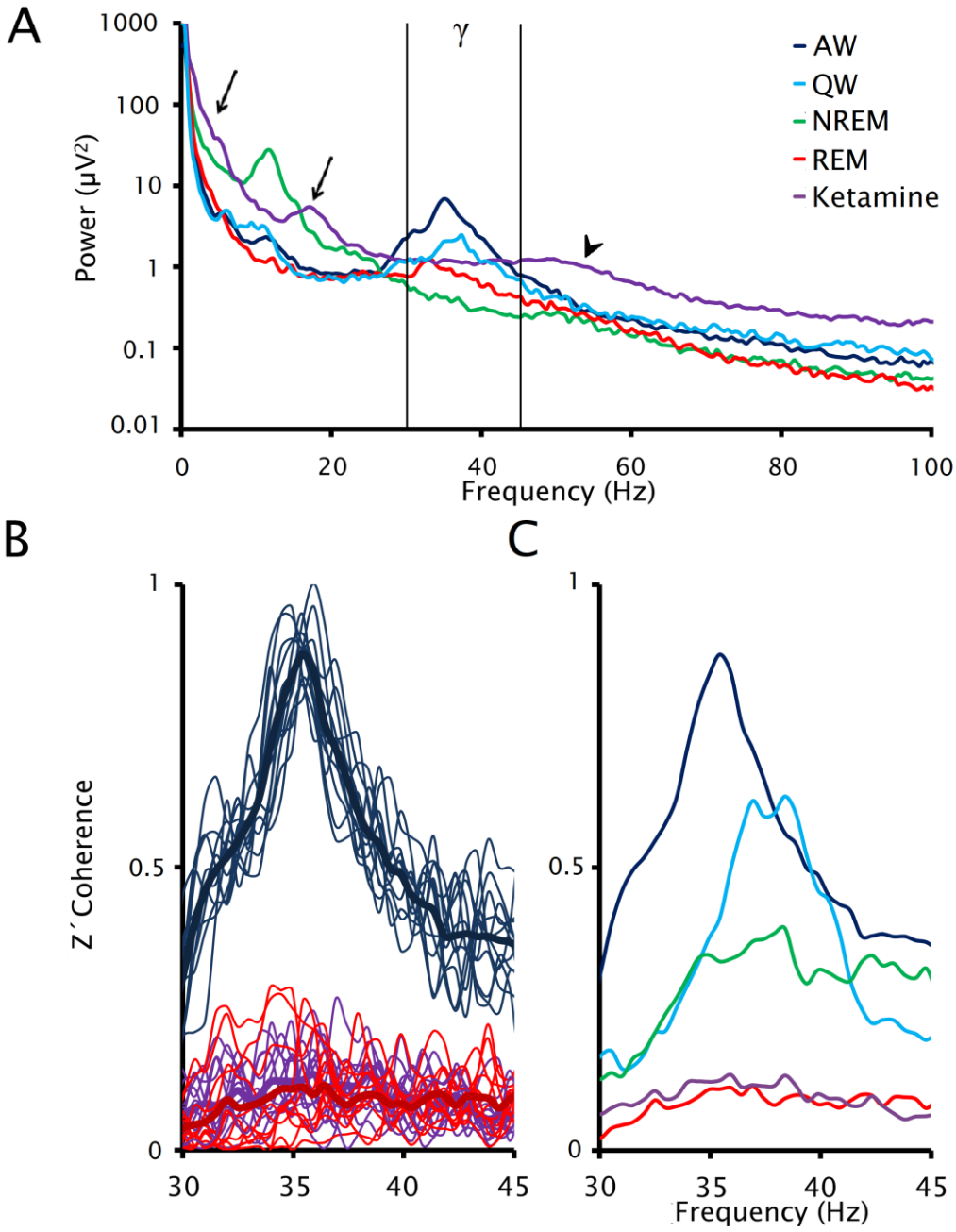

Figura III.4. **Potencia del EEG y coherencia gamma bajo el efecto de la ketamina.** A espectro de potencias (0.5-100 Hz), promedio de 10 ventanas de 100 segundos del EEG de la corteza prefrontal de C5 durante la AW, QW, sueño NREM, sueño REM y la administración de ketamina (15 mg/kg). Las flechas muestran los picos de potencia delta y beta bajo ketamina y la cabeza de flecha muestra la potencia gamma alta bajo la droga. B. Se muestran 12 perfiles de las coherencia z' (líneas delgadas) de las aéreas Pf y Pp del C5 (cortezas prefrontal y parietal posterior), así como los promedios de estos 12 perfiles (líneas gruesas)

para vigilia alerta el sueño REM y la administración de ketamina (15 mg/kg). C. Perfiles de coherencia z' gamma promedio durante la AW, QW, sueño NREM, sueño REM y la administración de ketamina (15 mg/kg).

En la Figura III.5A, mediante espectrogramas gamma y envolventes, es visualmente sencillo comparar la dinámica de las "ráfagas" entre AW, sueño REM y ketamina. Se puede observar un marcado acoplamiento entre las cortezas durante AW, este acoplamiento desaparece tanto durante el sueño REM como bajo el efecto de la ketamina. Las formas de onda de la ráfaga gamma durante el sueño REM y bajo el efecto de la ketamina son similares (Figura III.5B). Estas son diferentes a las de AW.

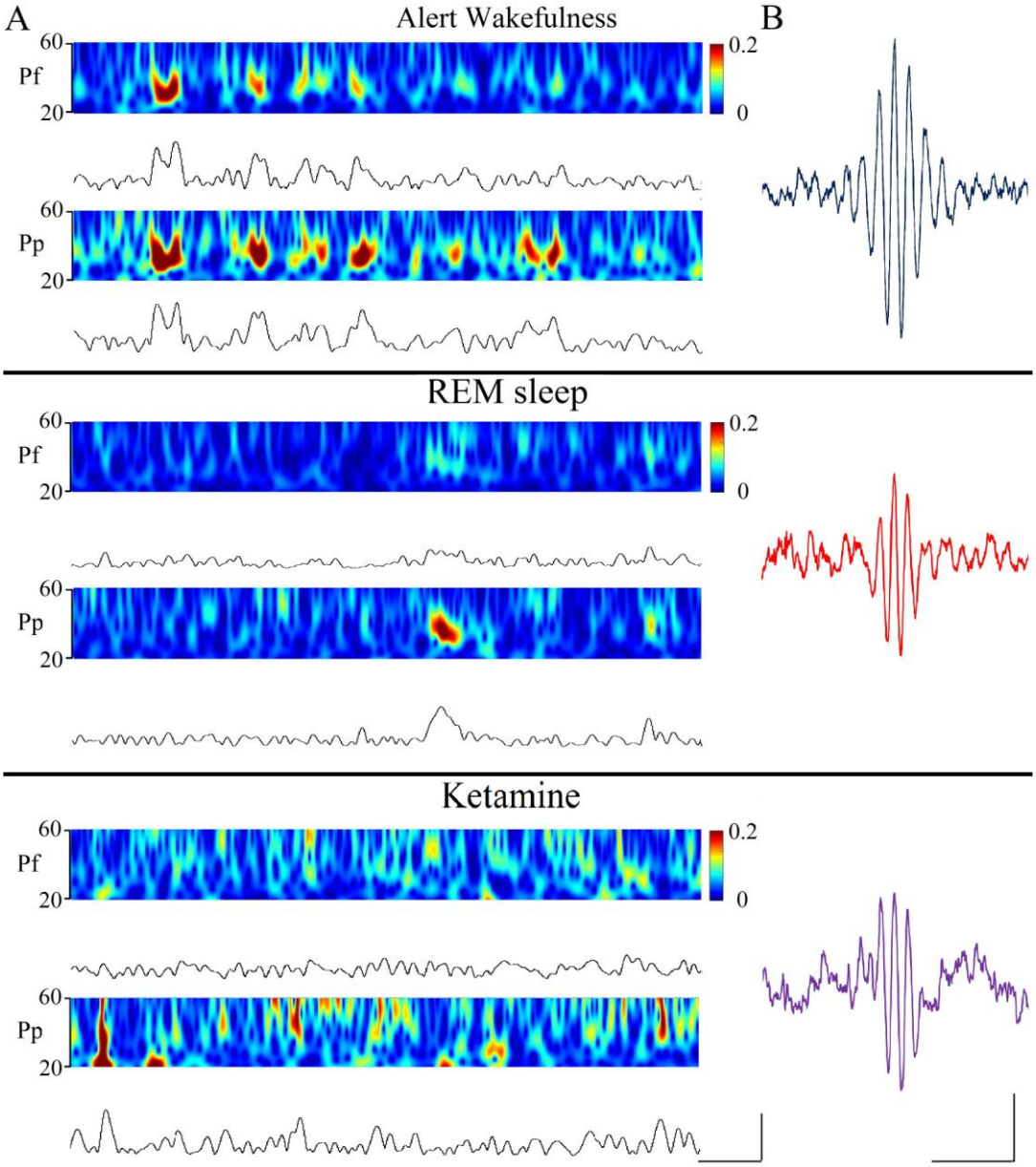

Figura III.5. A. Espectrogramas (por medio de la función wavelet) y banda gamma rectificada (30-45 Hz) o envolventes gamma, durante AW, sueño REM y bajo el efecto de la ketamina (15 mg/kg). Barras de calibración; 400 ms y 30 µV. B. "ráfagas" gamma promediados de un registro filtrado (pasa alto 3 Hz) seleccionado de la corteza prefrontal. 100 ráfagas aleatorias fueron seleccionadas y promediadas; el "trigger" fue el pico de la onda de mayor amplitud de la "ráfaga". Barras de calibración 200 ms y 10 µV.

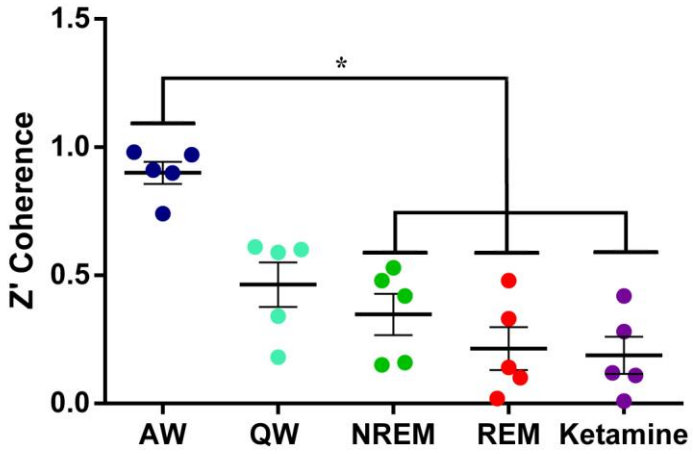

Figura III.6.Coherencia gamma promedio de los 5 animales. Coherencia z´ entre áreas corticales anteriores y posteriores para los 5 animales durante AW, QW, sueño NREM, sueño REM y 15 mg/kg de ketamina (Ketamine). El asterisco muestra los estados que tuvieron diferencias significativas, $F_{4, 24} = 75.4$, $p < 0.001$.

Figura III.6 muestra, para todos los animales, la coherencia gamma entre las cortezas anteriores y posteriores para todos los estados comportamentales y ketamina. Los niveles de coherencia bajo ketamina fueron similares al sueño REM. Si bien con mrANOVA solamente podemos distinguir entre ketamina y AW, cuando analizamos individualmente cada animal podemos ver diferencias significativas entre todos los estados. La Tabla III.2 muestra la coherencia para todas las combinaciones de cortezas estudiadas y para todos los animales. Claramente se observa que la ketamina desciende la coherencia gamma a niveles del sueño REM (o incluso menores) en todos los pares de cortezas estudiadas, de los 5 animales.

Tabla III.2. Valores de coherencia z' gamma (30-45 Hz) durante la W, sueño y luego de la administración de ketamina (15 mg/kg).

		AW	QW	NREM	REM	K	F
C1	Ppr-Ppl	1.13 ± 0.03*	0.84 ± 0.07*	0.77 ± 0.03*	0.55 ± 0.03	0.6 ± 0.03	28
	S1r-Ppr	0.98 ± 0.04*	0.41 ± 0.03*	0.53 ± 0.03*	0.33 ± 0.01	0.28 ± 0.01	87
C2	Pfl-Ppl	0.90 ± 0.06*	0.34 ± 0.05*	0.16 ± 0.01*	0.10 ± 0.01	0.11 ± 0.01	78
	Ppd-Ppi	0.95 ± 0.04*	0.46 ± 0.05*	0.27 ± 0.04*	0.20 ± 0.03	0.51 ± 0.03	60
C3	Ppr-Ppl	0.43 ± 0.01*	0.34 ± 0.04*	0.05 ± 0.01*	0.05 ± 0.01	0.04 ± 0.01	98
	S1r-Ppr	0.97 ± 0.02*	0.60 ± 0.04	0.48 ± 0.01*	0.48 ± 0.01*	0.42 ± 0.03	88
C4	M1r-V1r	0.91 ± 0.02*	0.18 ± 0.01*	0.15 ± 0.01*	0.02 ± 0.01	0.01 ± 0.01	857
C5	Pfd-Ppd	0.73 ± 0.04*	0.59 ± 0.04*	0.42 ± 0.07*	0.14 ± 0.06	0.12 ± 0.03	368
	S1d-Ppd	0.91 ± 0.04*	0.82 ± 0.06*	0.62 ± 0.06*	0.42 ± 0.03	0.47 ± 0.03	28

Los valores representan la media ± error estándar. Los asteriscos muestran la significancia con respecto a ketamina (K). $p < 0.05$, ANOVA con pruebas *post hoc* de Tamhane. Todas las combinaciones de áreas corticales tienen los mismos grados de libertad (4 entre grupos, 55 dentro de grupos). M1, corteza motora primaria; Pf, corteza prefrontal; Pp, corteza parietal posterior; S1, corteza primaria somato-sensorial; V1, corteza visual primaria; r, derecha; l, izquierda.

4.5. Curva dosis-respuesta

En la Figura III.7 A se muestran los valores promedio de coherencia gamma para AW y ketamina en dosis de 5, 10 y 15 mg/kg para las cortezas seleccionadas de los 5 animales. Se puede observar que en algunos animales las dosis de 5 y 10 mg/kg tuvieron valores de coherencia intermedios entre AW y la dosis de 15 mg/kg, mientras que en otros las dosis de 5 y 10 mg/kg mostraron una coherencia gamma mínima similar a la de la dosis de 15 mg/kg.

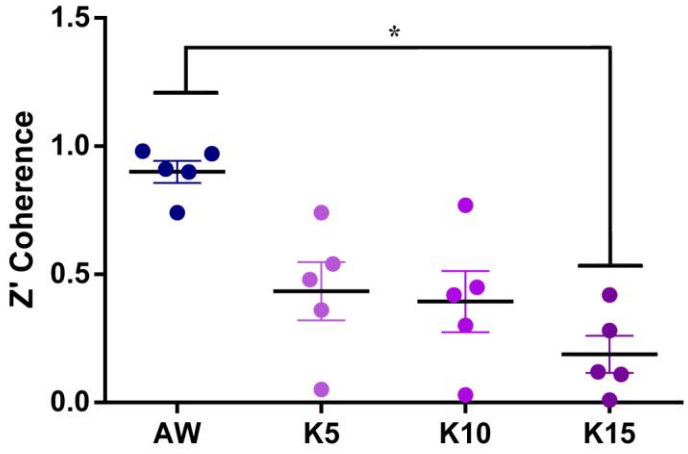

Figura III.7. **Curva dosis-respuesta de la coherencia gamma.** Coherencia z´ entre áreas corticales anteriores y posteriores para los 5 animales durante AW y tratados con ketamina en dosis de 5, 10 y 15 mg/kg (K5, K10 y K15 respectivamente). El asterisco muestra los estados que tuvieron diferencias significativas, $F_{3, 19} = 40.4$, $p < 0.003$.

5. Discusión

Hemos demostrado que la ketamina en dosis subanestésicas produce una disminución de la coherencia en la frecuencia gamma (30-45 Hz) de las regiones corticales estudiadas. Esta disminución de coherencia gamma fue similar a la que ocurre durante el sueño REM, y menor que durante la vigilia y el sueño NREM. La coherencia gamma no fue afectada por estímulos novedosos, que en condiciones basales alertan al animal provocando un gran aumento de la coherencia gamma.

La potencia gamma (30-45 Hz) se mantuvo en un nivel similar al de QW y sueño REM, pero mayor que la potencia gamma durante el sueño NREM. La potencia gamma también aumento a frecuencias mayores (45 a 100 Hz), pero no se profundizó en el estudio de esta banda.

5.1. Sueño REM como modelo natural de psicosis

El sueño REM y la psicosis comparten características fenomenológicas y neurofisiológicas importantes (Gottesmann, 2005; Manoach & Stickgold, 2009; Mota-Rolim & Araujo, 2013; Dresler et al., 2014). En términos de experiencia subjetiva, la actividad onírica durante el sueño y la psicosis presentan percepciones intrínsecas, independientes de la estimulación externa, asociadas a la falta de crítica (o juicio racional) con respecto a la realidad bizarra de estas experiencias (Cicogna & Bosinelli, 2001). Se ha propuesto que estas características como la violación de leyes físicas, incongruencias en el tiempo, espacio y personajes, proviene de la disminución de la actividad cerebral frontal que caracteriza la psicosis y el sueño REM (Corsi-Cabrera et al., 2003; Dresler et al., 2014; Voss et al., 2014).

Hobson (1997), considera que la psicosis y las experiencias oníricas tienen las siguientes similitudes:

- las intensas imágenes visuales de nuestras experiencias oníricas son como las alucinaciones visuales que ocurren frecuentemente en estados tóxicos causados especialmente por drogas que alteran la química del cerebro (psicosis tóxicas).
- la convicción de que incluso los eventos de experiencias oníricas físicamente imposibles son reales es como la creencia delirante que es el sello de toda psicosis.
- incapacidad para reconocer que estamos soñando, es similar a la tenacidad con que el paranoico se aferra a la creencia falsa.

- las historias que inventamos para explicar los sucesos imaginarios improbables e imposibles son como las confabulaciones del síndrome de Korsakoff.
- la intensidad de la ansiedad que sufrimos en las pesadillas se acerca a la experimentada por personas con trastorno de pánico.

Hobson concluye entonces que "soñar es, por definición, una psicosis".

A su vez, la vigilia en pacientes psicóticos y el sueño REM en sujetos normales muestran un EEG similar fuertemente activado (Gottesmann & Gottesman, 2007. La corteza prefrontal dorsolateral y la corteza cingular posterior se desactivan durante el sueño REM. Es importante destacar que la corteza prefrontal dorsolateral también se desactiva en la psicosis, particularmente cuando los rendimientos cognitivos están disminuidos (Weinberger et al., 1986; Fletcher et al., 1998).

Existen dos hipótesis principales relacionadas con la psicosis que involucran trastornos de la dopamina y el glutamato (Gottesmann & Gottesman, 2007). De hecho, los antagonistas de glutamato inducen síntomas psicóticos y al mismo tiempo generan sueños vívidos (Reeves et al., 2001; Grace, 2000; Heresco-Levy, 2000). Un déficit de glutamato en el núcleo accumbens parece ser el resultado de la disminución de la producción glutamatérgica del hipocampo que inhibe la liberación prefrontal de glutamato en el núcleo accumbens (Grace, 2000). Por lo tanto, la influencia glutamatérgica del núcleo medial de la amígdala podría predominar generando trastornos de los procesos emocionales. Esto ocurre tanto en la psicosis como durante el sueño debido a la fuerte activación de la amígdala durante esta etapa de sueño (Maquet y Franck, 1997).

Por otra parte, el exceso de dopamina en el núcleo accumbens se puede considerar parcialmente responsable de los síntomas positivos de la

psicosis (MacKay et al., 1982). Concordantemente con esto, se pudo determinar que la liberación de dopamina en el núcleo accumbens es máxima durante el sueño REM (Le´na et al., 2005), Además, agonistas de receptores dopaminérgicos, inducen tanto síntomas psicóticos como pesadillas (Buffenstein et al., 1999; Thompson & Pierce, 1999). A su vez, los neurolépticos, que bloquean la acción de la dopamina, suprimen tanto los síntomas psicóticos como las experiencias oníricas (Solms, 2000; Jakovljevic et al., 2003).

Por lo tanto, características electrofisiológicas, imagenológicas, farmacológicas y neuroquímicas del sueño REM se encuentran específicamente en la psicosis y constituyen candidatos a los endofenotipos de esta enfermedad. En consecuencia, el sueño REM se considera un modelo neurobiológico de este trastorno mental (Gottesmann & Gottesman, 2007).

5.2. Ketamina como modelo farmacológico de psicosis

Los receptores NMDA se encuentran en las sinapsis excitadoras y se expresan ubicuamente en el SNC. Estudios clínicos, preclínicos y teóricos sugieren que el receptor NMDA está involucrado en la fisiopatología de varias enfermedades psiquiátricas (Bergeron & Coyle, 2012; Kantrowitz & Javitt, 2012; Paul & Skolnick, 2003; Schwartz et al., 2012).

Dosis subanestésicas de antagonistas NMDA se usan ampliamente para modelar algunos de los síntomas de la psicosis (Abi-Saab et al., 1998; Krystal et al., 1994; Scorza et al., 2007; Corlett et al., 2007a); entre estas la ketamina. En voluntarios sanos, ésta induce cambios perceptivos, trastorno del pensamiento como delirios y síntomas negativos (Krystal et al., 1994; Krystal et al., 2005; Duncan et al., 2001; Stone & Pilowsky 2006; Malhotra et al., 1996; Pomarol-Clotet et al., 2006). Además, la ketamina induce deficiencias selectivas en la función cognitiva, que son comparables a las observadas en la psicosis (Fletcher & Honey., 2006; Morgan & Curran.,

2006). Por ejemplo, tanto la ketamina, como la psicosis están asociadas con dificultades para utilizar más que de mantener, la información en la memoria de trabajo (Honey et al., 2003, 2004; Perry et al., 2001; Kim et al., 2004). Algunos autores han argumentado que los cambios perceptivos y cognitivos que induce se asemejan más a los encontrados durante las etapas prodrómicas de la enfermedad (Pomarol-Clotet et al., 2006; Corlett et al., 2006, 2007a, 2007b, 2011).

A su vez, existe evidencia de hipofunción de los receptores NMDA en pacientes psicóticos. Estudios *post mortem* encontraron una disminución de los receptores NMDA en la corteza prefrontal dorsolateral y el hipocampo de pacientes esquizofrénicos (Konradi & Heckers, 2003).

5.3. Potencia y Coherencia gamma durante el sueño REM (modelo natural de psicosis)

Los resultados descriptos en el Capítulo II y en el presente Capítulo muestran claramente que la potencia gamma durante el sueño REM es similar a la de QW, mientras la coherencia desciende a niveles mínimos. Como se mencionó en el Capítulo II, este fenómeno podría estar relacionado con las características bizarras de los sueños.

5.4. Potencia y Coherencia gamma bajo dosis sub-anestésicas de ketamina (modelo farmacológico de psicosis)

En el presente trabajo encontramos que dosis subanestésicas de ketamina (que no provocan la pérdida de consciencia del animal) reducen la coherencia gamma entre diferentes áreas neocorticales a un nivel similar al de sueño REM, aunque la potencia gamma se mantiene a un nivel similar a QW.

En acuerdo con nuestros resultados, Pinault (2008) demostró en rata aumentos dependientes de la dosis en la potencia gamma frontoparietal que ocurren incluso a dosis relativamente bajas de ketamina (2.5 mg/kg) y MK801 (0.06 mg/kg) (otro antagonista NMDA). También se encontraron

incrementos de potencia equivalentes en la corteza visual, y en menor medida en la corteza motora, lo que indica aumentos de potencia en una variedad de regiones corticales (Phillips et al., 2012). En forma consistente con esto, Palenicek et al. (2011) demuestran aumentos en la potencia gamma en la mayoría de las regiones de la corteza.

Con respecto a la coherencia gamma, y también en armonía con nuestros resultados, Pal et al. (2015) identificaron una disminución de la coherencia y la potencia gamma con dosis anestésicas de ketamina en rata. Sin embargo, Akeju et al. (2017) encontraron un aumento de la potencia y la coherencia gamma en la inducción anestésica con ketamina en humanos, probablemente porque el análisis de coherencia lo realizaron entre electrodos frontales localizados a poca distancia, en registros estándar de EEG.

Los datos mencionados anteriormente sugieren que el acoplamiento entre diferentes áreas corticales estaría mediado por glutamato actuando a través de receptores NMDA, de modo que cuando estos son bloqueados por la ketamina disminuye el acoplamiento entre diferentes áreas corticales distantes sin disminuir la sincronización local.

La ketamina bloquea los receptores NMDA que son exitatorios, en las interneuronas corticales con alta frecuencia de disparo más eficazmente que en las neuronas piramidales. Esto da como resultado una regulación a la baja de la actividad de las interneuronas, y una disminución de la liberación de GABA en la sinapsis entre la neurona piramidal y las interneuronas (Homayoun et al., 2007; Seamans, 2008). Esta disminución en el tono inhibidor (disminución de la liberación de GABA) da como resultado que las neuronas piramidales se encuentren notablemente activas. Esto explica también por qué la ketamina se asocia con una mayor utilización de la glucosa cerebral y flujo sanguíneo (Langsjo et al., 2004; Langsjo et al; 2005), y con un aumento de las oscilaciones gamma (Ferrer-Allado et al; 1973, Schwartz et al; 1974, Schultz et al; 1990, Engelhardt et al; 1994, Hering et al; 1994, Lee et al; 2013, Blain-Moraes et al; 2014). No

obstante, estas oscilaciones gamma no se acoplan entre diferentes áreas corticales como lo hacen durante la vigilia (Figuras III 1 y III3), lo que sugiere que su acoplamiento entre áreas corticales distantes depende de las sinapsis glutamatérgicas con receptores NMDA entre las neuronas piramidales y las interneuronas corticales.

La ketamina induce síntomas psicóticos durante los primeros 40-60 minutos luego de su administración (Krystal et al., 2005). La dinámica temporal de estos síntomas coincide con la evolución dinámica de la disminución de la coherencia gamma observada en nuestros experimentos. Esta falta de acoplamiento de la actividad de frecuencia gamma durante el efecto máximo de la ketamina podría estar involucrada en las peculiaridades de las operaciones cognitivas que ocurren bajo el efecto de la ketamina. Es posible que este fenómeno también ocurra en pacientes que sufren de psicosis.

En relación a nuestros hallazgos, White & Siegel (2016), proponen que en la psicosis la potencia gamma esta aumentada durante QW. A su vez, un estudio en pacientes psicóticos durante el sueño encontró una disminución en la coherencia de la actividad en las frecuencias beta y gamma entre las áreas frontal derecha y central derecha (Yeragani et al., 2006). Además, estudios de la actividad gamma bajo estimulación sensorial visual o auditiva (AW) muestran que el aumento de la actividad gamma (30-50 Hz) y su acoplamiento de fase, inducida por dichos estímulos está reducida en pacientes psicóticos (Brenner et al., 2003; Kwon et al., 1999; Light et al., 2006; Adler et al., 1982; Freedman et al., 1996; Griffith et al., 1995; Waldo et al., 1995; Gallinat et al., 2004; Spencer et al., 2008; Lee et al., 2003; Sun et al., 2011). Estos hallazgos concuerdan con la falta de respuesta (tanto en potencia como en coherencia gamma) frente a estímulos sensoriales bajo el efecto de la ketamina (Figura III.3).

6. CONCLUSIONES

Concluimos que las interacciones funcionales entre las áreas corticales en la banda de frecuencia gamma disminuyen de manera similar en ambos modelos de psicosis, ketamina en dosis subanestésicas y sueño REM. Este desacoplamiento de la actividad de frecuencia gamma puede estar involucrado en las características cognitivas compartidas por las experiencias oníricas y la psicosis.

REFERENCIAS

Adams, B., & Moghaddam B. (1998) Corticolimbic dopamine neurotransmission is temporally dissociated from the cognitive and locomotor effects of phencyclidine. *Journal of Neuroscience.* 18, 5545–5554.

Adler, L.E., Pachtman, E., Franks, R.D., Pecevich, M., Waldo, M.C., Freedman, R., 1982. Neurophysiological evidence for a defect in neuronal mechanisms involved in sensory gating in schizophrenia. *Biology Psychiatry*. 17, 639–654.

Akeju, O., Song, A H., Hamilos, A E., Pavone, K J., Flores, F J., Brown, E N., & Purdon, P L. (2017) Electroencephalogram Signatures of Ketamine-Induced Unconsciousness. *Clinical Neurophysiology*. 127(6): 2414–2422.

Arnbjerg, J. (1979). Clinical use of ketamine-xylazine for anaesthesia in the cat *Nordisk veterinaermedicin.* 31(4):145-54

Babadi, B. & Brown, E.N. (2014) A review of multitaper spectral analysis. *IEEE Transactions on Biomedical Engineering.* 61, 1555-1564

Boucetta, S., Cisse, Y., Mainville, L., Morales, M. & Jones, B.E. (2014) Discharge Profiles across the Sleep-Waking Cycle of Identified Cholinergic, GABAergic, and Glutamatergic Neurons in the Pontomesencephalic Tegmentum of the Rat. *Journal of Neuroscience*. 34, 4708-4727.

Bauer, M., Oostenveld, R., Peeters, M., Fries, P. (2006) Tactile Spatial Attention Enhances Gamma-Band Activity in Somatosensory Cortex and Reduces Low-Frequency Activity in Parieto-Occipital Areas. *Journal of Neuroscience.* 26(2):490-501.

Bergeron, R., & Coyle, J.T. (2012) NAAG, NMDA receptor and psychosis. *Current Medicinal Chemistry.* 19: 1360–1364.

Berman, A.L., & Jones, E.G. (1982) The thalamus and basal telencephalum of the cat. A citoarchitectonic atlas with stereotaxic coordinates. University of Wisconsin. Madison.

Blain-Moraes, S., Lee, U., Ku, S., Noh, G., Mashour, GA. Electroencephalographic effects of ketamine on power, cross-frequency coupling, and connectivity in the alpha bandwidth. *Frontier in Systems Neuroscience*. 2014;8:114.

Bouyer, J.J., Montaron, M.F., & Rougeul, A. (1981) Fast fronto-parietal rhythms during combined focused attentive behavior and immobility in cat: cortical and thalamic localizations. *Electroencephalogram Clinical Neurophysiology*. 51. 244-252.

Bradley, P. B., & Elkes, J. (1953) On some effects of lysergic acid diethylamide (LSD 25) in normal volunteers. *Journal of. Physiology.* 120: 14P.

Bradley, P. B., & Elkes, J., (1957a) The effects of some drugs on the electrical activity of the brain. *Brain.* 80:77.

Bradley, P. B., & Elkes J. (1957b) in Metabolism of the Nervous System, ed. hı' I). Richter, pp. 515-522, Pergamon Press, London and New York,.

Bradley, P. B., & Key, B. J., (1958) The effect of drugs on arousal response produced by electrical stimulation of the reticular formation of the brain, *Electroencephalogram Clinical Neurophysiology*. 10: 97–110.

Bullock, T.H. (1997) Signals and signs in the nervous system: the dynamic anatomy of electrical activity is probably information-rich. *Proceedings of the National Academy of Science U S A*. 94. 1-6.

Bullock, T.H., & McClune, M.C. (1989) Lateral coherence of the electrocorticogram: a new measure of brain synchrony. *Electroencephalogram Clinical Neurophysiology*. 73. 479-498.

Bullock, T.H., McClune, M.C., Achimowic,. J.Z., Iragui-Madoz, V.J., Duckrow. R.B. & Spencer. S.S. (1995a) EEG coherence has structure in the millimeter domain: subdural and hippocampal recordings from epileptic patients. *Electroencephalogram Clinical Neurophysiology*. 95. 161-177.

Bullock, T.H., McClune, M.C., Achimowicz, J.Z., Iragui-Madoz, V.J., Duckrow, R.B. & Spencer, S.S. (1995b) Temporal fluctuations in coherence of brain waves *Proceedings of the National Academy of Science U S A*. 92. 11568-11572.

Bullock, T.H., McClune, M.C., & Enright, J.T. (2003) Are the electroencephalograms mainly rhythmic? Assessment of periodicity in wide-band time series. *Neuroscience*. 121. 233-252.

Buzsaki G, & Wang, X.J. (2012) Mechanisms of gamma oscillations. *Annu Rev Neuroscience.* 35. 203-225.

Buffenstein, A., Heaster, J., Ko, P., (1999). Chronic psychotic illness from amphetamine. *American Journal of Psychiatry*. 156, 662.

Braun, A.R., Balkin, T.J., Wesenten, N.J., Carson, R.E., Varga, M., Baldwin, P., Selbie, S., Belenky, G., & Herscovitch, P. (1997) Regional cerebral blood flow throughout the sleep-wake cycle. An H2 (15) O PET study. *Brain*. 120 (Pt 7) 1173-97

Brenner, C.A., Sporns, O., Lysaker, P.H., O'Donnell, B.F. (2003). EEG synchronization tomodulated auditory tones in schizophrenia, schizoaffective disorder, and schizotypal personality disorder. *American Journal of Psychiatry.* 160, 2238–2240

Cantero, J.L., Atienza, M., Madsen, J.R., & Stickgold, R., (2004) Gamma EEG dynamics in neocortex and hippocampus during human wakefulness and sleep. *Neuroimage*. 22. 1271-1280.

Cardin, J.A., Carlen, M., Meletis K., Knoblich, U., Zhang F., Deisseroth, K. (2009). Driving fast-spiking cells induces gamma rhythm and controls sensory responses *Nature*. 459 pp. 663-667

Carskadon, M. W. (2005). Normal Human Sleep: An Overview. In: Principles and practices of sleep medicine (Meir H. Kryger. T. R., William C. Dement. ed). pp 13-23 Philadelphia: Elsevier-Saunders.

Castro, S., Falconi, A., Chase, M. and Torterolo, P. (2013) Coherent neocortical 40-Hz oscillations are not present during REM sleep. *European Journal of Neuroscience*. 1–10. doi:10.1111/ejn.12143

Castro S., Cavelli M., Vollono P., Chase M H., Falconi A., Torterolo P. (2014) Inter-hemispheric coherence of neocortical gamma oscillations during sleep and wakefulness. *Neuroscience Letters.* 578 197–202.

Castro, S., Benedetto, L., Gutierrez, M., Falconi, A.., & Torterolo, P. (2010) "Coherence" in the cortical electrical activity during sleep and wakefulness 3rd *International Congress on Sleep Medicine and 12th Brazilian Congress on Sleep Medicine.*, San Pablo.

Castro, S., Gutierrez, M., Falconi, A., Chase, M. & Torterolo, P. (2011) Absence of EEG gamma (35-40Hz) coherence characterizes REM sleep and differentiates it from wakefulness *41st annual meeting of the Society for Neuroscience*., Washington.

Cavelli, M., Castro, S., Schwarzkopf, N., Chase, M H., Falconi A., Torterolo, P. (2015) Coherent neocortical gamma oscillations decrease during REM sleep in the rat *Behavioural Brain Research.* 281 318–325.

Cavelli, M., Castro, S., Mondino, A., Gonzales, J., Falconi, A., & Torterolo, P. (2017a) Absence of EEG gamma coherence in a local activated cortical

state: a conserved trait of REM sleep. *Translational Brain Rhythmicity.* 281 DOI10.1016/j.bbr.2014.12.050

Cavelli, M., Rojas-Líbano, Schwarzkopf, N., Castro, S., Gonzalez, J. D., Mondino, A., Santana, N., Benedetto, L., Falconi, A., &Torterolo, P. (2017b) Power and coherence of cortical High Frequency Oscillations during wakefulness and sleep. *European Journal of Neuroscience.* DOI10.1111/ejn.13718

Cavelli, M., Zoccolli, G., Silvani, A., Schwarzkopf, N., Castro-Zaballa, S., Gonzalez, J., Mondino, A., Santana, N., Falconi, A., Torterolo, P. (2017). Acoplamiento local y desacoplamiento de largo rango caracterizan a la actividad gamma (30-100 Hz) cortical durante el sueño REM. *Congreso Nacional de Biociencias,* Montevideo, 2017

Chow, K. L., Dement, W. C., & Mitchell, S. A. (1960) Electroenceph. din. Neurophysiol. 11: 107, 1959.Clide, Dean J.: Self ratings. In: *Drugs and Behavior*, ed. by J. G. Miller and L. Uhr, John Wiley & Sons, New York.

Cicogna, P. C., and Bosinelli, M. (2001). Consciousness during dreams. *Conscious. Cognition*. 10, 26–41. doi: 10.1006/ccog.2000.0471

Corsi-Cabrera, M., Miro, E., del-Rio-Portilla, Y., Perez-Garci, E., Villanueva, Y., & Guevara, M.A. (2003) Rapid eye movement sleep dreaming is characterized by uncoupled EEG activity between frontal and perceptual cortical regions. *Brain Cognition*. 51. 337-345.

Corlett, P. R., Honey, G. D., Aitken, M. R., Dickinson, A., Shanks, D. R., et al (2006) Frontal responses during learning predict vulnerability to the psychotogenic effects of ketamine: linking cognition, brain activity, and psychosis. *Archives of General Psychiatry.* 63:611–621

Corlett, P. R., Honey, G. D., Fletcher, P. C. (2007a) From prediction error to psychosis: ketamine as a pharmacological model of delusions. *Journal of Psychopharmacolgy.* 21:238–252

Corlett, P. R., Murray, G. K., Honey, G. D, Aitken, M. R, Shanks, D. R., Robbins, T. W., Bullmore, E. T., Dickinson, A., Fletcher, P. C. (2007b) Disrupted prediction-error signal in psychosis: evidence for an associative account of delusions. *Brain.* 130:2387–2400

Corlett, P. R., Frith, C. D., Fletcher, P. C. (2009) From drugs to deprivation: a Bayesian framework for understanding models of psychosis.Psychopharmacology. 206:515–530

Corlett, P. R., Honey, G. D., Krystal, J. H., Fletcher, P. C. (2011) Glutamatergic model psychoses: prediction error, learning, and inference. *Neuropsychopharmacology.* 36:294–315

Das, N.N. & Gastaut{ H. (1955) Variations de l'activite electrique du cerveau. du coeur et des muscles squellettiques au cours de la meditation et de l'extase yoguique. *Electroencephalogram Clinical Neurophysiology*. 6:211.

Dement, W., & Kleitman, N. (1957) The relation of eye movements during sleep to dream activity: an objective method for the study of dreaming. *Journal of Experimental Psychology*. 53 339-46.

Duncan, E. J, Madonick, S. H, Parwani, A., Angrist, B., Rajan, R., Chakravorty, S., Efferen, T. R., Szilagyi, S., Stephanides, M., Chappell, P. B., Gonzenbach, S., Ko, G. N., Rotrosen, J. P. (2001) Clinical and sensorimotor gating effects of ketamine in normals*. Neuropsychopharmacology.* 25:72–83

Dresler, M., Wehrle, R., Spoormaker, V. I., Steiger, A., Holsboer, F., Czisch, M., et al. (2014). Neural correlates of insight in dreaming and psychosis. *Sleep Medicine* Review. 20, 92–99. doi: 10.1016/j.smrv.2014. 06.004

Eckhorn, R., Bauer, R., Jordan, W., Brosch, M., Kruse, W., Munk, M., & Reitboeck. H.J., Coherent oscillations: a mechanism of feature linking in the visual cortex? Multiple electrode and correlation analyses in the cat. *Biology Cybernetics.* 60 (1988) 121-30.

Elkes, J. (1957) Effects of psychosomimetic drugs in animals and man. In: Neuropharmacology; Transactions of the Third Conference, ed. By H. A. Abramson, pp. 205-295, Josiah Macy, Jr. Foundation, New York,

Edelman, G.M., & Tononi, G. (2000) A universe of consciousness. Basic Books. New York.

Engelhardt, W., Stahl, K., Marouche, A., Hartung, E., Dierks, T. (1994) Ketamine racemate versus S-(+)-ketamine with or without antagonism with physostigmine. A quantitative EEG study on volunteers. *Anaesthesist*. 43(Suppl 2):S76–82.

Ferrer-Allado, T., Brechner, V. L., Dymond, A., Cozen, H., Crandal,l P., (1973) Ketamine-induced electroconvulsive phenomena in the human limbic and thalamic regions. *Anesthesiology.* 38:333–44.

Fletcher, P. C., Honey, G. D. (2006) Schizophrenia, ketamine and cannabis: evidence of overlapping memory deficits. *Trends Cognition Science.* 10:167–174

Fletcher, P.C., McKenna, P.J., Frith, C.D., Grasby, P.M., Friston, K.J., Dolan, R.J., 1998. Brain activation in schizophrenia during a graded memory taski studied with functional neuroimaging. *Archives of General Psychiatry.* 55, 1001–1008.

Fosse, R., Stickgold, R., & Hobson, J.A. (2001) Brain-mind states: reciprocal variation in thoughts and hallucinations. *Psychology Science*. 12. 30-36.

Fuchs, E.C., Zivkovic, A.R., Cunningham, M.O., Middleton, S., Lebeau, F.E., Bannerman, D.M. (2007) Recruitment of parvalbumin-positive interneurons determines hippocampal function and associated behavior. *Neuron*. 53 . 591-604

Fuster, J.M. (1989) *The prefrontal cortex*. Raven Press. New York.

Freedman, R., Adler, L.E., Myles-Worsley, M., Nagamoto, H.T., Miller, C., Kisley, M., McRae, K., Cawthra, E., Waldo, M., (1996). Inhibitory gating of an evoked response to repeated auditory stimuli in schizophrenic and normal subjects. Human recordings, computer simulation, and an animal model. *Archives of General Psychiatry*. 53, 1114–1121.

Galarreta, M., Hestrin, S. (1999) A network of fast-spiking cells in the neocortex connected by electrical synapses *Nature*. 402. 72-615

Gallinat, J., Winterer, G., Herrmann, C.S., Senkowski, D., (2004). Reduced oscillatory gamma-band responses in unmedicated schizophrenic patients indicate impaired frontal network processing. *Clinical Neurophysiology.* 115, 1863–1874.

Gottesmann, C. (2006) Dreaming and schizophrenia: a common neurobiological background? *Medical Science*. 22(2):201-5

Garzon, M., de Andres, I. & Reinoso-Suarez, F. (1997) Neocortical and hippocampal electrical activities are similar in spontaneous and cholinergic-induced REM sleep. *Brain Research*. 766, 266-270.

Gosseries, O., Bruno, M., Vanhaudenhuyse, A., Laureys, S. & Schnakers, C. (2009) Consciousness in the locked-in syndrome. In Laureys, S., Tononi, G. (eds.) The neurology of consciousness: cognitive neuroscience and neuropathology. Elsevier, San Diego. 191-203.

Gottesmann, C & Gottesman, I. (2007). The neurobiological characteristics of rapid eye movement (REM) sleep are candidate endophenotypes of depression, schizophrenia, mental retardation and dementia. *Progress in Neurobiology*. 81.4. 237-250.

Guilleminault, C. & Fromherz, S. (2011) Narcolepsy: Diagnosis and Management. In Kryger, M.H., Roth, T., Dement, W.C. (eds.) Principles and practices of sleep medicine. Saunders, Philadelphia, . 957-968.

Grace, A.A., 1991. Phasic versus tonic dopamine release and the modulation of dopamine system responsivity: a hypothesis for the etiology of schizophrenia. *Neuroscience.* 41, 1–24.

Griffith, J., Hoffer, L.D., Adler, L.E., Zerbe, G.O., Freedman, R., (1995). Effects of sound intensity on a midlatency evoked response to repeated auditory stimuli in schizophrenic and normal subjects. *Psychophysiology* 32, 460–466.

Hall, G.H. (1970) Effects of nicotine and tobacco smoke on the electrical activity of the cerebral cortex and olfactory bulb. *British Journal of Pharmacology*. 38, 271-286.

Hanna, R.M., Borchard, R.E. & Schmidt, S.L. Pharmacokinetics of ketamine HC1 and metabolite I in the cat: a comparison of i.v., i.m., and rectal administration. *Journal of veterinary Pharmacology Therapy.* 11, 84–93.

Harle, M., Rockstroh, B.S., Keil. A., Wienbruch. C. & Elbert. T.R. (2004) Mapping the brain's orchestration during speech comprehension: task-specific facilitation of regional synchrony in neural networks. *BMC Neuroscience*. 5. 40.

Hering, W., Geisslinger, G., Kamp, H. D., Dinkel, M., Tschaikowsky, K., Rugheimer, E., et al. (1994) Changes in the EEG power spectrum after midazolam anaesthesia combined with racemic or S- (+) ketamine. *Acta Anaesthesiologica Scandinavica*. 38:719–23.

Heresco-Levy, U., 2000. N-methyl-D-aspartate (NMDA) receptor-based treatmentapproaches in schizophrenia: the first decade. *International Journal of Neuropharmacology.* 3, 243–258.

Hipp, J. F. & Siegel, M. (2013) Dissociating neuronal gamma-band activity from cranial and ocular muscle activity in EEG. *Frontiers in human neuroscience.* doi:10.3389/fnhum.00338.

Hobson, J. A. (1997) Dreaming as Delirium: A Mental Status Analysis of our Nightly Madness. *Seminars in Neurology.* 17:2; 121-128

Hobson, J. A. (2009) REM sleep and dreaming: towards a theory of protoconsciousness. *National Review Neuroscience*. 10. 803-813.

Homayoun, H., Moghaddam, B. (2007) NMDA receptor hypofunction produces opposite effects on prefrontal cortex interneurons and pyramidal neurons*. Journal of Neuroscience.* 27:11496–500.

Honey, RA., Turner, D. C., Honey, G. D., Sharar, S. R., Kumaran, D., Pomarol-Clotet, E., McKenna, P., Sahakian, B. J., Robbins, T. W., Fletcher, P. C. (2003) Subdissociative dose ketamine produces a deficit in manipulation but not maintenance of the contents of working memory. *Neuropsychopharmacology.* 28:2037–2044

Honey, R. A., Honey, G. D., O'Loughlin, C., Sharar, S. R., Kumaran. D., Bullmore. E. T. et al (2004) Acute ketamine administration altersthe brain responses to executive demands in a verbal working memory task: an FMRI study. *Neuropsychopharmacology.* 29:1203–1214

Hunt., MJ & Kasicki S A (2013) systematic review of the effects of NMDA receptor antagonists on oscillatory activity recorded in vivo. *Journal of Psychopharmacology.* 27(11) 972–986

Jasper, H. H. & Andrews, H.L. (1938) Brain potentials and voluntary muscle activity in man. *Journal of Neurophysiology*. 1. 87-100.

Jakovljevic, M., Sagud, M., Mihaljevic-Peles, A., (2003). Olanzapine in the treatment-resistant, combat-related PTSD—a series of case reports. *Acta Psychiatrica Scandinavica.* 107, 394–396.

John, E.R. (2002) The neurophysics of consciousness. *Brain Research*. 39. 1-28

Jouvet, M. (1965) [The paradoxical phase of sleep]. *International Journal of Neurology*. 5, 131-150.

Kantrowitz, J., & Javitt DC (2012) Glutamatergic transmission in schizophrenia: From basic research to clinical practice. Current Opinion Psychiatry 25: 96–102.

Kim, T., Thankachan, S., McKenna, J.T., McNally, J.M., Yang, C., Choi, J.H., Chen, L., Kocsis, B., Deisseroth, K., Strecker, R.E., Basheer, R., Brown, R.E. & McCarley, R.W. (2015) Cortically projecting basal forebrain parvalbumin neurons regulate cortical gamma band oscillations. *Proceedings of the National Academy of Science U S A*. 112, 3535-3540.

Kim, J., Glahn, D. C., Nuechterlein, K. H., Cannon, T. D. (2004) Maintenance and manipulation of information in schizophrenia: further evidence for impairment in the central executive component of working memory. *Schizophrenia Research.* 68:173–187

Krystal, J. H., Karper, L. P., Seibyl, J. P., Freeman, G. K., Delaney, R. et al (1994) Subanesthetic effects of the noncompetitive NMDA antagonist, ketamine, in humans psychotomimetic, perceptual, cognitive, and neuroendocrine responses. *Archives of General Psychiatry.* 51:199–214

Krystal, J. H., Karper, L. P., Bennett. A., D'Souza, D. C., Abi-Dargham, A. et al (1998) Interactive effects of subanesthetic ketamine and subhypnotic lorazepam in humans. *Psychopharmacology.* 135:213–229

Krystal, J. H., Perry, E. B., Gueorguieva, R., Belger, A., Madonick, S. H., Abi-Dargham, A., Cooper, T. B., MacDougall, L., Abi-Saab, W., D'Souza, D. C. (2005) Comparative and Interactive Human Psychopharmacologic Effects of Ketamine and Amphetamine: Implications for Glutamatergic and Dopaminergic Model Psychoses and Cognitive Function. *Archives of General Psychiatry*. 62:985-995

Konradi, C., Heckers, S., (2003). Molecular aspects of glutamate dysregulation: implications for schizophrenia and its treatment. *Pharmacological Therapy*. 97, 153–179.

Kwon, J.S., O'Donnell, B.F., Wallenstein, G.V., Greene, R.W., Hirayasu, Y., Nestor, P.G., Hasselmo, M.E., Potts, G.F., Shenton, M.E., McCarley, R.W., (1999). Gamma frequency-range abnormalities to auditory stimulation in schizophrenia. *Archives of General Psychiatry*. 56, 1001–1005.

Langsjo, J. W., Maksimow, A., Salmi, E., Kaisti, K., Aalto, S., Oikonen, V., et al. (2005) S-ketamine anesthesia increases cerebral blood flow in excess of the metabolic needs in humans. *Anesthesiology*. 103: 258–68.

Langsjo, JW., Salmi, E., Kaisti, K. K., Aalto, S., Hinkka, S., Aantaa, R., et al. (2004) Effects of subanesthetic ketamine on regional cerebral glucose metabolism in humans. *Anesthesiology*. 100:1065–71.

Lazarewicz, M. T., Ehrlichman, R. S., Maxwell, C., Gandal, M, J., Finkel, L. H., &. Siegel S J. (2009) Ketamine Modulates Theta and Gamma Oscillations. *Journal of Cognitive Neuroscience.* 22:7, 1452–1464

Lee, U., Ku, S., Noh, G., Baek, S., Choi, B., Mashour, G. A., Disruption of frontal-parietal communication by ketamine, propofol, and sevoflurane. *Anesthesiology*. 2013;118:1264–75.

Lee, K.H., Williams, L.M., Haig, A., Gordon, E., (2003). "Gamma (40 Hz) phase synchronicity" and symptom dimensions in schizophrenia. *Cognitive. Neuropsychiatry*. 8, 57–71.

Le´na, I., Parrot, S., Deschaux, O., Muffat, S., Sauvinet, V., Renaud, B., Suaud-Chagny, M.F., Gottesmann, C., (2005). Variations in the extracellular levels of dopamine, noradrenaline, glutamate and aspartate across the sleep–wake cycle in the medial prefrontal cortex and nucleus accumbens of freely moving rats. *Journal of Neuroscience*. Res. 81, 891–899.

Lewis, D. A., Hashimoto, T., Volk, D.W. (2005). Cortical inhibitory neurons and schizophrenia *National Review Neuroscience*. 6 . 312-324

Lewis, D. A., Moghaddam, B. (2006). Cognitive dysfunction in schizophrenia: Convergence of gamma-aminobutyric acid and glutamate alterations *Arch ives of Neurol*ogy. 63 . 1372-1376

Libet, B., Pearl, D.K., Morledge, D.E., Gleason, C.A., Hosobuchi, Y. & Barbaro, N.M. (1991) Control of the transition from sensory detection to sensory awareness in man by the duration of a thalamic stimulus. The cerebral 'time-on' factor. *Brain*. 114 (Pt 4). 1731-1757.

Light, G.A., Hsu, J.L., Hsieh, M.H., Meyer-Gomes, K., Sprock, J., Swerdlow, N.R., Braff, D.L., (2006). Gamma band oscillations reveal neural network cortical coherence dysfunction in schizophrenia patients. *Biology Psychiatry* 60, 1231–1240.

Llinas, R., & Ribary, U. (1993) Coherent 40-Hz oscillation characterizes dream state in humans. *Proceedings of the National Academy of Science U S A*. 90. 2078-2081.

Llinas, R., Ribary, U., Contreras, D., & Pedroarena, C., (1998) The neuronal basis for consciousness. *Philosoohical Transactions of the Royal Society of London B Biological Sciences*. 353. 1841-1849.

Llinas, R.R., Grace, A.A. &Yarom, Y. (1991) In vitro neurons in mammalian cortical layer 4 exhibit intrinsic oscillatory activity in the 10- to 50-Hz frequency range. *Proceedings of the National Academy of Science U S A*. 88, 897-901.

Lisman, J., Buzsaki, G. (2008): A neural coding scheme formed by the combined function of gamma and theta oscillations. *Schizophrenia Bull*. 34:974–980.

Mann, E. O., Suckling, J. M., Hajos, N., Greenfield. S. A., Paulsen, O. (2005) Perisomatic feedback inhibition underlies cholinergically induced fast network oscillations in the rat hippocampus in vitro *Neuron*. 45. 105-117

Manoach, D. S., and Stickgold, R. (2009). Does abnormal sleep impair memory consolidation in schizophrenia? *Froniers in Human Neuroscience*. 3:21. doi: -10.3389/neuron.09.021.2009

MacKay, A.V., Iversen, L.L., Rossor, M., Spokes, E., Bird, E., Arregui, A., Snyder, S., (1982). Increased brain dopamine and dopamine receptors in schizophrenia. *Archives of General Psychiatry*. 39, 991–997.

Malhotra, A. K., Pinals, D. A., Weingartner, H., Sirocco, K., Missar, C. D., et al (1996) NMDA receptor function and human cognition: the effects of ketamine in healthy volunteers. *Neuropsychopharmacology.* 14:301–307

Maloney, K. J., Cape, E. G., Gotman, J., & Jones, B. E. (1997) High-frequency gamma electroencephalogram activity in association with sleep-wake states and spontaneous behaviors in the rat. *Neuroscience*. 76. 541-555.

Maquet, P. & Franck, G., (1997). REM sleep and amygdala. *Molecular Psychiatry*. 2, 195–196.

Maquet, P., Peters, J.M., Aerts, J., Delfiore, G., Degueldre, C., Luxen, A., Franck, G., (1996). Functional neuroanatomy of human rapid-eye-movement sleep and dreaming. *Nature.* 383, 163–166.

Markowitsch, H. J., & Pritzel, M. (1977) A stereotaxic atlas of the prefrontal cortex of the cat. *Acta Neurobiologiae Experimentalis (Wars)*. 37. 63-81.

Mashour, G. A. (2006) Integrating the science of consciousness and anesthesia. *Anesthesia & Analgesia*. 103. 975-982.

Mashour, G.A. & Avidan, M.S. (2015) Intraoperative awareness: controversies and non-controversies. *British Journal of Anaesthesiology*. 1:i20-i26. doi: 10.1093/bja/aev034.

Massimini, M., Ferrarelli, F., Huber, R., Esser, S.K., Singh, H. &Tononi, G. (2005) Breakdown of cortical effective connectivity during sleep. *Science*. 309, 2228-2232.

Miltner, W.H., Braun, C., Arnold, M., Witte, H., Taub, E., (1999). Coherence of gamma-band EEG activity as a basis for associative learning. *Nature.* 397, 434 – 436.

Morrison, A.R. (1983) A window on the sleeping brain. *Scientific America*. 248. 94-102.

Mota-Rolim, S. A., and Araujo, J. F. (2013). Neurobiology and clinical implications of lucid dreaming. *Medine Hypothesys.* 81, 751–756. doi: 10.1016/j.mehy.2013. 04.049

Morgan, C. J, Curran, H. V. (2006) Acute and chronic effects of ketamine upon human memory: a review*. Psychopharmacology.* 188:408– 424

Mota, N. B., Resende, A., Sérgio, A., Mota-Rolim, Copelli, M., & Ribeiro, S. (2016).Psychosis and the Control of Lucid Dreaming *Frontiers in Psychology.* 7(185) · March DOI: 10.3389/fpsyg.2016.00294 · License: CC BY 4.0

Nir, Y., Mukamel, R., Dinstein, I., Privman, E., Harel, M., Fisch, L., Gelbard-Sagiv, H., Kipervasser, S., Andelman, F., Neufeld, M.Y., Kramer, U., Arieli, A., Fried, I., & Malach, R., (2008) Interhemispheric correlations of slow spontaneous neuronal fluctuations revealed in human sensory cortex. *Nature Neuroscience*. 11. 1100-1108.

Nir, Y., & Tononi. G. (2010) Dreaming and the brain: from phenomenology to neurophysiology. *Trends in Cognitive Science*. 14. 88-100.

Nunez, P.L., Srinivasan, R., Westdorp, A.F., Wijesinghe, R.S., Tucker, D.M., Silberstein, R.B., & Cadusch, P.J., (1997) EEG coherency. I: Statistics. reference electrode. volume conduction. Laplacians. cortical imaging. and interpretation at multiple scales. *Electroencephalogram Clinical Neurophysiology*. 103. 499-515.

Pal, D., Hambrecht-Wiedbusch, V. S., Silverstein, B. H., Mashour, G. A-. (2015) Electroencephalographic coherence and cortical acetylcholine during ketamine-induced unconsciousness*. British Journal of Anaesthesiology*. 114:979–89

Palenicek, T., Fujakova, M., Brunovsky, M., et al. (2011) Electroencephalographic spectral and coherence analysis of ketamine in rats: Correlation with

behavioral effects and pharmacokinetics. *Neuropsychobiology.* 63: 202–218

Pace-Schott, E., (2005). The neurobiology of dreaming. In M.H. Kryger. T. Roth and W.C. Dement (Eds.). Principles and practices of sleep medicine. Elsevier-Saunders. Philadelphia. . 551-564.

Paul, J., C., Riehl, J. L., & Unna, K. R. (1959) Quantitation of the effects of depressant drugs on EEG activation response. *Federation. Proceedings*. 18: 431,

Paul, I. A., and Skolnick, P. (2003) Glutamate and depression: Clinical and preclinical studies. *Annals of the NY Academy of Science.* 1003: 250–272.

Perez-Garci, E., del-Rio-Portilla, Y., Guevara, M. A., Arce, C. & Corsi-Cabrera, M. (2001) Paradoxical sleep is characterized by uncoupled gamma activity between frontal and perceptual cortical regions. *Sleep*. 24. 118-126.

Perry, W., Heaton, R. K., Potterat, E., Roebuck, T., Minassian, A., Braff, D.L (2001) Working memory in schizophrenia: transient “online” storage versus executive functioning. *Schizophrenia Bull.* 27:157–176

Pinault, D- (2008) N-methyl d-aspartate receptor antagonists ketamine and MK-801 induce wake-related aberrant gamma oscillations in the ratneocortex. *Biology Psychiatry.* 63: 730–735.

Pomarol-Clotet, E., Honey, G. D., Murray, G. K,, Corlett, P. R., Absalom, A. R. et al (2006) Psychological effects of ketamine in healthy volunteers. Phenomenological study. *British Journal of Psychiatry.* 189:173–179

Phillips, K. G., Cotel, M. C., McCarthy, A. P., et al. (2012) Differential effects of NMDA antagonists on high frequency and gamma EEG oscillations in a neurodevelopmental model of schizophrenia. *Neuropharmacology.* 62: 1359–1370.

Rechtschaffen, A. (1978) The single-mindedness and isolation of dreams. *Sleep*. 1. 97-109.

Rieder, M. K., Rahm, B., Williams, J. D., & Kaiser, J. (2010) Human gamma-band activity and behavior. *International Journal of Psychophysiology*. 79. 39-48.

Rajkowski, J., Kubiak, P., & Aston-Jones, G., (1994) Locus coeruleus activity in monkey: phasic and tonic changes are associated with altered vigilance. *Brain Research Bull.* 35:607-616.

Reeves, M., Lindholm, D.E., Myles, P.S., Fletcher, H., Hunt, J.O., (2001). Adding ketamine to morphine for patient-controlled analgesia after major abdominal surgery: a double-blind, randomized trial. *Anesthesia & Analgesia*. 93, 116–120.

Reinoso-Suarez, F., de Andres, I., Rodrigo-Angulo, M.L. & Garzon, M. (2001) Brain structures and mechanisms involved in the generation of REM sleep. *Sleep Medicine Review*. 5, 63-77.

Roach, B.J., & Mathalon, D.H. (2008) Event-related EEG time-frequency analysis: an overview of measures and an analysis of early gamma band phase locking in schizophrenia. *Schizophrenia Bull*. 34, 907-926.

Sastre, J. P., & Jouvet, M. (1979). Oneiric behavior in cats. *Physiology Behaviour*. 22. 979-989.

Seamans, J. (2008) Losing inhibition with ketamine. *Nature Chemical Biology*. ;4:91–3.

Schwartz, S. & Maquet. P. (2002) Sleep imaging and the neuro-psychological assessment of dreams. *Trends in Cognitive Scencei*. **6**. 23-30.

Schwartz, T. L., Sachdeva, S., & Stahl, S. M. (2012) Genetic data supporting the NMDA glutamate receptor hypothesis for schizophrenia. *Current Pharmacology.* 18: 1580–1592.

Schultz, A., Schultz. B., Zachen, B., Pichlmayr, I. (1990). The effects of ketamine on the electroencephalogram--typical patterns and spectral representations. [Article in German]. *Anaesthesist.* 39:222–5.

Schwartz, M. S., Virden, S., Scott, D. F. (1974). Effects of ketamine on the electroencephalograph*. Anaesthesia*. 29:135–40.

Singer, W., 2002. Gamma oscillations and cognition. In: Reisin, R.C., Nuwer, M., Hallet, M., Medina, C. (Eds.), Advances in Clinical Neurophysiology. *Clinical. Neurophysiol.* (Suppl.), vol. 54. Elsevier, The Netherlands, 3 – 22.

Sirota, A., Montgomery, S., Fujisawa, S., Isomura, Y., Zugaro, M., & Buzsáki, G. (2008) Entrainment of Neocortical Neurons and Gamma Oscillations by the Hippocampal Theta Rhythm. *Neuron*. 60, 683–697.

Sohal, V. S., Zhang, F., Yizhar, O. (2009).Deisseroth Parvalbumin neurons and gamma rhythms enhance cortical circuit performance *Nature*. 459. 698-702

Solms, M., (2000). Dreaming and REM sleep are controlled by different brain mechanisms. *Behavioural Brain Science*. 23, 843–850.

Scorza, M. C., Meikle, M. N., Hill, X. L., Richeri, A., Lorenzo, D., & Artigas, F. (2007) Prefrontal cortex lesions cause only minor effects on the hyperlocomotion induced by MK-801 and its reversal by clozapine. The International *Journal of Neuropsychopharmacology.* 11(4):519-32DOI10.1017/S1461145708008432

Skosnik, P.D., Cortes-Briones, J.A., & Hajós, M. (2015). Cannabinoids, Neural Oscillations, and Psychosis. *Biological Psychiatry.* 79:568–577

Sun, Y., Farzana, F., Barra, M.S., Kiriharab, K., Fitzgeraldc, P.B., Lightb, G.A., Daskalakisa, Z.J. (2011). Gamma oscillations in schizophrenia: Mechanisms and clinical significance. *Brain Research.* 98 – 114 doi:10.1016/j.brainres.2011.06.065

Spencer, K.M., Niznikiewicz, M.A., Shenton, M.E., McCarley, R.W., (2008). Sensory-evoked gamma oscillations in chronic schizophrenia. *Biology Psychiatry.* 63, 744–747.

Steriade, M., Amzica, F., & Contreras, D. (1996) Synchronization of fast (30-40 Hz) spontaneous cortical rhythms during brain activation. *Journal of Neuroscience*. 16. 392-417.

Stone, J. M., Pilowsky L, S. (2006) Psychopathological consequences of ketamine. *British Journal of Psychiatry.* 189:565–566

Tamas, G., Buhl, E. H., Lorincz, A., Somogyi, P. (2000) Proximally targeted GABAergic synapses and gap junctions synchronize cortical interneurons *Nature Neuroscience*. 3 . 366-371

Thompson, D.F., & Pierce, D.R., (1999). Drug-indiced nightmares. *Annals of Pharmacotherapy*. 33, 93–98.

Thompson, R. F., Johnson, R. H., & Hoopes, J. J. (1963) Organization of auditory somatic sensory and visual projection to association fields of cerebral cortex in the cat. *Journal of Neurophysiology*. 26. 343-364.

Tiitinen, H., Sinkkonen, J., Reinikainen, K., Alho, K., Lavikainen, J. & Naatanen, R. (1993) Selective attention enhances the auditory 40-Hz transient response in humans. *Nature*. 364. 59-60.

Tononi, G. (2009) Sleep and dreaming. In Laureys, S., Tononi, G. (eds.) The neurology of consciousness: cognitive neuroscience and neuropathology. Elsevier, San Diego, . 89-107.

Tononi, G. (2010) Information integration: its relevance to brain function and consciousness. *Archives Italiannes de Biologia*. 148. 299-322.

Torterolo, P., Benedetto, L., Lagos, P., Sampogna, S., & Chase, M. H. (2009) State-dependent pattern of Fos protein expression in regionally-specific sites within the preoptic area of the cat. *Brain Research*. 1267. 44-56.

Torterolo, P., Castro, S., Cavelli, M., Velazques, N., Brando, V., Falconi, A., Chase, M. H., Migliaro, E. (2015) Heart rate variavility during carbachol-induced REM sleep and cataplexy. *Behavioural Brain Research*. 291. 72. 79

Torterolo, P., Castro, S., Cavelli, M., Chase, M. H., Falconi, A. (2016) Neocortical 40 Hz oscillations during carbachol-induced rapid eye movement sleep and

cataplexy. *European Journal of Neuroscience*. 1–10, 2016. doi:10.1111/ejn.13151.

Torterolo, P., & Vanini, G. (2010) Nuevos conceptos sobre la generación y el mantenimiento de la vigilia. *Review Neurology*. 50: 747-58.

Uhlhaas, P.J., Pipa, G., Lima, B., Melloni, L., Neuenschwander, S., Nikolic, D., & Singer, W. (2009) Neural synchrony in cortical networks: history. concept and current status. *Frontiers of Integrative Neuroscencei*. 3. 17.

Uhlhaas, P.J., Pipa, G., Neuenschwander, S., Wibral, M., & Singer, W. (2011) A new look at gamma? High- (>60 Hz) gamma-band activity in cortical networks: function. Mechanisms and impairment. *Progress in Biophysycs & Molecular Biology*. 105. 14-28.

Urbano, F.J., Kezunovic, N., Hyde, J., Simon, C., Beck, P. & Garcia-Rill, E. (2012) Gamma band activity in the reticular activating system. *Frontiers Neurology*. 3. 6.

Ursin, R., & Sterman, M. (1981) Manual for standardized scoring of sleep and waking states in adult cats. BIS/BRI. University of California. Los Angeles.

Vanini, G., Torterolo, P., Baghdoyan, H. A., & Lydic R. (2011) The shared circuits of sleep and anesthesia. Neuroscientific foundations of anesthesiology.

Von der Malsburg., C. (1995) Binding in models of perception and brain function. *Current Opinion Neurobiology*. 5. 520-526.

Voss, U., Holzmann, R., Hobson, A., Paulus, W., Koppehele-Gossel, J., Klimke, A. & Nitsche, M.A. (2014) Induction of self awareness in dreams through frontal low current stimulation of gamma activity. *Nature Neuroscience*. 17, 810-812.

Voss, U., Holzmann, R., Tuin, I. & Hobson. J.A. (2009) Lucid dreaming: a state of consciousness with features of both waking and non-lucid dreaming. *Sleep*. 32. 1191-1200.

Waldo, M., Myles-Worsley, M., Madison, A., Byerley, W., Freedman, R., (1995). Sensory gating deficits in parents of schizophrenics. *American Journal of Medical Genetics*. 60, 506–511.

Watson, C., Baghdoyan, H., & Lydic. R., (2010) A neurochemical perspective on states of consciousness. In Hudetz. A.G., Pearce. R. (eds.) Supressing the Mind. Contemporary Clinical Neuroscience. Humana Press. 33-79.

Weinberger, D.R., Berman, K.F., Zec, R.F., (1986). Physiological dysfunction of dorsolateral prefrontal cortex in schizophrenia. 1. Regional cerebral blood flow evidence. *Archives of General Psychiatry*. 43, 114–124.

White, R.S., & Siegel, S.J. (2016). Cellular and circuit models of increased resting state network gamma activity in schizophrenia. *Neuroscience*. 321 66–76

Whittington, M.A., Traub, R.D., Jefferys, J.G. (1995) Synchronized oscillations in interneuron networks driven by metabotropic glutamate receptor activation *Nature*. 373 . 612-615

Yeragani, V.K., Cashmere, D., Miewald, J., Tancer, M., Keshavan, M.S. (2006) Decreased coherence in higher frequency ranges (betaand gamma) between central and frontal EEG in patients with schizophrenia: A preliminary report. *Psychiatry Research*. 141:53–60.

Ylinen, A., Soltesz, I., Bragin, A., Penttonen, M., Sik, A., Buzsaki, G. (1995) Intracellular correlates of hippocampal theta rhythm in identified pyramidal cells, granule cells, and basket cells *Hippocampus*. 5 . 78-90

Yuval-Greenberg, S., Tomer, O., Keren, A.S., Nelken, I. & Deouell. L.Y. (2008) Transient induced gamma-band response in EEG as a manifestation of miniature saccades. *Neuron*. 58. 429-441.

CAPITULO IV

ROL DEL SISTEMA COLINÉRGICO EN LAS OSCILACIONES GAMMA DEL EEG

1. Introducción

Las neuronas colinérgicas mesopontinas y del cerebro basal anterior están involucradas en el control de los estados comportamentales y en las funciones cognitivas durante la vigilia (Torterolo et al., 2016).

La administración sistémica de atropina, un antagonista colinérgico muscarínico, en animales de experimentación, provoca un enlentecimiento del EEG, con ondas lentas y husos similares a los del sueño. Sin embargo, los animales permanecen activos (Wilker, 1952). Esta falta de correlación entre el EEG con características de sueño y el comportamiento se denomina “disociación”. Esta disociación fue observada en perros, gatos y conejos (Wilker, 1952; Bradley & Elkes, 1953; Bach et at., 1955; Longo, 1956; Bradley & Elkes, 1957a, b; Elkes, 1957; Chow et at., 1959; Yamamoto, 1988). La atropina disminuye la activación en el EEG generado tanto por estimulación sensorial como por estimulación de la formación reticulada del tronco encefálico (Rinaldi & Himwich, 1955; Bradley & Elkes, 1957b; Bradley & Key, 1958; Paul et at., 1959). No obstante, la respuesta comportamental a estos estímulos no se afecta (Bradley & Key, 1958).

Para encontrar pistas que expliquen la falta de correspondencia entre el comportamiento y los patrones de EEG inducidos por los antagonistas del receptor muscarínico, en el presente Capítulo estudiamos la potencia y la coherencia en la banda de gamma frecuencias de EEG del gato tratado con atropina y escopolamina. Estos son antagonistas

muscarínicos competitivos no selectivos empleados comúnmente. Comparamos estos resultados con la potencia y la coherencia gamma del EEG que está presente durante la W y el sueño.

1.2 Hipótesis de trabajo

Esperamos encontrar que si bien bajo el efecto de atropina y escopolamina, las ondas lentas del EEG tienen un patrón similar al sueño NREM, las oscilaciones gamma tienen un patrón similar al de vigilia. Esto explicaría la vigilia conductual bajo su efecto.

2. Objetivos

2.1. Objetivo general

Estudiar como las oscilaciones gamma y su nivel de acoplamiento entre áreas corticales es regulado por el sistema colinérgico.

2.2. Objetivos específicos

Analizar la potencia y el acoplamiento de las oscilaciones en la banda gamma entre distintas áreas corticales bajo el efecto de los antagonistas del receptor muscarínico (atropina y escopolamina).

3. Material y métodos.

Gran parte de la metodología fue descrita previamente. Solo se comentaran los detalles diferenciales en esta serie experimental.

3.1. Sesiones experimentales

Se realizaron registros poligráficos en 5 animales en los que se registraron simultáneamente la actividad múltiples áreas corticales con electrodos monopolares (las áreas corticales en cada animal se muestran en la Figura IV.1.A). Los datos fueron obtenidos luego de la administración de atropina o escopolamina, así como durante AW, QW, sueño NREM y REM.

La atropina (0.2 o 0.4 mg/kg s/c, Sigma) o escopolamina (1 mg/kg s/c., Sigma) fueron administradas en 4 sesiones experimentales (por dosis) en 5 y 3 animales respectivamente; las dosis fueron similares a la de estudios previos (Martin & Eades, 1960; Hall, 1970; Zagrodzka & Kubiak, 1991). La administración de las drogas se hizo en distintos días, en forma randomizada, dejando siempre por lo menos dos días de descanso entre ellas. En experimentos piloto se administró vehículo (salina) y el análisis del EEG durante la vigilia y el sueño mostraron resultados similares a los observados en registros basales; por lo tanto, se utilizaron registros basales (sin administración de solución salina) para el análisis.

3.2. Análisis de los datos

Además, los intervalos de RR de la señal de ECG también se analizaron y trazaron en función del tiempo (tacograma) (Brando et al., 2014; Torterolo et al., 2015).

Se compararon la potencia y la coherencia de la banda gamma baja (30-45 Hz) del EEG bajo los efectos de atropina y escopolamina con los estados de W y sueño. Para normalizar los datos y realizar pruebas estadísticas paramétricas, se utilizó la transformación Fisher z' para los valores de coherencia gamma. Posteriormente, se analizaron los perfiles de coherencia z' de la banda gamma en épocas de 100 segundos para cada par de registros de EEG, así como el promedio de doce épocas. La potencia y la coherencia z' de la banda gamma para cada canal de EEG o derivado (par de canales EEG) también se promediaron para los estados comportamentales y los tratamientos farmacológicos. Los efectos de las drogas se analizaron en el período de su máximo efecto; es decir, las ventanas de análisis se tomaron 10-20 minutos luego de la inyección de escopolamina, y 60-70 minutos luego de la administración de atropina.

Para las Figuras III.1 y III.5 se usaron los enfoques de multitaper y wavelet para estimar la potencia de EEG (ver Capítulo III).

Los datos se expresaron como media ± error estándar. Se evaluó la significancia de las diferencias entre estados conductuales para cada gato con ANOVA unidireccional y prueba de Tamhane. Para analizar el efecto de los fármacos en todo el grupo de animales (Figura IV.7), se estudio la media de la coherencia z' intra-hemisférica de la banda gamma entre áreas corticales anteriores (S1 para C1 y C3, Pf para C2 y C5 y M1 para C4; Figura IV.1A) y posteriores (V1 para C4, y Pp para el resto de los animales). Para este propósito, utilizamos ANOVA de medidas repetidas (rmANOVA) y la prueba *post hoc* de Bonferroni. El criterio utilizado para rechazar hipótesis nulas fue $p < 0.05$.

4. Resultados.

4.1. Comportamiento

Luego de la administración de atropina (0.2 y 0.4 mg/kg) o escopolamina (1 mg/kg), los animales estuvieron despiertos y pudieron seguir a los experimentadores con sus ojos. También fueron capaces de vocalizar. Cuando los animales, aún bajo los efectos de las sustancias, se volvieron a colocar en condición de libre movimiento (al final de los experimentos, 3 a 4 horas después de la inyección del fármaco), pudieron deambular normalmente.

4.2. Registros crudos y filtrados

Como era de esperar, ambas dosis de atropina aumentaron la frecuencia cardíaca y eliminaron su variabilidad (se muestra un ejemplo en el tacograma de la Figura IV.1B); sin embargo, la droga produjo efectos centrales claros solo a 0.4 mg/kg. Por lo tanto, solo analizamos los efectos de la dosis más alta.

La atropina (0.4 mg/kg) promovió vigilia comportamental acompañada de ondas lentas de alta amplitud y husos en el EEG; es decir, un EEG similar al de sueño NREM. Los efectos cardiovasculares alcanzaron su mayor valor entre 3 y 5 minutos después de la

administración, mientras que las ondas lentas y los husos se desarrollaron completamente después de 40-50 minutos. En la Figura IV.1B se muestra que la potencia delta (0.5-3 Hz) y sigma (11-14 Hz) aumentaron, mientras que la potencia gamma se redujo desde un nivel de AW (alerta inducida por inyección) a un nivel QW después de la administración de atropina.

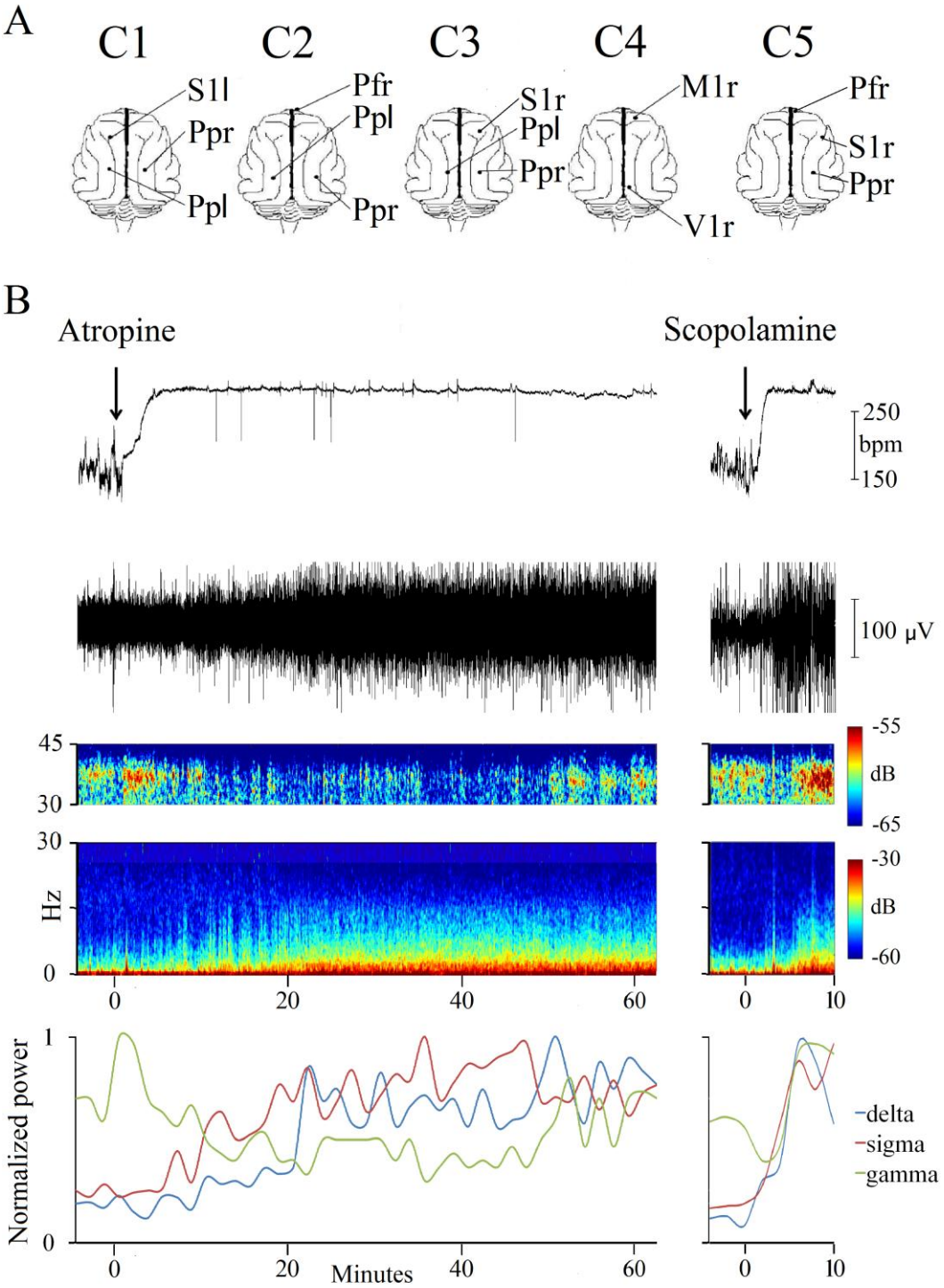

Figura IV.1. **Los antagonistas muscarínicos generan un EEG con ondas lentas y husos acompañados de actividad gamma.** A. Posición de los electrodos de registro. Los registros de estos electrodos se derivaron a un electrodo inactivo común, que se ubicó sobre el seno frontal. C1-C5, nombre

identificatorio de los animales. M1, corteza motora primaria; Pf, corteza prefrontal; Pp, corteza parietal posterior; S1, corteza somato-sensorial primaria; V1, corteza visual primaria; r, derecha; l, izquierda. B. El tacograma, el EEG de la corteza parietal posterior, su espectrograma y la potencia delta, sigma y gamma, se muestran después de la inyección de atropina o escopolamina (flechas). bpm, latidos por minuto; EEG, electroencefalograma. Los valores de potencia se normalizaron con la potencia máxima para cada banda de frecuencia.

En contraste con el sueño NREM, pero similar a AW, las "ráfagas" gamma estuvieron presentes bajo el efecto de la atropina. Estas "ráfagas" gamma se acoplaron entre las diferentes áreas corticales y se identifican fácilmente en los registros crudos (Figura IV.2).

Se obtuvieron resultados similares después de la administración de escopolamina; sin embargo, los efectos en el EEG aparecieron con una latencia más corta (aproximadamente 3 min; Figura IV.1B). La Figura IV.3 muestra registros crudos y filtrados después de la administración de escopolamina. En los registros filtrados (pasa-banda) entre 30 y 45 Hz, es evidente que la actividad gamma y el acoplamiento bajo el efecto de la escopolamina son similares al de AW, pero diferentes en comparación con el sueño NREM (Figura IV.3). Por el contrario, bajo escopolamina, las ondas lentas y los husos fueron muy similares a los del sueño NREM (Figura IV.3).

En resumen, siguiendo la administración de atropina o escopolamina, el EEG consistió en oscilaciones gamma acopladas en un fondo de ondas lentas y husos. Debido a que estos fenómenos similares a los del sueño NREM (ondas delta y husos) ya han sido descritos, no los analizamos (Wilker, 1952; Bradley & Elkes, 1953; Bach et at., 1955; Longo, 1956; Bradley & Elkes, 1957a, b; Elkes, 1957; Chow et at., 1959; Yamamoto, 1988).

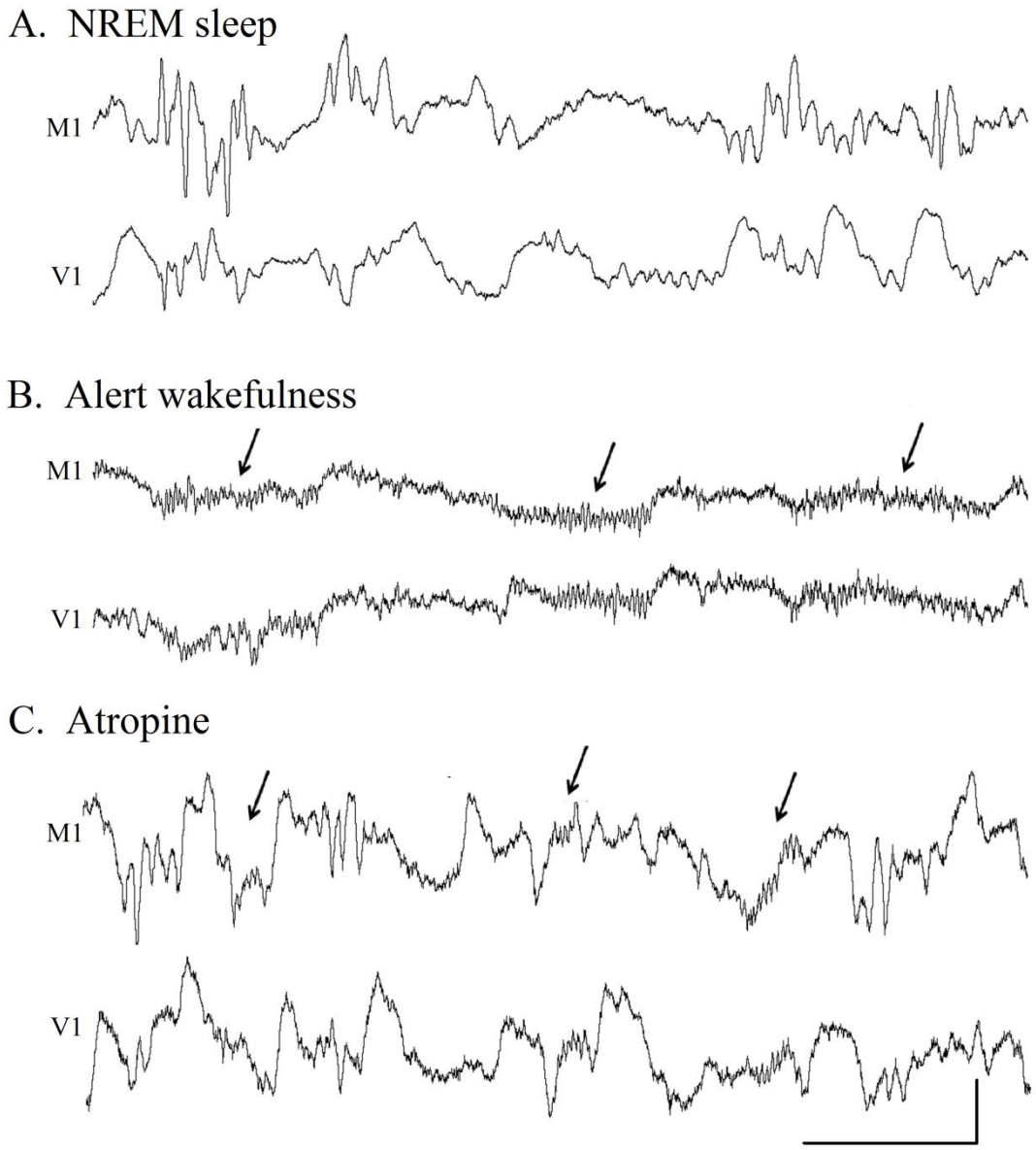

Figura IV.2. La atropina genera un EEG con oscilaciones gamma acopladas junto a ondas lentas y husos. Esta figura consiste en registros simultáneos de EEG de la corteza motora primaria (M1) y de la corteza visual primaria (V1) durante el sueño NREM (A), vigilia alerta (B) y después de la administración de atropina (C). Las flechas indican oscilaciones gamma. Barras de calibración, 1 segundo y 200 µV.

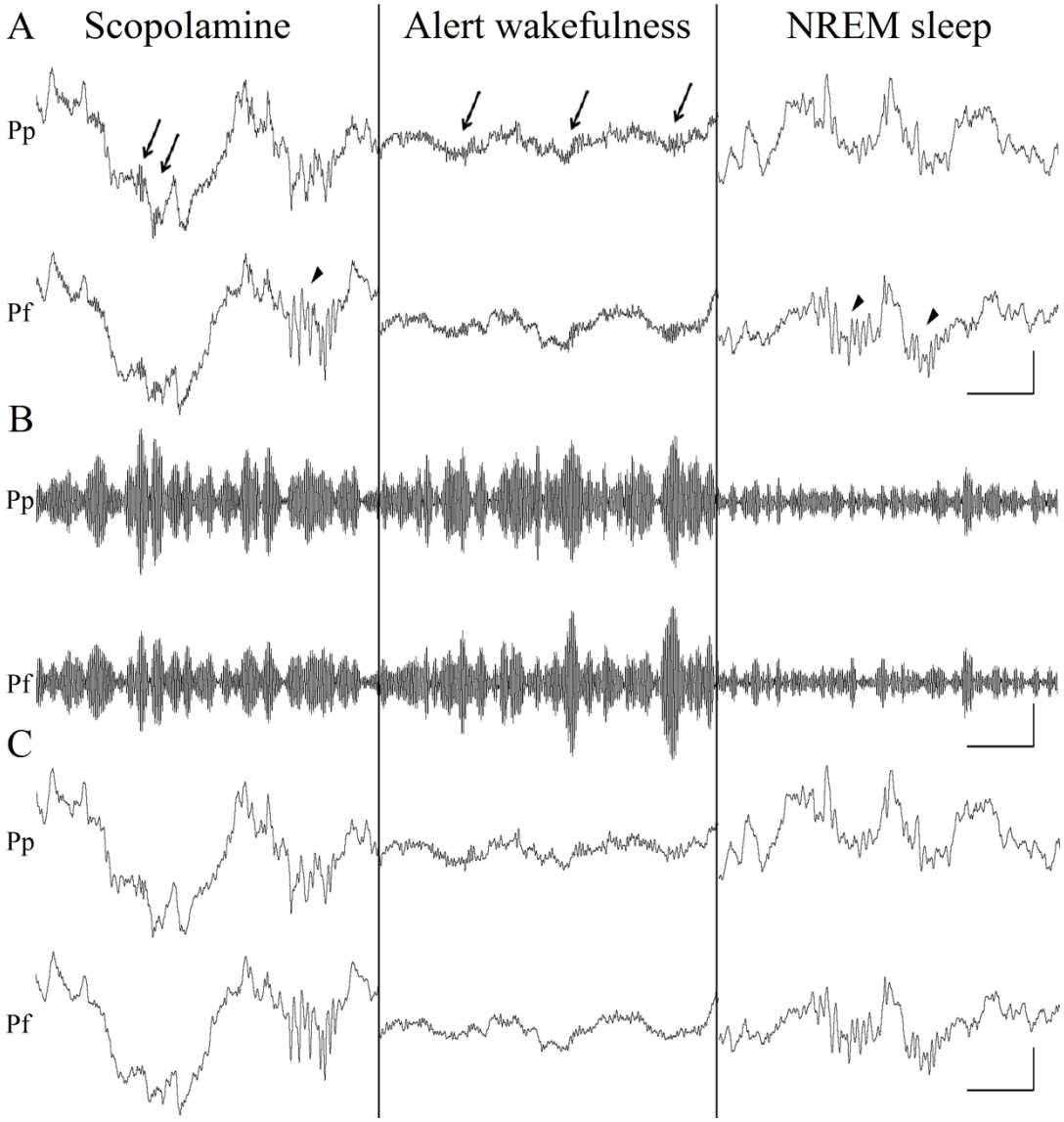

Figura IV.3. **Efectos de la escopolamina en el EEG.** Registros crudos simultáneos (A), actividad de 30 a 45 Hz (B) y 0.5 a 30 Hz (C), filtrados por filtro pasa-banda de la corteza prefrontal (Pf) y parietal posterior (Pp) durante sueño NREM, AW y después de la administración de escopolamina. Las flechas y las puntas de flecha indican "ráfagas" gamma y husos, respectivamente. Barras de calibración, 1 segundo y 200 µV para A y C; 20 µV para B.

4.3. Caracterización de las oscilaciones gamma después del tratamiento con atropina / escopolamina

Debido a que las "ráfagas" gamma estuvieron presentes tanto durante AW como después del tratamiento con antagonistas muscarínicos, analizamos sus características. Las funciones de autocorrelacion (ACF) y de correlación cruzada entre pares de cortezas (CCF) de registros seleccionados filtrados (30-45 Hz) durante AW y bajo de atropina se presentan en la Figura IV.4. Los CCF fueron similares en atropina y AW. Las "ráfagas" gamma promedio se acoplan con ondas lentas tanto en sueño NREM como luego de la administración de escopolamina.

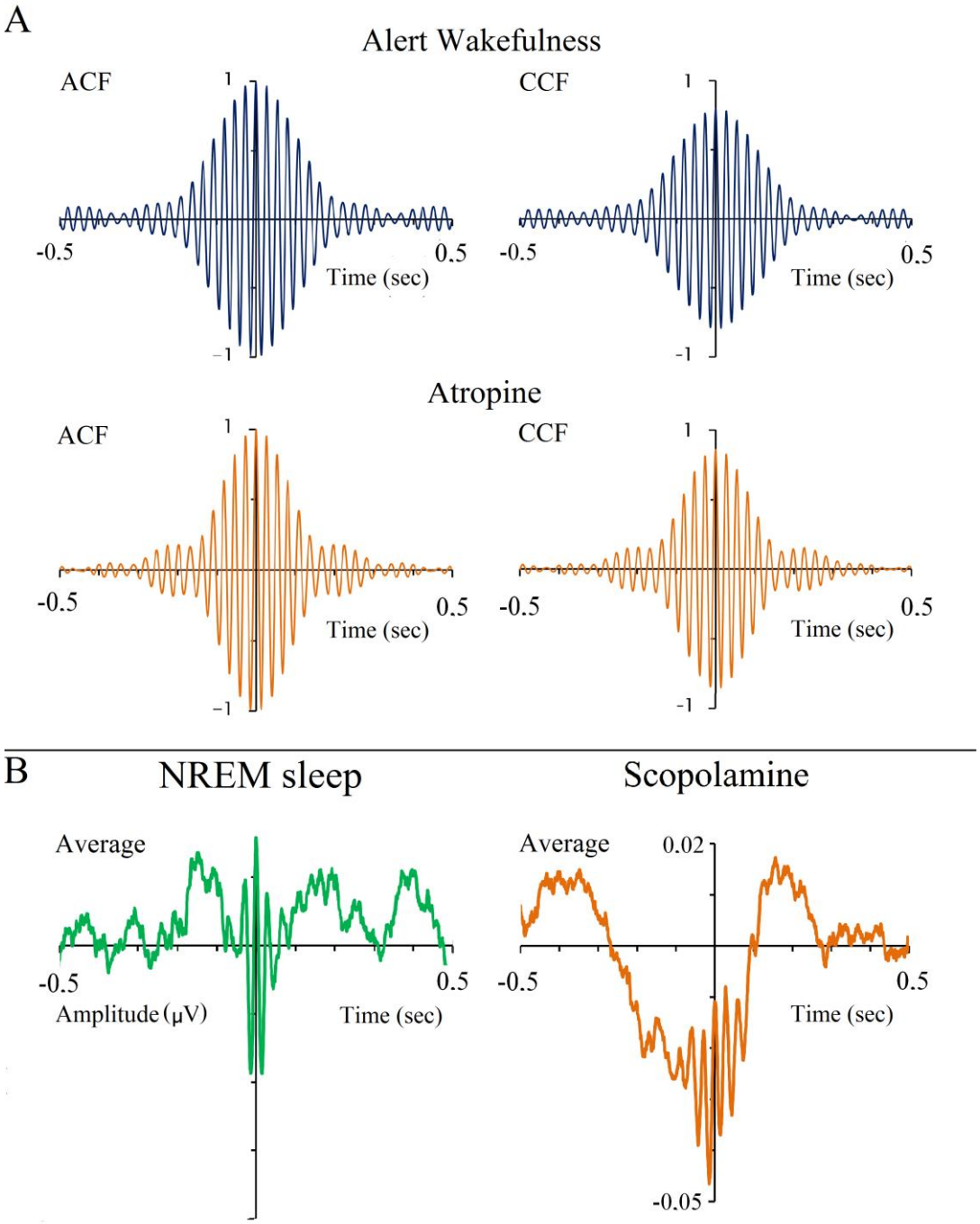

Figura IV.4.Oscilaciones gamma bajo el efecto de atropina y escopolamina. A. Se muestra la función de autocorrelacion (ACF) de los registros filtrados (30-45 Hz) durante AW y bajo el efecto de la atropina. También se muestran las funciones de correlación cruzada (CCF) de los registros filtrados (30-45 Hz). Las funciones se procesaron a partir de una ventana de registro de EEG de 300 segundos de registros simultáneos de EEG de la corteza prefrontal y la corteza

parietal posterior (CCF). La ACF y CCF se muestran durante la vigilia alerta y después de la administración de atropina. B. Oscilaciones gamma promediadas de un registro crudo seleccionado de la corteza prefrontal. Se seleccionaron y promediaron 100 ráfagas aleatorias; el disparador fue pico de la onda de mayor amplitud dentro de la oscilación gamma. Los promedios se muestran durante el sueño NREM y bajo el efecto de escopolamina.

En la Figura IV.5A, mediante espectrogramas gamma y envolventes, es visualmente fácil comparar la dinámica de las "ráfagas" entre AW, escopolamina y sueño NREM. Si bien existe un marcado acoplamiento entre las cortezas durante AW y después de la administración de escopolamina, este acoplamiento disminuye durante el sueño NREM. Las formas de onda del promedio de la ráfaga gamma son similares durante AW y después del tratamiento con escopolamina (Figura IV.5B). Como se observa en la Figura IV.5, la frecuencia gamma dominante fue similar en los 3 casos (aproximadamente 37 Hz); la amplitud y duración de la ráfaga fue menor en sueño NREM.

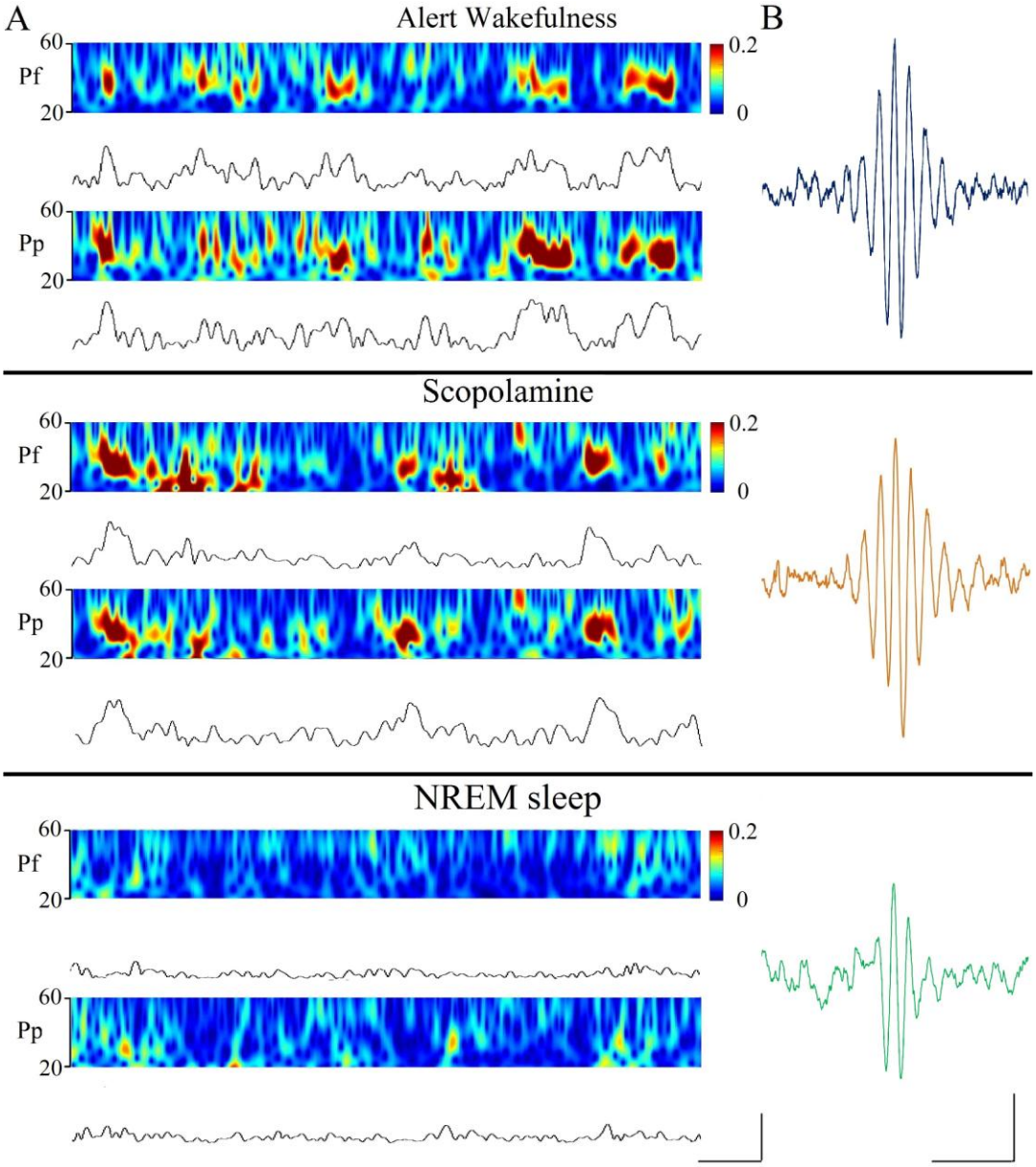

Figura IV 5. A. Espectrogramas (por medio de la función wavelet) y banda gamma rectificada (30-45 Hz) o envolventes gamma, durante AW, bajo escopolamina y durante el sueño NREM. Barras de calibración; 400 ms y 30 µV. B. "ráfagas" gamma promediados de un registro filtrado (pasa alto 3 Hz) seleccionado de la corteza prefrontal. 100 ráfagas aleatorias fueron seleccionadas y promediadas; el "trigger" fue el pico de la onda de mayor amplitud de la "ráfaga". Barras de calibración 200 ms y 10 µV

4.4. Potencia y coherencia gamma

El análisis del espectro de potencias del EEG en la corteza parietal posterior de un animal representativo se muestra en la Figura IV.6A. La potencia es similar durante el sueño NREM, la atropina y la escopolamina para frecuencias inferiores a 30 Hz. En contraste, la potencia de la banda gamma (30-45 Hz) es mayor después de la administración de atropina y escopolamina en comparación con la presente durante el sueño NREM. La potencia gamma bajo atropina y escopolamina mostro el "pico" característico de AW, aunque de menor amplitud en el caso de atropina (Figura IV.6C). El efecto sobre la potencia para el tratamiento con atropina y escopolamina se muestran de forma independiente para todos los animales y combinaciones de áreas corticales en las Tabla IV.1 y IV.2. Para ambas drogas la potencia fue significativamente mayor que durante el sueño NREM para todos los animales y para prácticamente todas las cortezas.

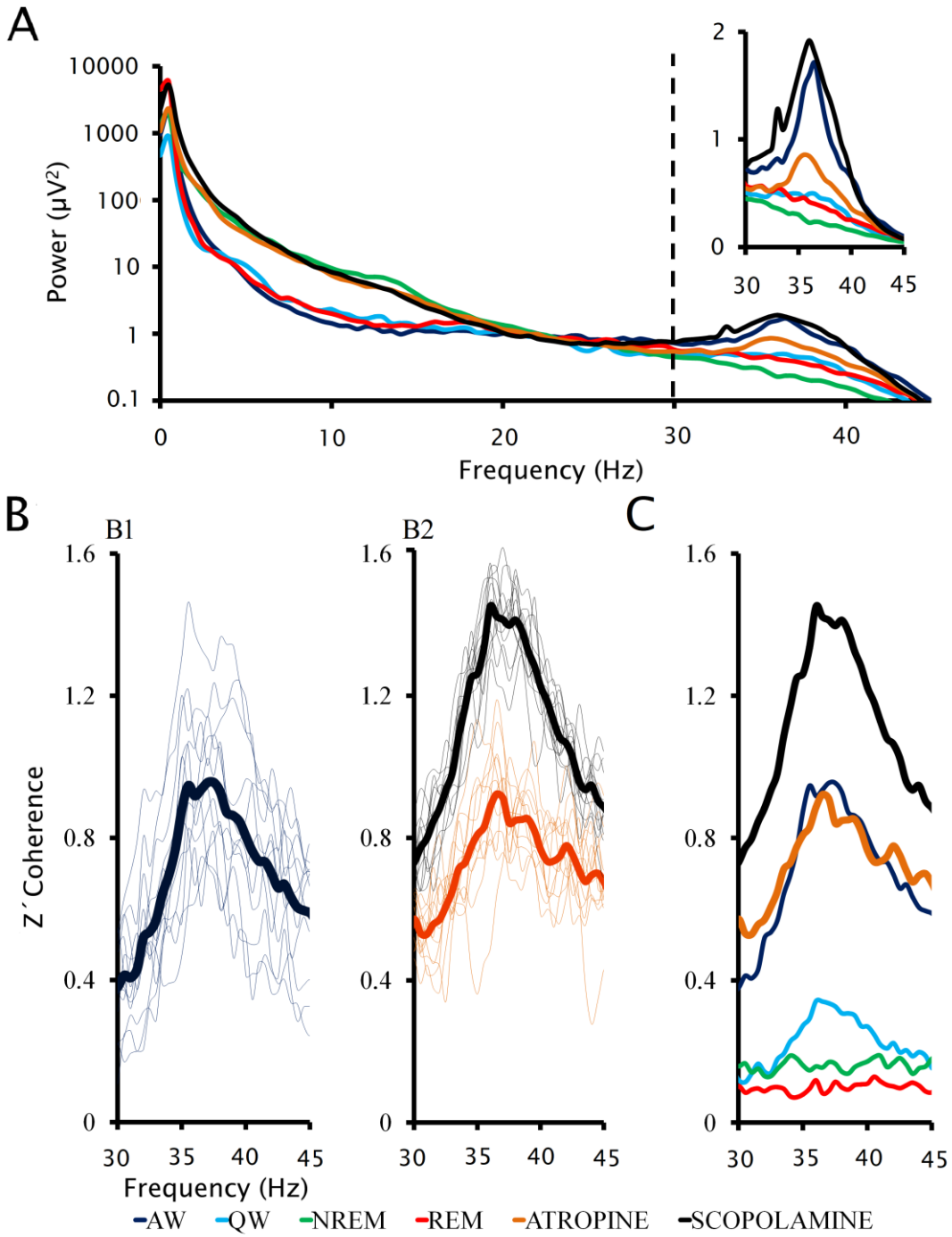

Figura IV.6. **Potencia y coherencia gamma del EEG bajo el efecto de la atropina y escopolamina.** A. Espectro de potencia promediado (0.5-45 Hz) durante AW, QW, NREM, sueño REM, administración de atropina y escopolamina. B. Se muestran doce perfiles de las coherencia z' (líneas delgadas) de un par representativo de registros (cortezas prefrontal y parietal posterior), así como los promedios de estos 12 perfiles (líneas gruesas) para vigilia alerta (B1),

administración de atropina y administración de escopolamina (B2). C. Perfiles de coherencia z' gamma promedio durante AW, QW, sueño NREM, sueño REM, administración de atropina y escopolamina.

Tabla IV.1. Valores de potencia gamma (30-45 Hz) durante vigilia, sueño y luego del tratamiento con atropina.

		AW	QW	NREM	REM	A	F
C1	Pp	64.4 ± 2.4*	18.3 ± 4.7*	8.9 ± 0.3*	15.1 ± 0.5*	81.1 ± 3.7	66
	S1	15.3 ± 0.6	13.1 ± 0.9*	7.6 ± 0.3*	13.0 ± 0.6*	17.8 ± 0.8	7
C2	Pf	60.9 ± 3.1*	23.8 ± 3.6	12.5 ± 0.3	20.9 ± 0.4	18.6 ± 1.6	50
	Pp	57.6 ± 2.6*	21.1 ± 3.9	10.3 ± 0.3*	18.5 ± 0.5	23.1 ± 1.3	37
C3	Pp	14.0 ± 0.8*	10.8 ± 0.9	6.5 ± 0.6*	9.7 ± 1.3	9.9 ± 0.8	26
	S1	26.2 ± 1.5*	13.1 ± 0.9*	6.1 ± 0.4	7.7 ± 0.5	8.4 ± 0.8	131
C4	M1	75.8 ± 4.3*	26.7 ± 0.9*	15.8 ± 0.5*	19.6 ± 0.9*	34.3 ± 1.2	73
	V1	57.4 ± 3.0*	8.4 ± 0.6*	5.8 ± 0.91*	10.2 ± 0.5*	28.2 ± 3.6	55
C5	Pf	132.0 ± 4.0*	57.2 ± 5	20.5 ± 1.3*	18.3 ± 1.1*	51.2 ± 7,7	113
	S1	121.2 ± 4.9*	69.8 ± 4.4*	18.6 ± 1.8*	37.0 ± 2.4	61.0 ± 3.9	121
	Pp	174.0 ± 11.2*	79.8 ± 4.4	35.3 ± 3.2*	39.9 ± 2.5*	63.8 ± 5.0	85

Los valores representan la media ± error estándar. $p < 0.05$. ANOVA con pruebas *post hoc* de Tamhane. Los asteriscos muestran la significancia con respecto a atropina (A). Todas las aéreas corticales tienen los mismos grados de libertad (5 entre grupos, 66 dentro de grupos). M1, corteza motora primaria; Pf, corteza prefrontal; Pp, corteza parietal posterior; S1, corteza primaria somato-sensorial; V1, corteza visual primaria; r, derecha; l, izquierda.

Tabla IV.2. Valores de potencia gamma (30-45 Hz) durante vigilia, sueño y luego del tratamiento con escopolamina.

		AW	QW	NREM	REM	S	F
C1	Pp	64.4 ± 2.4	18.3 ± 4.7*	8.9 ± 0.3*	15.1 ± 0.5*	61.1 ± 5.3	6
	S1	15.3 ± 0.6	13.1 ± 0.9	7.6 ± 0.3*	13.0 ± 0.6	14.8 ± 2.4	64
C2	Pf	60.9 ± 3.1*	23.8 ± 3.6	12.5 ± 0.3*	20.9 ± 0.4	24.8 ± 1.2	71
	Pp	57.6 ± 2.6*	21.1 ± 3.9	10.3 ± 0.3*	18.5 ± 0.5	35.3 ± 1.4	71
C5	Pf	132.0 ± 4.0	57.2 ± 5*	20.5 ± 1.3*	18.3 ± 1.1*	69.1 ± 3.0	187
	S1	121.2 ± 4.9*	69.8 ± 4.4*	18.6 ± 1.8*	37.0 ± 2.4*	38.9 ± 3.9	116
	Pp	174.0 ± 11.2*	79.8 ± 4.4	35.3 ± 3.2*	39.9 ± 2.5*	112.0 ± 5.2	86

Los valores representan la media ± error estándar. $p < 0.05$. ANOVA con pruebas *post hoc* de Tamhane. Los asteriscos muestran la significancia con respecto a escopolamina (S). Todas las áreas corticales tienen los mismos grados de libertad (5 entre grupos, 66 dentro de grupos). Pf, corteza prefrontal; Pp, corteza parietal posterior; S1, corteza primaria somato-sensorial; r, derecha; l, izquierda

La Figura IV.6B muestra perfiles de coherencia z' para un par representativo de áreas corticales de EEG, de doce periodos de 100 segundos y su promedio para AW, así como para estados inducidos por atropina y escopolamina. En este ejemplo los perfiles de coherencia z' con atropina fueron similares a los de AW. Bajo escopolamina, los perfiles de coherencia z' fueron aún mayores. En la Figura IV.6C se muestran los perfiles de coherencia promedio de la banda gamma en todos los estados.

Se realizó un análisis estadístico de la coherencia z´ entre las cortezas anteriores y posteriores para los 5 animales (Figura IV.7). El rmANOVA mostró que la coherencia z' para atropina fue similar a la de AW, y mayor que durante QW, NREM y sueño REM.

El efecto sobre la coherencia gamma para el tratamiento con atropina y escopolamina también se muestran de forma independiente para todos los animales y combinaciones de áreas corticales en las Tablas IV.3 y IV.4. Para la mayoría de animales y cortezas los resultados son similares a lo mostrado en la Figura IV.7.

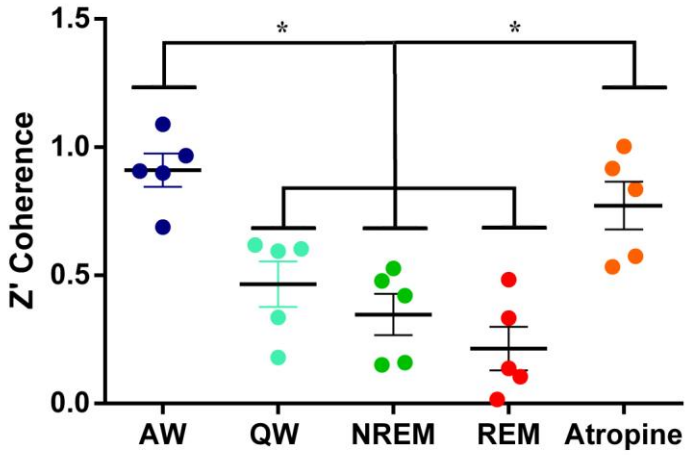

Figura IV.7. **Coherencia gamma en los 5 animales.** Coherencia z´ entre áreas corticales anteriores y posteriores para los 5 animales durante AW, QW, NREM, sueño REM y después de la aplicación de atropina (Atropine). $F_{4,\ 24} = 31.4$, $p < 0.0001$.

Tabla IV.3. Valores de coherencia z' gamma (30-45) durante vigilia, sueño y luego del tratamiento con atropina.

		AW	QW	NREM	REM	A	F
C1	Ppr-Ppl	1.13 ± 0.03	0.84 ± 0.07	* 0.77 ± 0.03	* 0.55 ± 0.03	1.52 ± 0.02	11
	S1r-Ppr	0.98 ± 0.04	* 0.41 ± 0.03	* 0.53 ± 0.03	* 0.33 ± 0.01	1.00 ± 0.08	31
C2	Pfl-Ppl	0.90 ± 0.06	* 0.34 ± 0.05	* 0.16 ± 0.01	* 0.10 ± 0.01	0.84 ± 0.03	38
	Ppd-Ppi	0.95 ± 0.04	* 0.46 ± 0.05	* 0.27 ± 0.04	* 0.20 ± 0.03	0.96 ± 0.02	67
C3	Ppr-Ppl	0.43 ± 0.01	0.34 ± 0.04	* 0.05 ± 0.01	* 0.05 ± 0.01	0.47 ± 0.08	12
	S1r-Ppr	0.97 ± 0.02	* 0.60 ± 0.04	* 0.48 ± 0.01	* 0.48 ± 0.01	0.92 ± 0.08	22
C4	M1r-V1r	* 0.91 ± 0.02	* 0.18 ± 0.01	* 0.15 ± 0.01	* 0.02 ± 0.01	0.53 ± 0.05	88
C5	Pfd-Ppd	* 0.69 ± 0.04	0.59 ± 0.04	* 0.42 ± 0.07	* 0.14 ± 0.06	0.57 ± 0.04	215
	S1d-Ppd	* 0.91 ± 0.04	0.82 ± 0.06	* 0.62 ± 0.06	* 0.42 ± 0.03	0.83 ± 0.03	190

Los valores representan la media ± error estándar. $p < 0.05$. ANOVA con pruebas *post hoc* de Tamhane. Los asteriscos muestran la significancia con respecto a atropina (A). Todas las combinaciones de aéreas corticales tienen los mismos grados de libertad (5 entre grupos, 66 dentro de grupos). M1, corteza motora primaria; Pf, corteza prefrontal; Pp, corteza parietal posterior; S1, corteza primaria somato-sensorial; V1, corteza visual primaria; r, derecha; l, izquierda.

Tabla IV.4. Valores de coherencia z' gamma (30-45 Hz) durante vigilia, sueño y luego del tratamiento con escopolamina.

		AW	QW	NREM	REM	S	F
C1	Ppr-Ppl	* 1.13 ± 0.03	* 0.84 ± 0.07	* 0.77 ± 0.03	* 0.55 ± 0.03	1.43 ± 0.02	70
	S1r-Ppr	* 0.98 ± 0.04	* 0.41 ± 0.03	* 0.53 ± 0.03	* 0.33 ± 0.01	1.26 ± 0.06	172
C2	Pfl-Ppl	* 0.90 ± 0.06	* 0.34 ± 0.05	* 0.16 ± 0.01	* 0.10 ± 0.01	1.30 ± 0.03	179
	Ppd-Ppi	* 0.95 ± 0.04	* 0.46 ± 0.05	* 0.27 ± 0.04	* 0.20 ± 0.03	1.09 ± 0.01	200
C5	Pfd-Ppd	* 0.69 ± 0.04	0.59 ± 0.04	* 0.42 ± 0.07	* 0.14 ± 0.06	0.56 ± 0.01	184
	S1d-Ppd	* 0.91 ± 0.04	0.82 ± 0.06	* 0.62 ± 0.06	* 0.42 ± 0.03	0.78 ± 0.03	178

Los valores representan la media ± error estándar. $p < 0.05$. ANOVA con pruebas *post hoc* de Tamhane. Los asteriscos muestran la significancia con respecto a escopolamina (S). Todas las combinaciones de áreas corticales tienen los mismos grados de libertad (5 entre grupos, 66 dentro de grupos). Pf, corteza prefrontal; Pp, corteza parietal posterior; S1, corteza primaria somato-sensorial; r, derecha; l, izquierda.

5. Discusión

Hemos confirmado que los antagonistas del receptor muscarínico inducen la vigilia conductual asociada con ondas lentas y husos en el EEG (como en el sueño NREM). Además, demostramos que bajo el efecto de atropina o escopolamina, las oscilaciones gamma coherentes (≈ 40 Hz) también se elevan como durante la vigilia.

Las oscilaciones gamma coherentes son una característica distintiva de la vigilia alerta en el gato (Capítulo II). Por lo tanto, este nuevo hallazgo genera dos conceptos importantes. En primer lugar, la acetilcolina, que actúa a través de los receptores muscarínicos, no es necesaria para generar oscilaciones EEG neocorticales a 40 Hz, ya que su bloqueo no las abole. En segundo lugar, estos datos sugieren fuertemente que las oscilaciones gamma de gran amplitud y coherentes están asociadas con la presencia de vigilia conductual, ya que esta se mantiene a pesar de que los antagonistas colinérgicos muscarínicos generan un perfil de EEG similar al sueño NREM. En suma, este EEG "disociado" con ondas lentas y husos, pero también con oscilaciones coherentes de 40 Hz (un rasgo de vigilia alerta), puede ser la base neurofisiológica de la "clásica" disociación electro-cortical y conductual que es producida por estas drogas.

5.1. Consideraciones farmacológicas

La acetilcolina produce sus efectos biológicos al actuar sobre receptores nicotínicos y muscarínicos. Se han clonado cinco receptores muscarínicos (Langmead et al., 2008). Mientras que los subtipos M1, M3 y M5 se unen a través de proteínas Gq/11 activando fosfolipasa C y movilizan el calcio intracelular, M2 y M4 ejercen su acción a través de la proteína Gi/o inhibiendo la adenilatocilasa y reduciendo las concentraciones intracelulares de AMPc (Langmead et al., 2008). El receptor muscarínico predominante en el SNC es el subtipo M1, que se

encuentra en corteza, tálamo, hipocampo y cuerpo estriado. Los receptores M2 se encuentran predominantemente en tronco encefálico y tálamo. Los receptores M4 se encuentran en muchas regiones cerebrales, pero son más prominentes en el cuerpo estriado. La densidad M3 y M5 es mucho menor (Langmead et al., 2008).

La escopolamina y atropina difieren en su farmacocinética; la primera tiene una corta vida media y fácilmente penetra en la barrera hematoencefálica, mientras que la atropina no (Ebert et al., 1998; Brunton & Parker, 2008). Por lo tanto, la escopolamina tiene efectos centrales más pronunciados en comparación con la atropina; esta propiedad puede explicar las diferencias en la latencia y cuantitativas de los efectos producidos por ambos fármacos.

5.2. Disociación electro-cortical y conductual

Como se muestra en el presente y en varios otros estudios (ver Introducción), la vigilia conductual está presente después del tratamiento con antagonistas de los receptores muscarínicos. Sin embargo, se han descrito sutiles efectos cognitivos. En el gato, la escopolamina altera la fase ejecutiva de la predación (es decir, la mordida letal) y el consumo de presas sin alterar la fase preparatoria (motivacional, generalmente expresada como interés por la presa, acecho, persecución y captura) (Zagrodzka & Kubiak, 1991).

Los estudios farmacológicos clásicos también han mostrado alteraciones cognitivas en humanos tratados con atropina (Ostfeld et al., 1960). Este medicamento produce una disminución en el habla y movimientos espontáneos, deterioro de la memoria, la atención, y somnolencia. Sin embargo, los sujetos pueden responder preguntas simples y realizar tareas sin el requisito de atención prolongada o memoria. Pueden sentarse, pararse, abrir o cerrar los ojos, extender sus extremidades a pedido, aunque se mueven más lentamente. La escopolamina también produce sedación, alteración de las habilidades de

coordinación y disminución de la memoria a corto plazo (Nuotto, 1983). Además, el fármaco afecta el tiempo de reacción simple y de selección, el pareo de números y las tareas de memoria. Por el contrario, no modifica el reconocimiento de palabras y el recuerdo a largo plazo de éstas (Ebert et al., 1998). Sahakian (1988) sugirió que los efectos más contundentes de la escopolamina son los que implican procesos de discriminación, vigilancia, atención selectiva, así como la consolidación y recuperación de recuerdos (Sahakian, 1988). Todo esto, sugiere que la atropina y la escopolamina disminuyen la memoria y la motivación, pero no abolen la consciencia.

Con el tratamiento con atropina o escopolamina, el comportamiento de vigilia en animales y humanos se acompaña de husos similares a los de sueño y ondas lentas en el EEG (Wikler, 1952; Longo, 1956; Bradley & Elkes, 1957; Bradley & Key, 1958; Ostfeld et al., 1960; Sannita et al., 1987a, b; Yamamoto, 1988). Nuestros resultados muestran claramente este hecho. Por lo tanto, los antagonistas del receptor muscarínico inducen una disociación electrográfica (perfil similar al sueño NREM en el EEG) y conductual (comportamiento de vigilia). Además, los antagonistas del receptor muscarínico inducen un aumento de la potencia y la coherencia (comparable a AW) gamma en comparación con el sueño.

5.3. Actividad Gamma anidada en ondas lentas

Las Figuras IV3, IV4 Y IV5 muestran claramente que la actividad gamma está presente durante el sueño NREM. Estudios previos ya han demostrado que la actividad gamma se puede observar anidada en las ondas lentas en los "up states" durante la anestesia y el sueño NREM (Mena-Segovia et al., 2008; Quyen et al., 2010; Valderrama et al., 2012; Valencia et al., 2013). En nuestros registros, las oscilaciones gamma, tanto durante la atropina/escopolamina como en el sueño NREM, están asociadas con el componente negativo de las ondas lentas, que probablemente esté asociado con los estos "up states". Por lo tanto, es probable que la atropina y la escopolamina potencien estas oscilaciones gamma.

5.4. Lecciones sobre las funciones cognitivas

Nuestros resultados sugieren que la presencia de husos y ondas lentas en el EEG, por sí mismos, no son responsables de la pérdida total de consciencia presente en el sueño NREM profundo (Tononi, 2009).

Ondas lentas. Se ha planteado la hipótesis de que la capacidad del cerebro para generar experiencias conscientes se reduce en presencia de ondas lentas (Edelman & Tononi, 2000; Tononi, 2009; Siclari et al., 2017). En este sentido, las neuronas tálamo-corticales se hiperpolarizan durante las ondas lentas del sueño NREM. Esta hiperpolarización reduce la transmisión de información sensorial a través del tálamo, lo que hace que la corteza esté parcialmente desconectada funcionalmente de las experiencias sensoriales (Steriade et al., 1993a). Además, debido a que el nivel de consciencia depende de la capacidad del cerebro para integrar información (Tononi, 2010), es probable que la reducción de la comunicación intracortical durante el sueño NREM esté directamente involucrada en la pérdida del conocimiento (Massimini et al., 2005).

Actividad gamma. Como muestra Maloney et al. (1997) y se muestra en el Capítulo II, durante el sueño NREM, además de ondas lentas y husos

de sueño, hay una disminución de la potencia gamma en comparación con la vigilia (AW y QW) y el sueño REM. Además, la coherencia gamma se reduce cuando se compara con la vigilia (tanto AW como QW), pero es mayor a la del sueño REM (Capítulo II; Anexo 1; Anexo 2). Por el contrario, los antagonistas del receptor muscarínico inducen una alta coherencia gamma en el EEG.

La potencia gamma, que es una medida de la sincronización local, y la actividad gamma coherente, que refleja las interacciones funcionales entre las áreas corticales distantes, contribuyen de manera significativa al mantenimiento de un estado cognitivo funcional durante la vigilia. Durante el sueño NREM profundo, donde se pierde la consciencia hay una disminución de la potencia y coherencia gamma con respecto a la vigilia (Capítulo II). Por lo tanto, es probable que la potencia y coherencia gamma sean fundamentales para la consciencia. De hecho, los estudios que utilizan anestesia general como un "interruptor" para la consciencia, han demostrado que una fuerte reducción de la coherencia gamma (principalmente entre regiones corticales lejanas) se correlaciona con la pérdida de conocimiento (John, 2002; Mashour, 2006; Pal et al., 2016).

5.5. La activación de los receptores muscarínicos no es necesaria para la actividad gamma.

Las neuronas que contienen acetilcolina y forman parte de los sistemas activadores, están presentes en los núcleos tegmentales latero-dorsal y pedunculopontino (LDT-PPT), así como en el cerebro basal anterior (Jones, 2005; Torterolo & Vanini, 2010).

Las neuronas colinérgicas del LDT-PPT y cerebro basal anterior son reconocidas para desempeñar un papel crucial en la generación de activación cortical durante W y el sueño REM (Jones, 2005, 2004; Torterolo & Vanini, 2010). Sin embargo, observamos que la atropina y la escopolamina no bloquean la actividad cortical rápida ni la coherencia gamma. De acuerdo con estos hallazgos, se ha negado el papel de las

neuronas colinérgicas del cerebro basal anterior en la generación de oscilaciones gamma en el EEG (Kim et al., 2015); sin embargo, las neuronas GABAérgicas del prosencéfalo basal que se proyectan a la corteza cerebral juegan un papel importante en la generación de actividad gamma (Kim et al., 2015). El hecho de que las neuronas colinérgicas estén activas durante el sueño REM (Boucetta et al., 2014) y la coherencia de gamma virtualmente ausente durante este estado de comportamiento (Capítulo II), está en total acuerdo con nuestros resultados. Además un trabajo reciente encontró que la coherencia gamma cortico-cortical elevada se correlaciona con la excitación conductual y no está mediada por mecanismos colinérgicos (Pal et al., 2016).

Los sistemas monoaminérgicos e hipocretinérgicos, que pueden permanecer activos después de la administración de antagonistas del receptor muscarínico, podrían inducir la potencia y coherencia gamma, actuando a través del tálamo y/o corteza a pesar de la presencia de husos y ondas lentas. Se necesitan nuevos experimentos para probar esta hipótesis.

5.6. Patología, toxicología y abuso de drogas

Una disminución de la actividad colinérgica cortical está presente en la enfermedad de Alzheimer, la enfermedad de Parkinson y la demencia de cuerpos de Lewy. Estas enfermedades implican la falta de concentración en la información más relevante y la dificultad para mantener un flujo apropiado de consciencia (Perry & Perry, 1995). Es interesante destacar, que los pacientes con enfermedad de Alzheimer no solo mantienen la actividad gamma, sino que tienen un aumento de la coherencia gamma evocada por estímulos sensoriales o eventos en comparación con los controles sanos (Basar et al., 2017).

Los fármacos anticolinérgicos se han utilizado con fines recreativos o rituales. Una de las experiencias religiosas o mágicas más ampliamente descritas que se remonta a los tiempos antiguos, es la alteración de la

consciencia con la inducción de alucinaciones por parte de un miembro de la familia de plantas Solanaceae (Belladonna, Henbane o Datura), que contienen escopolamina, atropina y otras relacionadas estrechamente con estos alcaloides (Perry & Perry, 1995). Efectos similares ocurren con la intoxicación con medicamentos médicos antimuscarínicos prescritos, o con organofosforados (Perry & Perry, 1995). Quizás el ejemplo más extraordinario de disfunción cognitiva es el uso criminal de sustancias anticolinérgicas presentes en los extractos de Datura (llamados "burundanga") para inducir amnesia y comportamiento sumiso o "obediencia" en las víctimas (Ardila & Moreno, 1991; Ardila-Ardila et al., 2006). Nuestros resultados, que demuestran la presencia de potencia y coherencia gamma después del tratamiento con drogas antimuscarínicas, son importantes para avanzar en la comprensión de los síndromes que ocurren cuando el sistema colinérgico central es disfuncional.

6. CONCLUSIONES

Aunque la atropina y la escopolamina produjeron un EEG "sincronizado" con ondas lentas y husos que se asemeja al sueño NREM, las interacciones funcionales entre las áreas corticales en la banda gamma permanecieron altas, similares a AW. Este fenómeno podría explicar la disociación entre el EEG y el comportamiento que provocan los fármacos antagonistas del receptor muscarínico.

REFERENCIAS

Ardila, A. & Moreno, C. (1991) Scopolamine intoxication as a model of transient global amnesia. *Brain Cognition*. 15, 236-245.

Ardila-Ardila, A., Moreno, C.B. & Ardila-Gomez, S.E. (2006) [Scopolamine poisoning ('burundanga'): loss of the ability to make decisions]. *Review Neurology*. 42, 125-128.

Babadi, B. & Brown, E.N. (2014) A review of multitaper spectral analysis. *IEEE Transactions on Biomedical Engineering.* 61, 1555-1564

Basar, E., Femir, B., Emek-Savas, D.D., Guntekin, B. & Yener, G.G. (2017) Increased long distance event-related gamma band connectivity in Alzheimer's disease. *Neuroimage Clinical.* 14, 580-590.

Boucetta, S., Cisse, Y., Mainville, L., Morales, M. & Jones, B.E. (2014) Discharge Profiles across the Sleep-Waking Cycle of Identified Cholinergic, GABAergic, and Glutamatergic Neurons in the Pontomesencephalic Tegmentum of the Rat. *Journal of Neuroscience*. 34, 4708-4727.

Bouyer, J.J., Montaron, M.F., & Rougeul, A. (1981) Fast fronto-parietal rhythms during combined focused attentive behavior and immobility in cat: cortical and thalamic localizations. *Electroencephalogram Clinical Neurophysiology*. 51. 244-252.

Bradley, P. B., & Elkes, J., (1957a).The effects of some drugs on the electrical activity of the brain. *Brain.* 80:77.

Bradley, P. B. & Key, B.J. (1958).The effect of drugs on arousal responses produced by electrical stimulation of the reticular formation of the brain. *Electroencephalogram Clinical Neurophysiology*. 10, 97-110.

Brando, V., Castro-Zaballa, S., Falconi, A., Torterolo, P. & Migliaro, E.R. (2014) Statistical, spectral and non-linear analysis of the heart rate variability during wakefulness and sleep. *Archives Italiannes de Biologia*, 152, 32-46.

Brunton, L. & Parker, K. (2008) *Goodman and Gilman's Manual of Pharmacology and Therapeutics*. McGraw Hill Medical, New York.

Bullock, T.H., McClune, M.C. & Enright, J.T. (2003) Are the electroencephalograms mainly rhythmic? Assessment of periodicity in wide-band time series. *Neuroscience*. 121, 233-252.

Buzsaki, G. & Wang, X. J. (2012) Mechanisms of gamma oscillations. *Annual Review Neuroscience.* 35. 203-225.

Cantero, J.L., Atienza, M., Madsen, J.R. & Stickgold, R. (2004) Gamma EEG dynamics in neocortex and hippocampus during human wakefulness and sleep. *Neuroimage*. 22, 1271-1280.

Castro, S., Cavelli, M., Vollono, P., Chase, M.H., Falconi, A. & Torterolo, P. (2014) Inter-hemispheric coherence of neocortical gamma oscillations during sleep and wakefulness. *Neuroscience Letters*. 578, 197-202.

Castro, S., Falconi, A., Chase, M.H. & Torterolo, P. (2013) Coherent neocortical 40-Hz oscillations are not present during REM sleep. *European Journal of Neuroscience*. 37, 1330-1339.

Cavelli, M., Castro, S., Schwarzkopf, N., Chase, M.H., Falconi, A. & Torterolo, P. (2015) Coherent neocortical gamma oscillations decrease during REM sleep in the rat. *Behaioralv Brain Research*. 281, 318-325.

Cavelli, M., Castro, S., Mondino, A., Gonzales, J., Falconi, A. & Torterolo, P. (2017) Absence of EEG gamma coherence in a local activated cortical state: a conserved trait of REM sleep. Translational Brain Rhythmicity. DOI10.15761/TBR.1000115.

Chow, K.L. & John, E.R. (1959) Acetylcholine Metabolism and Behavior of Rats. *Science*. 129, 64.

Ebert, U., Siepmann, M., Oertel, R., Wesnes, K.A. & Kirch, W. (1998) Pharmacokinetics and pharmacodynamics of scopolamine after subcutaneous administration. *Journal of Clinical Pharmacology*. 38, 720-726.

Edelman, G.M. & Tononi, G. (2000) A universe of consciousness. Basic Books, New York.

Gottesmann, C. (2006) The dreaming sleep stage: a new neurobiological model of schizophrenia? *Neuroscience*. 140, 1105-1115.

Hall, G.H. (1970) Effects of nicotine and tobacco smoke on the electrical activity of the cerebral cortex and olfactory bulb. *British Journal of Pharmacology*. 38, 271-286.

Hobson, J.A. (2009) REM sleep and dreaming: towards a theory of protoconsciousness. *Natiure Reviews Neuroscience*. 10, 803-813.

John, E.R. (2002) The neurophysics of consciousness. *Brain Research Review*. 39, 1-28.

Jones, B. (2005) Basic mechanisms of sleep-wake states. In Kryger, M.H., Roth, T., Dement, W.C. (eds) Principles and practices of sleep medicine. Elsevier-Saunders, Philadelphia, 136-153.

Jones, B.E. (2004) Activity, modulation and role of basal forebrain cholinergic neurons innervating the cerebral cortex. *Progress in Brain Research*. 145, 157-169.

Kim, T., Thankachan, S., McKenna, J.T., McNally, J.M., Yang, C., Choi, J.H., Chen, L., Kocsis, B., Deisseroth, K., Strecker, R.E., Basheer, R., Brown, R.E. & McCarley, R.W. (2015) Cortically projecting basal forebrain parvalbumin neurons regulate cortical gamma band oscillations. *Proceedings of the National Academy of Science U S A*. 112, 3535-3540.

Langmead, C.J., Watson, J. &Reavill, C. (2008) Muscarinic acetylcholine receptors as CNS drug targets. *Pharmacology &Therapeutics*. 117, 232-243.

Lee, M.G., Hassani, O.K. & Jones, B.E. (2005) Discharge of identified orexin/hypocretin neurons across the sleep-waking cycle. *Journal of Neuroscience*. 25, 6716-6720.

Llinas, R. & Ribary, U. (1993) Coherent 40-Hz oscillation characterizes dream state in humans. *Proceedings of the National Academy of Science U S A*. 90, 2078-2081.

Llinas, R., Ribary, U., Contreras, D. & Pedroarena, C. (1998) The neuronal basis for consciousness. *Philoophical Transactions of the Royal Society of London B Biological Sciences*. 353, 1841-1849.

Llinas, R.R., Grace, A.A. & Yarom, Y. (1991) In vitro neurons in mammalian cortical layer 4 exhibit intrinsic oscillatory activity in the 10- to 50-Hz frequency range. *Proceedings of the National Academy of Science U S A*. 88, 897-901.

Longo, V.G. (1956) Effects of scopolamine and atropine electroencephalographic and behavioral reactions due to hypothalamic stimulation. *J Pharmacological Experimental Therapy*. 116, 198-208.

Maloney, K.J., Cape, E.G., Gotman, J. & Jones, B.E. (1997) High-frequency gamma electroencephalogram activity in association with sleep-wake states and spontaneous behaviors in the rat. *Neuroscience*. 76, 541-555.

Martin, W.R. & Eades, C.G. (1960) A comparative study of the effect of drugs on activating and vasomotor responses evoked by midbrain stimulation: atropine, pentobarbital, chlorpromazine and chlorpromazine sulfoxide. *Psychopharmacologia*. 1, 303-335.

Mashour, G.A. (2006) Integrating the science of consciousness and anesthesia. *Anesthesia & Analgesia*. 103, 975-982.

Massimini, M., Ferrarelli, F., Huber, R., Esser, S.K., Singh, H. & Tononi, G. (2005) Breakdown of cortical effective connectivity during sleep. *Science*. 309, 2228-2232.

Mena-Segovia, J., Sims, H.M., Magill, P.J. & Bolam, J.P. (2008) Cholinergic brainstem neurons modulate cortical gamma activity during slow oscillations. *Journal of Physiology*. 586, 2947-2960.

Mileykovskiy, B.Y., Kiyashchenko, L.I. & Siegel, J.M. (2005) Behavioral correlates of activity in identified hypocretin/orexin neurons. *Neuron*. 46, 787-798.

Monti, J.M. (2013) The neurotransmitters of sleep and wake, a physiological reviews series. *Sleep Med Review*. 17, 313-315.

Munk, M.H., Roelfsema, P.R., Konig, P., Engel, A.K. & Singer, W. (1996) Role of reticular activation in the modulation of intracortical synchronization. *Science*, 272, 271-274.

Nuotto, E. (1983) Psychomotor, physiological and cognitive effects of scopolamine and ephedrine in healthy man. *European Journal of Clinical Pharmacology*. 24, 603-609.

Ostfeld, A.M., Machne, X. & Unna, K.R. (1960) The effects of atropine on the electroencephalogram and behavior in man. *Journal of Pharmacological Experimental Therapy*. 128, 265-272.

Pal D, Silverstein BH, Lee H, Mashour GA (2016) Neural Correlates of Wakefulness, Sleep, and General Anesthesia: An Experimental Study in Rat. *Anesthesiology* 125: 929-942.

Perez-Garci, E., del-Rio-Portilla, Y., Guevara, M.A., Arce, C. &Corsi-Cabrera, M. (2001) Paradoxical sleep is characterized by uncoupled gamma activity between frontal and perceptual cortical regions. *Sleep*. 24, 118-126.

Perry, E.K. & Perry, R.H. (1995) Acetylcholine and hallucinations: disease-related compared to drug-induced alterations in human consciousness. *Brain Cognition*. 28, 240-258.

Quyen, M.L.V., Muller, L.E., Telenczus, B., Halgrem, E., Cash, S., et al. (2016) High-frequency oscillations in human and monkey neocortex during the wake–sleep cycle. *Proceedings of the National Academy of Science.* 113, 9363–9368

Rieder, M.K., Rahm, B., Williams, J.D. & Kaiser, J. (2010) Human gamma-band activity and behavior. *International Journal of Psychophysiology*. 79, 39-48.

Rinaldi, F. &Himwich, H.E. (1955) Alerting responses and actions of atropine and cholinergic drugs. *AMA Archives of Neurology & Psychiatry*. 73, 387-395.

Roach, B.J., & Mathalon, D.H. (2008) Event-related EEG time-frequency analysis: an overview of measures and an analysis of early gamma band phase locking in schizophrenia. *Schizophrenia Bull*. 34, 907-926.

Rodriguez, E., George, N., Lachaux, J.P., Martinerie, J., Renault, B. & Varela, F.J. (1999) Perception's shadow: long-distance synchronization of human brain activity. *Nature*. 397, 430-433.

Sahakian, B. (1988) Cholinergic drugs and human cognitive performance *Handbook of Psychopharmcology*. 66, 393-424.

Sannita, W.G., Fioretto, M., Maggi, L. &Rosadini, G. (1987a) Effects of scopolamine parenteral administration on the electroretinogram, visual evoked potentials, and quantitative electroencephalogram of healthy volunteers. *Documenta Ophthalmology*. 67, 379-388.

Sannita, W.G., Maggi, L. &Rosadini, G. (1987b) Effects of scopolamine (0.25-0.75 mg i.m.) on the quantitative EEG and the neuropsychological status of healthy volunteers. *Neuropsychobiology*. 17, 199-205.

Siclari F, Baird B, Perogamvros L, et al. (2017) The neural correlates of dreaming. Nature Neuroscience 20: 872-878.

Steriade, M., Amzica, F. & Contreras, D. (1996) Synchronization of fast (30-40 Hz) spontaneous cortical rhythms during brain activation. *Journal Neuroscience*. 16, 392-417.

Steriade, M., McCormick, D.A. &Sejnowski, T.J. (1993a) Thalamocortical oscillations in the sleeping and aroused brain. *Science*. 262, 679-685.

Steriade M, Nuñez A, Amzica F. (1993b). A novel slow (<1 hz) oscillation of neocortical neurons in vivo : Depolarizing and hyperpolarizing components. *Journal of Neuroscience.* 1993b;13:3252–3265. [PubMed]

Tiitinen, H., Sinkkonen, J., Reinikainen, K., Alho, K., Lavikainen, J. &Naatanen, R. (1993) Selective attention enhances the auditory 40-Hz transient response in humans. *Nature*. 364, 59-60.

Tononi, G. (2009) Sleep and dreaming. In Laureys, S., Tononi, G. (eds) *The neurology of consciousness: cognitive neuroscience and neuropathology*. Elsevier, San Diego, 89-107.

Tononi, G. (2010) Information integration: its relevance to brain function and consciousness. *Archives Italiannes de Biologia*. 148, 299-322.

Torterolo, P., Monti, J., Pandi-Perumal, S.R. (2016). Neuroanatomy and neuropharmacology of sleep and wakefulness En: Synopsis of Sleep Medicine. Editor: Pandi-Perumal S.R. Apple Academic Press.

Torterolo, P., Castro-Zaballa, S., Cavelli, M., Chase, M.H. &Falconi, A. (2016) Neocortical 40-Hz oscillations during carbachol-induced REM sleep and cataplexy. *European Journal of Neuroscience*. 43, 580-589.

Torterolo, P., Castro-Zaballa, S., Cavelli, M., Velasquez, N., Brando, V., Falconi, A., Chase, M.H. &Migliaro, E.R. (2015) Heart rate variability during carbachol-induced REM sleep and cataplexy. *Behavioral Brain Research*. 291, 72-79.

Torterolo, P. & Chase, M.H. (2014) The hypocretins (orexins) mediate the "phasic" components of REM sleep: a new hypothesis. *Sleep Science*. 7, 19-29.

Torterolo, P. &Vanini, G. (2010) [New concepts in relation to generating and maintaining arousal]. *Review Neurology*. 50, 747-758.

Torterolo, P., Yamuy, J., Sampogna, S., Morales, F.R. & Chase, M.H. (2003) Hypocretinergic neurons are primarily involved in activation of the somatomotor system. *Sleep*. 1, 25-28.

Uhlhaas, P.J., Pipa, G., Lima, B., Melloni, L., Neuenschwander, S., Nikolic, D. & Singer, W. (2009) Neural synchrony in cortical networks: history, concept and current status. *Frontiers of Integrative Neuroscience*. 3, 17.

Uhlhaas, P.J., Pipa, G., Neuenschwander, S., Wibral, M. & Singer, W. (2011) A new look at gamma? High- (>60 Hz) gamma-band activity in cortical networks: function, mechanisms and impairment. *Progress in Biophysics & Molecular Biology*. 105, 14-28.

Valderrama, M., Crepon, B., Botella-Soler, V., Martinerie, J., Hasboun, D., Alvarado-Rojas, C., Baulac, M., Adam, C., Navarro, V. & Le Van Quyen, M. (2012) Human gamma oscillations during slow wave sleep. *PLoS One*. 7, e33477.

Valencia, M., Artieda, J., Bolam, J.P. & Mena-Segovia, J. (2013) Dynamic interaction of spindles and gamma activity during cortical slow oscillations and its modulation by subcortical afferents. *PLoS One*. 8, e67540.

Velik, R. (2009) From single neuron-firing to consciousness--towards the true solution of the binding problem. *Neuroscience Biobehaviour Review*. 34, 993-1001.

von der Malsburg, C. (1995) Binding in models of perception and brain function. *Current Opinion Neurobiology*. 5, 520-526.

Voss, U., Holzmann, R., Tuin, I. & Hobson, J.A. (2009) Lucid dreaming: a state of consciousness with features of both waking and non-lucid dreaming. *Sleep.* 32, 1191-1200.

Wikler, A. (1952) Pharmacologic dissociation of behavior and EEG "sleep patterns" in dogs; morphine, n-allylnormorphine, and atropine. *Proceedingsof the Society of Experimental Biology and Medicine*. 79, 261-265.

Yamamoto, J. (1988) Roles of cholinergic, dopaminergic, noradrenergic, serotonergic and GABAergic systems in changes of the EEG power spectra and behavioral states in rabbits. *Japan Journal of Pharmacology*. 47, 123-134.

Zagrodzka, J. & Kubiak, P. (1991) Scopolamine-induced alterations in predatory behaviour pattern in cats. *Acta Neurobiologiae Experimentalis (Wars)*. 51, 29-36.

PERSPECTIVAS

En base a los resultados encontrados, las investigaciones a realizar en el futuro serán las siguientes:

- Analizar la potencia y la coherencia de frecuencias más elevadas del EEG como las high frequency oscilations (HFO), así como su relación con las oscilaciones de baja frecuencia durante la vigilia y el sueño.
- Estudiar las variaciones relativas en la coherencia gamma de diferentes combinaciones de áreas corticales durante la vigilia alerta desencadenada por diferentes tipos y modalidades de estímulos.
- Comprobar si el nivel de acoplamiento de la banda gamma entre áreas corticales y subcorticales que incrementan su actividad durante el sueño REM, como las cortezas límbicas y la amígdala.
- Investigar si el nivel de acoplamiento de la banda gamma entre áreas corticales es regulado por otros sistemas moduladores como sistemas noradrenérgicos, dopaminérgico, serotoninérgicos, hipocretinérgicos y MCHérgicos.
- Conocer si el nivel de acoplamiento de la banda gamma entre áreas corticales es alterado por la privación de sueño.

ANEXO 1.LAS OSCILACIONES GAMMA NEOCORTICALES COHERENTES DISMINUYEN DURANTE EL SUEÑO REM EN LA RATA

Las funciones cognitivas más complejas requieren la integración y coordinación de grandes poblaciones de neuronas en regiones corticales y subcorticales. Se han postulado que las oscilaciones en la banda de alta frecuencia (30-100 Hz) del electroencefalograma (EEG) son un producto de esta interacción. Éstas están implicadas en la unión de eventos neuronales espacialmente separados pero temporalmente correlacionados, lo que da como resultado una experiencia perceptual unificada. La extensión de esta conectividad funcional se puede examinar por medio del algoritmo matemático llamado "coherencia", que se correlaciona con la "fuerza" de las interacciones funcionales entre áreas corticales. Como continuación de estudios previos en el gato (Capítulo II) el presente estudio se realizó para analizar la coherencia del EEG en la banda gamma de la rata durante la (W), el sueño (NREM) y el sueño REM.

Las ratas fueron implantadas con electrodos en diferentes áreas corticales para registrar la actividad del EEG, y se determinaron los valores de coherencia y potencia dentro de la banda gamma de frecuencia de EEG (30-48 y 52-100 Hz).

La coherencia entre todas las regiones corticales en las bandas gamma baja y alta de frecuencias fue mayor durante W en comparación con el sueño. La coherencia EEG en las bandas gamma baja y alta fue menor durante el sueño REM.

Behavioural Brain Research 281 (2015) 318–325

Contents lists available at ScienceDirect

Behavioural Brain Research

journal homepage: www.elsevier.com/locate/bbr

Research report

Coherent neocortical gamma oscillations decrease during REM sleep in the rat

Matías Cavelli[a], Santiago Castro[a], Natalia Schwarzkopf[a], Michael H. Chase[b,c], Atilio Falconi[a], Pablo Torterolo[a,*]

[a] Laboratorio de Neurobiología del Sueño, Departamento de Fisiología, Facultad de Medicina, Universidad de la República, General Flores 2125, 11800 Montevideo, Uruguay
[b] WebSciences International, 1251 Westwood Blvd., Los Angeles, CA 90024, USA
[c] UCLA School of Medicine, Los Angeles, CA 90095, USA

HIGHLIGHTS

- The electroencephalogram of adult rats was recorded during sleep and wakefulness.
- The intra and inter-hemispheric coherence of the EEG gamma band was analyzed.
- The coherence was larger in W and almost absent during REM sleep.

ARTICLE INFO

Article history:
Received 8 October 2014
Received in revised form
19 December 2014
Accepted 23 December 2014
Available online 31 December 2014

Keywords:
Cortex
Consciousness
EEG
Synchronization
Coherence

ABSTRACT

Higher cognitive functions require the integration and coordination of large populations of neurons in cortical and subcortical regions. Oscillations in the high frequency band (30–100 Hz) of the electroencephalogram (EEG), that have been postulated to be a product of this interaction, are involved in the binding of spatially separated but temporally correlated neural events, which results in a unified perceptual experience. The extent of this functional connectivity can be examined by means of the mathematical algorithm called "coherence", which is correlated with the "strength" of functional interactions between cortical areas. As a continuation of previous studies in the cat [6,7], the present study was conducted to analyze EEG coherence in the gamma band of the rat during wakefulness (W), non-REM (NREM) sleep and REM sleep.

Rats were implanted with electrodes in different cortical areas to record EEG activity, and the magnitude squared coherence values within the gamma frequency band of EEG (30–48 and 52–100 Hz) were determined.

Coherence between all cortical regions in the low and high gamma frequency bands was greater during W compared with sleep. Remarkably, EEG coherence in the low and high gamma bands was smallest during REM sleep.

We conclude that high frequency interactions between cortical areas are radically different during sleep and wakefulness in the rat. Since this feature is conserved in other mammals, including humans, we suggest that the uncoupling of gamma frequency activity during REM sleep is a defining trait of REM sleep in mammals.

1. Introduction

Electroencephalographic (EEG) oscillations in the gamma frequency (30–100 Hz) band are involved in the integration or binding of spatially separated but temporally correlated neural events [1–3]. An increase in gamma power typically appears during states/behaviors that are characterized by the active cognitive processing of external percepts or internally generated thoughts and images in humans and during alert wakefulness in animals [4–7].

The degree of EEG coherence between two cortical regions is correlated with the strength of the functional interconnections

* Corresponding author. Tel.: +598 2924 34 14x3234.
E-mail address: ptortero@fmed.edu.uy (P. Torterolo).

http://dx.doi.org/10.1016/j.bbr.2014.12.050
0166-4328/

that occur between them [1,2,8,9]. Recently, Siegel et al. (2012) have proposed that frequency-specific correlated oscillations in distributed cortical networks provide indices, or 'fingerprints', of the network interactions that underlie cognitive processes [10].

Gamma coherence between different brain areas, which is greatest during wakefulness (W) has been viewed as a possible neural correlate of consciousness [11]. In effect, coherence in the gamma frequency band decreases during narcosis (unconsciousness) induced by anesthesia [12,13].

During deep non-REM (NREM) sleep there is an absence, or at least a strong reduction in cognitive functions. In contrast, dreams that occur more prominently during rapid eye movement (REM) sleep, are considered a special kind of cognitive activity or proto-consciousness [14]. Recently, we demonstrated in the cat that there is high level of neocortical intra and interhemispheric gamma coherence during alert wakefulness, it decreases during quiet W and NREM sleep, and is almost absent during REM sleep [6,7].

In the present report, we evaluated the extent of EEG 30–100 Hz coherence between intra and interhemispheric neocortical activity during naturally occurring sleep and W in the rat.

2. Materials and methods

2.1. Experimental animals

Twelve adult male Wistar rats (300–350 g) were used in this study. The animals were determined to be in good health by the Institutional Animal Care Facility. All of the animals were maintained on a 12:12-h light-dark cycle under controlled temperature (21–24 °C) conditions with free access to food and water. All of the experimental procedures were conducted in accord with the *Guide for the Care and Use of Laboratory Animals* (8th edition, National Academy Press, Washington, DC, 2010) and approved by the Institutional Animal Care Commission (protocol No. 071140-001931-12, Facultad de Medicina, Universidad de la República). Adequate measures were taken to minimize pain, discomfort or stress of the animals. In addition, all efforts were made in order to use the minimal number of animals necessary to produce reliable scientific data.

2.2. Surgical procedures

The surgical procedures employed were similar to those in our previous studies [15,16]. The animals were chronically implanted with electrodes to monitor the states of sleep and W. Anesthesia was induced with a mixture of ketamine-xylazine (90 mg/kg; 5 mg/kg i.p. respectively). The animal's head was positioned in a stereotaxic frame and the skull was exposed. In order to record the EEG, stainless steel screw electrodes were placed in the calvarium, overlying the parietal and occipital cortices and the cerebellum (Fig. 1). Bipolar electrodes were inserted into the neck muscle in order to record the electromyogram (EMG). The electrodes were connected to a plug that was bonded to the skull with acrylic cement.

At the end of the surgical procedures, an analgesic was administered. Incision margins were kept clean and a topical antibiotic was administered on a daily basis. After the animals had recovered from the preceding surgical procedures, they were adapted to the recording environment for a period of at least one week.

2.3. Experimental sessions

Experimental sessions of 6 h in duration were conducted during the light period, between 12 A.M. and 6 P.M, in a temperature controlled (21–24 °C) and sound attenuated chamber. All animals had free access to water and food. During these sessions (as well as during the adaptation sessions), the animals were able to move freely within the confines of the recording-chamber.

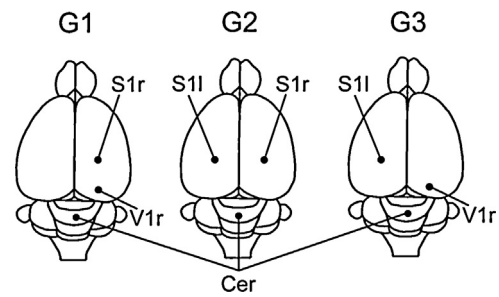

Fig. 1. Position of recording electrodes. The figure presents a summary of the position of the recording electrodes on the surface of the primary somatosensory and primary visual cortices (according to Ref. [31]). The electrodes were referred to a common electrode that was located over the cerebellum (Cer). G1–G3, are groups of animals with different electrode locations (four animals per group). S1, somatosensory primary cortex; V1, visual primary cortex; r, right; l, left.

EEG and EMG of each rat were recorded daily for a period of approximately 2 weeks in order to obtain a complete data set. The activity of two cortical areas was recorded simultaneously with monopolar electrodes. A common electrode reference montage was placed on the cerebellar surface; this montage is critical for the analysis of coherence [17–21]. For each pair of recordings, data were obtained during four recording sessions, and for every combination of electrodes, in three groups (G1–G3) of 4 rats (Fig. 1).

Bioelectric signals were amplified (×1000), filtered (0.1–200 Hz), sampled (512 Hz, 16 bits) and stored in a PC using Spike 2 software (Cambridge Electronic Design). Data were obtained during spontaneously occurring W, NREM and REM sleep. The presence of low voltage fast waves in the parietal cortex, a mixed theta rhythm (4–7 Hz) in the occipital cortex and relatively high electromyographic activity were used to identify W. Light and deep NREM sleep were determined, but only epochs of established periods of deep NREM sleep were utilized for coherence analysis. Deep NREM sleep was identified by the presence of continuous high amplitude slow (0.5–4 Hz) frontal and occipital waves and sleep spindles (9–15 Hz) combined with a reduced EMG activity. REM sleep was identified by the occurrence of low voltage fast parietal waves, a regular theta rhythm in the occipital cortex, and the absence of EMG activity except for occasional muscular twitches [15].

2.4. Data analysis

Sleep and waking states were determined in epochs of 10 s [15]. In order to obtain power spectral and coherence values between a pair of EEG channels, we used procedures that we have previously employed [6,7]. Artifacts were detected in the raw recording and in the spectrogram (with a 0.5 s resolution); artifacts produced a general increase in power and were usually associated with movements. Twelve independent artifact-free periods of 100 s were selected and examined during each behavioral state (1200 s for each behavioral state per rat).

For each 100 s period, the Magnitude Squared Coherence was determined as follows: $coh_{ab}(f) = [\sum csd_{ab}(f)]^2/[\sum psd_a(f) \sum psd_b(f)]$, where psd is the power spectral density and a and b are the waves that are analyzed. csd is the cross spectra density, or the Fourier transform of the cross covariance function, which provides a statement of how common activity between two processes is distributed across frequencies. Coherence between two waveforms is a function of frequency and ranges from 0 for totally incoherent waveforms to 1 for maximal coherence. In order for two waveforms to be completely coherent at a particular frequency over a

given time range, the phase shift between the waveforms must be constant and the amplitudes of the waves must have a constant ratio.

We obtained power spectrum and the magnitude squared coherence using the Spike 2 script COHER 1S (Cambridge Electronic Design). By employing this method, we were able to analyze the coherence between two EEG channels that were recorded simultaneously during 100 s periods. This analysis period was divided into 100 time-blocks with a sampling rate of 512 Hz, a bin size of 1024 samples (512 for each channel) and a resolution of 0.5 Hz. Analyses of serial, non-overlapping, 10 s epochs were also used to determine the temporal dynamic of the coherence (Figs. 5 and 6).

We concentrated on examining the coherence of the EEG in the gamma frequency band (30–48 and 52–100 Hz); low and high gamma bands were also analyzed in our previous studies in cats, where they exhibited differences in relation to attentive behaviors [6,7]. Fifty Hz electrical noise was also avoided with this partition. In order to eliminate the possibility that gamma activity and coherence were produced by extra-cerebral potentials, we performed the same procedures and analysis than in our previous studies (see [6,7] for details).

In order to normalize the data and evaluate them by means of parametric statistical tests, we applied the Fisher z′ transform to the gamma coherence values. The z′-coherence of the gamma band for each pair of EEG channels was averaged across behavioral states. z′-Coherence was expressed as the mean ± standard error. The significance of the differences among behavioral states, cortical sites and interactions were evaluated with two-ways ANOVA and Tukey tests. The z′-coherence across behavioral states for the intra or interhemispheric combination of electrodes was also evaluated by one-way ANOVA and Tamhane tests. The gamma power for the different cortices among behavioral states was also evaluated with

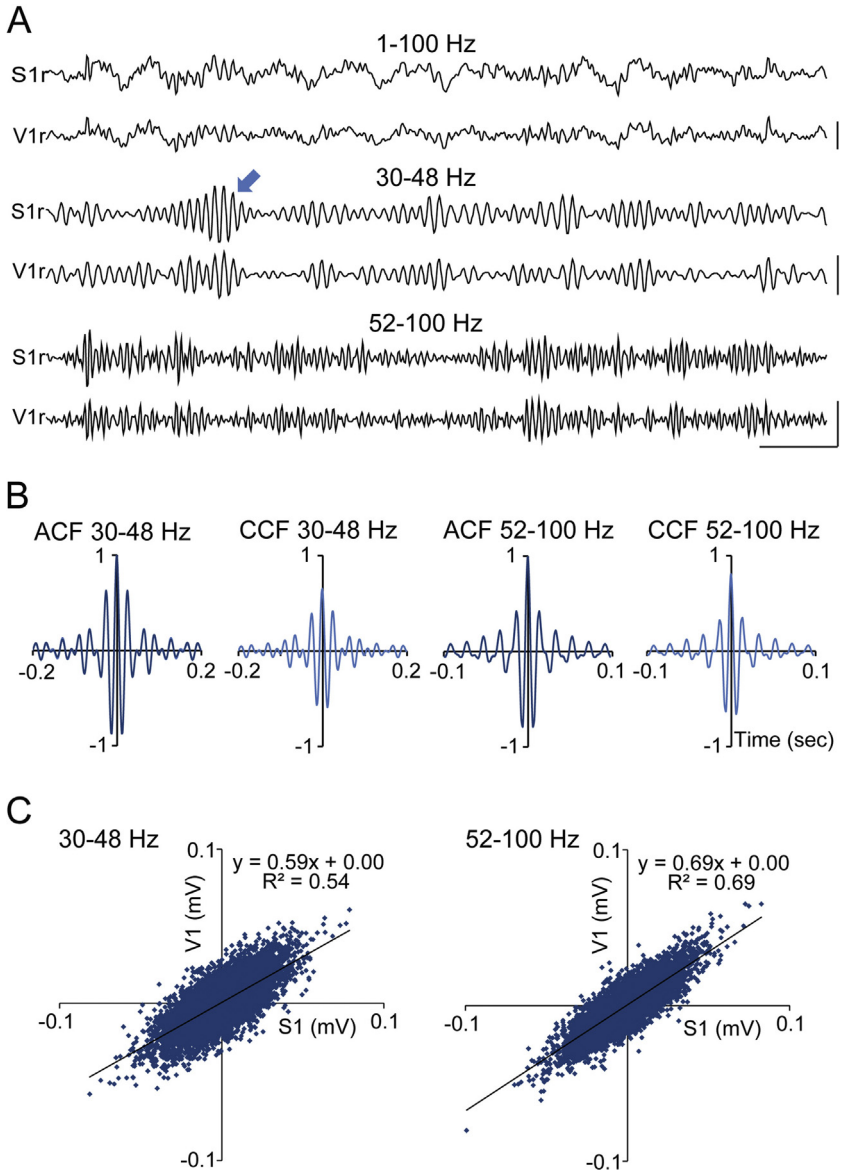

Fig. 2. Gamma oscillations during wakefulness. (A) Simultaneous raw and filtered (35–48 and 52–100 Hz) recordings from the right somatosensory primary (S1r) and right visual primary (V1r) cortices during wakefulness. Gamma oscillations, which are readily observed in the raw recordings, are highlighted after filtering. An arrow signals a "burst" of gamma oscillations. Calibration bars: 200 ms and 200 μV for raw recordings and 100 μV for filtered recordings. (B) Autocorrelation function (ACF) and cross-correlation functions (CCF) from filtered (35–48 Hz and 52–100 Hz) periods of 100 s of simultaneous EEG recordings from S1r and V1r are shown during W. The ACF of both channels are superimposed. (C) Linear regression between the amplitudes of S1r and V1r was performed on representative filtered recordings (30–48 and 52–100 Hz) during 20 s of wakefulness. The determination coefficients and regression line equations are shown.

one-way ANOVA and Tamhane tests. The criterion used to reject the null hypotheses was $p < 0.05$.

Selected recordings were filtered, with a band pass of 30–48 and 52–100 Hz, using Spike 2 digital finite impulse response filters. The amplitude of simultaneously recorded pairs of filtered EEG signals was also analyzed by means of the Pearson correlation. Autocorrelations and cross-correlations functions were also computed.

3. Results

3.1. Raw and filtered (30–48 and 52–100 Hz) EEG recordings during wakefulness and REM sleep

The EEG fluctuates between a desynchronized pattern of activity in the presence of theta rhythm during W and REM sleep and synchronized slow wave activity during NREM sleep. Although EEG activity during W and REM sleep is similar, there are subtle differences. Representative EEG recordings during W and REM sleep are shown in Figs. 2 and 3, respectively. Oscillations of approximately 30–48 Hz can be observed in raw recordings during W (Fig. 2); these electrographic events are not clear during REM sleep (Fig. 3).

Gamma oscillations 30–48 or 52–100 Hz, were unmasked after digital filtering of the recordings. During W, gamma oscillations at 30–48 Hz exhibited some burst of activity with spindle morphology (see example in Fig. 2, arrow); on the other hand, 52–100 Hz oscillations were irregular without a clear pattern. In spite of this, the autocorrelation functions show the presence of an oscillatory pattern of gamma activity (for 30–48 and 52–100 Hz) both during W and REM (Figs. 2 and 3).

Fig. 2 also illustrates a representative example of the coupling of EEG signals recorded from different cortical sites of the same hemisphere during W. Coupling was highlighted when the amplitudes of the signals between pairs of simultaneous EEG recordings were

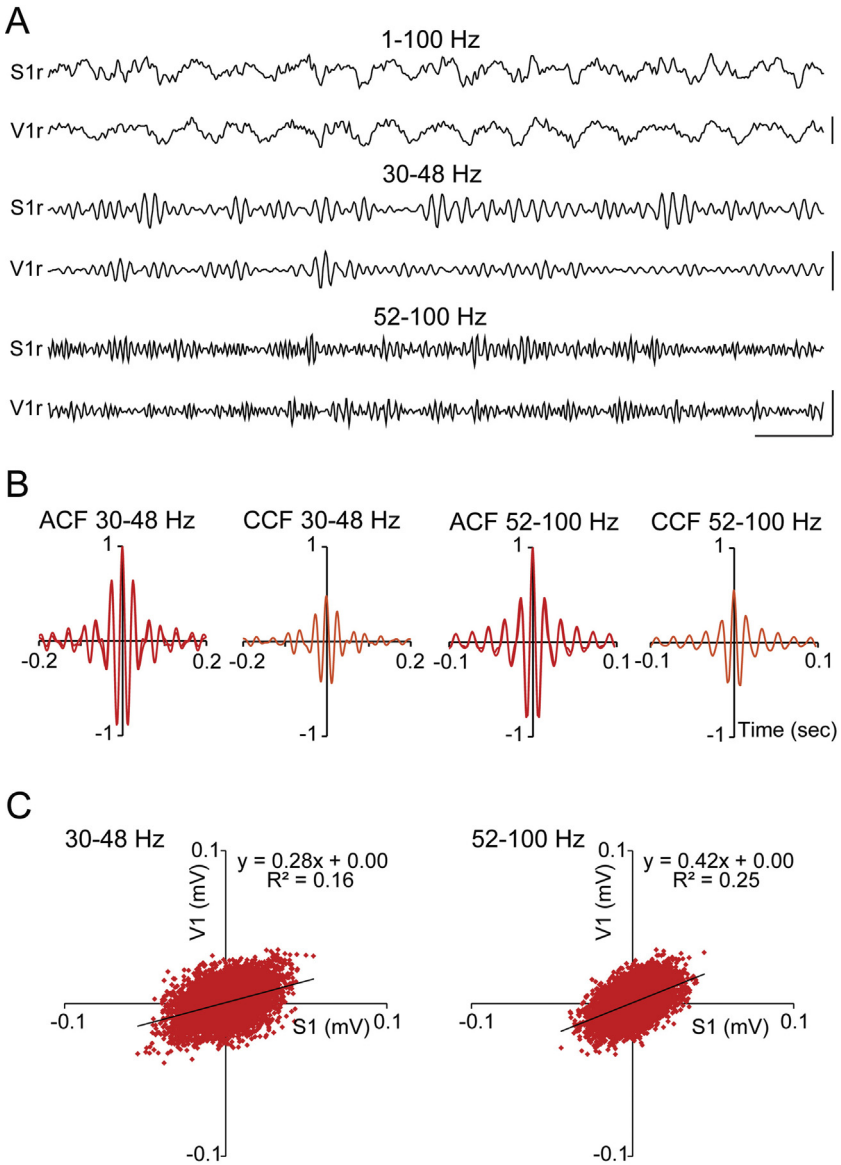

Fig. 3. Gamma oscillations during REM sleep. (A) Simultaneous raw and filtered (35–48 and 52–100 Hz) recordings from the right somatosensory primary (S1r) and right visual primary (V1r) cortices during REM sleep. The amplitude and duration of gamma oscillations decreased compared to wakefulness (see Fig. 2). Calibration bars: 200 ms and 200 μV for raw recordings and 100 μV for filtered recordings. (B) Autocorrelation (ACF) and cross-correlation functions (CCF) from filtered (35–48 Hz and 52–100 Hz) periods of 100 s of simultaneous EEG recordings from S1r and V1r are shown during REM sleep. The ACF of both channels are superimposed. (C) Linear regression between the amplitudes of S1r and V1r were analyzed from representative filtered recordings (30–48 and 52–100 Hz) during 20 s of REM sleep. The determination coefficients and regression line equations are shown.

correlated; the cross-correlation function also shows that both waves are strongly coupled. During REM sleep, the intrahemispheric EEG coupling is reduced, which can be observed in the filtered recordings, the correlation and the cross-correlation histogram exhibited in Fig. 3.

3.2. Coherent 30–48 and 52–100 Hz activity is reduced during REM sleep

In addition to the fact that EEG coupling was minimal during REM sleep when analyzed by filtered recordings and correlation methods, we utilized the magnitude-squared coherence for an in-depth analysis of different pairs of EEG signals that were simultaneously recorded during W and sleep.

As a first step, by means of the two-ways ANOVA we analyzed z′-coherence using behavioral states, and intra- or interhemispheric combination of electrodes (derivates) as factors. The analyses revealed a significant effect of behavioral states (30–48 Hz, $F_{2,423} = 47.28$, $p < 0.0001$; 52–100 Hz, $F_{2,423} = 232.2$, $p < 0.0001$), derivates (30–48 Hz, $F_{2,423} = 335.5$, $p < 0.0001$; 52–100 Hz, $F_{2,423} = 242.4$, $p < 0.0001$) and interactions (30–48 Hz, $F_{4,423} = 8.508$, $p < 0.0001$; 52–100 Hz, $F_{4,423} = 4.497$, $p = 0.001$). Tukey *post hoc* analyses showed that, disregarding the derivates, 30–48 Hz z′-coherence during REM sleep was different than during the other behavioral states ($p < 0.001$). In addition, disregarding behavioral states, 30–48 Hz z′-coherence in the heterotopic interhemispheric combination was different than in the others derivates ($p < 0.001$). All of the combination (behavioral states and derivates) were statistically significant ($p < 0.001$) for 52–100 Hz z′-coherence.

As a second step, we analyzed the z′-coherence in each combination of electrodes across behavioral states using one-way ANOVA. There were significant differences for the intrahemispheric (30–48 Hz, $F_{2,141} = 27.81$, $p < 0.0001$; 52–100 Hz, $F_{2,141} = 94.39$, $p < 0.0001$); the interhemispheric homotopic (30–48 Hz, $F_{2,141} = 8.501$, $p < 0.0001$; 52–100 Hz, $F_{2,141} = 58.95$, $p < 0.0001$) and interhemispheric heterotopic derivates (30–48 Hz, $F_{2,141} = 32.52$, $p < 0.0001$; 52–100 Hz, $F_{2,141} = 95.68$, $p < 0.0001$).

In Fig. 4 is readily observed that, for all the derivates, the minimum values of the z′-coherence for both 30–48 and 52–100 Hz were during REM sleep. For the 30–48 Hz band, in the intrahemispheric derivates, maximum values were present during W. In interhemispheric heterotopic combination, the maximum value of z′-coherence was during NREM sleep. The z′-coherence for 52–100 Hz band was significantly greater during W both for intra and interhemispheric derivates (Fig. 4). The schematic presented in Fig. 4B summarizes the gamma z′-coherence during W and sleep.

For an in-depth analysis of the transitions (t) into and from REM sleep, we analyzed the mean gamma z′-coherence during t (Fig. 5). REM sleep onset was accompanied by a decrease in z′-coherence that was maintained at a low level during this state (Fig. 5A). In contrast, during the transition from REM sleep either to W or NREM sleep, z′-coherence increased (Fig. 5B).

An example of the dynamic evolution of EEG coherence in gamma (30–48 and 52–100 Hz) across behavioral states is shown in Fig. 6 for the intrahemispheric combination of electrodes. While the maximal values of z′-coherence were present during W, the minimal values occurred during REM sleep episodes (Fig. 6).

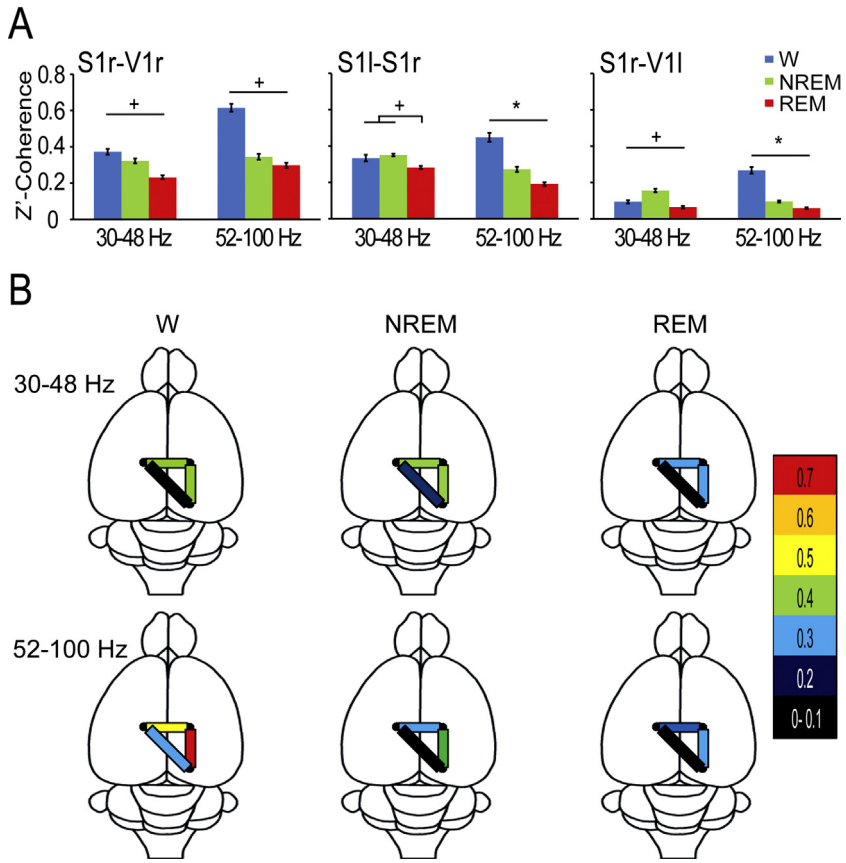

Fig. 4. Gamma band z′-coherence during wakefulness and sleep. (A) Mean z′-coherence (30–48 and 52–100 Hz) of intrahemispheric (G1, S1r–V1r), interhemispheric homotopic (G2, S1l–S1r) and interhemispheric heterotopic (G3, S1r–V1l) combination of electrodes. Data were obtained from 4 rats per group; 12 windows of 100 s per rat for each behavioral state. The values represent the mean ± standard error. Statistical significance: $^{+}P < 0.05$ and $^{*}P < 0.0001$; ANOVA and Tamhane tests. (B) Summary of the gamma band EEG z′-coherence. The lines represent derivates and the color represents the level of z′-coherence. (For interpretation of the references to color in this figure legend, the reader is referred to the web version of this article.)

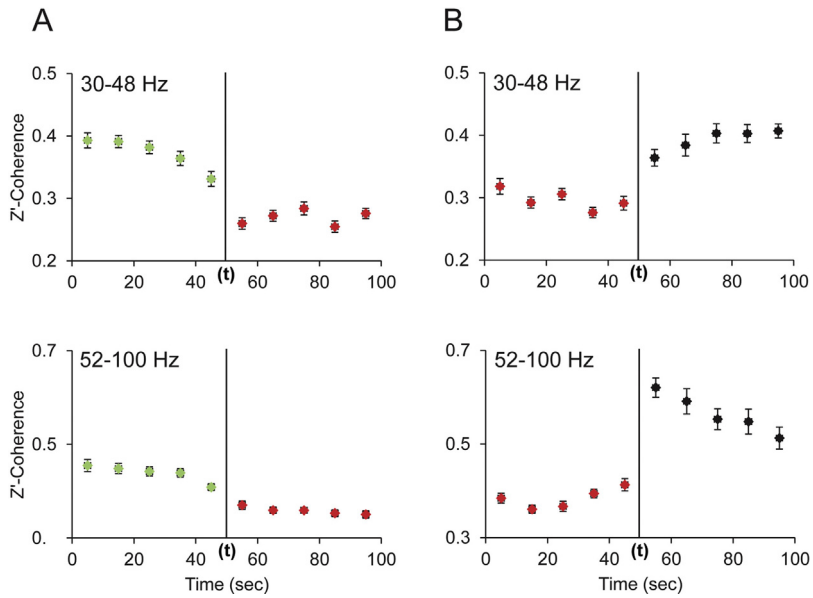

Fig. 5. z′-Coherence during REM sleep transitions. (A) The graphs depict the mean z′-coherence ± standard error (for 30–48 and 52–100 Hz) of 25 transitions of one rat of the G1 group (S1r–V1r, intrahemispheric coherence). (*t*) indicates the onset of REM sleep. (B) Waking from REM sleep. The graphs show the mean z′-coherence ± standard deviation (for 30–48 and 52–100 Hz) of 25 transitions of one rat of the G1 group (S1r–V1r, intrahemispheric coherence). (*t*) indicates the end of the REM sleep episodes. NREM episodes are symbolized in green; REM episodes in red. The states that followed the REM sleep episodes are indicated in black (these epochs were mainly wakefulness but NREM sleep episodes also followed REM sleep). (For interpretation of the references to color in this figure legend, the reader is referred to the web version of this article.)

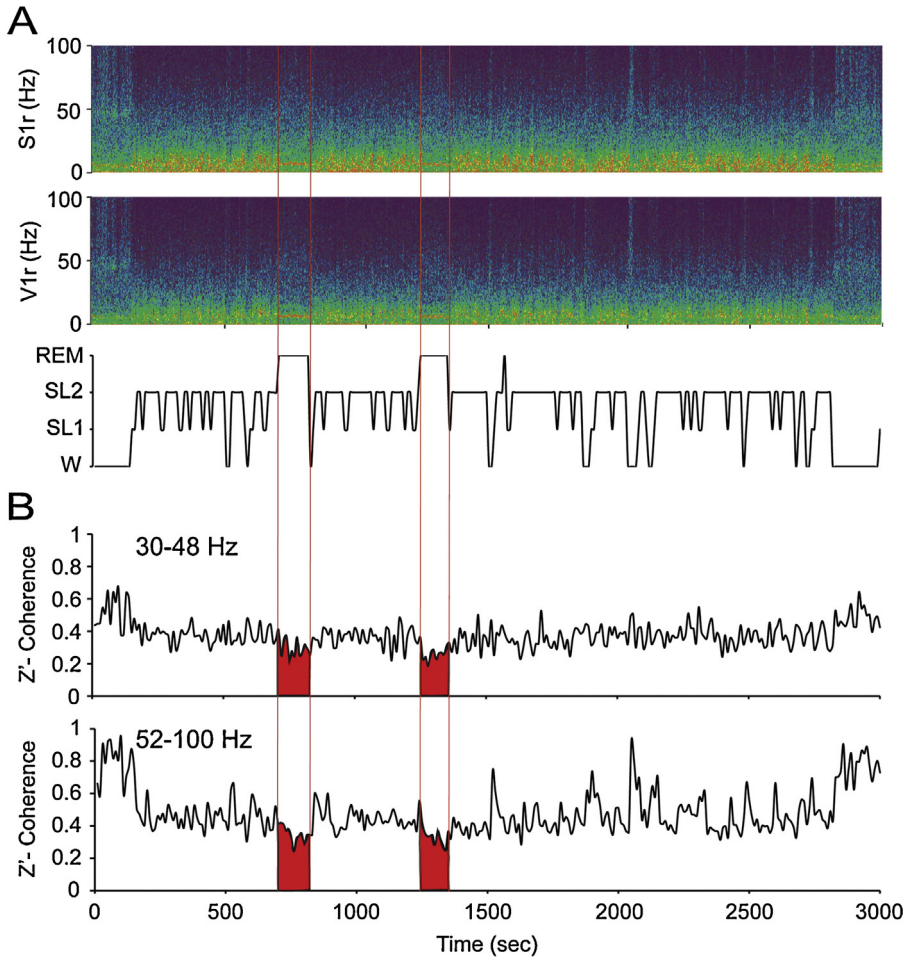

Fig. 6. Dynamic of the gamma coherence during wakefulness and sleep. (A) The spectrogram (0.1–100 Hz) of primary visual (V1r) and primary somatosensory (S1r) cortical recordings and the accompanying hypnogram are shown. During W and REM sleep the theta activity (4–9 Hz) in the spectrograms can be readily observed. Gamma activity is larger during W. During NREM sleep, delta activity (0.5–4 Hz) is more prominent and there are intermittent episodes of sigma activity (9–15 Hz), which correspond to the presence of sleep spindles. (B) The z′-coherence for both gamma bands (30–48 and 52–100 Hz) was analyzed in 10-s epochs. The maximum values of z′-coherence occurred during W; z′-coherence decreased to an intermediate level during NREM sleep and minimum values were present during the periods of REM sleep (segments in red). (For interpretation of the references to color in this figure legend, the reader is referred to the web version of this article.)

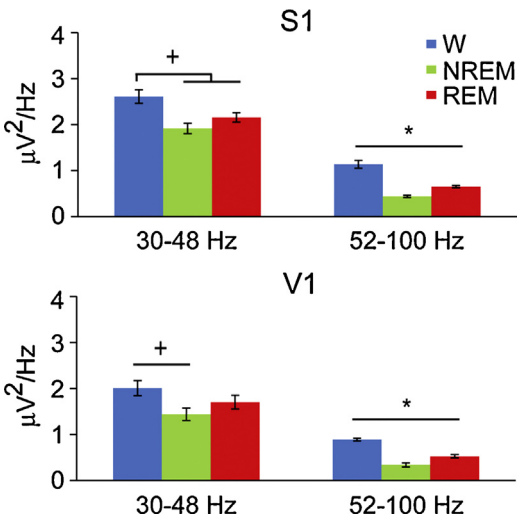

Fig. 7. Gamma power during wakefulness and sleep. Mean gamma band power of the EEG recorded from 3 rats of the intra-hemispheric S1r and V1r cortices of group G1 (see Fig. 1) during wakefulness (W), NREM and REM sleep. The values represent mean ± standard error. Statistical significance: $^{+}P<0.05$ and $^{*}P<0.0001$, ANOVA with Tamhane tests.

3.3. Gamma power during wakefulness and sleep

The gamma power was different across behavioral states for S1 (30–48 Hz, $F_{2,105}=7.941$, $p=0.001$; 52–100 Hz, $F_{2,105}=49.37$, $p<0.0001$) and V1 cortices (30–48 Hz, $F_{2,105}=6.092$, $p=0.003$; 52–100 Hz, $F_{2,105}=45.06$, $p<0.0001$). Fig. 7 shows that gamma power was significantly greater during W than during REM sleep for 52–100 Hz in S1 and V1 cortices, and for 30–48 Hz in S1 cortex. However, in contrast to z′-coherence values, the minimum power values occurred during NREM sleep.

4. Discussion

In the present study, we demonstrated in rats that the EEG intra-hemispheric and interhemispheric coherence in the gamma (30–48 and 52–100 Hz) frequency band is smaller during REM sleep that during W or NREM sleep. Therefore, these data suggest that during REM sleep, high-frequency functional interaction between different cortical regions is lower compared with other behavioral states.

4.1. Gamma coherence during wakefulness

It is well established that gamma power and gamma coherence increase during W in cats and humans, mainly for intrahemispheric combination of electrodes [4,6,7]. In the cat, gamma band coherence at ≈40 Hz increases during alert W; this fact that can be clearly observed in raw recordings [6,7]. In the present study, the largest gamma power and intrahemispheric coherence was present during W states, but the differences depending on waking conditions were not studied. In this regards, Maloney et al. (1998) showed that the largest values of gamma power occur during periods of active W [22].

4.2. Gamma coherence during REM sleep

In the present report, we demonstrated in rats that gamma intra and interhemispheric coherence reaches a nadir during REM sleep. This result accords with the results of our previous studies in the cat [6,7], where gamma coherence was almost absent during REM sleep in intrahemispheric and interhemispheric derivates. The demonstration that there is a radical reduction in gamma coherence between different cortical regions during REM sleep does not contradict the findings of Steriade el al. (1996), which showed an increase in local coupling (within a column or among closely cortical sites) during activated states [23]. In fact, as shown in Fig. 7, gamma power (as a reflection of local gamma synchronization) during REM sleep was close to W, and larger than during NREM sleep. Therefore, although gamma activity was large during REM sleep, the coupling of gamma oscillations between different cortical areas (reflected by gamma coherence) was minimal.

In humans, an early report showed that during REM sleep magneto-EEG 40-Hz oscillations were similar in distribution, phase and amplitude to those observed during W. In contrast, Perez-Garci et al. (2001) reported that there is a decrease in correlation spectra in 2-s epochs of fast (27–48 Hz) frequencies restricted to intra-hemispheric frontal-perceptual cortical regions during REM sleep. On the contrary, the gamma synchrony between homologous cortical regions of both hemispheres increases during REM sleep in humans [24,25]. Cantero et al. (2004) employed human intracranial EEG recordings for coherence analyses during sleep, which allowed a much finer spatial scale than scalp-recorded signals. They found that local (within neocortical regions) and long-range (between intra-hemispheric neocortical regions) gamma (35–58 Hz) coherence was significantly greater during wakefulness than during sleep. However, no differences in coherence were found between NREM and REM sleep. Furthermore, functional gamma-range coupling between the neocortex and hippocampus was observed during wakefulness, but not during REM sleep. Finally, Voss et al. (2009) demonstrated that gamma coherence decreases during REM sleep compared with wakefulness; during lucid dreaming, coherence values are intermediate between W and REM sleep.

As with other EEG rhythms, gamma oscillations remains remarkable conserved in mammals irrespective of brain size [26]. The decrease in gamma coherence during REM sleep in rats (present report), in cats [6,7] and in humans [24,27,28], indicates that during this behavioral state there is a decrease in the capacity for integration among different cortices within high frequency ranges.

A recent study demonstrated that electrical stimulation of the prefrontal cortex in the lower gamma band (≈40 Hz) during REM sleep influences ongoing brain activity and induces self-reflective awareness (a feature of W) in dreams (*i.e.*, lucid dreams), while other stimulation frequencies were not effective [29]. Thus, the data support the concept that synchronous oscillations of ≈40 Hz are an electrophysiological pattern of activity that is indicative of attentive wakefulness. On the contrary, the reduction of gamma coherence during REM sleep [6,7,24,27,28], may underlie the unique pattern of REM sleep mentation, *i.e.*, dreams [14,30].

5. Conclusions

During REM sleep in the rat, despite an activated EEG, there is an uncoupling of the gamma frequency activities between neocortical sites. Therefore, functional interactions among different cortical areas, which are critical for cognitive functions, are different during W and REM sleep. Since this feature is conserved in other mammals, including humans, we consider that this uncoupling of gamma frequency activity during REM sleep is a defining trait of REM sleep in mammals.

Acknowledgments

We are grateful to Dr. Horacio Igarzabal for his assistance in the experimental procedures. This study was partially supported by the “Programa de Desarrollo de Ciencias Básicas” (PEDECIBA) and the “Agencia Nacional de Investigacion e Innovación” (ANII), Uruguay.

References

[1] Rieder MK, Rahm B, Williams JD, Kaiser J. Human gamma-band activity and behavior. Int J Psychophysiol 2010;79:39–48.
[2] Uhlhaas PJ, Pipa G, Lima B, Melloni L, Neuenschwander S, Nikolic D, et al. Neural synchrony in cortical networks: history, concept and current status. Front Integr Neurosci 2009;3:17.
[3] Uhlhaas PJ, Pipa G, Neuenschwander S, Wibral M, Singer W. A new look at gamma? High- (>60 Hz) gamma-band activity in cortical networks: function, mechanisms and impairment. Prog Biophys Mol Biol 2011;105:14–28.
[4] Llinas R, Ribary U. Coherent 40-Hz oscillation characterizes dream state in humans. Proc Natl Acad Sci U S A 1993;90:2078–81.
[5] Tiitinen H, Sinkkonen J, Reinikainen K, Alho K, Lavikainen J, Naatanen R. Selective attention enhances the auditory 40-Hz transient response in humans. Nature 1993;364:59–60.
[6] Castro S, Falconi A, Chase MH, Torterolo P. Coherent neocortical 40-Hz oscillations are not present during REM sleep. Eur J Neurosci 2013;37:1330–9.
[7] Castro S, Cavelli M, Vollono P, Chase MH, Falconi A, Torterolo P. Interhemispheric coherence of neocortical gamma oscillations during sleep and wakefulness. Neurosci Lett 2014;578:197–202.
[8] Bullock TH, McClune MC, Enright JT. Are the electroencephalograms mainly rhythmic? Assessment of periodicity in wide-band time series. Neuroscience 2003;121:233–52.
[9] Edelman GM, Tononi G. A universe of consciousness. New York: Basic Books; 2000.
[10] Siegel M, Donner TH, Engel AK. Spectral fingerprints of large-scale neuronal interactions. Nat Rev Neurosci 2012;13:121–34.
[11] Llinas R, Ribary U, Contreras D, Pedroarena C. The neuronal basis for consciousness. Philos Trans R Soc Lond B: Biol Sci 1998;353:1841–9.
[12] John ER. The neurophysics of consciousness. Brain Res Brain Res Rev 2002;39:1–28.
[13] Mashour GA. Integrating the science of consciousness and anesthesia. Anesth Analg 2006;103:975–82.
[14] Hobson JA. REM sleep and dreaming: towards a theory of protoconsciousness. Nat Rev Neurosci 2009;10:803–13.
[15] Benedetto L, Rodriguez-Servetti Z, Lagos P, D'Almeida V, Monti JM, Torterolo P. Microinjection of melanin concentrating hormone into the lateral preoptic area promotes non-REM sleep in the rat. Peptides 2013;39C:11–5.
[16] Lagos P, Torterolo P, Jantos H, Chase MH, Monti JM. Effects on sleep of melanin-concentrating hormone microinjections into the dorsal raphe nucleus. Brain Res 2009;1265:103–10.
[17] Bullock TH, Buzsaki G, McClune MC. Coherence of compound field potentials reveals discontinuities in the CA1-subiculum of the hippocampus in freely-moving rats. Neuroscience 1990;38:609–19.
[18] Bullock TH. Signals and signs in the nervous system: the dynamic anatomy of electrical activity is probably information-rich. Proc Natl Acad Sci U S A 1997;94:1–6.
[19] Bullock TH, McClune MC, Achimowicz JZ, Iragui-Madoz VJ, Duckrow RB, Spencer SS. EEG coherence has structure in the millimeter domain: subdural and hippocampal recordings from epileptic patients. Electroencephalogr Clin Neurophysiol 1995;95:161–77.
[20] Cantero JL, Atienza M, Salas RM. Clinical value of EEG coherence as electrophysiological index of cortico-cortical connections during sleep. Rev Neurol 2000;31:442–54.
[21] Nunez PL, Srinivasan R, Westdorp AF, Wijesinghe RS, Tucker DM, Silberstein RB, et al. EEG coherency. I: Statistics, reference electrode, volume conduction, Laplacians, cortical imaging, and interpretation at multiple scales. Electroencephalogr Clin Neurophysiol 1997;103:499–515.
[22] Maloney KJ, Cape EG, Gotman J, Jones BE. High-frequency gamma electroencephalogram activity in association with sleep-wake states and spontaneous behaviors in the rat. Neuroscience 1997;76:541–55.
[23] Steriade M, Amzica F, Contreras D. Synchronization of fast (30–40 Hz) spontaneous cortical rhythms during brain activation. J Neurosci 1996;16:392–417.
[24] Perez-Garci E, del-Rio-Portilla Y, Guevara MA, Arce C, Corsi-Cabrera M. Paradoxical sleep is characterized by uncoupled gamma activity between frontal and perceptual cortical regions. Sleep 2001;24:118–26.
[25] Corsi-Cabrera M, Sifuentes-Ortega R, Rosales-Lagarde A, Rojas-Ramos OA, Del Rio-Portilla Y. Enhanced synchronization of gamma activity between frontal lobes during REM sleep as a function of REM sleep deprivation in man. Exp Brain Res 2014;232:1497–508.
[26] Buzsaki G, Logothetis N, Singer W. Scaling brain size, keeping timing: evolutionary preservation of brain rhythms. Neuron 2013;80:751–64.
[27] Cantero JL, Atienza M, Madsen JR, Stickgold R. Gamma EEG dynamics in neocortex and hippocampus during human wakefulness and sleep. Neuroimage 2004;22:1271–80.
[28] Voss U, Holzmann R, Tuin I, Hobson JA. Lucid dreaming: a state of consciousness with features of both waking and non-lucid dreaming. Sleep 2009;32:1191–200.
[29] Voss U, Holzmann R, Hobson A, Paulus W, Koppehele-Gossel J, Klimke A, et al. Induction of self awareness in dreams through frontal low current stimulation of gamma activity. Nat Neurosci 2014;17:810–2.
[30] Nir Y, Tononi G. Dreaming and the brain: from phenomenology to neurophysiology. Trends Cogn Sci 2010;14:88–100.
[31] Paxinos G, Watson C. The rat brain. New York: Academic Press; 2005.

ANEXO 2. AUSENCIA DE COHERENCIA GAMMA DE EEG EN UN ESTADO CORTICAL ACTIVADO LOCALMENTE: UN RASGO CONSERVADO DE SUEÑO REM

Durante los procesos cognitivos, hay interacciones entre varias regiones de la corteza cerebral. Las oscilaciones en la banda gamma de frecuencias (30-100 Hz) del electroencefalograma están implicadas en la unión de eventos neuronales espacialmente separados pero temporalmente correlacionados, lo que da como resultado una experiencia perceptual unificada.

Al igual que la vigilia, el sueño REM se caracteriza por la presencia de oscilaciones gamma en el EEG. Los sueños, que se consideran un tipo especial de actividad cognitiva o proto-consciencia, ocurren principalmente durante este estado. La potencia de la banda gamma, evaluada por la transformada rápida de Fourier, refleja el grado de sincronización local a esa frecuencia. Por otro lado, el alcance de las interacciones entre las diferentes áreas corticales en la banda gamma de frecuencias se puede explorar mediante una función matemática llamada "coherencia", que refleja la "fuerza" de las interacciones funcionales entre las áreas corticales.

El objetivo del presente trabajo fue estudiar en la rata la relación dinámica entre la potencia gamma y la coherencia en las bandas gamma baja (30-48 Hz) y alta (52-98 Hz) durante la vigilia y el sueño, en áreas neocorticales occipitales, parietales y frontales, así como en el bulbo olfatorio, que es un sitio crítico de génesis del ritmo gamma. Además, volvimos a analizar los registros anteriores en gatos para evaluar la misma relación dinámica que en las ratas.

En ambas especies, el resultado principal fue que durante el sueño REM, la potencia gamma aumentó, mientras que la coherencia gamma

entre áreas neocorticales distantes disminuyó. El hecho de que este perfil esté presente tanto en *rodenthia* como en *carnivora* sugiere que este es un rasgo que caracteriza el sueño REM en mamíferos.

Translational Brain Rhythmicity

Research Article

Absence of EEG gamma coherence in a local activated cortical state: a conserved trait of REM sleep

Matías Cavelli*, Santiago Castro-Zaballa, Alejandra Mondino, Joaquin Gonzalez, Atilio Falconi and Pablo Torterolo

Laboratory of Sleep Neurobiology, Department of Physiology, School of Medicine, Universidad de la República, Montevideo, Uruguay

Abstract

During cognitive processes, there are extensive interactions between various regions of the cerebral cortex. Oscillations in the gamma frequency band (30-100 Hz) of the electroencephalogram are involved in the binding of spatially separated but temporally correlated neural events, which results in a unified perceptual experience.

Like wakefulness, REM sleep is characterized by gamma oscillations in the EEG. Dreams, that are considered a special type of cognitive activity or proto-consciousness, mostly occur during this state.

The power of the gamma band, assessed by the fast Fourier transform, reflects the local degree of synchronization at that frequency. On the other hand, the extent of interactions between different cortical areas at the gamma frequency band can be explored by means of a mathematical function called 'coherence', which reflects the 'strength' of functional interactions between cortical areas.

The objective of the present report was to study in the rat the dynamic relationship between gamma power and coherence in the low (30-48 Hz) and high (52-98 Hz) gamma bands during waking and sleep, in occipital, parietal, and frontal neocortical areas, as well as in the olfactory bulb, that is a critical site of gamma rhythm-genesis. In addition, we re-analyzed previous recordings in cats, in order to evaluate the same dynamic relationship as in rats. In both species, the main result was that during REM sleep, gamma power increased, while gamma coherence between distant neocortical areas decreased. The fact that this profile is present in *rodenthia* as well as in *carnivora* suggests that this is a trait that characterize REM sleep in mammals.

Introduction

The brain is a complex, self-organized system with non-linear dynamics, in which distributed and parallel processing coexist with serial operations within highly interconnected networks, but without a single coordinating center [1,2]. This organ integrates fragmentary neural events that occur at different times and locations into a unified perceptual experience. Understanding the mechanisms that are responsible for this integration, "the binding problem", is one of the most important challenges that cognitive neuroscience has to solve [3,4].

One of the binding mechanisms appears to be the synchronization of neuronal activity by phase-locking of self-generated network oscillations [5,6]. The first experimental evidence supporting the potential role of synchrony as a relational code, was described in simultaneously recorded but spatially segregated neurons that engaged in synchronous oscillation when activated by visual stimuli. The frequency of these synchronized oscillations was in the range of 40 Hz [7,8]. This coordinating mechanisms was named "binding-by-synchrony" [2,4]; and this theory assumes that coherence in neuronal activity is critical for information processing [9].

Jasper and Andrews first used the term gamma waves to designate low-amplitude waves at 35-45 Hz in the electroencephalogram (EEG) [10]. These oscillations were later described in the olfactory bulb (OB) of hedgehogs by Adrian [11]. An increase in gamma activity typically appears during states/behaviors that are characterized by the active cognitive processing of external percepts or internally generated thoughts and images [12-16].

Cognitive activities not only occur during wakefulness (W). Dreams, which occur mostly during REM sleep, are considered a special kind of cognitive activity or proto-consciousness [17]. In contrast, during deep non-REM (NREM) sleep, there is an absence, or at least a strong reduction, in oneiric activity [17]. REM sleep dreams are characterized by their vividness, single-mindedness, bizarreness and loss of voluntary control over the plot. Attention is unstable and rigidly focused, facts and reality are not checked, violation of physical laws and bizarreness are passively accepted, contextual congruence is distorted, time is altered and memories become labile [17,18]. Interestingly, some authors have suggested that cognition during REM sleep resembles psychosis [19]. High gamma activity is also present during REM sleep, both in humans and animals [20-23].

Local cortical oscillations in the gamma band can be examined by means of the fast Fourier transform (FFT). The results are expressed in gamma power that reflects the local degree of synchronization of the extracellular potential at that frequency [24]. Local gamma oscillations are higher during REM sleep compared to NREM sleep [21-23,25]. On the other hand, the extent of interactions between different cortices at the gamma frequency band can be explored through a mathematical function called 'coherence', which reflects the 'strength' of functional interactions between cortical areas [26-28]. Gamma coherence between distant areas has been proposed as a neural correlate of

Correspondence to: Dr. Pablo Torterolo, Department of Physiology, Faculty of Medicine, University of the Republic, General Flores 2125, 11800 Montevideo-Uruguay, Tel: (598) 2924 34 14 ext. 3234; E-mail: ptortero@fmed.edu.uy

Key words: *wakefulness, paradoxical sleep, cortex, dreams, synchronization, NREM sleep*

Received: June 29, 2017; **Accepted:** July 28, 2017; **Published:** July 31, 2017

conscious perception and self-awareness [29-33]. In this regard, coherence in the gamma frequency band is lost during anesthesia-induced unconsciousness [34-36], and is severely altered in psychiatric disorders [37,38].

In previous studies, we showed in cats and rats, that gamma coherence is high during W, decreases during NREM sleep and is almost absent during REM sleep [23,39-41]. However, these studies were limited in the extent of the cortical loci studied, as well as in the examination of the dynamic relationship between local and long-range gamma synchronization. Therefore, the aim of the present report was the following: 1. To study in the rat low (30-48 Hz) and high (52-98 Hz) gamma power and coherence during W and sleep in neocortical areas (such as frontal cortices) that were not yet studied. We also aimed to analyze the OB, that is a critical site of gamma rhythm-genesis [11,14,15]. In addition, we evaluated in detail the dynamic relationship between local or short-range synchronization (power) and long-range synchronization (coherence) during W, sleep and transitions into and out REM sleep. 2. To re-analyze previous recordings in cats, in order to evaluate the same dynamic relationships proposed for rats.

Material and methods

Experimental animals

We analyzed data obtained from nine adult Wistar rats and six adult cats. Data from four of these cats were utilized in previous studies [39,41]. The animals were determined to be in good health by veterinarians of the Department of Laboratory Medicine of the School of Medicine, Universidad de la República, Uruguay. All experimental procedures were conducted in accordance with the National Animal Care Law (#18611) and with the "Guide to the care and use of laboratory animals" (8th edition, National Academy Press, Washington D. C., 2010). Furthermore, the Institutional Animal Care Committee approved the experimental procedures. Adequate measures were taken to minimize pain, discomfort or stress of the animals, and efforts were made to use the minimum number of animals necessary to produce reliable data.

Surgical procedures and experimental sessions are summarized below; for details [23,39].

Surgical procedures

Animals were chronically implanted with electrodes to monitor the states of sleep and W. In rats, anesthesia was induced with a mixture of ketamine-xylazine. Cats were pre-medicated with xylazine, atropine and antibiotics, and anesthesia was induced with ketamine and maintained with a gas mixture of isoflourane in oxygen.

The animal's head was positioned in a stereotaxic frame and the skull was exposed. In order to record the EEG, stainless steel screw electrodes (diameter: 1.4 mm cats and 1.0 mm for rats) were placed on the surface (above the dura mater) in different cortices. Figure 1 presents a summary of the positions of the recording electrodes on the surface of the cortex for rats and cats. In the rats, six electrodes were located on the neocortex forming two anterior-posterior consecutive squares centered with respect to the midline and the frontal square centered with respect to Bregma (Figure 1). Each side of the squares has a length of 5 mm. The electrodes were located in primary motor cortex (M1, L: ±2.5 mm, AP: +2.5 mm), primary somato-sensory cortex (S1, L: ±2.5 mm, AP: -2.5 mm), and secondary visual cortex (V2, L: ±2.5 mm, AP: -7.5 mm). The other electrode was located over the right OB (L: +1.25 mm, AP: +7.5 mm). Each cat was implanted with several electrodes throughout the neocortex. However, in this report, we analyzed the signals from the electrodes positioned in the anterior (frontal) and posterior (occipital or parietal) cortices of the same hemisphere.

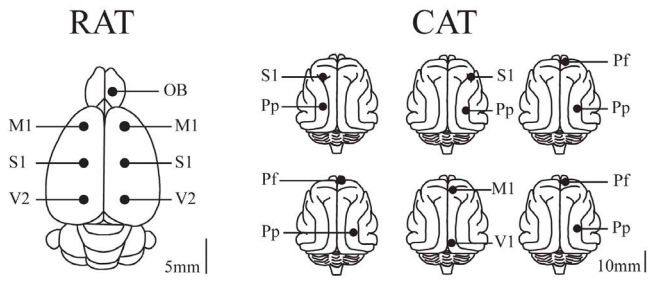

Figure 1. Position of recording electrodes. The figure presents a summary of the positions of the recording sites on the surface of the cerebral cortex of a group of 9 rats sharing the same location of electrodes, and 6 cats with similar but not the same electrode locations as in rats. The electrodes were referred to a common electrode that was located over the cerebellum (rats) or left frontal sinus (cats). OB, olfactory bulb; M1, primary motor cortex; S1, primary somato-sensory cortex; V1, primary visual cortex; V2, secondary visual cortex; Pf, pre-frontal cortex; Pp, posterior parietal cortex.

The electrodes were soldered to a plug and bonded to the skull with acrylic cement. In order to record the electromyogram (EMG), two electrodes were inserted into the neck muscle chronically in the rat, and contact electrodes (with EEG-paste interphase) were acutely positioned on the neck skin of the cat. In the cat, two plastic tubes (which were used to maintain the animal's head fixed without pain or pressure), were also bonded to the skull with acrylic cement.

At the end of the surgical procedures, an analgesic was administered. Incision margins were kept clean and a topical antibiotic was administered on a daily basis. After the animals had recovered from the preceding surgical procedures, they were adapted to the recording environment for a period of at least one week (rats) and two months (cats).

Experimental sessions

Experimental sessions of 4-6 h in duration were conducted during the light period, between 12 AM and 6 PM (rats) and 11 AM to 3 PM (cats) in a temperature-controlled environment (21-24 °C). In rats, the recordings were obtained via a rotating connector in a sound-attenuated chamber which is also a Faraday box; during these sessions (as well as during adaptation sessions), the animals were able to move freely within the confines of the recording chamber (transparent cages (40 x 30 x 20 cm) containing wood shavings) and had free access to water and food. Cats were recorded in a Faraday box in semi-restricted conditions; during experimental sessions' the head of the cat was held in a stereotaxic frame by a head-restraining device, while the body rested in a sleeping bag.

The simultaneous activity of different cortical areas was recorded with monopolar arrangement of electrodes [42]. A common electrode reference montage was employed; it was located in the left frontal sinus of the cats [39], and in the cerebellum of the rats [23]. The EMG was also monitored. Each cat and rat was recorded daily for a period of approximately 30 days and 2 weeks, respectively, in order to obtain a complete data set.

Bioelectric analog signals were amplified with differential AC amplifiers (AM-systems model 1700; 1000 x), filtered (0.1-500 Hz), digitized (1024 Hz, 2^{16} bits) and stored on a PC using the Spike2 software (Cambridge Electronic Design). Data were obtained during W, REM sleep, and NREM sleep.

Data analysis

Sleep and waking states were determined for every 10-seconds epoch for rats and cats. W, light sleep (SL1), deep or slow wave sleep (SL2), NREM sleep (SL1 + SL2) and REM sleep were identified in rats [23,43]. Alert W (AW), quiet W (QW), W (AW+QW), NREM sleep and REM sleep were identified in cats [39]. AW was induced for a period of 300 sec by a sound stimulus, which was introduced approximately 30 minutes after the beginning of the recording. The sound stimulus consisted of clicks (0.1 ms in duration) of 60 to 100 dB SPL in intensity with a variable frequency of presentation (1 to 500 Hz, modified at random by the operator) in order to avoid habituation [39].

We focused on the analysis of low (LG: 30-48 Hz) and high (HG: 52-98 Hz) gamma frequency bands of the EEG; 50 Hz electrical noise was avoided with this partitioning. In rats, we analyzed gamma power in the maximum number of channels and coherence in all the possible cortical combinations. In cats, we focused on a pair of electrodes with similar location in all animals, one in a frontal position and one in a posterior position of the brain. In order to analyze gamma power and gamma coherence between these EEG channels, we used similar procedures as in our previous studies [23,39,41]; however, the analysis in cats and rats were not exactly the same (see below).

CAT

We employed the same methodology that we described in our previous studies [39-41]. Twelve artifact-free periods of 100 seconds were examined during each behavioral state (1200 seconds for each behavioral state, per animal; data were selected from three different recordings).

RAT

The maximum number of non-transitional and artifact-free periods of 30 seconds was selected during each behavioral state to determine the mean power and coherence for each rat. For each animal, we analyzed two complete (6 h) recordings (recordings with the minimal amount of artifacts were selected).

The coherence between two EEG channels that were recorded simultaneously was analyzed in windows of 30 second (rat) or 100 second (cat) windows. For each period, the Magnitude Squared Coherence as well as the power spectrum for each channel, were calculated by means of Spike2 script COHER-HOL 1S (for details about coherence definition see [26,39]). For the coherence analysis, each period was divided into 30 (rat) and 100 (cat) time-blocks with a bin size of 2048 samples, and a resolution of 0.5 Hz. We applied the Fisher z' transform to the gamma coherence values in order to normalize and evaluate them by means of parametric statistical tests. The data was then analyzed through custom-built Python routines.

Analyses of 10-second epochs were also used to determine the temporal dynamic of power and coherence. Hence, low and high gamma power and coherence were normalized, and referred to as normalized power (NP) and normalized z'-coherence (NC). For dynamic analysis (see Results), normalization was undertaken by dividing each value by the maximum value (of either power or coherence) recorded in each analyzed segment. For statistical analysis, the normalization was performed for each animal by dividing each mean value by the maximum-recorded value.

We also analyzed the LG and HG mean global power (MGP) and mean global coherence (MGC) in each rat, by averaging the power measured in all the channels, and the coherence for all combinations of electrodes [36].

In order to determine the relationship between local or short-range synchronization (power) and long-range synchronization (coherence) we applied the following function: ((NP of Ch1 + NP Ch2) / 2)) - (NC between Ch1-Ch2). We named this function Power-Coherence difference (NP-NC). A similar approach was employed for the global power and coherence (MGP – MGC). In previous preliminary analyses, we constructed the function utilizing the ratio between normalized power and coherence with similar results. However, we considered the NP-NC function a more suitable analysis given that the signs of the results differed between states; W (close to zero), NREM sleep (negative values) and REM sleep (positive values).

The data were expressed as mean ± standard deviation of the NP, NC and NP-NC. The significance of the differences across behavioral states was evaluated with one-way ANOVA and Tamhane post hoc tests (for each animal) and repeated measures ANOVA (for comparison between the means of the whole group of cats or rats), along with Tukey post hoc tests. The criterion used to reject the null hypothesis was $p < 0.05$.

Results

Gamma activity in rat

Dynamics of gamma activity in the rat: The gamma dynamic during sleep and W in a representative rat is shown in Figure 2; the spectrograms and hypnograms of Figure 2A, indicate the different states of W and sleep. Low and high gamma NP is shown in Figure 2B. For primary somatosensory (S1) and secondary visual (V2) cortices, both low and high gamma NP was higher during W than during sleep. For the low gamma band in this animal there were not clear changes in the NP between NREM sleep and REM sleep. On the contrary, high gamma NP was minimal in NREM sleep but increased during REM sleep (Figure 2B).

Low and high gamma NC between S1 and V2 were the highest during W and decreased during NREM sleep (Figure 2C). The largest decrement in low and high gamma NC occurred during REM sleep.

In order to analyze the relationship between gamma power (that reflects local or short-range synchronization) and gamma coherence (that reveals long-range or distant synchronization), the NP-NC function was applied (Figure 2C). During W this relationship was close to zero, had negative values during NREM sleep and reverted to positive values during REM sleep. This dynamic profile was similar for both low and high gamma bands.

Cortical extent of LG and HG power and coherence: To study the cortical extent of power and coherence of gamma bands, we analyzed a group of nine rats that shared the same electrode positions. Statistical analyses of gamma power and coherence are shown in Tables 1, 2 and 3; these results are graphically summarized in Figure 3. LG and HG NP showed significant differences across behavioral states in all the cortical regions (Table 1). These results revealed that LG and HG power is high during W than during sleep, both in neocortex and OB. The lowest values were recorded during NREM sleep, while during REM sleep the HG NP increased to an intermediate level in all the cerebral areas recorded. On the other hand, LG showed similar values to those of W in the parietal and frontal areas of the neocortex (Table 1).

For LG, NC displayed significant differences across behavioral states from sixteen of twenty-one possible electrode pair combinations (Table 2). Interestingly, seven combinations displayed a greater coherence during NREM sleep than during W. In contrast, only two

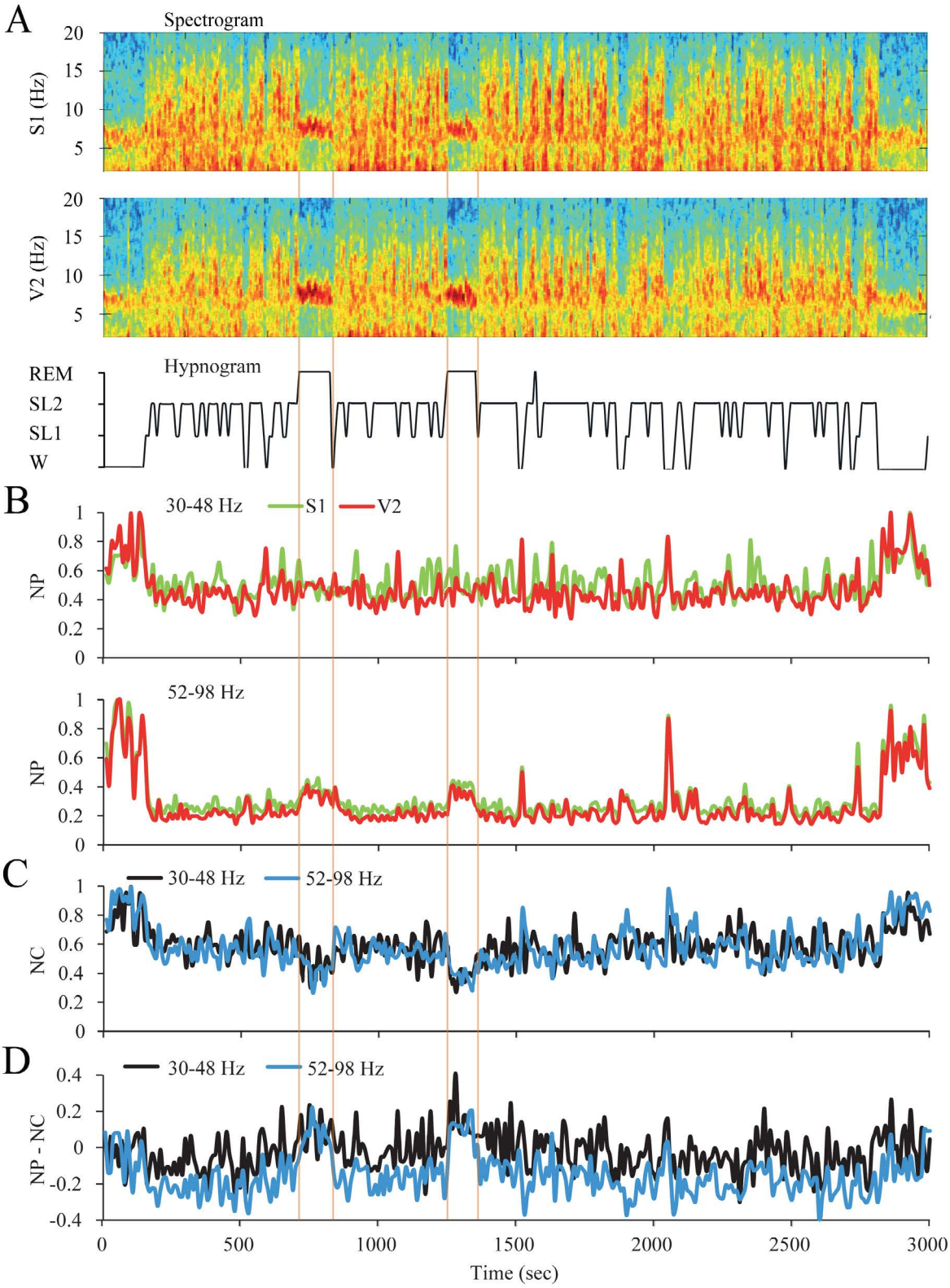

Figure 2. Dynamic of the gamma activity in the rat. A. The spectrograms (1-20 Hz) of secondary visual (V2) and primary somatosensory (S1) cortical recordings and the hypnogram are shown. During W and REM sleep, theta activity (4-9 Hz) in the spectrograms can be readily observed. During NREM sleep, delta activity (0.5-4 Hz) was more prominent and there were intermittent episodes of sigma activity (9-15 Hz), which correspond to the presence of sleep spindles. Color calibration of the spectrogram is not shown. B. Normalized power (NP) of S1 (green) and V1 (red) cortices for low (upper traces) and high (lower traces) gamma bands are shown. C. Normalized z'-coherence (NC) for both gamma bands (30-48 and 52-98 Hz). D. Power-coherence difference function (NP-NC) discriminates between REM sleep with positive values and the rest of states with zero or negative values. All the parameters were analyzed in 10 second epochs. W, wakefulness; SL1, light sleep; SL2, slow wave sleep; REM, REM sleep.

Table 1. Normalized power during sleep and wakefulness in the rat.

		Descriptive Statistics (NP)			Repeated measures ANOVA		Multiple Comparisons-Tukey		
Band	Electrode	W (mean ± SD)	NREM (mean ± SD)	REM (mean ± SD)	F	Sig. (p)	W vs NREM (p)	W vs REM (p)	REM vs NREM (p)
LG	OBr	1.0 ± 0.0	0.48 ± 0.05	0.84 ± 0.10	142.7	**<0.001**	**<0.001**	**< 0.001**	**<0.001**
	M1l	0.89 ± 0.13	0.51 ± 0.11	0.98 ± 0.03	70.9	**<0.001**	**<0.001**	0.122	**<0.001**
	M1r	0.89 ± 0.12	0.52 ± 0.08	0.97 ± 0.04	71.3	**<0.001**	**<0.001**	0.130	**<0.001**
	S1l	0.86 ± 0.15	0.64 ± 0.18	0.95 ± 0.07	13.9	**<0.001**	**0.007**	0.263	**<0.001**
	S1r	0.91 ± 0.15	0.71 ± 0.16	0.96 ± 0.06	12.1	**<0.000**	**0.004**	0.691	**<0.001**
	V2l	1.0 ± 0.0	0.57 ± 0.18	0.81 ± 0.13	38.1	**<0.000**	**<0.000**	**0.003**	**<0.000**
	V2r	0.98 ± 0.03	0.57 ± 0.14	0.78 ± 0.13	36.3	**<0.000**	**<0.000**	**0.001**	**0.001**
HG	OBl	1.0 ± 0.0	0.32 ± 0.10	0.44 ± 0.12	190.1	**<0.001**	**<0.001**	**< 0.001**	**0.001**
	M1r	0.99 ± 0.01	0.33 ± 0.08	0.77 ± 0.16	69.8	**<0.001**	**<0.001**	**0.003**	**<0.001**
	M1l	0.99 ± 0.01	0.36 ± 0.10	0.78 ± 0.12	98.6	**<0.001**	**<0.001**	**< 0.001**	**<0.001**
	S1r	0.99 ± 0.01	0.49 ± 0.10	0.87 ± 0.08	106.3	**<0.001**	**<0.001**	**0.007**	**<0.001**
	S1l	0.99 ± 0.00	0.53 ± 0.09	0.89 ± 0.06	129.1	**<0.001**	**<0.001**	**0.008**	**<0.001**
	V2r	0.99 ± 0.02	0.45 ± 0.15	0.74 ± 0.19	46.8	**<0.001**	**<0.001**	**0.001**	**<0.001**
	V2d	0.99 ± 0.01	0.38 ± 0.17	0.63 ± 0.27	35.4	**<0.001**	**<0.001**	**< 0.001**	**0.011**

The analysis was performed in 9 animals. The degrees of freedom were 2 (between groups) and 16 (within groups). OB, olfactory bulb; M1, primary motor cortex; S1, primary somatosensory cortex; V2, secondary visual cortex r, right; l, left. W, wakefulness; NREM, non-REM sleep; REM, REM sleep. *, $p < 0.05$.

Table 2. LG normalized coherence during sleep and wakefulness in the rat.

	Descriptive Statistics (NC)			Repeated measures ANOVA		Multiple Comparisons-Tukey		
Electrode pairs	W (mean ± SD)	NREM (mean ± SD)	REM (mean ± SD)	F	Sig. (p)	W vs SWS (p)	W vs REM (p)	REM vs NREM (p)
OBr-M1r	0.91 ± 0.09	0.86 ± 0.12	0.92 ± 0.07	0.9	0.409	0.506	0.994	0.449
OBr-M1l	0.93 ± 0.08	0.86 ± 0.12	0.93 ± 0.07	1.6	0.225	0.285	0.999	0.289
OBr-S1r	0.93 ± 0.07	0.79 ± 0.17	0.82 ± 0.16	2.2	0.135	0.138	0.281	0.898
OBr-S1l	0.93 ± 0.07	0.79 ± 0.15	0.85 ± 0.14	2.4	0.121	0.105	0.401	0.674
OBr-V2r	0.93 ± 0.09	0.90 ± 0.07	0.81 ± 0.16	2.4	0.120	0.870	0.119	0.272
OBr-V2l	0.90 ± 0.09	0.96 ± 0.06	0.83 ± 0.12	4.2	**0.033**	0.370	0.304	**0.025**
M1r-M1l	0.98 ± 0.02	0.95 ± 0.05	0.81 ± 0.09	17.4	**< 0.001**	0.480	**< 0.001**	**0.001**
M1r-S1r	0.98 ± 0.03	0.90 ± 0.05	0.91 ± 0.06	4.4	**0.030**	**0.041**	0.066	0.965
M1r-S1l	0.97 ± 0.04	0.90 ± 0.09	0.80 ± 0.09	11.8	**< 0.001**	0,105	**< 0.001**	**0.042**
M1r-V2r	0.94 ± 0.09	0.94 ± 0.06	0.69 ± 0.12	17.7	**< 0.001**	0,991	**< 0.001**	**< 0.001**
M1r-V2l	0.88 ± 0.08	0.99 ± 0.01	0.68 ± 0.10	31.7	**< 0.001**	**0.031**	**< 0.001**	**< 0.001**
M1l-S1l	0.97 ± 0.03	0.88 ± 0.05	0.92 ± 0.07	4.6	**0.025**	**0.019**	0.275	0.333
M1l-V2l	0.85 ± 0.09	0.99 ± 0.01	0.66 ± 0.11	35.3	**< 0.001**	**< 0.001**	**< 0.001**	**< 0.001**
S1r-M1l	0.98 ± 0.03	0.93 ± 0.06	0.79 ± 0.09	20.4	**< 0.001**	0.296	**< 0.001**	**< 0.001**
S1r-S1l	0.94 ± 0.06	0.97 ± 0.03	0.79 ± 0.10	17.7	**< 0.001**	0.682	**< 0.001**	**< 0.001**
S1r-V2l	0.69 ± 0.13	1.0 ± 0.0	0.59 ± 0.12	77.9	**< 0.001**	**< 0.001**	**0.020**	**< 0.001**
V2r-M1l	0.89 ± 0.13	0.96 ± 0.05	0.73 ± 0.17	8.41	**0.003**	0.544	**0.027**	**0.003**
V2r-S1l	0.77 ± 0.13	1.0 ± 0.0	0.63 ± 0.17	27.1	**< 0.001**	**< 0.001**	**0.041**	**< 0.001**
V2r-V2l	0.61 ± 0.09	1.0 ± 0.0	0.55 ± 0.12	91.4	**< 0.001**	**< 0.001**	0.269	**< 0.001**
S1l-V2l	0.81 ± 0.11	1.0 ± 0.0	0.71 ± 0.06	50.1	**< 0.001**	**< 0.001**	**0.005**	**< 0.001**
S1r-V2r	0.81 ± 0.13	0.98 ± 0.03	0.75 ± 0.15	11.7	**< 0.001**	**0.009**	0.443	**< 0.001**

The analysis was performed in 9 animals. The degrees of freedom were 2 (between groups) and 16 (within groups). OB, olfactory bulb; M1, primary motor cortex; S1, primary somatosensory cortex; V2, secondary visual cortex r, right; l, left. W, wakefulness; NREM, non-REM sleep; REM, REM sleep. *, $p < 0.05$.

electrode combinations showed the opposite pattern. In adition, NC during W was higher than during REM sleep for eleven combinations while in REM sleep NC was lower than during NREM sleep in fourteen electrode combinations. Interestingly, LG coherence between most of the OB and neocortical combinations were not modified across behavioral states.

For HG, NC also displayed significant differences across behavioral states for nineteen out of twenty-one combinations (Table 3). Coherence was higher during W than during NREM sleep in eighteen combinations, and higher than during REM sleep in nineteen combinations. REM sleep showed lower NC than during NREM sleep in nine combinations of cortical electrodes.

Mean global gamma activity during sleep and wakefulness in the rat: Figure 4A illustrates the MGP, MGC and their difference in nine rats, during the W and sleep. Gamma MGP showed significant differences across behavioral states (LG, $F_{2,16}$= 58.1, $p < 0.001$; HG, $F_{2,16}$= 178.1, $p < 0.001$). Figure 4A reveals that LG MGP did not present significant differences between W and REM sleep. Both during W and REM sleep, LG MGP was higher than during NREM sleep. On the other hand, HG MGP was highest during W, had an intermediate value during REM sleep and reached the minimum value during NREM sleep.

There was a significant difference in MGC across behavioral states (LG, $F_{2,16}$= 26.6, $p < 0.001$; HG, $F_{2,16}$= 86.7, $p < 0.001$). Figure 4B shows that LG MGC did not present significant differences between W and NREM sleep. The lowest values of low and high gamma coherence were present during REM sleep (Figure 4B).

NP-NC was significantly different for low and high gamma bands (LG, $F_{2,16}$= 97.1, $p < 0.001$; HG, $F_{2,16}$= 55.3, $p < 0.001$). During W, the

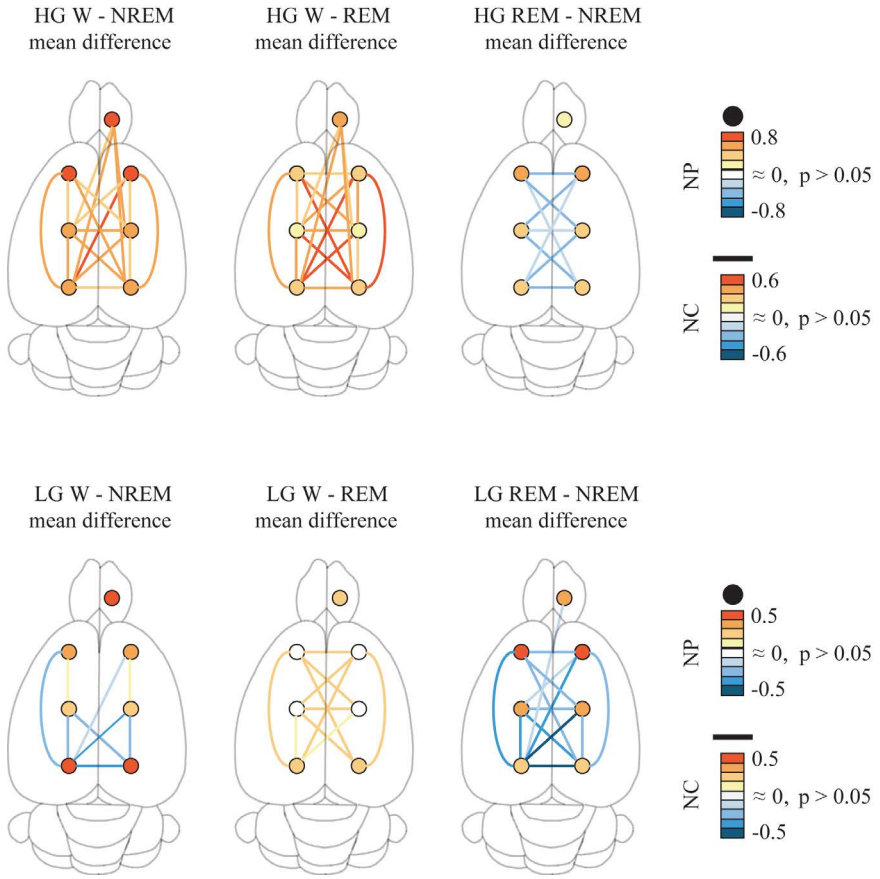

Figure 3. Low (LG) and high gamma (HG) band power and coherence in the rat. Summary of the statistically significant differences between behavioral states of the LG and HG normalized power (NP) and normalized coherence (NC) over the surface of the cerebral cortex. The circles represent the power for the different cortical regions, while the lines represent the coherence for the different combinations of electrodes. The colors represent the mean difference level of NP and NC. Data were obtained from the mean values of all available, non-transitional artifact-free windows per rat for each behavioral state (9 rats). Repeated mesures ANOVA and Tukey paired comparisons tests. OB, olfactory bulb; M1, primary motor cortex; S1, primary somato-sensory cortex; secondary V2, visual cortex.

Table 3. HG normalized coherence during sleep and wakefulness in the rat.

	Descriptive Statistics (NC)			**Repeated measures ANOVA**		**Multiple Comparisons-Tukey**		
Electrode pairs	W (mean ± SD)	NREM (mean ± SD)	REM (mean ± SD)	F	Sig. (p)	W vs SWS (p)	W vs REM (p)	REM vs NREM (p)
OBr-M1r	0.93 ± 0.10	0.76 ± 0.16	0.83 ± 0.16	2.9	0.081	0.0686	0.363	0.580
OBr-M1l	0.93 ± 0.09	0.77 ± 0.12	0.84 ± 0.16	3.5	0.055	0.044	0.325	0.495
OBr-S1r	0.96 ± 0.11	0.64 ± 0.21	0.67 ± 0.22	8.7	**0.002***	**0.004***	**0.008***	0.955
OBr-S1l	0.95 ± 0.13	0.67 ± 0.15	0.72 ± 0.21	6.9	**0.006***	**0.008***	**0.028***	0.806
OBr-V2r	1.0 ± 0.0	0.57 ± 0.19	0.57 ± 0.27	22.1	**< 0.001***	**< 0.001***	**< 0.001***	0.997
OBr-V2l	1.0 ± 0.0	0.60 ± 0.12	0.56 ± 0.18	39.6	**< 0.001***	**< 0.001***	**< 0.001***	0.676
M1r-M1l	0.98 ± 0.03	0.92 ± 0.11	0.74 ± 0.13	12.7	**< 0.001***	0.510	**< 0.001***	**0.005***
M1r-S1r	1.0 ± 0.0	0.72 ± 0.08	0.68 ± 0.08	56.1	**< 0.001***	**< 0.001***	**< 0.001***	0.361
M1r-S1l	0.99 ± 0.01	0.79 ± 0.12	0.63 ± 0.11	38.8	**< 0.001***	**< 0.001***	**< 0.001***	**0.004***
M1r-V2r	0.98 ± 0.05	0.57 ± 0.14	0.52 ± 0.22	26.5	**< 0.001***	**< 0.001***	**< 0.001***	0.805
M1r-V2l	1.0 ± 0.0	0.54 ± 0.12	0.43 ± 0.10	116.5	**< 0.001***	**< 0.001***	**< 0.001***	**0.010***
M1l-S1l	1.0 ± 0.0	0.79 ± 0.08	0.78 ± 0.07	36.4	**< 0.001***	**< 0.001***	**< 0.001***	0.967
M1l-V2l	0.99 ± 0.03	0.59 ± 0.16	0.50 ± 0.13	51.1	**< 0.001***	**< 0.001***	**< 0.001***	0.203
S1r-M1l	1.0 ± 0.0	0.77 ± 0.09	0.56 ± 0.10	89.1	**< 0.001***	**< 0.001***	**< 0.001***	**< 0.001***
S1r-S1l	1.0 ± 0.0	0.68 ± 0.09	0.56 ± 0.04	148.5	**< 0.001***	**< 0.001***	**< 0.001***	**< 0.001***
S1r-V2l	0.98 ± 0.03	0.68 ± 0.17	0.52 ± 0.16	36.6	**< 0.001***	**< 0.001***	**< 0.001***	**0.032***
V2r-M1l	1.0 ± 0.0	0.57 ± 0.15	0.46 ± 0.13	88.4	**< 0.001***	**< 0.001***	**< 0.001***	**0.045***
V2r-S1l	1.0 ± 0.0	0.60 ± 0.16	0.45 ± 0.13	82.3	**< 0.001***	**< 0.001***	**< 0.001***	**0.007***
V2r-V2l	1.0 ± 0.0	0.74 ± 0.16	0.56 ± 0.18	38.4	**< 0.001***	**< 0.001***	**< 0.001***	**0.008***
S1l-V2l	1.0 ± 0.0	0.67 ± 0.12	0.67 ± 0.12	44.9	**< 0.001***	**< 0.001***	**< 0.001***	0.980
S1r-V2r	0.96 ± 0.10	0.76 ± 0.11	0.74 ± 0.13	7.9	**0.004***	**0.013***	**0.006***	0.927

The analysis was performed in 9 animals. The degrees of freedom were 2 (between groups) and 16 (within groups). OB, olfactory bulb; M1, primary motor cortex; S1, primary somato-sensory cortex; V2, secondary visual cortex r, right; l, left. W, wakefulness; NREM, non-REM sleep; REM, REM sleep. *, $p < 0.05$.

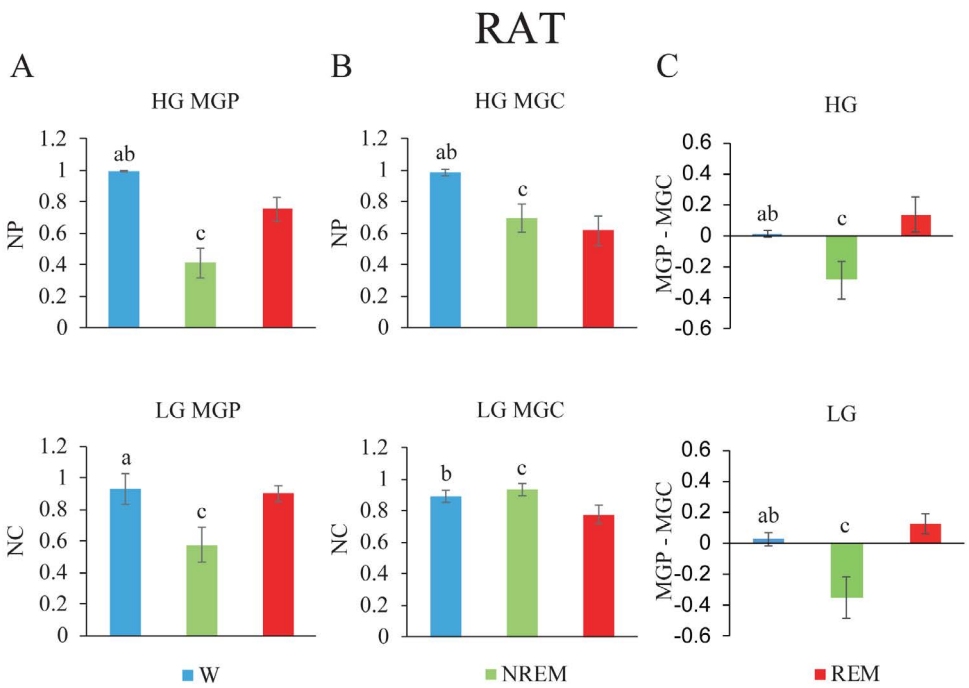

Figure 4. Gamma band mean global power (MGP), mean global coherence (MGC) and their normalized difference during wakefulness and sleep in the rat. A. Low gamma (lower) and high gamma (upper) MGP. B. MGC is depicted. C. Power-coherence difference (NP-NC). The values represent the mean ± standard deviation. Repeated measures ANOVA and Tamhane tests. a, W vs NREM sleep, $p < 0.05$; b, W vs REM sleep, $p < 0.05$; c, NREM sleep vs REM sleep, $p < 0.05$.

value was close to zero, it was negative during NREM sleep and positive during REM sleep (Figure 4C).

Gamma activity in cats

Dynamics of gamma activity in the cat: The dynamic changes in gamma activity in a representative cat are exhibited in Figure 5. The spectrograms and hypnograms of Figure 5A, reflect the different behavioral states of the animal. The NP for the low and high gamma bands was modified along the W-sleep cycle (Figure 5B). Pre-frontal (Pf) and parietal posterior (Pp) NP were highest during AW and decreased progressively during the transition to QW and NREM sleep. During REM sleep, there was a clear increase in the low and high gamma NP in both cortices.

We also analyzed the dynamic changes in gamma NC between Pf and Pp electrodes across behavioral states (Figure 5C). Low and high gamma NC were highest during AW and decreased during QW and NREM sleep to an intermediate value. In contrast to the NP, low and high gamma coherence during REM sleep decreased to its lowest level.

When the NP-NC function was applied (Figure 5D), during AW and QW NP-NC values were close to zero, they decreased to negatives values during NREM sleep, and inverted to positive values during REM sleep.

Gamma activity during sleep and wakefulness in the cat: The analysis in the cat was limited to two cortical areas (anterior and posterior) of the same hemisphere. In cats, the mean NP of the gamma band was different across behavioral states (LG, $F_{2,10}$= 132.1, $p < 0.001$; HG Hz, $F_{2,10}$= 36.9, $p < 0.001$). Figure 6A shows that low and high gamma band power was significantly higher during W than during other states. The minimum level of power was recorded during NREM sleep and reached intermediate values during REM sleep.

These animals showed significant differences in the NC (LG, $F_{2,10}$= 46.8, $p < 0.001$; HG, $F_{2,10}$= 56.1, $p < 0.001$) (Figure 6B). During W, low and high gamma coherence was greater and significantly different compared to the rest of the behavioral states. The lowest values for LG and HG coherence were present during REM sleep.

NP-NC was calculated in the cat. NP-NC was significantly different for the low and high gamma bands across behavioral states (LG Hz, $F_{2,10}$= 19.7, $p < 0.001$; HG, $F_{2,10}$= 38.3, $p < 0.001$) (Figure 6C). During W, NP-NC in LG and HG was nearly zero, while in NREM sleep it presented negative values. Positive values were observed during REM sleep.

Gamma activity during REM sleep transitions: For an in-depth examination of the transitions (t) into and from REM sleep, we analyzed the mean gamma power and mean z'-coherence in 10-second windows in cats (Figure 7) and rats (Figure 8). In both animal models, REM sleep onset was accompanied by a reduction in low and high gamma z'-coherence (Figures 7A and 8A, upper charts). Interestingly, this reduction in gamma coherence tended to precede REM sleep onset by several seconds; we considered EEG activation (desynchronization) as the beginning of REM sleep (time 0). In contrast, at the end of REM sleep episode, z'-coherence increased (Figures 7B and 8B, upper charts).

Low and high gamma power increased during REM sleep onset (Figures 7A and 8A, lower charts). At the end of the REM sleep episodes, on average there was an increase in gamma power (reflecting W) that was followed by a decrease in this parameter (probably driven by NREM sleep) (Figures 7B and 8B, lower charts). A short bout of W (microarousal) followed by NREM sleep, or a sustained period of W, usually followed REM sleep episodes. This phenomenon could determine a more variable low and high gamma power following REM sleep episodes.

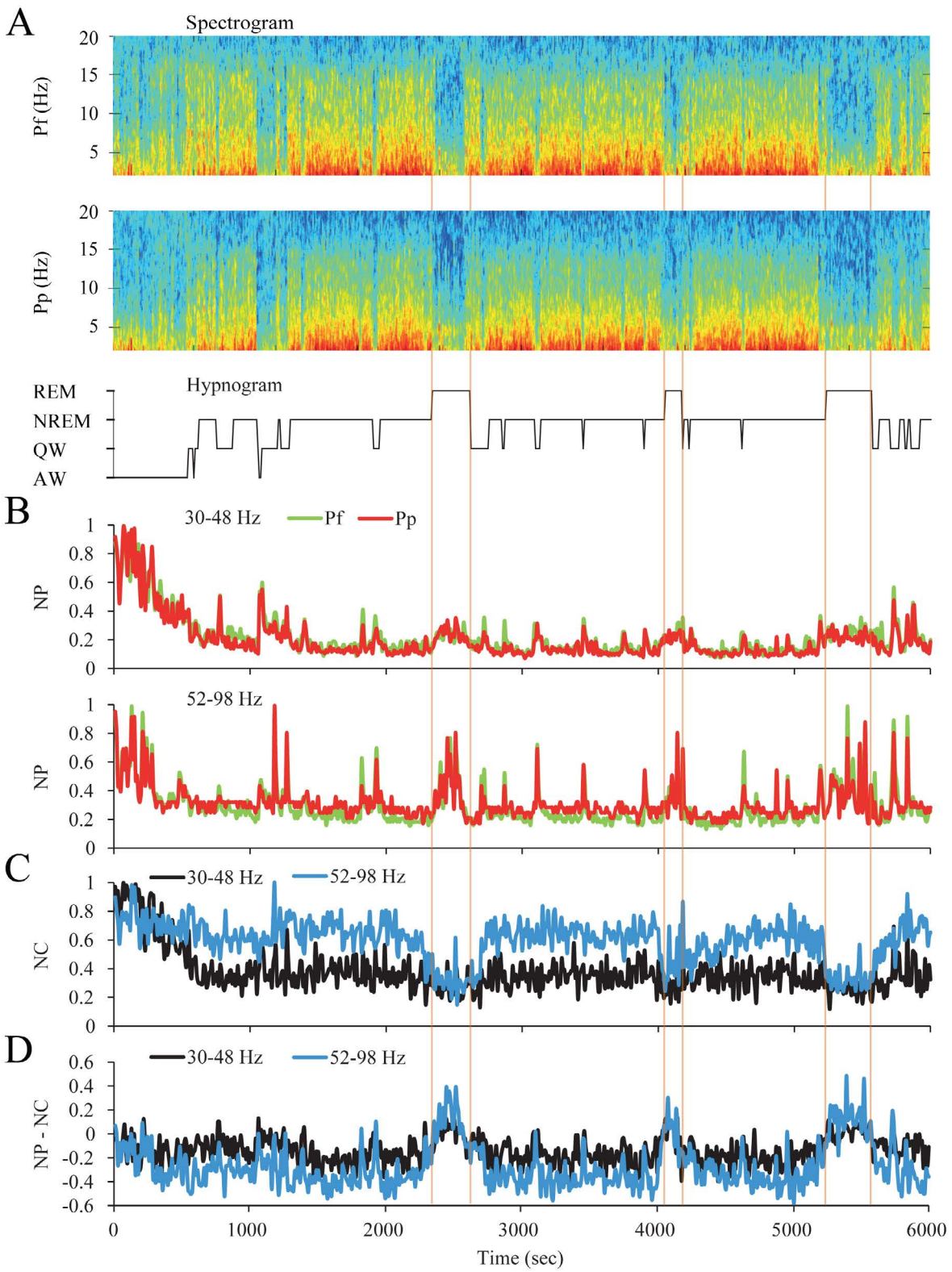

Figure 5. Dynamics of gamma activity in the cat. A. The spectrograms (1-20 Hz) of prefrontal (Pf) and posterior parietal (Pp) cortical recordings and the hypnogram are shown. During W and REM sleep there was weak slow wave activity. During NREM sleep, delta activity (0.5-4 Hz) was more prominent and there were intermittent episodes of sigma activity (9-15 Hz), which correspond to the presence of sleep spindles. Color calibration of the spectrogram is not shown. B. Normalized power (NP) of Pf (green) and Pp (red) cortices for low (upper traces) and high (lower traces) gamma bands are shown. C. Normalized z'-coherence (NC) for both gamma bands (30-48 and 52-98 Hz). D. Power-coherence difference representation (NP-NC) shows near zero values for AW and QW, negative values during NREM sleep and inversion to positives values during REM sleep. All the parameters were analyzed in 10 seconds epochs. AW, alert wakefulness; QW, quiet wakefulness; NREM, NREM sleep; REM, REM sleep.

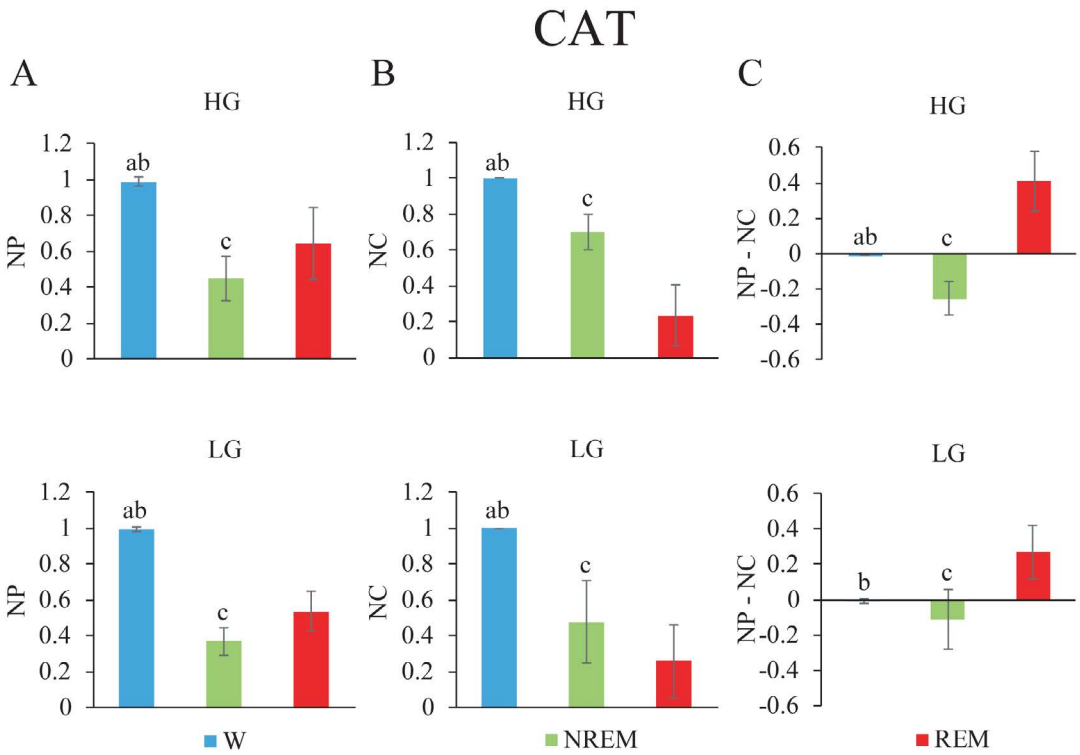

Figure 6. Gamma band normalized power (NP), normalized coherence (NC) and their normalized difference during wakefulness and sleep in the cat. A. Low gamma (lower) and high gamma (upper) mean NP of frontal (f) and posterior (p) electrodes. B. NC between both channels f and p are depicted. C. Power-coherence difference (NP-NC). The values represent the mean ± standard deviation. Repeated measures ANOVA and Tamhane tests. a, W vs NREM sleep, $p < 0.05$; b, W vs REM sleep, $p < 0.05$; c, NREM sleep, vs REM sleep, $p < 0.05$.

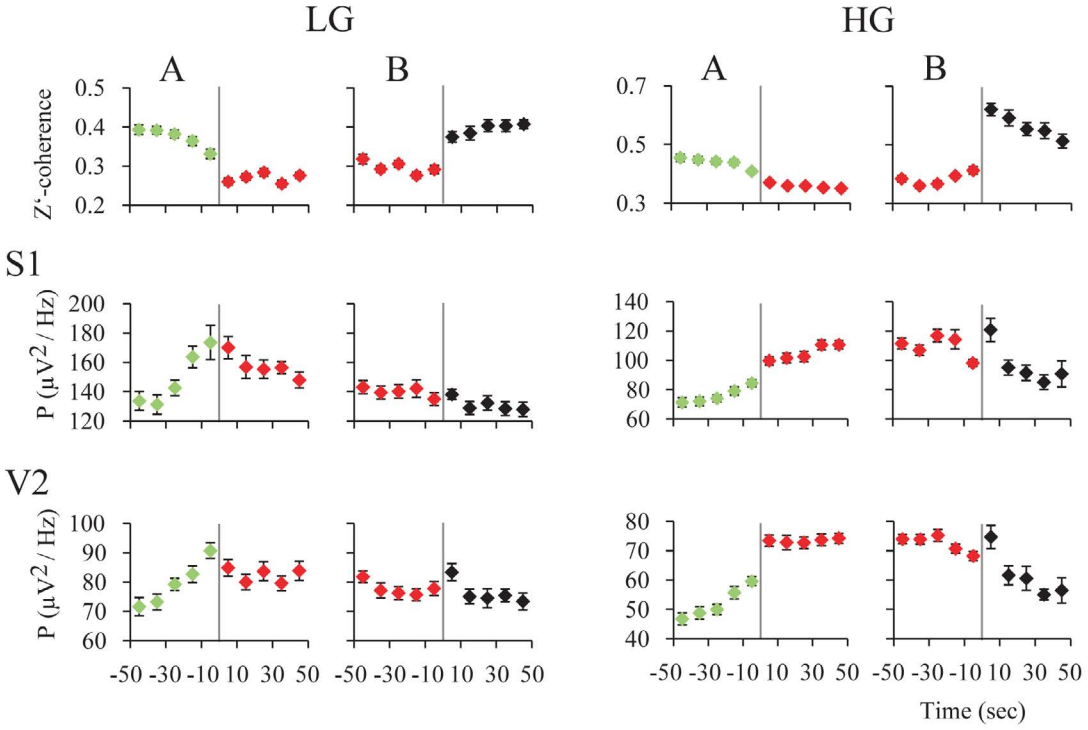

Figure 7. z'-coherence and power during REM sleep transitions in the rat. A. Transition into REM sleep. The graphics depict the mean z'-coherence and power ± standard error for 30-48 and 52-98 Hz, of 30 transitions of one representative rat. Data were taken from recordings of primary somatosensory (S1) and secondary visual (V2) cortices. Change of colors and the vertical line indicate the phase transition. NREM sleep episodes are symbolized in green; REM sleep episodes in red. B. Transition out of REM sleep. The mean z'-coherence and power ± standard error for 30-48 and 52-98 Hz, of 30 transitions of the same rat are shown. Red to black transition indicates the end of the REM sleep episode. The states indicated in black were mainly micro-awakenings but some NREM sleep episodes also followed REM sleep.

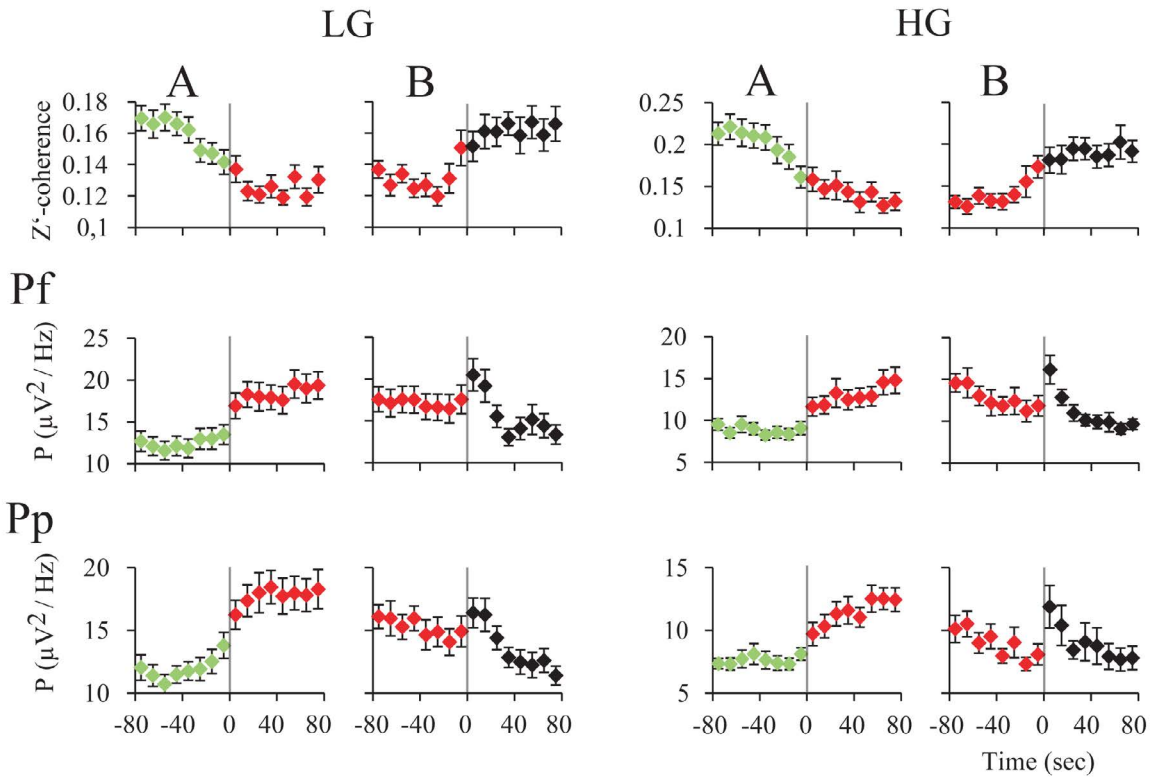

Figure 8. z'-coherence and power during REM sleep transitions in the cat. A. Transition into REM sleep. The graphics represent the mean z'-coherence and power ± standard error for 30-48 and 52-98 Hz, of 30 transitions of one representative cat. Data were taken from recordings of prefrontal (Pf) and posterior parietal (Pp) cortices. Change of colors and the vertical line indicate the phase transition. NREM episodes are symbolized in green; REM sleep episodes in red. B. Transition out of REM sleep. The mean z'-coherence and power ± standard error for 30-48 and 52-98 Hz, of 30 transitions of the same cat are shown. Red to black transition indicates the end of the REM sleep episode. The states indicated in black were mainly micro-awakenings but some NREM sleep episodes also followed REM sleep.

The main relationships during W and sleep between gamma power, reflecting local or short-range synchronization, and gamma coherence, representing distant or large-range coupling, is schematized in Figure 9. High short (local) and long-range (distant) gamma coupling is present during W. In contrast, high local gamma synchronization with long-range gamma uncoupling is present during REM sleep.

Discussion

In the present study, we performed a thorough analysis of gamma power and coherence in rat neocortical areas and OB; and we also performed a more spatially-limited analysis in the cat. The main result of this report is the demonstration in two different animal models (rats and cats), that during REM sleep there was a strong local (short-range) synchronization of the neural population in both gamma (30-48 and 52-98 Hz) frequency bands, while this synchronization was strongly reduced between distant areas. These data suggest that during REM sleep, in spite of a local activated state, high-frequency functional interactions between different cortical regions are lost (or highly diminished).

The relationship between local and distant gamma synchronization was further explored utilizing the gamma NP-NC function as an index (Figures 4 and 6). This index reflects the difference between the normalized power (reflecting local or short-range synchronization) and normalized coherence (distant areas or long-range synchronization); which was close to zero during W, consisted of negative values during NREM sleep, while positive values were found during REM sleep. Therefore, this index of gamma activity was capable of differentiating between W, NREM sleep, and REM sleep both in cats and rats.

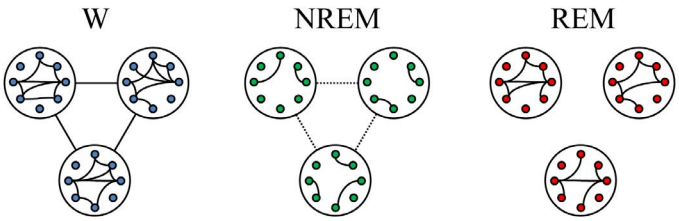

Figure 9. Schematic representation of the short and long-range gamma synchronization during wakefulness (W), NREM sleep and REM sleep. The small circles represent neurons while large circles represent the areas of the cortex where these neurons are located. Colors of neurons represent the behavioral states (blue, W; green, NREM sleep; red, REM sleep) and connecting lines between the circles represent gamma synchronization between distant cortical areas. Short-range (local) and long-range (distant) gamma synchronization occurs during W. During NREM sleep both short and long-range gamma synchronization decrease. During REM sleep, while gamma synchronization is present at local level, distant gamma coupling is absent.

Gamma power and coherence during wakefulness and NREM sleep

It is well established that gamma power and gamma intra-hemispheric coherence is high during W in cats, rats, and humans [21-23,25,39,44]. In the cat, gamma band coherence increases during alert W; a fact that can be clearly observed in raw recordings [39]. Gamma coherence is also high during cataplexy (W with REM sleep atonia) induced by carbachol microinjections into the nucleus pontis oralis (NPO) of the cat [41].

In the present report, we extend previous data in rats [23], showing the cortical extent of gamma power and coherence. As shown in Figure 3, low and high gamma power is higher in W than in NREM sleep and

REM sleep in most of the neocortical areas and OB. The exemption was that low gamma power during W and REM sleep was similar in frontal and parietal cortices (Figure 3).

Coherence for high gamma during W was higher than during NREM sleep and REM sleep across all the combinations of cortical loci. However, low gamma coherence differences between W and NREM sleep varied between different cortices (Figure 4) [23].

Gamma power and coherence during REM sleep

In the present report, we demonstrated in rats and cats that gamma coherence reached a nadir during REM sleep. In the rat, high and low gamma coherence decreased in most combinations of electrodes in comparison to W and NREM sleep (Figure 3). However, the power in this frequency band increased compared to NREM sleep. This power-coherence relationship was also readily observed in the dynamic analysis (Figures 2 and 5), as well as in the transition into and out REM sleep (Figure 7 and 8).

This result is in accordance with the results of our previous analyses in cat [39] and rat [23]. Interestingly, gamma coherence is also lost during REM sleep induced by carbachol microinjections into the NPO of the cat [41].

In preliminary studies in human newborns, cortical gamma coherence was almost absent during REM sleep [45]. The demonstration that there is a reduction in gamma coherence between different cortical regions during REM sleep was also shown in adult humans [20,33,46]. In addition, Voss et al. (2009) demonstrated that gamma coherence during lucid dreaming was intermediate between W and REM sleep [33].

As with other EEG rhythms, gamma oscillations remain remarkably conserved in mammals irrespective of brain size [47]. The decrease in gamma coherence during REM sleep in rats, cats and humans, indicates that during this behavioral state there is a decrease in the capacity for integration across different cortices within this high frequency band, despite high local activity at these frequencies.

A recent study demonstrated that scalp fronto-temporal electrical stimulation in the lower gamma band (≈40 Hz) during REM sleep influences ongoing brain activity and induces self-reflective awareness (a feature of W) in dreams (i.e., lucid dreams), while other stimulation frequencies were not effective [32]. Thus, the data support the concept that synchronous long-range oscillations of ≈40 Hz are an electrophysiological pattern of activity that is indicative of attentive wakefulness. On the contrary, the reduction in gamma coherence during REM sleep together with increased local gamma activity (accompanied by a decrease in low frequency activity), may underlie the unique pattern of REM sleep mentation, i.e., dreams [17,18,48]. During NREM sleep the decrease in local and a small reduction in distant gamma coupling accompanied by an increase in low frequency oscillations (delta waves) and sleep spindles, may be the neurophysiological foundation for the reduction or absence of oneiric activity during deep NREM sleep. Interestingly, Siclari *et al.*, (2017) have demonstrated that reports of dream experience in either REM sleep and NREM sleep were associated with decreases in delta power and increases in gamma power (25-50 Hz) mainly in posterior cortical regions [48].

Gamma power and coherence in the OB during W and sleep

It is well established that local slow field potentials in the OB are associated with breathing, and these oscillations would aid in the exchange of information between olfactory areas and other parts of the brain [49-51]. These respiratory potentials in the OB reflect respiratory rhythms during W and REM sleep, but not during NREM sleep [52], and entrain gamma oscillations in the OB as well as in other areas of the brain [11,14,15,53].

Our data show that in the OB, the maximum gamma power is present during W, decreases during NREM sleep, and increases to intermediate values during REM sleep. LG coherence between OB and most neocortical areas did not differ across behavioral states (Figure 3 and Table 2). However, HG coherence between the OB and medial and posterior areas of neocortex was higher during W than sleep (Figure 3 and Table 3). New studies are needed to shed light in the functional interrelation between the OB and neocortical areas during W and sleep.

Gamma coherence and the waking-promoting systems

Cognitive activity and different EEG rhythms are generated by the activity of cortical and thalamic neurons, which are reciprocally connected [29,54]. Gamma-band rhythmogenesis is also inextricably tied to perisomatic inhibition in the neocortex, wherein the key ingredient is $GABA_A$ receptor-mediated inhibition [12]. However, both neocortical gamma power and coherence during W and sleep are modulated by the activating or waking-promoting systems of the brainstem, hypothalamus and basal forebrain that directly or indirectly project to the thalamus and/or cortex [55,56]. By regulating thalamo-cortical activities, these activating systems produce electrographic and behavioral arousal.

The activating systems decrease their activity during the NREM sleep. However, the activity of the various components of these systems differs markedly during REM sleep. While most monoaminergic systems decrease their firing rate during REM sleep (REM-off neurons), cholinergic neurons increase their discharge during this behavioral state (REM-on neurons), which contributes to the cortical activation [55,56]. Therefore, it is expected that cholinergic REM-on neurons, whose soma are located in the mesopontine and basal forebrain region, may contribute in the promotion of local gamma synchronization (gamma power). In addition, because these cholinergic neurons turn on during REM sleep, they should not be critical to the generation of gamma coherence (distant coupling), which is absent during this state. In fact, systemic muscarinic antagonists do not block gamma coherent activity [57].

Noradrenergic, serotonergic and histaminergic neurons that are active during W [55,56], may be crucial in promoting gamma coherence during this behavioral state. Their lack of activity during REM sleep may be involved in the absence of gamma coherence during this state.

Other neuronal systems, such as hypocretinergic and dopaminergic neurons that are active during W, as well as GABAergic or glutamatergic neurons which are located in the mesopontine reticular formation and basal forebrain, may also contribute to the profile of gamma activity during W and sleep [55,56]. In fact, Kim *et al.*, [58], highlighted the role of cortical-projecting GABAergic neurons of the basal forebrain in the generation of gamma oscillations in the EEG [58]. In addition, the authors suggest that cholinergic neurons within this area are not critical for the generation of these oscillations.

It is important to note that firing within the gamma band range is present in different sites of the reticular activating system, including the pedunculo-pontine tegmental nucleus (PPN) [59]. In this area, gamma oscillations are modulated by two independent pathways related to different Ca2+ channel types which suggests different ways

of modulating waking and REM sleep [60,61]. This subcortical gamma activity possibly contribute to "bottom up" neocortical gamma activity during W and REM sleep [62].

Local and distant gamma coupling relationship

The NP-NC index clearly shows that short and long-range gamma synchronization is deeply modified across behavioral states; this fact is illustrated in the model presented in Figure 9. As discussed above, this electrophysiological phenomenon could be related to the cognitive features that characterize W, NREM sleep and REM sleep. Moreover, NREM sleep and REM sleep dream content, and different drugs or processes that affect cognition, must all modify the NP-NC index. We hypothesize that dissociative drugs such as ketamine, or psychiatric conditions such as psychosis, will also increase the index values as in REM sleep. Finally, this NP-NC index, that signals the presence of REM sleep, should be applied to confirm the absence of REM sleep in aquatic mammals, that for its obligate swimming behavior during sleep do not have REM sleep atonia [63-65].

Conclusions

During REM sleep, despite a locally activated EEG, there is uncoupling of gamma frequency oscillations between distant neocortical sites. In spite of regional variations, this gamma activity pattern extends, in rats, from the posterior cortices to the OB. Therefore, although local gamma coupling is similar to W, functional interactions among different cortical area, which are critical for cognitive functions, are radically different during REM sleep. Since this feature is conserved in rats, cats and likely in humans, we consider that this short-range gamma coupling along with gamma long-range uncoupling during REM sleep is a defining trait of REM sleep in mammals.

Acknowledgement

This study was partially supported by a grant of the Comisión Sectorial de Investigación Científica (CSIC) and the "Programa de Desarrollo de Ciencias Básicas, PEDECIBA". S. Castro, A. Mondino and M. Cavelli currently have a postgraduate fellowship from the Agencia Nacional de Investigación en Innovación (ANII) and Comisión de Apoyo a Postgrados (CAP), respectively.

Competing interests

All the authors declare no conflict of interest.

Author contributions

Financial support. P.T., A.F., M.C.

Experimental design. M.C., P.T., S.CZ.

Experimental procedures. M.C., S.CZ., A.M., J.G., P.T.

Analysis of the data. M.C., S.CZ., A.M., J.G.

Discussion and interpretation of the data. M.C., P.T., S.CZ., A.M., J.G., A.F.

Wrote the manuscript. M.C., P.T.

All the authors participated in critical revision the manuscript, added important intellectual content, and approved the definitive version.

References

1. Singer W (2015) Complexity as Substrate for Neuronal Computations. Acad Sci. Pontif. City, Vatican. PP: 1-10.
2. Singer W (2007) Binding by synchrony. *Scholarpedia* 2: 1657.
3. von der Malsburg C, Schneider W (1986) A neural cocktail-party processor. *Biol Cybern* 54: 29-40. [Crossref]
4. von der Malsburg C (1995) Binding in models of perception and brain function. *Curr Opin Neurobiol* 5: 520-526. [Crossref]
5. Singer W (1999) Neuronal Synchrony?: A Versatile Code for the Definition of Relations?? Most of our knowledge about the functional organization. *Neuron* 24: 49-65.
6. Varela F, Lachaux JP, Rodriguez E, Martinerie J (2001) The brainweb: phase synchronization and large-scale integration. *Nat Rev Neurosci* 2: 229-239. [Crossref]
7. Eckhorn R, Bauer R, Jordan W, Brosch M, Kruse W, et al. (1988) Coherent oscillations: a mechanism of feature linking in the visual cortex? Multiple electrode and correlation analyses in the cat. *Biol Cybern* 60: 121-130. [Crossref]
8. Gray CM, König P, Engel AK, Singer W (1989) Oscillatory responses in cat visual cortex exhibit inter-columnar synchronization which reflects global stimulus properties. *Nature* 338: 334-337.
9. Fries P (2005) A mechanism for cognitive dynamics: neuronal communication through neuronal coherence. *Trends Cogn Sci* 9: 474-480. [Crossref]
10. Jasper HH, Andrews HL (1938) Brain potentials and voluntary muscle activity in man. *J Neurophysiol* 1: 87-100.
11. Adrian ED (1942) Olfactory reactions in the brain of the hedgehog. *J Physiol* 100: 459-473. [Crossref]
12. Buzsáki G, Wang XJ (2012) Mechanisms of gamma oscillations. *Annu Rev Neurosci* 35: 203-225. [Crossref]
13. Rieder MK, Rahm B, Williams JD, Kaiser J (2011) Human Î³-band activity and behavior. *Int J Psychophysiol* 79: 39-48. [Crossref]
14. Rojas-Líbano D, Kay LM (2008) Olfactory system gamma oscillations: the physiological dissection of a cognitive neural system. *Cogn Neurodyn* 2: 179-194.
15. Freeman WJ, Schneider W (1982) Changes in spatial patterns of rabbit olfactory EEG with conditioning to odors. *Psychophysiology* 19: 44-56. [Crossref]
16. Uhlhaas PJ, Pipa G, Lima B, Melloni L, Neuenschwander S, et al. (2009) Neural synchrony in cortical networks?: history , concept and current status. *Front Integr Neurosci* 3: 1-19.
17. Hobson JA (2009) REM sleep and dreaming: towards a theory of protoconsciousness. *Nat Rev Neurosci* 10: 803-813. [Crossref]
18. Nir Y, Tononi G (2010) Dreaming and the brain: from phenomenology to neurophysiology. *Trends Cogn Sci* 14: 88-100. [Crossref]
19. Gottesmann C (2006) The dreaming sleep stage: a new neurobiological model of schizophrenia? *Neuroscience* 140: 1105-1115. [Crossref]
20. Cantero JL, Atienza M, Madsen JR, Stickgold R (2004) Gamma EEG dynamics in neocortex and hippocampus during human wakefulness and sleep. *Neuroimage* 22: 1271-1280. [Crossref]
21. Llinás R, Ribary U (1993) Coherent 40-Hz oscillation characterizes dream state in humans. *Proc Natl Acad Sci U S A* 90: 2078-2081. [Crossref]
22. Maloney KJ, Cape EG, Gotman J, Jones BE (1997) High-frequency gamma electroencephalogram activity in association with sleep-wake states and spontaneous behaviors in the rat. *Neuroscience* 76: 541-555.
23. Cavelli M, Castro S, Schwarzkopf N, Chase MH, Falconi A, et al. (2015) Coherent neocortical gamma oscillations decrease during REM sleep in the rat. *Behav Brain Res* 281: 318-325.
24. Buzsáki G, Anastassiou CA, Koch C (2012) The origin of extracellular fields and currents--EEG, ECoG, LFP and spikes. *Nat Rev Neurosci* 13: 407-420. [Crossref]
25. Chrobak JJ, Buzsáki G (1998) Gamma oscillations in the entorhinal cortex of the freely behaving rat. *J Neurosci* 18: 388-398. [Crossref]
26. Bullock TH, McClune MC (1989) Lateral coherence of the electrocorticogram: a new measure of brain synchrony. *Electroencephalogr Clin Neurophysiol* 73: 479-498. [Crossref]
27. Bullock TH, McClune MC, Achimowicz JZ, Iragui-Madoz VJ, Duckrow RB, et al. (1995) Temporal fluctuations in coherence of brain waves. *Proc Natl Acad Sci U S A* 92: 11568-11572. [Crossref]

28. Cantero JL, Atienza M, Salas RM (2000) Valor clínico de la coherencia EEG como índice electrofisiológico de conectividad córtico-cortical durante el sueño. *Rev Neurol* 31: 442-454.

29. Llinás R, Ribary U, Contreras D, Pedroarena C (1998) The neuronal basis for consciousness. *Philos Trans R Soc Lond B Biol Sci* 353: 1841-1849. [Crossref]

30. Hadjipapas A, Hillebrand A, Holliday IE, Singh KD, Barnes GR (2005) Assessing interactions of linear and nonlinear neuronal sources using MEG beamformers: a proof of concept. *Clin Neurophysiol* 116: 1300-1313. [Crossref]

31. Melloni L, Molina C, Pena M, Torres, W. Singer, E. Rodriguez (2007) Synchronization of neural activity across cortical areas correlates with conscious perception. *J Neurosci* 27: 2858-2865.

32. Voss U, Holzmann R, Hobson A, Paulus W, Koppehele-Gossel J, et al. (2014) Induction of self awareness in dreams through frontal low current stimulation of gamma activity. *Nat Neurosci* PP: 1-5.

33. Voss U, Holzmann R, Tuin I, Hobson JA (2009) Lucid dreaming: a state of consciousness with features of both waking and non-lucid dreaming. *Sleep* 32: 1191-1200. [Crossref]

34. John ER (2002) The neurophysics of consciousness. *Brain Res Brain Res Rev* 39: 1-28. [Crossref]

35. Mashour GA (2006) Integrating the science of consciousness and anesthesia. *Anesth Analg* 103: 975-982. [Crossref]

36. Pal D, Silverstein BH, Lee H, Mashour GA (2016) Neural Correlates of Wakefulness, Sleep, and General Anesthesia: An Experimental Study in Rat. *Anesthesiology* 125: 929-942. [Crossref]

37. Uhlhaas PJ, Singer W (2010) Abnormal neural oscillations and synchrony in schizophrenia. *Nat Rev Neurosci* 11: 100-113. [Crossref]

38. Sun Y, Farzan F, Barr MS, Kirihara K, Fitzgerald PB, et al. (2011) Î³ oscillations in schizophrenia: mechanisms and clinical significance. *Brain Res* 1413: 98-114. [Crossref]

39. Castro-Zaballa S, Falconi A, Chase MH, Torterolo P (2013) Coherent neocortical 40-Hz oscillations are not present during REM sleep. *Eur J Neurosci* 37: 1330-1339.

40. Castro-Zaballa S, Cavelli M, Vollono P, Chase MH, Falconi A, et al. (2014) Inter-hemispheric coherence of neocortical gamma oscillations during sleep and wakefulness. *Neurosci Lett* 578: 197-202.

41. Torterolo P, Castro-Zaballa S, Cavelli M, Chase MH, Falconi A (2016) Neocortical 40 Hz oscillations during carbachol-induced rapid eye movement sleep and cataplexy. *Eur J Neurosci* 43: 580-589.

42. Bullock TH, Buzsáki G, McClune MC (1990) Coherence of compound field potentials reveals discontinuities in the CA1-subiculum of the hippocampus in freely-moving rats. *Neuroscience* 38: 609-619.

43. Benedetto L, Rodriguez-Servetti Z, Lagos P, D'Almeida V, Monti JM, et al. (2013) Microinjection of melanin concentrating hormone into the lateral preoptic area promotes non-REM sleep in the rat. *Peptides* 39: 11-15.

44. Steriade M, Amzica F, Contreras D (1996) Synchronization of fast (30-40 Hz) spontaneous cortical rhythms during brain activation. *J Neurosci* 16: 392-417.

45. Castro S, Cavelli M, Torterolo P, Falconi A, Rava M, et al. (2014) Congr Int Neuropediatría Colonia.

46. Pérez-Garci E, del-Río-Portilla Y, Guevara M, Arce C, Corsi-Cabrera M (2001) Paradoxical sleep is characterized by uncoupled gamma activity between frontal and perceptual cortical regions. *Sleep* 24: 118-126.

47. Buzsáki G, Logothetis N, Singer W (2013) Scaling brain size, keeping timing: Evolutionary preservation of brain rhythms. *Neuron* 80: 751-764.

48. Siclari F, Baird B, Perogamvros L, et al. (2017) The neural correlates of dreaming. *Nat Neurosci* 20: 872-878. [Crossref]

49. Rojas-Líbano D, Frederick DE, Egaña JI, Kay LM (2014) The olfactory bulb theta rhythm follows all frequencies of diaphragmatic respiration in the freely behaving rat. *Front Behav Neurosci* 8: 214.

50. Lockmann AL, Laplagne DA, Leão RN, Tort AB (2016) A Respiration-Coupled Rhythm in the Rat Hippocampus Independent of Theta and Slow Oscillations. *J Neurosci* 36: 5338-5352. [Crossref]

51. Nguyen Chi V, Muller C, Wolfenstetter T, Yanovsky Y, Draguhn A, et al. (2016) Hippocampal Respiration-Driven Rhythm Distinct from Theta Oscillations in Awake Mice. *J Neurosci* 36: 162-177.

52. Jessberger J, Zhong W, Brankack J, Draguhn A (2016) Olfactory Bulb Field Potentials and Respiration in Sleep-Wake States of Mice. *Neural Plast* 2016: 1-9.

53. Zhong W, Ciatipis M, Wolfenstetter T, Jessberger J, Müller C, et al. (2017) Selective entrainment of gamma subbands by different slow network oscillations. *Proc Natl Acad Sci U. S. A.*.

54. Llinás R, Ribary U (2001) Consciousness and the brain. The thalamocortical dialogue in health and disease. *Ann N Y Acad Sci* 929: 166-175. [Crossref]

55. Torterolo P, Vanini G (2010) [New concepts in relation to generating and maintaining arousal]. *Rev Neurol* 50: 747-758. [Crossref]

56. Torterolo P, Monti JM, Pandi-Perumal S (2016) Synposis Sleep Med., Apple Academic Press, pp. 1-22.

57. Castro s, Cavelli M, Falconi A, Torterolo P (2016) 23rd Congr Eur Sleep Res Soc Bol, Italy.

58. Kim T, Thankachan S, McKenna JT, McNally JM, Yang C, et al. (2015) Cortically projecting basal forebrain parvalbumin neurons regulate cortical gamma band oscillations. *Proc Natl Acad Sci* 201413625.

59. Garcia-Rill E, Luster B, D'Onofrio S, Mahaffey S, Bisagno V, et al. (2016) Implications of gamma band activity in the pedunculopontine nucleus. *J Neural Transm (Vienna)* 123: 655-665. [Crossref]

60. Luster B1, D'Onofrio S, Urbano F, Garcia-Rill E (2015) High-threshold Ca2+ channels behind gamma band activity in the pedunculopontine nucleus (PPN). *Physiol Rep* 3. [Crossref]

61. Luster br, Urbano FJ, Garcia-rill E (2016) Intracellular mechanisms modulating gamma band activity in the pedunculopontine nucleus (PPN). *Physiol Rep* 4: 1-16.

62. Garcia-Rill E (2017) Bottom-up gamma and stages of waking. *Med Hypotheses* 104: 58-62. [Crossref]

63. Lyamin OI, Kosenko PO, Lapierre JL, Mukhametov LM, Siegel JM (2008) Fur seals display a strong drive for bilateral slow-wave sleep while on land. *J Neurosci* 28: 12614-12621. [Crossref]

64. Lyamin OI, Manger PR, Ridgway SH, Mukhametov LM, Siegel JM (2008) Cetacean sleep: an unusual form of mammalian sleep. *Neurosci Biobehav Rev* 32: 1451-1484. [Crossref]

65. Madan V, Jha SK (2012) Sleep alterations in mammals: did aquatic conditions inhibit rapid eye movement sleep? *Neurosci Bull* 28: 746-758. [Crossref]

ANEXO 3.POTENCIA Y COHERENCIA DE LAS OSCILACIONES CORTICALES DE ALTA FRECUENCIA DURANTE LA VIGILIA Y EL SUEÑO

Recientemente, se describió un nuevo tipo de actividad oscilatoria cortical rápida que ocurre entre 110 y 160 Hz (oscilaciones de alta frecuencia (HFO)). Las HFO son modulados por el ritmo theta en el hipocampo y la neocorteza durante la vigilia activa y el sueño REM. Dado que el acoplamiento theta-HFO aumenta durante REM, se ha propuesto un papel para HFO en la consolidación de memoria. Sin embargo, las propiedades globales, como la distribución topográfica en toda la corteza, y la coherencia cortico-cortical siguen siendo desconocidas. En el presente estudio, registramos el electroencefalograma durante el sueño y la vigilia en la rata, y analizamos la extensión espacial de la potencia y la coherencia de la banda de HFO.

Confirmamos que la amplitud de HFO se sincroniza en fase con las oscilaciones theta y se modifica en los diferentes estados comportamentales. Durante la vigilia activa, la potencia de HFO fue relativamente mayor en la neocorteza y el bulbo olfatorio en comparación con el sueño. La potencia de HFO disminuyó durante el sueño NREM y tuvo un nivel intermedio durante el sueño REM. Además, la coherencia fue mayor durante la vigilia activa que durante el sueño NREM, mientras que el sueño REM mostró un patrón complejo en el que la coherencia aumentaba solo entre áreas intrahemisféricas y disminuía entre interhemisféricas. Este patrón de coherencia es diferente al de la coherencia gamma (30-100 Hz), que se reduce durante el sueño REM.

Los datos actuales muestran un importante diálogo cortico-cortical HFO durante la vigilia activa incluso cuando el nivel de co-modulación theta es menor que en sueño REM. Por el contrario, durante el sueño REM, este

diálogo está muy modulado por theta, y restringido a las regiones corticales medial-posteriores intrahemisféricas.

EJN European Journal of Neuroscience FENS Federation of European Neuroscience Societies

European Journal of Neuroscience, pp. 1–10, 2017 doi:10.1111/ejn.13718

Power and coherence of cortical high-frequency oscillations during wakefulness and sleep

Matías Cavelli,[1] Daniel Rojas-Líbano,[2] Natalia Schwarzkopf,[1] Santiago Castro-Zaballa,[1] Joaquín Gonzalez,[1] Alejandra Mondino,[1] Noelia Santana,[1] Luciana Benedetto,[1] Atilio Falconi[1] and Pablo Torterolo[1]
[1]Laboratorio de Neurobiología del Sueño, Departamento de Fisiología, Facultad de Medicina, Universidad de la República, General Flores 2125, 11800 Montevideo, Uruguay
[2]Laboratorio de Neurociencia Cognitiva y Social, Facultad de Psicología, Universidad Diego Portales, Santiago, Chile

Keywords: CFC, gamma, paradoxical sleep, rat, REM, theta

Abstract

Recently, a novel type of fast cortical oscillatory activity that occurs between 110 and 160 Hz (high-frequency oscillations (HFO)) was described. HFO are modulated by the theta rhythm in hippocampus and neocortex during active wakefulness and REM sleep. As theta-HFO coupling increases during REM, a role for HFO in memory consolidation has been proposed. However, global properties such as the cortex-wide topographic distribution and the cortico-cortical coherence remain unknown. In this study, we recorded the electroencephalogram during sleep and wakefulness in the rat and analyzed the spatial extent of the HFO band power and coherence. We confirmed that the HFO amplitude is phase-locked to theta oscillations and is modified by behavioral states. During active wakefulness, HFO power was relatively higher in the neocortex and olfactory bulb compared to sleep. HFO power decreased during non-REM and had an intermediate level during REM sleep. Furthermore, coherence was larger during active wakefulness than non-REM, while REM showed a complex pattern in which coherence increased only in intra and decreased in inter-hemispheric combination of electrodes. This coherence pattern is different from gamma (30–100 Hz) coherence, which is reduced during REM sleep. This data show an important HFO cortico-cortical dialog during active wakefulness even when the level of theta comodulation is lower than in REM. In contrast, during REM, this dialog is highly modulated by theta and restricted to intra-hemispheric medial-posterior cortical regions. Further studies combining behavior, electrophysiology and new analytical tools are needed to plunge deeper into the functional significance of the HFO.

Introduction

The synchronous activity of large population of neocortical neurons generates oscillatory activities in the electroencephalogram (EEG) that vary according to behavior and cognitive functions (Buzsáki *et al.*, 2012). Among the faster oscillations, gamma band activity (30–100 Hz) has been extensively explored (Adrian, 1942; Freeman & Schneider, 1982; Gray *et al.*, 1989; Joliot *et al.*, 1994; Rojas-Líbano & Kay, 2008; Fries, 2009; Buzsáki & Wang, 2012). An increase in gamma activity typically emerges during behaviors characterized by active processing of external percepts or internally generated thoughts and images (Freeman & Schneider, 1982; Tiitinen *et al.*, 1993; Rieder *et al.*, 2011; Uhlhaas *et al.*, 2011). Cognitive activities do not only occur during wakefulness (W). Dreaming, the cognitive counterpart of REM sleep, reveals the existence of another form of cognitive activity or proto-consciousness (Hobson, 2009). Accordingly, gamma power during REM sleep has similar values than W and it is larger compared to deep non-REM (NREM) sleep, where cognitive activity is reduced (Maloney *et al.*, 1997; Chrobak & Buzsáki, 1998; Cavelli *et al.*, 2015).

The coupling of EEG gamma activity between two different cortical areas, as analyzed by spectral coherence, increases during several behaviors and cognitive activities in both animals and humans (Bouyer *et al.*, 1981; Bressler *et al.*, 1993; Härle *et al.*, 2004; Daume *et al.*, 2017). Recently, we showed in cats and rats that long-range gamma coherence is maximum during W, decreases during NREM sleep and reaches its lowest value during REM sleep (Castro-Zaballa *et al.*, 2013, 2014; Cavelli *et al.*, 2015; Torterolo *et al.*, 2016). Also, gamma coherence between distant areas has been proposed as a neural correlate of conscious perception and self-awareness (Llinás *et al.*, 1998; Rodriguez *et al.*, 1999; Melloni *et al.*, 2007; Voss *et al.*, 2009, 2014). In this regard, coherence in the gamma frequency band is lost during anesthesia-induced unconsciousness (John, 2002; Mashour, 2006; Pal *et al.*, 2016) and is severely altered in psychiatric disorders (Uhlhaas & Singer, 2010; Sun *et al.*, 2011).

Correspondence: Dr Pablo Torterolo, as above.
E-mail: ptortero@fmed.edu.uy

Received 19 May 2017, revised 13 September 2017, accepted 13 September 2017

Edited by Gregor Thut

Reviewed by Adriano Tort, Federal University of Rio Grande do Norte, Brazil and Francisco Urbano, University of Buenos Aires, Argentina

The associated peer review process communications can be found in the online version of this article.

Few studies have dealt with EEG oscillations at frequencies higher than 100 Hz (Uhlhaas *et al.*, 2011). Nevertheless, a novel type of fast cortical oscillatory activity occurring between 110 and 160 Hz both in the hippocampus and in the parietal neocortex has been described (Sirota *et al.*, 2008; Tort *et al.*, 2008). Some authors dubbed high-frequency oscillations (HFO) to this activity (Scheffer-Teixeira *et al.*, 2012; Caixeta *et al.*, 2013; Tort *et al.*, 2013), while others called it fast or high gamma (Sirota *et al.*, 2008; Canolty *et al.*, 2009; Jackson *et al.*, 2011; Scheffzük *et al.*, 2011; Pal *et al.*, 2016). Similar to gamma oscillations, HFO are larger during active W and REM sleep (Scheffzük *et al.*, 2011; Scheffer-Teixeira & Tort, 2017) and its amplitude is modulated by theta oscillations both in hippocampus and in parietal neocortex (Sirota *et al.*, 2008; Tort *et al.*, 2013). HFO can co-occur with gamma oscillations nested in the same theta cycle but reach their maximum amplitude at a different theta phase (Scheffzük *et al.*, 2011; Tort *et al.*, 2013). In addition, like gamma activity, HFO have also been related to cognitive functions, such as decision making (Tort *et al.*, 2008). Because of their implication in the neocortex-hippocampal interaction and also due to the mnemonic role of REM sleep (Paller & Voss, 2004), it has been suggested that HFO may specifically be related to memory processing (Tort *et al.*, 2013).

Only a handful of studies have aimed to characterize the HFO, and several key features of these rhythms, such as their spatial patterns and coherence, remain unknown. A crucial step in the assignment of functionality to HFO is to have a larger spatial map of its occurrence across the cortical surface, as well as an assessment of its coherence between cortical regions. Hence, in this report, we studied the HFO spectral power and coherence along several recording sites spanning the entire neocortex and olfactory bulb (OB) of the rat, during W, NREM and REM sleep.

Experimental procedures

Experimental animals

Twenty-one adult male Wistar rats (270–300 g) were used in this study. The animals were obtained from URBE (Unidad de Reactivos Biológicos para Experimentación), of the Department of Laboratory Medicine of the School of Medicine, Universidad de la República, Uruguay. All experimental procedures were conducted in agreement with the National Animal Care Law (#18611) and with the 'Guide to the care and use of laboratory animals' (8th edition, National Academy Press, Washington D. C., 2010). Furthermore, the Institutional Animal Care Committee approved the experimental procedures (File: 071140-001931-12; Registration: CNEA N° 0011/11). Adequate measures were taken to minimize pain, discomfort or stress of the animals, and efforts were made to use the smallest number of animals necessary to obtain reliable data.

Surgical procedures

We employed similar surgical procedures as in our previous studies (Lagos *et al.*, 2009; Benedetto *et al.*, 2013; Cavelli *et al.*, 2015). The animals were chronically implanted with electrodes to monitor the states of sleep and W. Anesthesia was induced with a mixture of ketamine-xylazine (90 mg/kg; 5 mg/kg i.p., respectively). The rat was positioned in a stereotaxic frame, and the skull was exposed. Several craniotomies were made to insert the electrodes. To record the EEG, stainless steel screw electrodes (1 mm diameter) were screwed on the craniotomies to have their tips touching the brain's surface (above the dura mater) in different cortices and the OB. As shown in Fig. 1, four groups of animals (G0–G3) were implanted with different spatial distributions of electrodes on the skull.

G0 group (n = 9). Six electrodes were located on the neocortex forming two anterior–posterior consecutive squares centered with respect to the midline and the frontal square centered with respect to Bregma (Fig. 1). Each side of the squares has a length of 5 mm. The electrodes were located in primary motor cortex (M1, L: ±2.5 mm, AP: +2.5 mm), primary somato-sensory cortex (S1, L: ±2.5 mm, AP: −2.5 mm) and secondary visual cortex (V2, L: ±2.5 mm, AP: −7.5 mm). The other electrode was located over the right OB (L: +1.25 mm, AP: +7.5 mm).

G1, G2 and G3 groups (n = 4 per group). To confirm and extend the results obtained in G0, we analyzed the HFO from recordings that were used in Cavelli *et al.* (2015). G1 group presents intra-hemispheric, while G2 and G3 groups have inter-hemispheric (homotopic and heterotopic, respectively) combinations of electrodes. Note that in G1 and G3, V1 was used instead of V2 (that was used in G0 group).

To record the electromyogram (EMG), two electrodes were inserted into the neck muscle. The electrodes were soldered into a six to 12 pin socket (depending of the number of electrodes) and fixed onto the skull with acrylic cement.

At the end of the surgical procedures, an analgesic (Ketoprofen, 1 mg/Kg s.c.) was administered. Incision margins were kept clean, and a topical antibiotic was applied daily. After the animals recovered from the surgical procedures (minimal recovering time of 4 days), they were adapted to the recording chamber for 1 week.

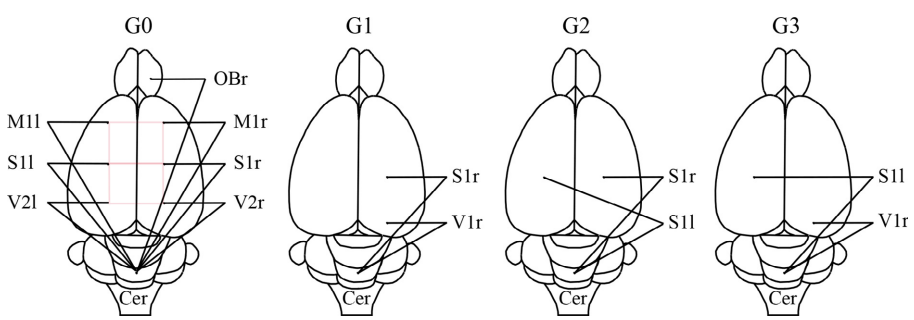

FIG. 1. Position of recording electrodes. The figure presents a summary of the cortical and OB positions of the recording electrodes. The electrodes were referred to a common electrode that was located over the cerebellum (Cer). In this group, the electrodes form two anterior–posterior consecutive squares centered with respect to the midline and with the frontal square centered with respect to Bregma (highlighted in red). OB, olfactory bulb; M1, primary motor cortex; S1, primary somato-sensory cortex; V2, secondary visual cortex; r, right; l, left.

Experimental sessions

All animals were housed individually in transparent cages (40 × 30 × 20 cm) containing wood shavings in a temperature-controlled (21–24 °C) room, with water and food *ad libitum*. Experimental sessions were conducted during the light period, between 12 A.M. and 6 P.M in a sound-attenuated chamber, which was also a Faraday box. The recordings were performed through a rotating connector, to allow the rats to move freely within the recording box.

The simultaneous activity of different cortical areas was recorded using a monopolar configuration with a common reference electrode located in the cerebellum (Bullock *et al.*, 1990; Cavelli *et al.*, 2015) (Fig. 1). The EMG was also monitored. Each rat was recorded daily for approximately 1 week to obtain a complete data set.

Bioelectric analog signals were amplified with a differential AC amplifier (AM-systems model 1700; 1000×), filtered (0.1–500 Hz), digitized (1024 Hz, 2^{16} bits) and stored on a PC using the Spike2 software (Cambridge Electronic Design).

Data analysis

Sleep and waking states were determined for 10-s epochs according to standard criteria (Cavelli *et al.*, 2015). For the analysis of the G0 group of animals, W was divided into active (AW) and quiet (QW) according to the mean level of theta activity averaged from the four posterior electrodes. Epochs that had a theta power above percentile 70 were classified as AW, while the remaining epochs were assigned as QW.

To analyze power spectrum (in each channel) and coherence (between pairs of EEG channels), we used similar procedures as in our previous studies (Castro-Zaballa *et al.*, 2013, 2014; Cavelli *et al.*, 2015; Torterolo *et al.*, 2016); however, the analysis in G0 and G1-G3 groups was not exactly the same (see below).

G0 group. The maximum number of non-transitional and artifact-free periods of 30 s was selected during each behavioral state to determine the mean power and coherence for each rat. For each animal, we analyzed two complete (6 h) recordings (the recordings with the lower number of artifacts were selected).

G1 to G3 groups. We employed exactly the same methodology as in our previous studies (Castro-Zaballa *et al.*, 2013, 2014; Cavelli *et al.*, 2015; Torterolo *et al.*, 2016). Twelve artifact-free periods of 100 s were examined during each behavioral state (1200 s for each behavioral state, per animal; data were selected from three different recordings). For these groups of animals, the 100-s windows of W consisted of a mixture of AW and QW.

The coherence between two EEG channels that were recorded simultaneously was analyzed in 30 s (for G0) or 100 s (for G1- G3) windows. For each period, the magnitude-squared coherence as well as the power spectrum for each channel was calculated by means of Spike2 script COHER-HOL 1S (for details about coherence definition see (Bullock & McClune, 1989; Castro-Zaballa *et al.*, 2013)). For the coherence analysis, each period was divided into 30 (G0) and 100 (G1-G3) time-blocks with a bin size of 2048 samples and a resolution of 0.5 Hz. The data were then analyzed through custom-built Python routines.

We examined the power and coherence of HFO between 105 and 148 Hz, to avoid any possible interference due to 50 Hz electrical noise (power line hum). To normalize the data and use parametric statistical tests, we applied the Fisher z- transform to the coherence values. The power of the HFO for each channel (expressed as the total power (TP) per band; absolute values), and the z'-coherence for each pair of EEG channels, was averaged across behavioral states. The data were expressed as mean ± standard deviation. The significance of the differences among behavioral states was evaluated with one-way ANOVA (for each rat) and repeated measures ANOVA (RMANOVA) (for comparison between the means of the whole group of rats), along with Tamhane and Bonferroni *post hoc* tests, respectively. The criterion used to reject null hypotheses was $P < 0.05$. When the ANOVA test resulted in a significant difference, a measure of effect size (MES) was also reported. The MES was reported as η^2, which was calculated as follows: $\eta^2 = (SS_{effect}/SS_{total})$, where SS_{effect} is the sum of squares between groups, and SS_{total} is the overall sum of squares. Therefore, the range of η^2 goes from 0 to 1 (0 means no effect). This measure estimates the proportion of the total variance of a given variable explained by a treatment (Kline, 2004).

Selected recordings were band-pass filtered to obtain HFO and theta bands using digital finite impulse response filters (FIR). The amplitude relation between simultaneously recorded pairs of filtered HFO epochs was analyzed using regression and correlation analysis. Autocorrelations (ACF) and cross-correlations functions (CCF) were also calculated.

A CCF-map (Fig. 2C) was generated between the theta rhythm (4–9 Hz) and the envelopes of frequencies higher than 20 Hz. To obtain the CCF-map, several band-pass filtered signals were generated from the raw recording. We filtered one in the theta range; for the others band-passed signals, we used 10-Hz bandwidth and 5-Hz steps, covering from 20 up to 190 Hz. The CCF-map was then generated by means of a raster plot of CCFs calculated between theta and the root mean square (RMS) envelopes of each filtered signal.

A RMS coherence map was also constructed to study the coherence of the HFO amplitude in the theta range (Fig. 6A). To construct this map, several pairs of band-pass filtered signals were obtained exactly as before, using a 10-Hz bandwidth and 5-Hz steps, covering from 20 up to 190 Hz. For each pair of filtered signals, the RMS was computed and the coherence calculated. The *X*-axis represents the frequency of coherence below 20 Hz, the *Y*-axis represents the mean frequency of the band-passed signals (the envelope's own frequency) and the Z-axis corresponds to the level of z'-coherence between each pairs of envelopes at a given frequency.

With the purpose of analyzing the modulation of the HFO amplitude by the phase of the theta oscillation, a comodulation map or 'co-modulogram' was performed in Matlab (see Figs 2D and 3A). To build the comodulogram, each pair composed by one slow (phase) and one fast (envelopes) oscillation was assessed by a measure called modulation index (MI); these data were processed in Matlab following previously described procedures (Tort *et al.*, 2010, 2013).

Results

Identification of the HFO: modulation by behavioral states and theta rhythm

As a first step, we confirmed that HFO activity was present in our recordings. As previously described, HFO are modulated by theta rhythm and modified by behavioral states. Figure 2A exhibits the power spectrum profiles of the EEG during W and sleep. This figure shows that there is a larger power between 25 and 250 Hz during W than during sleep states. During REM sleep, the power in S1 and V1 recording sites reveals a peak in the theta band. Also, a small, but clear power peak at the HFO band (arrows) is readily observed, which although lower than waking values, and it was larger than during NREM sleep.

Figure 2B shows raw and filtered recordings during REM sleep of a representative rat. In the raw recordings of S1 and V1 (right

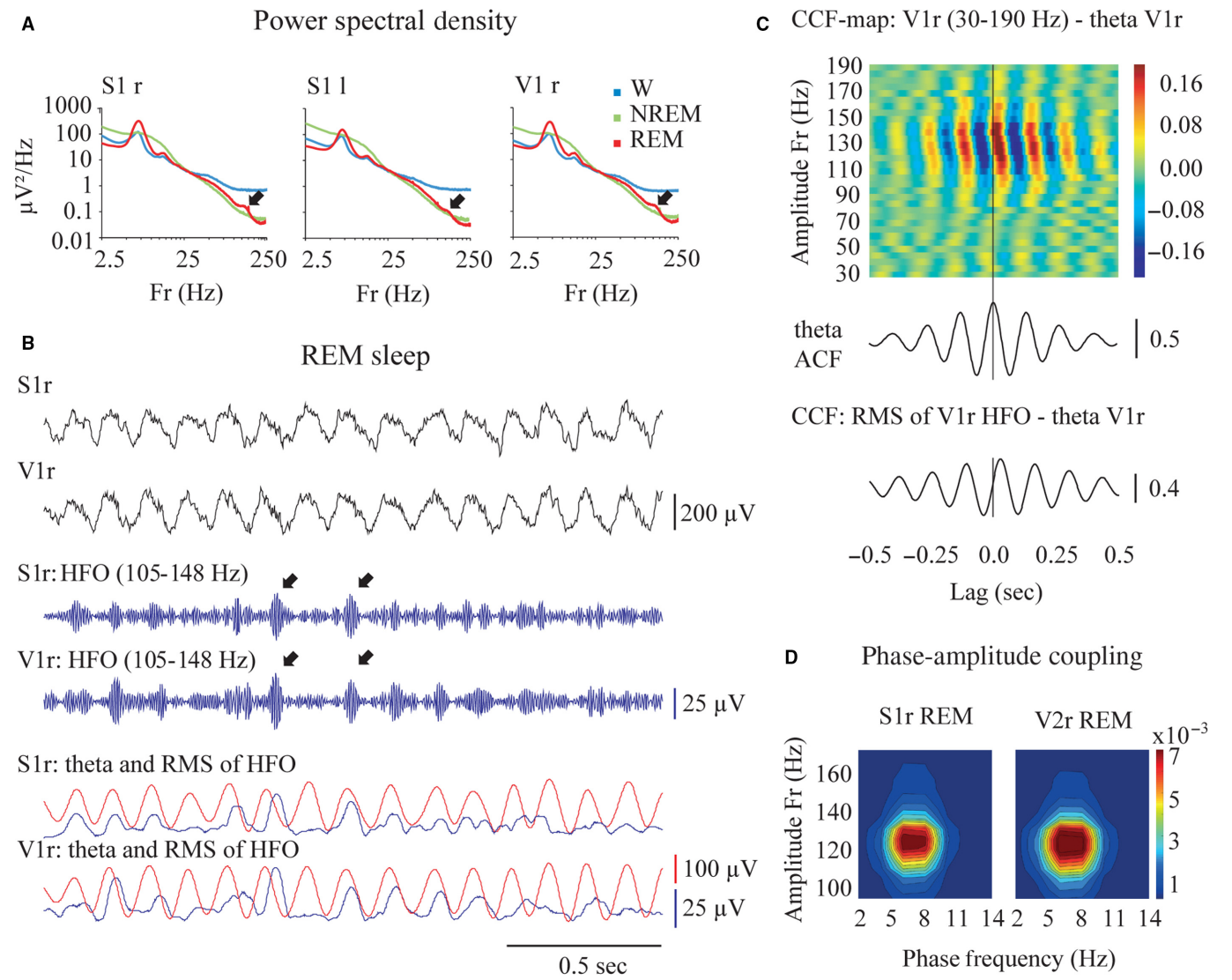

FIG. 2. High-frequency oscillations (HFO) are associated with theta oscillations during REM sleep. (A) S1r, S1l and V1r mean power spectral density during W (blue), NREM (green) and REM sleep (red) is shown. Each trace is the mean of 12 independent 100 s windows per animal (four rats). The arrows point the HFO peaks in the power profile during REM sleep. (B) Simultaneous raw and filtered (105–148 Hz) recordings from the right somato-sensory primary (S1r) and right visual primary (V1r) cortices during REM sleep. HFO were highlighted after filtering. Arrows in the filtered recordings indicate 'bursts' of HFO. The traces in the bottom show that the HFO RMS amplitude envelope (blue traces) seems to follow the theta oscillations (4–12 Hz band-pass filter, red traces). (C) Cross-correlation function (CCF) map of V1 theta and V1 RMS envelop (30–200 Hz, 10-Hz bandwidth and 5-Hz steps), autocorrelation function (ACF) of V1 theta, and CCF of V1 theta and V1 HFO (RMS) envelope are shown. These data were analyzed from 100 s windows during REM sleep. Coupling between HFO RMS and theta are readily observed in both CCF and CCF-map. (D) The comodulation map expressing theta-HFO phase-amplitude coupling (PAC) for S1 and V1 during REM sleep is shown. In the two plots, the modulation maximum reveals correlations between theta and HFO bands.

hemisphere), there is prominent theta activity, while high-frequency activity is present with smaller amplitude. HFO during REM sleep were unmasked after digital filtering of the recordings, and spindle-like 'bursts' of HFO were commonly observed (arrows). The RMS of the HFO amplitude is also shown (blue traces); in this case, the RMS peaks come out predominantly following the theta cycles' maxima (red traces). This strong association between the envelope of the HFO and the theta rhythm during REM sleep can be seen in the CCF and the cross-correlogram map of Fig. 2C. Furthermore, the comodulogram of Fig. 2D shows a high phase-amplitude coupling (PAC) between the amplitude of HFO and the phase of the theta rhythm during REM sleep, both in S1r and in V2r.

In contrast to REM sleep, during W there was not a clear peak in the HFO band power, even when the HFO power level was the highest (Fig. 2A). However, during W, HFO were also modulated by theta rhythm. Figure 3A exhibits by means of PAC that HFO are modulated by theta rhythm during AW (that is accompanied by high theta activity). In fact, AW showed higher modulation than QW, both in S1 and in V2. However, theta modulation during AW remained lower than during REM sleep (Figs 3A and 2D; see calibration bars). Figure 3B shows the z'-coherence between the raw recordings and HFO band envelopes of the same recording. This analysis revealed a clear peak of HFO coherence in the theta range (7–9 Hz) during AW; this modulation is not present during QW, neither in S1 nor in V2 (Fig. 3B).

All these analyses confirmed that the recorded HFO present the same features that have been previously described (Scheffzük *et al.*, 2011; Tort *et al.*, 2013).

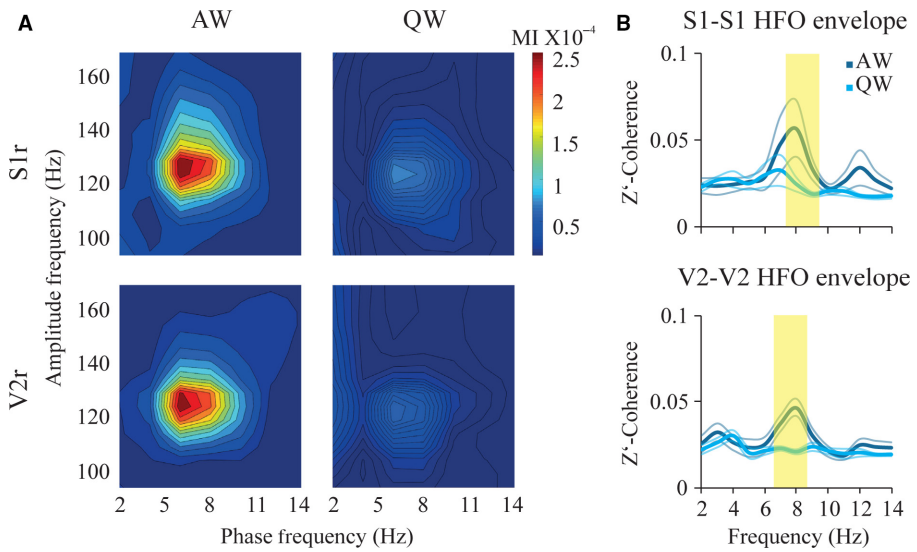

FIG. 3. High-frequency oscillations (HFO) are associated with theta oscillations during AW and not QW. (A) The comodulation map expressing theta-HFO phase-amplitude coupling (PAC) for S1 and V2 during AW (left) and QW (right) is shown. In S1 and V2 plots, the maximum value of modulation index (MI) between theta and HFO bands was observed during AW. (B) The graphics show the z'-coherence between the raw and the HFO envelope of the same record. This analysis reveals a clear peak in the theta range (7–9 Hz) coherence during AW but not during QW for S1 and V2 electrodes. The shaded yellow represents significant differences between AW and QW, paired *t*-test, $P < 0.05$.

Neocortical extent of the HFO power and coherence

To study the neocortical extent of power and coherence of HFO band, we analyzed a group of nine rats with the same electrode position (Fig. 1, G0). Statistical analyses of HFO band power and coherence are shown in Tables 1 and 2, respectively. HFO TP showed significant differences across behavioral states for all the electrodes (Table 1). These results revealed that HFO band power is larger during AW than during sleep, both in neocortex and in OB. The lowest values were recorded during NREM, while during REM sleep, the TP increased to an intermediate level in all the cerebral areas recorded.

Z'-coherence also displayed significant differences across behavioral states for all twenty-one possible electrode pair combinations (Table 2). HFO band coherence was larger during AW than during NREM sleep. During REM sleep, a significant increase in coherence was observed compared with NREM sleep but only for posterior intra-hemispheric combination of electrodes (Table 2, highlighted in a red frame). The rest of the electrodes combinations showed either no change (most of the combinations) or a decrease in coherence compared with NREM; this was the case of six inter-hemispheric combinations of electrodes (Table 2). The schematic presented in Fig. 4 summarizes the statistically significant mean differences of HFO band power and coherence during AW and sleep.

We also analyzed the HFO 'mean global coherence' by averaging the twenty-one electrode combinations (Pal *et al.*, 2016). This estimate of global coherence showed significant differences across behavioral states ($F_{2,24} = 112.3$, $P < 0.001$, $\eta^2 = 0.934$). Global coherence was higher during AW (0.53 ± 0.10), decreased during NREM (0.27 ± 0.07, $P < 0.001$) and reached a minimum during REM sleep (0.23 ± 0.07, $P = 0.032$).

The analyses of HFO band power, as well as intra- and inter-hemispheric coherence, were also performed on twelve animals corresponding to G1, G2 and G3 groups. In these groups, the results were comparable to the G0 group; in spite of that, W was analyzed as whole (AW + QW). The complete analyses for each group of animals and for each rat are shown in Supplementary Information (Fig. S1 and Tables S1 and S2, respectively).

TABLE 1. RMANOVA and Bonferroni tests. The analysis was performed in nine animals. The degrees of freedom were 2 (between groups) and 16 (within groups) for all the cortical regions that were analyzed

	Descriptive statistics (TP μV^2/Hz)			RMANOVA			Multiple comparisons-Bonferroni		
Electrode	AW (mean ± SD)	NREM (mean ± SD)	REM (mean ± SD)	*F*	Sig. (*P*)	Partial Eta Squared (η^2)	AW vs. SWS (*P*)	AW vs. REM (*P*)	REM vs. NREM (*P*)
OBr	124.1 ± 48.3	18.2 ± 9.5	29.6 ± 14.5	58.9	**<0.001**	0.880	**<0.001**	**<0.001**	**0.002**
M1l	71.6 ± 33.1	9.1 ± 1.8	16.5 ± 6.3	30.7	**<0.001**	0.793	**0.001**	**0.002**	**0.023**
M1r	74.5 ± 30.9	9.4 ± 2.6	16.3 ± 6.4	40.5	**<0.001**	0.835	**0.001**	**0.005**	**0.005**
S1l	63.4 ± 24.9	9.7 ± 2.4	23.5 ± 11.3	33.5	**<0.001**	0.808	**<0.001**	**0.004**	**0.010**
S1r	71.1 ± 24.9	17.6 ± 17.4	32.4 ± 19.5	82.9	**<0.001**	0.912	**<0.001**	**<0.001**	**0.001**
V2l	41.3 ± 20.7	10.9 ± 16.5	17.1 ± 19.7	67.7	**<0.001**	0.894	**<0.001**	**<0.001**	**0.015**
V2r	50.3 ± 24.3	12.5 ± 19.5	20.3 ± 23.8	59.5	**<0.001**	0.882	**<0.001**	**<0.001**	**0.024**

OB, olfactory bulb; M1, motor primary cortex; S1, somato-sensory primary cortex; V2, visual secondary cortex; r, right; l, left; AW, active wakefulness; NREM, non-REM sleep; REM, REM sleep, in bold $P < 0.05$.

TABLE 2. RMANOVA and Bonferroni tests. The analysis was performed in nine animals. The degrees of freedom were 2 (between groups) and 16 (within groups) for all the combinations that were analyzed. A significant increase in coherence in the posterior intra-hemispheric combination of electrodes was highlighted in a red frame

	Descriptive statistics (Z'-coherence)			RMANOVA			Multiple comparisons-Bonferroni		
Electrode pairs	AW (mean ± SD)	NREM (mean ± SD)	REM (mean ± SD)	*F*	Sig. (*P*)	Partial Eta Squared (η^2)	AW vs. SWS (*P*)	AW vs. REM (*P*)	REM vs. NREM (*P*)
OBr-M1r	0.66 ± 0.22	0.39 ± 0.25	0.35 ± 0.22	53.8	**<0.001**	0.871	**0.001**	**<0.001**	0.151
OBr-M1l	0.60 ± 0.33	0.33 ± 0.28	0.31 ± 0.27	45.7	**<0.001**	0.851	**0.001**	**<0.001**	0.712
OBr-S1r	0.42 ± 0.17	0.15 ± 0.11	0.11 ± 0.07	54.2	**<0.001**	0.872	**<0.001**	**<0.001**	0.295
OBr-S1l	0.41 ± 0.17	0.15 ± 0.10	0.11 ± 0.01	64.5	**<0.001**	0.890	**<0.001**	**<0.001**	**0.036**
OBr-V2r	0.31 ± 0.13	0.11 ± 0.06	0.09 ± 0.04	25.9	**<0.001**	0.764	**0.002**	**0.002**	0.696
OBr-V2l	0.28 ± 0.11	0.08 ± 0.05	0.06 ± 0.03	46.8	**<0.001**	0.854	**<0.001**	**<0.001**	0.468
M1r-M1l	0.79 ± 0.19	0.42 ± 0.15	0.34 ± 0.17	98.5	**<0.001**	0.925	**<0.001**	**<0.001**	0.145
M1r-S1r	0.80 ± 0.23	0.33 ± 0.12	0.30 ± 0.13	82.1	**<0.001**	0.911	**<0.001**	**<0.001**	0.592
M1r-S1l	0.70 ± 0.23	0.31 ± 0.12	0.19 ± 0.14	75.2	**<0.001**	0.904	**<0.001**	**<0.001**	**0.004**
M1r-V2r	0.51 ± 0.23	0.18 ± 0.10	0.18 ± 0.08	25.6	**<0.001**	0.762	**0.001**	**0.004**	1.000
M1r-V2l	0.45 ± 0.17	0.13 ± 0.07	0.10 ± 0.07	53.1	**<0.001**	0.869	**<0.001**	**<0.001**	0.608
M1l-S1l	0.87 ± 0.13	0.41 ± 0.12	0.38 ± 0.11	201.5	**<0.001**	0.962	**<0.001**	**<0.001**	0.345
M1l-V2l	0.49 ± 0.14	0.14 ± 0.08	0.17 ± 0.09	95.3	**<0.001**	0.923	**<0.001**	**<0.001**	0.179
S1r-M1l	0.59 ± 0.15	0.21 ± 0.07	0.15 ± 0.11	88.9	**<0.001**	0.918	**<0.001**	**<0.001**	0.234
S1r-S1l	0.66 ± 0.31	0.25 ± 0.15	0.11 ± 0.07	39.98	**<0.001**	0.833	**<0.001**	**0.001**	**0.011**
S1r-V2l	0.62 ± 0.28	0.28 ± 0.21	0.16 ± 0.14	51.7	**<0.001**	0.753	**<0.001**	**<0.001**	**0.011**
V2r-M1l	0.41 ± 0.15	0.14 ± 0.05	0.08 ± 0.04	42.2	**<0.001**	0.841	**0.001**	**<0.001**	**0.043**
V2r-S1l	0.40 ± 0.22	0.13 ± 0.06	0.08 ± 0.03	20.3	**<0.001**	0.718	**0.005**	**0.006**	0.071
V2r-V2l	0.49 ± 0.29	0.30 ± 0.22	0.15 ± 0.11	15.8	**<0.001**	0.665	**0.025**	**0.008**	**0.018**
S1l-V2l	0.72 ± 0.21	0.28 ± 0.13	0.44 ± 0.16	50.2	**<0.001**	0.863	**<0.001**	**0.001**	**0.002**
S1r-V2r	0.70 ± 0.35	0.39 ± 0.23	0.53 ± 0.27	17.3	**<0.001**	0.685	**0.003**	**0.034**	**0.031**

OB, olfactory bulb; M1, motor primary cortex; S1, somato-sensory primary cortex; V2, visual secondary cortex; r, right; l, left; W, wakefulness; NREM, non-REM sleep; REM, REM sleep, in bold $P < 0.05$.

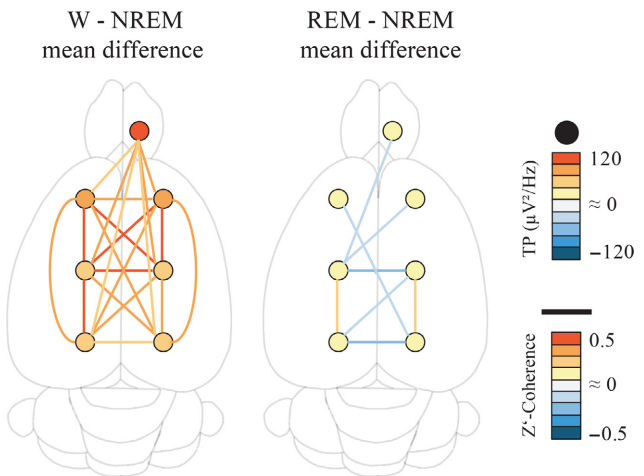

FIG. 4. High-frequency oscillations (HFO) band power and z'-coherence during wakefulness and sleep. Summary of the statistical significance differences between behavioral states of the HFO' total power and z'-coherence over the surface of the cerebral cortex (G0 group, Figure 1). The circles represent the power for the different electrode positions, while the lines represent the coherence for the different combination of electrodes. The colors represent the mean difference level of power and z'- coherence. RMANOVA and Bonferroni paired comparisons tests. Data were obtained from the mean values of all available, non-transitional artifact-free windows per rat for each behavioral state (nine rats). OB, olfactory bulb; M1, motor primary cortex; S1, somato-sensory primary cortex; V2, visual secondary cortex.

Inter-hemispheric differences in HFO coherence during REM sleep

One intriguing result of the analysis was that compared to NREM sleep, HFO coherence during REM increases only in the posterior intra-hemispheric electrode pairs.

Coherence values during REM sleep for three different electrode configurations S1r-V1r (intra-hemispheric), S1r-S1l (inter-hemispheric homotopic) and V1r-S1l (inter-hemispheric heterotopic) are shown in Fig. 5A. This plot highlights that the HFO coherence during REM sleep is relatively large for the intra-hemispheric electrode combinations, but it is absent in the inter-hemispheric configurations. This difference in HFO coupling during REM sleep between intra- and inter-hemispheric configurations is also evident in the filtered recordings (Fig. 5B) and in the cross-correlation and regression/correlation analyses (Fig. 5C and D). In contrast, we consistently observed that during W, the coupling is present for both types of combination of electrodes (Fig 5C and D).

To analyze whether the increase in intra-hemispheric HFO synchronization during REM sleep was associated with HFO bursts that oscillated at the theta frequency, we developed a RMS coherence map (Fig. 6A). This map shows an increase in the HFO RMS coherence at theta frequency, for the intra-hemispheric electrode combinations. Then, the intra- and inter-hemispheric coherence of the HFO RMS was analyzed. This analysis revealed a clear peak in the theta range both for intra- (7.10 ± 0.20 Hz; mean ± SD) and for inter-hemispheric homotopic (7.27 ± 0.26 Hz; mean ± SD) electrode combinations (Fig. 6B). However, HFO RMS theta peak coherence was larger for intra- (0.87 ± 0.07; mean ± SD) than for inter-hemispheric (0.55 ± 0.07; mean ± SD) combination of electrodes (*t*-test; $P < 0.001$). Hence, during REM sleep, the HFO burst envelopes oscillated at theta frequency and were more coupled within hemispheres than between hemispheres.

Discussion

In the present study, we analyzed the neocortical distribution of the HFO band (105–148 Hz), as well as its intra- and inter-hemispheric

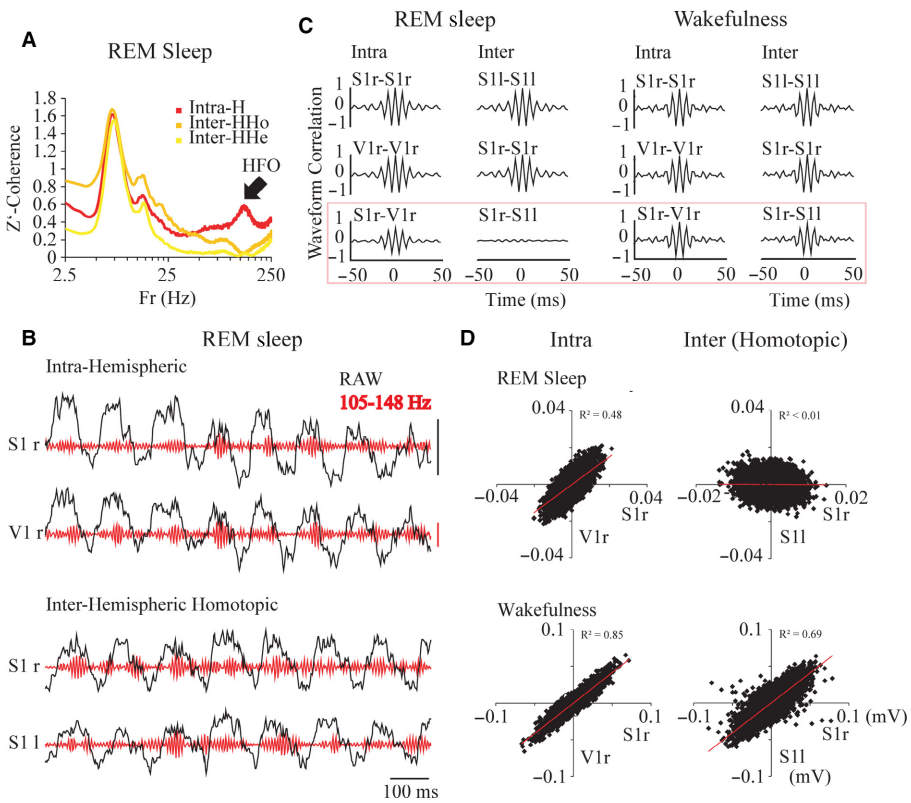

FIG. 5. High-frequency oscillations (HFO) intra- and inter-hemispheric coupling during REM sleep. (A) Mean coherence profiles during REM sleep. Traces from intra-hemispheric (red), inter-hemispheric homotopic (orange) and heterotopic (yellow) configuration of electrodes are shown. A peak of coherence in the HFO band is observed in the intra-hemispheric configuration (arrow), while in the inter-hemispheric combinations, the HFO coherence expressed its lowest values. (B) Simultaneous raw and filtered (105–148 Hz, red traces) recordings from the right somato-sensory primary (S1r) and right visual primary (V1r) cortices (top traces) and from the right somato-sensory primary (S1r) and left somato-sensory primary cortex (S1l) (bottom traces) during REM sleep. HFO, which are readily observed in the raw recordings, were highlighted after filtering. Synchrony in the HFO 'bursts' is more pronounced in the intra-hemispheric combination of electrodes. (C) Autocorrelation functions (ACF; two superior traces) and cross-correlation functions (CCF; inferior traces, framed in red) from filtered (105–148 Hz) periods of 100 s of simultaneous EEG recordings from somato-sensory and visual cortices are shown during W and REM sleep. (D) Linear regressions between the amplitudes of S1r-V1r and S1r-S1l were performed on representative filtered recordings (105–148 Hz) during 50 s of wakefulness and REM sleep. The determination coefficients are also shown. S1, somato-sensory primary cortex; V1, visual primary cortex; r, right; l, left.

(homotopic and heterotopic) cortico-cortical coherence, during W and sleep. We showed that the HFO band power, as well as the intra- and inter-hemispheric HFO band coherence, was greater during W than during sleep throughout the neocortex and OB. Similar results were obtained when W, or just AW, was analyzed. We also found an increase in the HFO band coherence during REM sleep, but only for the intra-hemispheric combination of electrodes located in the medial and posterior neocortical regions. Furthermore, we presented evidences that support the hypothesis that these levels of intra-hemispheric coherence are related to the burst of activity that is effectively modulated by theta waves generated by the hippocampal networks.

HFO characterization

We verified the presence of HFO activity in our recordings through filtering, correlation analysis and an estimate of cross-frequency coupling. Furthermore, we found HFO-theta coupling during AW and REM sleep in neocortical areas, consistent with previously published data (Scheffzük *et al.*, 2011).

We also confirmed a precise comodulation of HFO amplitude and theta activity. In fact, we observed that HFO envelope maxima appeared predominantly after the maximum of the theta wave (Fig. 2B and C), consistent with previous reports (Sirota *et al.*, 2008; Scheffzük *et al.*, 2011). This selective comodulation of HFO and theta activity, both during AW and REM sleep, makes it difficult to postulate another source than the brain contributing to this theta-coupled HFO. However, we cannot totally discard that muscle activity may contribute to part of the raw signal during AW and contributed to the high HFO power, even when the coherence of each channel with the EMG was negligible (data not shown). In other words, during W, although the theta-modulated HFO signal exists, part of the HFO band might include either an intracranial HFO not modulated by theta or an extracranial source. Hence, new studies would be important to develop new analytical tools to figure out how much of the HFO power and coherence levels are effectively modulated by the theta rhythm of the hippocampal network.

In contrast to W, during REM sleep, there is muscle atonia and is during this state where the maximum modulation between theta and HFO is expressed ((Scheffzük *et al.*, 2011) and present study); these facts practically discard the possibility that this signal has an extracranial source. Finally, it is worth to note that the HFO coherence decreases with electrode distance, as expected for signals of cortical origin (Bullock *et al.*, 1990) (Fig. S2).

HFO power and coherence during wakefulness and REM sleep

In all the neocortical areas explored as well as in the OB, the largest HFO band power was recorded during W. Compared to W, HFO

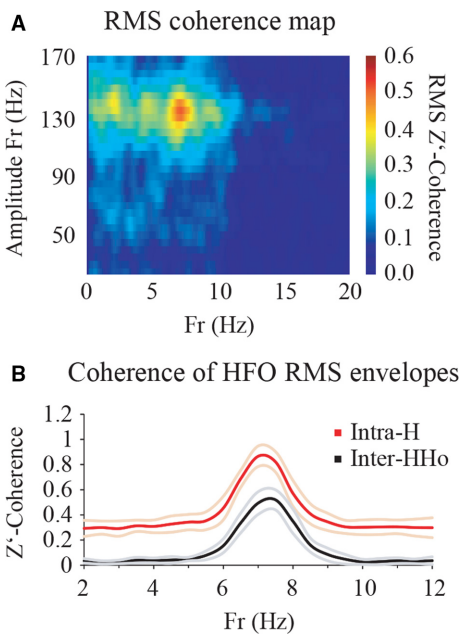

FIG. 6. Spectral z'-coherence of HFO root mean square (RMS) envelopes. (A) The plot shows the RMS coherence map between the envelopes of V1r and S1r (30–180 Hz, 10-Hz bandwidth and 5-Hz steps). This map shows an increase in envelopes coherence in the HFO band at theta frequency. (B) The graphic shows the mean ± standard deviation of the z'-coherence RMS amplitude envelopes of the filtered HFO for the intra- and inter-hemispheric combination of electrodes. The HFO RMS envelopes coherence shows only one peak in the theta range. The envelope coherence is greater for the intra-hemispheric (red trace) compared to the inter-hemispheric (black trace) combination of electrodes ($P < 0.001$). H, hemispheric; HHo, hemispheric homotopic.

power decreased during NREM and increased to intermediate values during REM sleep. This result agrees with Scheffzük *et al.* (2011), who showed that, in the parietal cortex, the HFO band power was more prominent during W compared to REM sleep.

We also showed that intra- and inter-hemispheric coherence was larger during W compared to sleep. While HFO band coherence decreases during NREM sleep, an interesting pattern emerged during REM sleep; there were major differences between intra- and inter-hemispheric HFO band coherence. Intra-hemispheric HFO band coherence values during REM sleep were intermediate between NREM and W. This fact was observed only for the medial and posterior electrode combinations. In contrast, HFO band coherence during REM sleep dropped in the inter-hemispheric (both homotopic and heterotopic) combinations of electrodes. In other words, cortical coupling in the HFO band during REM sleep occurs predominantly between posterior-medial cortical sites of the same hemisphere. Accordingly, the coherence of the HFO envelopes (which oscillate at theta frequencies) for the intra-hemispheric combination of electrodes was significantly higher than the one of the inter-hemispheric combination (Fig. 6B), even when theta coherence values were high and similar for the posterior intra- and inter-hemispheric combinations (Fig. 5A).

The present results suggest that the cortico-cortical dialog within the HFO band during REM sleep is high for each hemisphere but low or absent across them. These data also suggest that during REM sleep, sensory cortices (medial to posterior) are the main active participants of this cortico-cortical dialog at high frequency, while more motor-executive (anterior) cortices are not. In accordance, a recent work demonstrated an absence of theta-HFO coupling in the anterior lateral prefrontal cortex (Zhang *et al.*, 2016). Further studies are needed to identify the functional consequences of this phenomenon, and if subcortical areas such as the thalamus, whose neurons present high-frequency discharge bursts (Llinas & Steriade, 2006), are involved in the development of this cortico-cortical coherence.

HFO and gamma oscillations

In the parietal cortex, both HFO and gamma (30–100 Hz) are associated with theta oscillations (Tort *et al.*, 2008; Scheffer-Teixeira *et al.*, 2012) but in a different phase of the theta cycle (Scheffzük *et al.*, 2011). In contrast, in the lateral prefrontal cortex, only gamma activity (but not HFO) emerges during active W and REM sleep associated with theta (Zhang *et al.*, 2016). Hence, both gamma and HFO are related to the theta generated in the hippocampal network (Sirota *et al.*, 2008; Tort *et al.*, 2013).

In recent studies, we found both in rats and in cats that the long-range neocortical synchronization in the gamma frequency band (30–100 Hz), coherence is almost absent during REM sleep (Castro-Zaballa *et al.*, 2013, 2014; Cavelli *et al.*, 2015), even when gamma power is similar to W (Maloney *et al.*, 1997; Chrobak & Buzsáki, 1998; Cavelli *et al.*, 2015). Although HFO and gamma band coherence during REM sleep were almost absent in the inter-hemispheric electrode combinations (both for homotopic and for heterotopic cortices), HFO but not gamma band coherence increase in the posterior-medial combination of intra-hemispheric electrodes during this behavioral state. This pattern of activity differentiates HFO from gamma oscillations.

Recently, Pal *et al.* (2016) confirmed the loss of gamma band coherence during REM in rats. In addition, they showed a decrease in the HFO band (the authors dubbed HFO as high gamma), 'mean global coherence' during NREM and even more during REM sleep. The 'mean global coherence' was obtained by averaging the coherence for individual channel pairs for each animal. When we calculated the average of the twenty-one electrode combinations, the result was identical to Pal *et al.* (2016). Nevertheless, the 'mean global coherence' masks subtle changes that are generated in specific combinations of electrodes such as the case of the posterior intra-hemispheric combination of electrodes (Fig. 3).

HFO and cognition

The role of HFO in cognition is an unexplored area. During REM sleep, where dreams occur, high HFO coherence coexists with low gamma coherence, in posterior-medial intra-hemispheric cortices. We hypothesize that this may have cognitive implications. In this regard, due to the similarities between the neurobiology of REM sleep dreams with the neurobiology of the psychosis, REM sleep is considered a natural model of psychosis (Gottesmann, 2006; Gottesmann & Gottesman, 2007; Hobson & Voss, 2011). In fact, HFO is prominent in a pharmacological model of psychosis, such as the induced by Ketamine or MK-801 (both NMDA-receptor glutamatergic antagonists) (Caixeta *et al.*, 2013; Hunt & Kasicki, 2013; Cordon *et al.*, 2015).

Interestingly, HFO have been also recorded during epileptic seizures (Bragin *et al.*, 1999; Jirsch *et al.*, 2006; Zijlmans *et al.*, 2012). More studies are needed to understand the functional relationships between physiological HFO and HFO recorded in pathological conditions such as psychosis and seizures.

Conclusions

In the present study, we described the cortical spatial extent of HFO power and intra- and inter-hemispheric coherence across behavioral states in the rat. We identified and described previously unknown features of neocortical HFO during W and sleep. While there is a high-frequency cortico-cortical dialog throughout the cortex during W in the HFO band, this dialog is restricted during REM sleep to the intra-hemispheric medial-posterior (sensory/perceptual) cortical regions. We presented evidences that support the hypothesis that these levels of intra-hemispheric coherence during REM sleep are related to the burst of activity that is effectively modulated by theta. Further studies are needed to directly address the functional significance of the HFO.

Supporting Information

Additional supporting information can be found in the online version of this article:

Fig. S1. HFO band mean total power (TP) and coherence during wakefulness and sleep in each rat of the G1, G2 and G3 groups.
Fig. S2. HFO coherence as a function of the electrode distance.
Table S1. HFO Total Power during sleep and wakefulness in each rat of the G1, G2 and G3 groups.
Table S2. HFO z'-coherence during sleep and wakefulness in each rat of the G1, G2 and G3 groups.

Acknowledgements

This study was partially supported by the 'Programa de Desarrollo de Ciencias Básicas, PEDECIBA' and 'Comision Sectorial de Investigacion Cientifica', CSIC. S. CZ. and A. M. currently have a postgraduate fellowship from the 'Agencia Nacional de Investigación en Innovación (ANII)', while M. C. has a fellowship from 'Comisión de Apoyo a Postgrados (CAP)' D.RL. acknowledges funding from Proyecto Fondecyt 3120185.

Abbreviations

ACF, autocorrelation function; ANOVA, ANalysis Of VAriance; AP, antero-posterior; CCF, cross-correlation function; CFC, cross-frequency coupling; EEG, electroencephalogram; EMG, electromyogram; FIR, finite impulse response; HFO, high-frequency oscillations; i.p., intraperitoneal; L, lateral; M1, primary motor cortex; MES, measure of effect size; MI, modulation index; NREM, non-REM sleep; OB, olfactory bulb; PAC, phase-amplitude coupling; REM, rapid eyes movement; RMANOVA, repeated measures ANOVA; RMS, root mean square; s.c., subcutaneous; S1, primary somato-sensory cortex; SD, standard deviation; SS, sum of square; TP, total power; V1, primary visual cortex; V2, secondary visual cortex; W, wakefulness.

Conflict of interest

All the authors declare no conflict of interest.

Authors contributions

P.T., A.F., and M.C. financially supported. M.C., P.T., and S.CZ. did experimental design. M.C., and N.Schwarzkopf involved in experimental procedures. M.C., D.RL., J.G., A.M., and N.Santana analyzed the data. M.C., P.T., D.RL., S.CZ., J.G., A.F., and L.B. discussed and interpreted the data. M.C., and P.T. wrote the manuscript. All the authors participated in critical revision of the manuscript, added important intellectual content and approved the definitive version.

Data accessibility

For access to data contact Dr. Pablo Torterolo (ptortero@fmed.edu.uy).

References

Adrian, E.D. (1942) Olfactory reactions in the brain of the hedgehog. *J. Physiol.*, **100**, 459–473.
Benedetto, L., Rodriguez-Servetti, Z., Lagos, P., D'Almeida, V., Monti, J.M. & Torterolo, P. (2013) Microinjection of melanin concentrating hormone into the lateral preoptic area promotes non-REM sleep in the rat. *Peptides*, **39**, 11–15.
Bouyer, J.J., Montaron, M.F. & Rougeul, A. (1981) Fast fronto-parietal rhythms during combined focused attentive behaviour and immobility in cat: cortical and thalamic localizations. *Electroen. Clin. Neuro.*, **51**, 244–252.
Bragin, A., Engel, J., Wilson, C.L., Fried, I. & Buzsáki, G. (1999) High-frequency oscillations in human brain. *Hippocampus*, **9**, 137–142.
Bressler, S.L., Coppola, R. & Nakamura, R. (1993) Episodic multiregional cortical coherence at multiple frequencies during visual task performance. *Nature*, **366**, 153–156.
Bullock, T.H. & McClune, M.C. (1989) Lateral coherence of the electrocorticogram : a new measure of brain synchrony. *Electroen. Clin. Neuro*, **73**, 479–498.
Bullock, T.H., Buzsáki, G. & McClune, M.C. (1990) Coherence of compound field potentials reveals discontinuities in the CA1-subiculum of the hippocampus in freely-moving rats. *Neuroscience*, **38**, 609–619.
Buzsáki, G. & Wang, X.-J. (2012) Mechanisms of gamma oscillations. *Annu. Rev. Neurosci.*, **35**, 203–225.
Buzsáki, G., Anastassiou, C.A. & Koch, C. (2012) The origin of extracellular fields and currents — EEG, ECoG, LFP and spikes. *Nat. Rev. Neurosci.*, **13**, 407–420.
Caixeta, F.V., Cornélio, A.M., Scheffer-Teixeira, R., Ribeiro, S. & Tort, A.B.L. (2013) Ketamine alters oscillatory coupling in the hippocampus. *Sci. Rep.*, **3**, 2348.
Canolty, R.T., Edwards, E., Dalal, S.S., Soltani, M., Nagarajan, S.S., Berger, M.S., Barbaro, N.M., Knight, R.T. *et al.* (2009) High gamma power is phase-locked to theta oscillations in human neocortex. *Science*, **313**, 1626–1628.
Castro-Zaballa, S., Falconi, A., Chase, M.H. & Torterolo, P. (2013) Coherent neocortical 40-Hz oscillations are not present during REM sleep. *Eur. J. Neurosci.*, **37**, 1330–1339.
Castro-Zaballa, S., Cavelli, M., Vollono, P., Chase, M.H., Falconi, A. & Torterolo, P. (2014) Inter-hemispheric coherence of neocortical gamma oscillations during sleep and wakefulness. *Neurosci. Lett.*, **578**, 197–202.
Cavelli, M., Castro, S., Schwarzkopf, N., Chase, M.H., Falconi, A. & Torterolo, P. (2015) Coherent neocortical gamma oscillations decrease during REM sleep in the rat. *Behav. Brain Res.*, **281**, 318–325.
Chrobak, J.J. & Buzsáki, G. (1998) Gamma oscillations in the entorhinal cortex of the freely behaving rat. *J. Neurosci.*, **18**, 388–398.
Cordon, I., Nicolás, M.J., Arrieta, S., Lopetegui, E., López-Azcárate, J., Alegre, M., Artieda, J. & Valencia, M. (2015) Coupling in the cortico-basal ganglia circuit is aberrant in the ketamine model of schizophrenia. *Eur. Neuropsychopharm.*, **25**, 1375–1387.
Daume, J., Gruber, T., Engel, A.K. & Friese, U. (2017) Phase-amplitude coupling and long-range phase synchronization reveal frontotemporal interactions during visual working memory. *J. Neurosci.*, **37**, 313–322.
Freeman, W.J. & Schneider, W. (1982) Changes in spatial patterns of rabbit olfactory EEG with conditioning to odors. *Psychophysiology*, **19**, 44–56.
Fries, P. (2009) Neuronal gamma-band synchronization as a fundamental process in cortical computation. *Annu. Rev. Neurosci.*, **32**, 209–224.
Gottesmann, C. (2006) The dreaming sleep stage: a new neurobiological model of schizophrenia? *Neuroscience*, **140**, 1105–1115.
Gottesmann, C. & Gottesman, I. (2007) The neurobiological characteristics of rapid eye movement (REM) sleep are candidate endophenotypes of depression, schizophrenia, mental retardation and dementia. *Prog. Neurobiol.*, **81**, 237–250.
Gray, C.M., König, P., Engel, A.K. & Singer, W. (1989) Oscillatory responses in cat visual cortex exhibit inter-columnar synchronization which reflects global stimulus properties. *Nature*, **338**, 334–337.
Härle, M., Rockstroh, B.S., Keil, A., Wienbruch, C. & Elbert, T.R. (2004) Mapping the brain's orchestration during speech comprehension: task-specific facilitation of regional synchrony in neural networks. *BMC Neurosci.*, **5**, 40.

Hobson, J.A. (2009) REM sleep and dreaming: towards a theory of protoconsciousness. *Nat. Rev. Neurosci.*, **10**, 803–813.

Hobson, A. & Voss, U. (2011) A mind to go out of: reflections on primary and secondary consciousness. *Conscious. Cogn.*, **20**, 993–997.

Hunt, M.J. & Kasicki, S. (2013) A systematic review of the effects of NMDA receptor antagonists on oscillatory activity recorded in vivo. *J. Psychopharmacol.*, **27**, 972–986.

Jackson, J., Goutagny, R. & Williams, S. (2011) Fast and slow γ rhythms are intrinsically and independently generated in the subiculum. *J. Neurosci.*, **31**, 12104–12117.

Jirsch, J.D., Urrestarazu, E., LeVan, P., Olivier, A., Dubeau, F. & Gotman, J. (2006) High-frequency oscillations during human focal seizures. *Brain*, **129**, 1593–1608.

John, E.R. (2002) The neurophysics of consciousness. *Brain Res. Rev.*, **39**, 1–28.

Joliot, M., Ribary, U. & Llinás, R. (1994) Human oscillatory brain activity near 40 Hz coexists with cognitive temporal binding. *Proc. Natl. Acad. Sci. USA*, **91**, 11748–11751.

Kline, R.B. 2004. *Beyond Significance Testing: Reforming Data Analysis Methods in Behavioral Research*. American Psychological Association, Washington, DC.

Lagos, P., Torterolo, P., Jantos, H., Chase, M.H. & Monti, J.M. (2009) Effects on sleep of melanin-concentrating hormone (MCH) microinjections into the dorsal raphe nucleus. *Brain Res.*, **1265**, 103–110.

Llinas, R.R. & Steriade, M. (2006) Bursting of thalamic neurons and states of vigilance. *J. Neurophysiol.*, **95**, 3297–3308.

Llinás, R., Ribary, U., Contreras, D. & Pedroarena, C. (1998) The neuronal basis for consciousness. *Philos. T. Roy. Soc. B.*, **353**, 1841–1849.

Maloney, K.J., Cape, E.G., Gotman, J. & Jones, B.E. (1997) High-frequency gamma electroencephalogram activity in association with sleep-wake states and spontaneous behaviors in the rat. *Neuroscience*, **76**, 541–555.

Mashour, G.A. (2006) Integrating the science of consciousness and anesthesia. *Anest. Analg.*, **103**, 975–982.

Melloni, L., Molina, C., Pena, M., Torres, D., Singer, W. & Rodriguez, E. (2007) Synchronization of neural activity across cortical areas correlates with conscious perception. *J. Neurosci.*, **27**, 2858–2865.

Pal, D., Silverstein, B.H., Lee, H. & Mashour, G.A. (2016) Neural correlates of wakefulness, sleep, and general anesthesia. *Anesthesiology*, **125**, 929–942.

Paller, K.A. & Voss, J.L. (2004) Memory reactivation and consolidation during sleep. *Learn. Memory*, **11**, 664–670.

Rieder, M.K., Rahm, B., Williams, J.D. & Kaiser, J. (2011) Human γ-band activity and behavior. *Int. J. Psychophysiol.*, **79**, 39–48.

Rodriguez, E., George, N., Lachaux, J.P., Martinerie, J., Renault, B. & Varela, F.J. (1999) Perception's shadow: long-distance synchronization of human brain activity. *Nature*, **397**, 430–433.

Rojas-Líbano, D. & Kay, L.M. (2008) Olfactory system gamma oscillations: the physiological dissection of a cognitive neural system. *Cogn. Neurodynamics*, **2**, 179–194.

Scheffer-Teixeira, R. & Tort, A.B.L. (2017) Unveiling fast field oscillations through comodulation. *eNeuro*, **4**, https://doi.org/10.1523/ENEURO.0079-17.2017. [Epub ahead of print].

Scheffer-Teixeira, R., Belchior, H., Caixeta, F.V., Souza, B.C., Ribeiro, S. & Tort, A.B.L. (2012) Theta phase modulates multiple layer-specific oscillations in the CA1 region. *Cereb. Cortex*, **22**, 2404–2414.

Scheffzük, C., Kukushka, V.I., Vyssotski, A.L., Draguhn, A., Tort, A.B.L. & Brankačk, J. (2011) Selective coupling between theta phase and neocortical fast gamma oscillations during REM-sleep in mice. *PLoS One*, **6**, e28489.

Sirota, A., Montgomery, S., Fujisawa, S., Isomura, Y., Zugaro, M. & Buzsáki, G. (2008) Entrainment of neocortical neurons and gamma oscillations by the hippocampal theta rhythm. *Neuron*, **60**, 683–697.

Sun, Y., Farzan, F., Barr, M.S., Kirihara, K., Fitzgerald, P.B., Light, G.A. & Daskalakis, Z.J. (2011) Gamma oscillations in schizophrenia: mechanisms and clinical significance. *Brain Res.*, **1413**, 98–114.

Tiitinen, H., Sinkkonen, J., Reinikainen, K., Alho, K., Lavikainen, J. & Näätänen, R. (1993) Selective attention enhances the auditory 40-Hz transient response in humans. *Nature*, **364**, 59–60.

Tort, A.B.L., Kramer, M.A., Thorn, C., Gibson, D.J., Kubota, Y., Graybiel, A.M. & Kopell, N.J. (2008) Dynamic cross-frequency couplings of local field potential oscillations in rat striatum and hippocampus during performance of a T-maze task. *P. Natl. Acad. Sci. USA*, **105**, 20517–20522.

Tort, A.B.L., Komorowski, R., Eichenbaum, H. & Kopell, N. (2010) Measuring phase-amplitude coupling between neuronal oscillations of different frequencies. *J. Neurophysiol.*, **104**, 1195–1210.

Tort, A.B.L., Scheffer-Teixeira, R., Souza, B.C., Draguhn, A. & Brankačk, J. (2013) Theta-associated high-frequency oscillations (110-160 Hz) in the hippocampus and neocortex. *Prog. Neurobiol.*, **100**, 1–14.

Torterolo, P., Castro-Zaballa, S., Cavelli, M., Chase, M.H. & Falconi, A. (2016) Neocortical 40 Hz oscillations during carbachol-induced rapid eye movement sleep and cataplexy. *Eur. J. Neurosci.*, **43**, 580–589.

Uhlhaas, P.J. & Singer, W. (2010) Abnormal neural oscillations and synchrony in schizophrenia. *Nat. Rev. Neurosci.*, **11**, 100–113.

Uhlhaas, P.J., Pipa, G., Neuenschwander, S., Wibral, M. & Singer, W. (2011) A new look at gamma? High- (>60 Hz) γ-band activity in cortical networks: function, mechanisms and impairment. *Prog. Biophys. Mol. Bio.*, **105**, 14–28.

Voss, U., Holzmann, R., Tuin, I. & Hobson, J.A. (2009) Lucid dreaming: a state of consciousness with features of both waking and non-lucid dreaming. *Sleep*, **32**, 1191–1200.

Voss, U., Holzmann, R., Hobson, A., Paulus, W., Koppehele-Gossel, J., Klimke, A. & Nitsche, M.A. (2014) Induction of self awareness in dreams through frontal low current stimulation of gamma activity. *Nat. Neurosci.*, **17**, 1–5.

Zhang, X., Zhong, W., Brankačk, J., Weyer, S.W., Müller, U.C., Tort, A.B.L. & Draguhn, A. (2016) Impaired theta-gamma coupling in APP-deficient mice. *Sci. Rep.*, **6**, 21948.

Zijlmans, M., Jiruska, P., Zelmann, R., Leijten, F.S.S., Jefferys, J.G.R. & Gotman, J. (2012) High-frequency oscillations as a new biomarker in epilepsy. *Ann. Neurol.*, **71**, 169–178.